Sustainable future CSP fleet deployment in South Africa: A hydrological approach to strategic management

by

Dries Frank Duvenhage

Dissertation presented for the degree of Doctor of Philosophy in Industrial Engineering in the Faculty of Engineering at Stellenbosch University

The financial assistance of the National Research Foundation (NRF) towards this research is hereby acknowledged. Opinions expressed and conclusions arrived at, are those of the author and are not necessarily to be attributed to the NRF

Supervisor: Prof AC Brent

Co-supervisor: Prof WHL Stafford

Co-supervisor: Prof SS Grobbelaar

December 2019

DECLARATION

By submitting this dissertation electronically, I declare that the entirety of the work contained therein is my own, original work, that I am the sole author thereof (save to the extent explicitly otherwise stated), that reproduction and publication thereof by Stellenbosch University will not infringe any third party rights and that I have not previously in its entirety or in part submitted it for obtaining any qualification.

Date: December 2019

This dissertation includes six (6) original papers published in peer-reviewed journals [1] or books [0] or peer-reviewed conference proceedings [2] and unpublished publications [3 in review]. The development and writing of the papers (published and unpublished) were the principal responsibility of myself and, for each of the cases where this is not the case, a declaration is included in the dissertation indicating the nature and extent of the contributions of co-authors.

Abstract

The global growth in renewable energy, as a means to mitigate climate change, has seen the large-scale deployment of solar photovoltaics (PV) and wind in the electricity generation mix. However, this presents several challenges; primarily that both wind and PV are unpredictable and therefore cannot supply reliable electricity. This necessitates energy storage or the other, more flexible electricity generators to meet the shortfall. Concentrating solar power (CSP) can supply this shortfall in electricity through the concentration of solar irradiation and thermal storage of this heat.

This thermal process requires cooling, best achieved with a finite resource, namely water. Paradoxically, CSP is ideally suited to areas of high solar irradiation that are characteristically arid with low and variable water availability. However, the need for water, mainly as a source of cooling, is often neglected in the planning and development of CSP at a national scale, with few studies that explicitly assess and quantify these hydrological constraints.

This study aims to fill this research gap by improving our understanding of the constraints imposed by water resources on CSP development in arid regions, using South Africa as a case study. A systematic approach was used to model the hydrological constraints to CSP plants' operation and its wide-spread deployment. To determine to what extent CSP might play a role in supplying electricity to the South African grid, a review of future energy mix plans was performed. Although the theoretical potential of CSP based on the solar resource and suitable land is around 12,000 TWh (for the most efficient commercial CSP technologies), the current plans limit this potential considerably to between only 1.87 TWh and 142 TWh. Furthermore, these allocated capacities to CSP in the South African electricity supply are well below the limitations imposed by water resources, especially if dry-cooled plants are used.

CSP performance varies according to design and location, since meteorological conditions vary spatially and temporally. A high-level efficiency model (HLEM) was developed to quantify this variability in South Africa. It uses validated equations and assumptions from literature with CSP energy transfer efficiencies to determine monthly performance in terms of net electricity generation, water consumption factor and total volume of water consumption. Parabolic Trough and Central Receiver CSP plants were modelled with either wet or dry cooling and the CSP performance analysed at thousands of suitable locations in South Africa.

To assess water availability for CSP deployment at these locations, publicly available hydrological data for river flows, dam storage levels and groundwater reserves were used. The water demand from the four CSP-cooling configurations was then measured against the monthly available water per quaternary catchment area. The hydrological limitations were calculated for each configuration, and it was found that, depending on the CSP-cooling configuration, water availability will reduce the theoretical potential for CSP deployment to between 1 - 5% thereof (from 12,000 TWh to 120 – 566 TWh). These results provide guidelines for policy and planning of CSP deployment in South Africa, to ensure the sustainable management of water resources.

Uittreksel

Die wêreldwye groei in hernubare energie, as 'n wyse om klimaatsverandering te beveg, het die grootskaalse ontplooiing van fotovoltaïese sonkrag (PV) en windkrag in die elektrisiteit opwekkings netwerk meegebring. Dit bied egter verskeie uitdagings; hoofsaaklik dat wind en PV onvoorspelbaar is en dus nie betroubare elektrisiteit kan lewer nie. Dit noodsaak energie berging of ander, buigsamer kragopwekkers om aan die tekort te voldoen. Gekonsentreerde sonkrag (GSK) kan hierdie tekort aan elektrisiteit voorsien deur die konsentrasie van sonbestraling en termiese berging van hierdie hitte.

Hierdie termiese proses vereis egter verkoeling, wat die beste bereik word met 'n beperkte hulpbron, naamlik water. GSK is, teenstrydig hiermee, ideaal geskik vir gebiede met hoë sonbestraling wat kenmerkend droog is met 'n lae en veranderlike water beskikbaarheid. Die behoefte aan water, hoofsaaklik as verkoelings bron, word egter gereeld verwaarloos tydens die beplanning en ontwikkeling van GSK op nasionale skaal, met min studies wat hierdie hidrologiese beperking eksplisiet analiseer en kwantifiseer.

Hierdie studie het ten doel om hierdie leemte in die navorsing te vul deur ons begrip van die beperkinge wat deur waterbronne op GSK-ontwikkeling in droë streke plaas, te verbeter en Suid-Afrika as 'n gevallestudie te gebruik. 'n Stelselmatige benadering is gebruik om die hidrologiese beperkings op die werking van GSK-aanlegte en die wydverspreide implementering daarvan te modelleer. Om vas te stel in watter mate GSK 'n rol kan speel in die verskaffing van elektrisiteit aan die Suid-Afrikaanse krag voorsieningsnetwerk, is 'n oorsig van toekomstige energie-mengsel-planne uitgevoer. Alhoewel die teoretiese potensiaal van GSK, gebaseer op die sonbestraling en geskikte grond ongeveer 12,000 TWh is (vir die doeltreffendste kommersiële GSK-tegnologie), beperk die huidige planne hierdie potensiaal aansienlik. Vanaf ses-en-twintig scenario's met betrekking tot die Geïntegreerde Hulpbron Plan (IRP), kan die aandeel van GSK in die toekomstige jaarlikse elektrisiteit opwekking mengsel teen 2030 wissel van 1,87 TWh tot 142 TWh; afhangend van Suid-Afrika se beleid, groei en ekonomiese klimaat.

GSK -werkverrigting wissel volgens ontwerp en ligging, aangesien meteorologiese toestande ruimtelik en tydelik verskil. 'n Hoëvlak-doeltreffendheid model (HLEM) is ontwikkel om hierdie veranderlikheid in Suid-Afrika te kwantifiseer. Dit maak gebruik van gevalideerde vergelykings en aannames uit literatuur met GSK-energie-oordragdoeltreffendhede om die maandelikse prestasie te bepaal ten opsigte van netto elektrisiteit opwekking, water verbruiksfaktor en totale volume waterverbruik. Paraboliese trog- en sentrale ontvanger- GSK -aanlegte is met nat of droë verkoeling gemodelleer en die GSK-prestasie is op duisende geskikte plekke in Suid-Afrika geanaliseer.

Om die beskikbaarheid van water vir GSK-ontplooiing op hierdie plekke te bepaal, is hidrologiese data vir rivier vloei, dam opbergingsvlakke en grondwater reserwes gebruik, wat beskikbaar is in die publieke domein. Die water behoefte van die vier GSK-afkoelkonfigurasies is daarna gemeet aan die maandelikse beskikbare water per kwaternêre opvanggebied. Die hidrologiese beperkings is vir elke konfigurasie bereken, en daar is gevind dat die beskikbaarheid van water, afhangend van die GSK-verkoelingskonfigurasie, die teoretiese potensiaal vir GSK-ontplooiing tot tussen 1 - 5% daarvan sal verminder (van 12,000 TWh tot 120 - 566 TWh). Hierdie resultate bied riglyne vir beleid en beplanning van GSK-ontplooiing in Suid-Afrika om die volhoubare bestuur van waterbronne te verseker.

Acknowledgements

All glory and honour to God Almighty.

To my wife, Anneke, for supporting me through all my studies, endeavours, interests and life in total; thank you, I love you.

To my parents, Dries and Kim Duvenhage, for always loving me, always guiding me, but still allowing me to make my own decisions and mistakes; thank you, you are the best parents anyone could ask for, I love you.

Aan my skoon familie, dankie dat julle my vertrou het om vir Anneke te kan sorg en hierdie te voltooi, en dat julle my ondersteun het en gedeel het in alles en in die opwinding.

To my friends and colleagues along the journey; thank you for your support, friendship, support and kind words.

To Chris Gouws and Harrie Pritzen in Namibia; thank you for giving the opportunity to study in South Africa and for believing in me till the end.

To my study leaders Prof William and Prof Saartjie, thank you for your assistance and inputs. Particular thanks go out to my lead promoter, Prof Alan Brent, for being a fun, but wise and supportive study leader.

Thanks go out to STERG, Fraunhofer ISE, the hydrology officers at the Department of Water and Sanitation, the National Research Fund and Stellenbosch University for support, both institutional and financial.

Thanks to the team at Facilities Management, Stellenbosch University for their willingness to employ me temporarily during the last year of studies, and share in my career experience.

Table of Content

List of Figures

Chapter 2

Chapter 3

Chapter 4

Chapter 5

Chapter 6

Chapter 7

List of Tables

Chapter 2

Chapter 3

Chapter 4

Chapter 5

Chapter 6

Chapter 7

List of Equations

Chapter 4

Chapter 5

Chapter 6

Glossary and nomenclature

AADE	Annual Average Difference Error
BP	Bokpoort Location
CAPEX	Capital Expenditure
CSP	Concentrating Solar Power
CR	Central Receiver
CRWC	Central Receiver Wet-cooled
CRDC	Central Receiver Dry-cooled
DC	Dry cooled
DHIS	Detailed Hourly-Interval Simulation
DNI	Direct Normal Irradiance
DoE	Department of Energy of South Africa
DWS	Department of Water and Sanitation
GIS	Geographic Information System
GL	Gigalitres (equal to Mm^3)
GWh	Gigawatt Hour
HLEM	High-level Efficiency Model
ILL	Illanga Location
IRP	Integrated Resource Plan
IWRM	Integrated Water Resource Management
KaXSO	Kaxu Solar One Location
KSP	Katu Solar Park Location
KSO	Khi Solar One Location
LCOE	Levelised Cost Of Electricity
LUE	Land Use Efficiency
LUF	Land Use Factor
Mm^3	Million cubic meters
NERSA	National Energy Regulator of South Africa
PT	Parabolic Trough
PTWC	Parabolic Trough Wet-cooled
PTDC	Parabolic Trough Dry-cooled
QC	Quaternary Catchment
RBS	Resource Base Sheet
REI4P	Renewable Energy Independent Power Producer Procurement Program
RET	Renewable Energy Technology
RMSE	Root Mean Square Error
SF	Solar Field
PV	Solar photovoltaic
StE	Solar-to-electric
SWRM	Sustainable Water Resource Management
TES	Thermal Energy Storage
TWh	Terawatt Hour
VRE	Variable Renewable Energy
WC	Wet cooled
WEF	Water-energy-food
WRC	Water Research Commission
WWF	World Wildlife Fund

Chapter 1 – Introduction

1.1. Motivation for study

CSP is becoming a more popular option in countries with high solar irradiation and is being installed at greater rates and in larger amounts. This increase in global CSP installed capacities is taking the form of mega-projects like those in Morocco [1] and Dubai [2]. These projects include large capacities of CSP, which are co-located to make use of advantages due to shared infrastructure and financing mechanisms. While this is promising for the CSP industry, and driving down the costs of this technology, it poses a tangible risk to the water resources in these areas. CSP relies on locations with high-quality DNI for effective and affordable electricity. These areas, however, are typically arid and already experiencing water stress [3]. While dry cooling plants are an obvious choice, they are more costly and slightly less efficient, especially in the hot climates they are located. Dry cooling, however, does not discount the need for water at these plants, and water is still required for plant operation, albeit at between 80% and 90% lower rates than that of wet cooled plants [4].

While there are many initiatives aiming to reduce the reliance of CSP on water, little is being done to determine the potential impact of continued and increased growth in this technology on existing water supplies. A need, therefore, exists to contextualise, understand, and finally quantify the constraints imposed by water resources on CSP development in arid regions. This need, however, extends further into the sphere of national regulation, since both the development of the electricity supply network as well as the management of water resources is overseen by governments.

While the availability of water resources has already constrained the operation of other thermal power plants the world-over, it has the potential to drastically limit the planned deployment of CSP in arid areas, and with unmanaged development, can result in losses in electricity capacity and revenue. To improve our understanding of the water constraints to CSP development in semi-arid areas, South Africa was used as a case study to model and assess how water availability contains or limits CSP deployment. This contextualisation, understanding and assessment of hydrological constraints on CSP in South Africa must therefore be such that it can inform policy guidelines and form part of continuous national integrated water management.

The motivation for this study stems from these needs, specifically for the case of South Africa. This study is intended to provide a clear, systematic approach to quantify the hydrological constraints placed on CSP development potential. This quantification, however, should be usable in decision making processes, and as such must be adaptable to the different CSP technology configuration available and varying spatiotemporal conditions.

This work therefore aims to provide the first such documented approach for South Africa to assess and quantify the limits impose by water resources in high-DNI arid regions on CSP development potential, as laid out in the Study Objectives.

1.2. Study objectives and scope

- To understand the dependence of thermal energy infrastructure on water resources.
- To contextualize this dependence for the case of CSP in high-DNI, arid regions.
- To identify the likely future CSP development scenarios in South Africa as determined by national policy and the studies that inform them.

- To develop a validated, sub-annual, spatiotemporal model to assess CSP performance and water consumption across large areas for the most commercially mature CSP and cooling technologies, namely Parabolic Trough and Central Receiver CSP plants, and evaporative wet-cooling and dry-cooling (dry-cooled condenser).

- To identify areas suitable for CSP development within South Africa based on literature, as well as South Africa-specific screening criteria.

- To apply the spatiotemporal model to these areas.

- To quantify this resulting varying water demand per Quaternary Catchment.

- To quantify water availability per Quaternary Catchment based on historical data records.

- To evaluate the amount of CSP that can be hydrologically sustained along each primary river catchment with the key criteria being that the minimum aggregated water balance along the catchment can not fall below a certain threshold during any one month.

- To determine the value of optimizing CSP development in Quaternary Catchments with higher CSP potential (a combined consideration of amount of suitable area and annual DNI), as compared to only considering the minimum aggregated threshold.

- To provide a first attempt at using this information to inform policy guidelines for CSP development in South Africa to ensure hydrological sustainability.

1.3. Dissertation structure and list of publications

This manuscript employed the writing of separate, yet coherent scientific papers on the specific topics identified, which needed to be studied in order to achieve the contributions put forward in Section 1.1. It therefore consist of six (6) scientific papers, three of which were presented at conferences with peer-reviewed proceedings, and three of which were submitted to peer-reviewed international journals (one of these have already been successfully published, while the last two are in various stages of review by the respective journal editorial teams).

The manuscript makes use of continuous referencing, and does not have a reference list per chapter, since certain sources were cited multiple times between the six papers. Each chapter has its own Figure, Table and Equation numbering convention as follows:

- Figures: “*Figure #1 #2*.”.

- Tables: “*Table #1 #2*.”.

- Equations: “*Equation #1 #2*.”.

Where #1 refers to the CHAPTER NUMBER and #2 refers to the FIGURE/TABLE/EQUATION number within that chapter.

The dissertation structure, consisting of the following list of publications, is provided, with a short abstract of each chapter.

Chapter 2 - The need to strategically manage CSP fleet development and water resources: A structured review and way forward

Declaration with signature in possession of candidate and supervisor.

Status: Published

Citation: Duvenhage DF, Brent AC, Stafford WHL. The need to strategically manage CSP fleet development and water resources: A structured review and way forward. Renew Energy 2019;132:813–25. doi:10.1016/J.RENENE.2018.08.033.

The purpose of this paper was to establish the position of the research undertaken within existing literature. It serves both as the broader introduction to the overarching topic of the research, as well as the literature review conducted therefore. It deals with the dualistic problem of the need for water at CSP plants, and the lack thereof in high DNI areas. Furthermore, it covers the nature of the various consumptive water uses within different CSP plant configurations and introduces the concept of consumption factor for CSP plants (alternatively know as specific consumption, measured in volume per unit energy, i.e. m^3/MWh). Concerning water availability, it discusses the concept of Integrated Water Resource Management (IWRM) and the approaches used to quantify availability and implement IWRM. Additionally, it highlights the risks posed by variable and constrained water resources to thermal power plants, and identifies the need for strategic management of CSP plant development and water resources in arid regions. It concludes with a general description of how this problem should be addressed in a more sustainable way, namely through a detailed evaluation of the spatio-temporal variation in water demands for CSP plants, and the capability of water resources to supply this demand.

Chapter 3 - Future CSP in South Africa – A review of generation mix models, their assumptions, methods, results and implications

Declaration with signature in possession of candidate and supervisor.

Status: Published

Citation: Duvenhage DF, Craig OO, Brent AC, Stafford WHL. Future CSP in South Africa – A review of generation mix models, their assumptions, methods, results and implications. AIP Conf. Proc., vol. 2033, 2018, p. 120002. doi:10.1063/1.5067131

South Africa has experienced great uncertainty in its electricity supply sector. Many energy system modelling efforts have been undertaken. This is to determine the most appropriate energy mix and manage uncertainty. We review all available, relevant studies and summarize their results, modelling approaches, and input assumptions. From this, we try to understand their impact on CSP development in South Africa.

Chapter 4 - Concentrating Solar Power Potential in South Africa – an Updated GIS Analysis

Declaration with signature in possession of candidate and supervisor.

Status: Presented at conference, final review process

Citation: Duvenhage DF, Brent AC, Stafford W, van den Heever D. Concentrating Solar Power Potential in South Africa – an Updated GIS Analysis. In preprint. Int J Smart Grid Clean Energy 2019

Concentrating Solar Power (CSP) has become a leading Renewable Energy Technology (RET), and the only one inherently equipped with large-scale thermal energy storage for increased dispatchability. There are many studies that aim to determine the potential for CSP development in certain regions or countries. South Africa (SA) is a country with high solar irradiation by global standards, but few studies have been carried out to determine the potential for CSP. As part of a broader study on determining the impact of CSP on SA's water resources, an updated geospatial approach was used to determine this potential based on technological changes and improved spatial data. A tiered approach using a comprehensive set of criteria to exclude unsuitable areas was used to allow for the identification of suitable areas, as well as the modelling of electricity generation potential.

Chapter 5 - Water and CSP – a preliminary methodology for strategic water demand assessment

Declaration with signature in possession of candidate and supervisor.

Status: Published

Citation: D. Frank Duvenhage, Alan C. Brent, William H.L. Stafford, Omotoyosi Craig. Water and CSP – a preliminary methodology for strategic water demand assessment. AIP Conf. Proc., vol. 2126, 2019, p. 220002. doi:10.1063/1.5117761.

The purpose of this paper was to document the process of developing a spatio-temporal model of CSP water consumption and performance for South Africa. The spatial resolution must be high enough to capture spatial changes in atmospheric and meteorological conditions but also represent actual likely CSP plants. For this reason, a high spatial resolution of a grid of 1kmx1km was chosen. Each grid was evaluated for suitability based on a detailed list of criteria from literature, from slope and DNI, to a long list of excluded areas based on unsuitability due to current land uses and biodiversity protection. The resulting grid of suitable areas was then used to characterise CSP performance and water consumption for parabolic trough, central receiver and dry- and wet cooled systems. A monthly temporal resolution was used since it is capable of reflecting the seasonal variance in performance without being computationally laborious. The methodology employed an annual efficiency-based approach which was adapted to reflect monthly efficiency changes. These monthly efficiencies and solar resource quality (DNI) was used to calculate monthly generation potential. Thereafter, the monthly consumption factor was calculated based on efficiency assumptions for the different CSP technologies and atmospheric influences. This generation potential in GWh per month and monthly average consumption factor in m^3/MWh, was then calculated for each 1km x 1km cell in the entire grid and resulted in total monthly water consumption for a specific CSP configuration at a specific location, at a certain time of the year.

Chapter 6 - Water and CSP – A validated high-level CSP performance and water consumption model based on monthly efficiency calculations

Declaration with signature in possession of candidate and supervisor.

Status: Under review, comments received and first revision submitted

Submitted to: Journal of Solar Energy.

The work uses a novel, updated method to estimate CSP performance and water consumption for varying spatiotemporal meteorological conditions. The work builds on tried and tested theoretical annual efficiency calculation methods. It incorporates simplified monthly dependent boiler-turbine efficiency and solar field efficiency for Parabolic Troughs. The high-level

estimation of monthly net electricity generation for Parabolic Trough plants has a root mean square error (RMSE) of between 3.05% and 4.99%, and a annual average difference error (AADE) from hourly modelled results of between -4.67% and -0.38%. For Central Receiver plants, the RSME for monthly net electricity was found to vary between 2.04% and 3.20%, and showed an AADE of between -2.05% and 0.11% from the detailed hourly interval simulations results. Furthermore, through incorporating these efficiencies with the known System-Level Generic Model for water consumption factor calculation, presented an acceptably accurate estimation of total monthly water consumption. For wet-cooled Parabolic Trough plants the RMSE was between 3.32% and 4.75% and the AADE between -0.82% and 1.25%, while for wet-cooled Central Receiver plants, the RMSE ranges between 1.18% and 3.93%, with the AADE being between 1.18% and 3.93%. The model is capable of estimating plant performance for different CSP technologies, cooling technologies, locations, and monthly conditions. The validation method employed, included the hourly simulation of both a Parabolic Trough plant, and Central Receiver plant, at 50MW and 100MW installed capacities, and with both dry-cooled and wet-cooled condensing, at 5 different locations in South Africa with hourly weather data for a representative meteorological year. These results were then used to refine the annual efficiency assumptions to a monthly scale. Once more accurate monthly efficiencies were obtained, the high-level model was run for the same locations with total monthly DNI, and average monthly dry-bulb and wet-bulb temperatures as inputs. The model can be used for fast estimations of plant performance in many locations at different times of the year, and is intended for use in spatiotemporal modelling of large geographic areas.

Chapter 7 - Water and CSP – Linked CSP water demand models and national hydrology data to manage CSP development and water resource sustainability in arid regions

Declaration with signature in possession of candidate and supervisor.

Status: In review

Submitted to: Journal of Energy Policy

A systematic approach to develop management guidelines for CSP fleet deployment and sustainable water resource use in arid regions is presented. An overview is given of previous work done leading preceding this work. Once CSP development scenarios, suitable areas for development, and the water demand from CSP operations were evaluated, appropriate spatiotemporal CSP performance models were developed. The resulting consumptive patterns and the impact of variable resource availability on CSP plant operation, are analysed. This evaluation considered the entire South Africa, with focus on the areas identified as suitable for CSP, to study the impact on local water resources. It was found that the hydrological limitations imposed by variable water resources on CSP development are severe. Wet cooled Parabolic Troughs' national annual theoretical net generation potential reduced from 11,277 TWh to only 120 TWh, and wet cooled Central Receivers from 12,003 TWh to 170 TWh. Dry cooled versions also experience severe limitations, but to a lesser extent, with Parabolic Troughs decreasing from 11,038 TWh to 512 TWh, and Central Receivers from 11,824 TWh to 566 TWh. Accordingly, policy guidelines are suggested for sustainable CSP development and water resource management within the context of current South African water use regulation.

Chapter 8 – Thesis conclusions

This chapter provides and overview of the work's novel contributions and an overview of its limitations, serving as a point of departure for future work on similar topics relating to water resources and energy infrastructure, in particular CSP.

Chapter 2 – The need to strategically manage CSP fleet development and water resources: A structured review and way forward

2.1. Introduction

Thermal electricity generation requires water in large quantities; accounting for around 40% of the national annual water withdrawals in the United States (U.S.) in 2006, and 45% in 2010 [5], [6]. Globally, water withdrawals for thermal electricity constituted 15% of available fresh water resources in 2010 [7]. Due to improved access to technology by lower- and middle-income groups, and the growth in population, it is estimated that electricity demands will double in regions like China, India and Brazil over the next 40 years, and increase sevenfold in Africa by 2050. This population growth and increased consumption patterns will result in greater demands for both water and electricity [7] [8]. This increase in demand for both resources will take place against a backdrop of greater climate uncertainty, with more people living in areas that are under severe water stress [9], [10].

There is a gradual global transition away from conventional electricity generation towards Renewable Energy Technologies (RETs). Solar photovoltaic (PV) and onshore wind turbines have seen the greatest increase in adoption, and are expected to reach 48% and wind 35% (82% combined) of new renewable installed capacity by 2022 [11], [12]. The costs of these technologies have decreased greatly from their inception in the late 1980's and early 1990's, with the technology-specific costs of PV and onshore wind having decreased by 70% and 50% since 2010, respectively [11], [13]. These technologies, however, experience a major limitation due to resource intermittency [14], and the capacity factors of PV (25%) and wind (33%), are much lower than coal or nuclear [15]. Therefore, as the proportion of PV and wind in the power supply mix increases, there is a growing need for storage or more dispatchable supply of electricity in order to meet peaking demands and decreased grid stability [16]–[18]. Dispatchable renewable energy options include the use of PV and wind with storage in batteries (currently still considered a more expensive solution [19]), power-to-gas[1], hydro-pumped storage, bioenergy, and CSP with thermal storage [20]. However, to date gas turbines using natural fossil fuel has been the favoured dispatchable power generation option, because of flexibility, low capital costs and short lead times [21], [22].

CSP is a renewable energy technology that generates electricity similarly to other fossil-driven thermal power plants. Its source of heat, concentrated solar irradiance, makes it completely independent from fossil fuels. The addition of heat storage to CSP offers dispatchable electricity by enabling power generation at night and times when there is little or no solar irradiation [23]–[29]. In this study, the term CSP refers only to either parabolic trough or central receiver technologies with varying amounts of storage. Combined with an international push for carbon emissions reduction from the electricity sector, the global demand for dispatchable renewable energy, in the form of CSP, is likely to increase in regions with high solar irradiation, such as Southern Africa, Australia, and the MENA[2] region [11, p. 161]. As the development of CSP increases in countries with favourable solar resources, "solar parks" will emerge, where CSP and PV plants are grouped together in large quantities to exploit as much high-quality solar resources as possible. Examples of such solar parks can already be found in Morocco and the

[1] This is especially an option in European countries where heating is an important energy driver, and where supply from renewables like wind regularly exceed demand [20].
[2] Middle East and North Africa

UAE [30], [31]. In South Africa alone, as part of the ministerial determinations on Renewable Energy, a solar park of 5 GW has been planned in the arid Northern Cape Province [32], [33].

Similar to all thermal power generation technology, such as conventional fossil fuel power-plants, CSP requires a heat sink and, therefore, some form of cooling technology. The most cost-effective and efficient cooling technology is of the "wet-cooling" group, where water is actively used to cool and condense the steam after it has passed through the last steam turbine [34]. An alternative option that is more costly, but uses 90% less water, is "dry-cooling", which uses ambient air to cool and condense the steam [35]. Its efficiency, therefore, depends on the temperature and humidity of the air [34]. The higher capital cost, combined with its inherently lower efficiency, results in a double cost-penalty for CSP with "dry cooling", compared to "wet cooling". At CSP plants, 90% of water is typically used for cooling, while the rest is predominately used for cleaning of the solar-field and steam-cycle make-up [4]. Alternative water sources like seawater, and the combined generation of desalinated water and renewable electricity, are technically viable options and have received much attention, but typically require even more piping and pumping infrastructure, adding extra cost [36], [37]. Combined CSP and desalination are also best-suited in close proximity to coastal areas which unfortunately suffer from lower solar DNI due to higher cloud cover and air-moisture [38]. Many studies have assessed various countries' land potential for CSP based on certain suitability criteria. A summary of the criteria used in literature is given in Table 2. 1.

However, despite the fact that both water and solar resource availability varies spatially and temporally, and the growing evidence of the important linkages between water and energy planning [8], [39]–[53], water resource availability is often poorly considered in CSP planning and deployment [54]. With CSP being a viable solution as a large-scale, fully dispatchable RET, able to counter the intermittency issues associated with higher percentages of PV and wind in countries' energy mixes, its adoption rates are likely to rise. Due to the reliance on high solar irradiation, regions between 15^{O} and 40^{O} North and South of the equator, which are typically arid, will experience the most CSP development [55]. With this in mind, it is foreseeable that this increase in CSP adoption in such arid regions might place further pressure on already stressed water resources, and that constraints on water availability may curtail CSP performance and pose risks to the stranding of CSP assets. This is particularly true if CSP planning does not carefully consider water consumption and water availability at a local level. While there have been many studies on the reduction of CSP technology costs [56]–[62], cost escalations due to loss of production from reduced water availability poses a tangible risk that can be mitigated through appropriate planning. Therefore, there is a need to assess the potential of CSP in areas of high solar irradiation in light of the constraints imposed by water availability, and strategically manage CSP deployment so that it does not increase water scarcity.

This paper aims to provide an approach to the strategic management and planning of CSP infrastructure through the lens of the water-energy nexus. We assess the constraints of water availability on CSP deployment and propose an approach to the sustainable management and planning of CSP infrastructure. The methodology used in this paper is that of a narrative literature review in order to present a broad perspective of this subject, describe the problem, its context, and opportunities for management [63], [64]. The need for improved management and planning of CSP infrastructure in light of the water constraints point to the physical asset management of CSP being integrated with water resource management [65]–[67].

Table 2. 1: Suitability criteria for CSP plants from literature

Criteria	[68]	[69]	[70]	[71]	[72]	[73]	[74]	[75]	[76]	[77]	[78]	[79]	[80]	[81]	[82]
Min DNI ($MWh/m^2/y$)	2	2	1.8	2.2	1.7	1.8	1.8	2.6	1.5	2	1.5	2	1.8	1.8	NA
Max Slope(%)	2.1	1-4	3	2	3	0-3	2	1	1-5	4	2[g]	2.1	3	2.1	2
Excluded areas, buffer(km)*															
Wetlands	NA	0.5	NA	0	0[a]	NA	NA	NA	NA[d]	0	NA	0	NA	0	0
Lakes	NA	0.5	NA	0	0[a]	NA	0	0	NA	0	NA	0	NA	0	0
Rivers	NA	0.5	NA	0.5	0[a]	NA	0.5	0	NA	0	NA	0	NA	0	0
Sandy soil	NA	0.5	NA	10	0	NA	NA	NA	NA	NA	NA	NA	NA	NA	NA
Forests	NA	1	NA	0	0	NA	0	NA	NA	NA	NA	NA	NA	0	0
Protected areas	NA	1	NA	0	0[b]	NA	0	0[c]	NA	0[e]	0	0[e]	NA	0	NA
Agriculture	NA	2	NA	0	0[b]	NA	NA	NA	NA	NA	35%[h]	NA	NA	0	0
Roads	NA	2.5	NA	0.05	NA	NA	0.5	NA	NA	NA	NA	NA	NA	NA	NA
Railways	NA	NA	NA	NA	NA	NA	0.5	NA	NA	NA	NA	NA	NA	NA	NA
Mines	NA	NA	NA	3	NA	NA	NA	NA	NA	NA	NA	NA	NA	NA	NA
Populated areas	NA	0	NA	0	0	NA	0	0	NA	NA	NA	0	NA	6-8	0
High Wind Areas**	NA	NA	NA	NA	NA	NA	NA	NA	NA	NA	NA	0	NA	NA	NA
Min area (km^2)	NA	NA	NA	NA	NA	NA	NA	2	NA	NA	4	NA	NA	NA	NA
Maxi distance to (km)															
Grid	NA	NA	NA	NA	NA	NA	NA	20	20-100	NA[f]	NA	30[i]	40	50[i]	NA[j]
Roads/Rail	NA	NA	NA	NA	NA	NA	NA	NA	NA	NA	NA	NA	40	20[i]	NA[j]
Dams	NA	NA	NA	NA	NA	NA	NA	NA	NA	NA	NA	NA	NA	9[i]	NA[j]
Rivers	NA	NA	NA	NA	NA	NA	NA	NA	NA	NA	NA	NA	NA	NA	NA[j]

***** - An area beyond the explicit reach of the unsuitable area, also considered unsuitable, i.e. 0km means only the area itself, 0.5km means the area itself with an extended perimeter of 0.5km around it. ****** - Areas identified to pose potential risks to CSP structures. **a** - The use of buffers is mentioned but no detail on their extent is given. **b** - The study considered three different scenarios: one excluding, one including protected areas, and one including agricultural areas. **c** - The study used vegetation maps categorized as "critically endangered", "endangered", "vulnerable" and "least threatened", excluding all categories but "least threatened". **d** - The study limited all areas remaining after applying the other suitability criteria to only 1% of the identified area, in order to allow for reduced availability due to other exclusion considerations. **e** - "Environmentally sensitive lands" and Aboriginal Heritage sites are excluded. f - While the benefit of closer proximity to transmission infrastructure is discussed, it is not used as a limiting factor. **g** - Slopes up to 7% are considered along with restrictions on the orientation of the slope (North or South), but only <2% is considered explicitly suitable. **h** - Percentage of land cover type considered for CSP development. Similar percentages are applied to other land cover types. **i** - The study used a weighted approach to identify more and less suitable areas according to stakeholder inputs; thus, areas closer to the grid are considered more suitable, an those further are less. **j** - The study modelled the costs associated with building the required infrastructure according to the distance from the infrastructure.

2.2. Energy infrastructure management and planning

The physical asset management of CSP involves the integration of CSP generation with the national power generation mix and requires a process of integrated energy infrastructure management. It becomes increasingly challenging to integrate and coordinate energy infrastructure management and planning when the electricity supply market is liberalized or partially deregulated and independent power producers are allowed to enter the regulated market and supply electricity to the national grid [83]. The challenge is to integrate and plan the developments so that supply can be optimised with demand. In South Africa, energy mix expansion is regulated by policy and the future generation mix options are determined by national plans such as the Integrated Resource Plan, Integrated Energy Plan, National Infrastructure Plan and departmental strategic plans [84]–[87].

Infrastructure asset management is defined in the globally recognised International Infrastructure Management Manual, as "a systematic approach to the procurement, maintenance, operation, rehabilitation and disposal of one or more assets, integrating the utilization of assets and their performance with the business requirements of asset owners or users, with the main focus being the continuous alignment of asset performance to meet service delivery outputs to deliver the desired outcomes" [88]. It considers all phases of infrastructure projects and how they are to be managed in order to continuously ensure optimum performance and cost-effectiveness. When considering the planning phase of electricity infrastructure, there are three categories; strategic, tactical and operative planning [83]. Strategic planning focuses on long-term decisions like investment planning, tactical plans are medium-term ones that focus on, amongst others, project management and budgeting activities, and operational planning looks at short-term tasks like grid stability and plant operation. This paper focusses on strategic infrastructure planning, since the investment-intensive expansion of CSP fleets is under consideration.

Strategic energy infrastructure planning determines the long-term investment timelines for new power plants, and the decommissioning of old ones, in order to maintain a desired power generation and specific mix of technologies in the electricity power supply [88], [89]. These studies make use of multi-criteria modelling packages, such as PLEXOS, in order to determine the optimal mix of power generation options- based on their technical and practical capabilities, cost of capital, operation and maintenance costs, and future forecasted electricity demand [90]. However, this type of planning does not provide detailed insight into spatial planning or resource distribution, particularly in the case of RETs [27]. The challenge with RETs is that their operation is highly variable spatially, necessitating more detailed approaches to strategic energy infrastructure planning. Furthermore, these plans do not always carefully consider the water availability for electrical power generation, although a few studies have assessed the amount of water that will be needed to accommodate various power generation mixes with different associated cooling technologies [91]–[93]. It is argued that this combined total water consumption of energy mixes can be minimized through appropriate technology (power and cooling) selection during the strategic planning phase of energy infrastructure [94].

In the case of South Africa, the Integrated Resource Plan contains the details and schedules for the addition of particular capacities and power generation technologies to the grid, and responds to the White Paper on Energy Policy (1998), and White Paper on Renewable Energy (2003) that highlights the need for affordable renewables in the energy supply mix [95]–[97]. The Integrated Resource Plan informs the targets of the Renewable Energy Independent Power Producer Procurement Program and results in a competitive bidding process by independent power producers [98], [99]. This has resulted in the allocation of 6428 MW of RET capacity between 2010 and 2015 through five rounds of bidding, of which 2372 MW are PV, 3367 MW are Wind and 600 MW are CSP, with the rest being small hydro, landfill gas, biomass and biogas

projects [100], [101]. The National Energy Regulator of South Africa (NERSA) has also assisted independent power producers to sell electricity through enabling grid access and the partial liberalisation of power supply markets. The Integrated Resource Plan is used by the Department of Energy of South Africa (DoE) to place targets and timelines for installed capacities of different technologies, thereby serving as the long-term strategic energy mix expansion plan [102].

There are various CSP modelling software packages available and these have been reviewed previously [103]. The particular models that can be used to assess plant output, water consumption and economics include: DELSOL, SAM, SOLENERGY, EXCELERGY, TRNSYS and ColSimCSP, of which the System Advisor Model (SAM) is most notable in academic literature [103], [104]. ColSimCSP was recently specifically adapted to simulate CSP operation and water consumption for the international MinWaterCSP project by the European Union [105], [106].

2.3. Integrated water resource management

Integrated Water Resource Management (IWRM) is a process that promotes the coordinated development and management of water, land and related resources, in order to maximize the resultant economic and social welfare in an equitable manner without compromising the sustainability of vital ecosystems [107]. It is the response from practitioners and academics within the natural resource management industry to what has since been identified as a lacking approach to rapidly changing natural systems [108]. IWRM acknowledges that water resources within catchments or river basins are complex, and that their interaction with equally (if not more) complex socio-economic and ecological systems add another level of complexity to their interactions [109], [110].

In a detailed bibliometric analysis of research trends in the water resource sector, Zare et al. (2017) found that since the 1980s, when there were less than a total of 50 publications per year in the broad field of “Integrated water assessment and modelling”, this has increased to in excess of 1100 per year in the 2010s [111]. Furthermore, the analysis found that the word most prevalent in titles, keyword lists and abstracts was “management”, alluding to the growing realization of the importance of the concept of active involvement and planning in how human activities interact with water resources. A sharp increase in research focussed on IWRM is seen from 1992 and this is likely due to the publication and formalization of the United Nations (UN) Agenda 21, chapter 18, which emphasises the importance of all UN member states in establishing sound IWRM practices [112], and provides definitions on what constitutes IWRM and guidelines on how to establish such strategies [113]. It suggests that IWRM should be carried out at the catchment or sub-catchment level in the pursuit of the following four cardinal principles:

- IWRM strategies should be dynamic, collaborative, iterative and cross-sectoral with a special focus on identifying and protecting potential freshwater supply sources, and which considers not only environmental and human health wellbeing, but also technological means and socio-economic goals;
- Planning for sustainable and balanced use, and conservation and management of water resources should be based on local community needs within the agenda of national economic development policies;
- IWRM must include the design, implementation and reassessment phases of on-going projects and programmes to ensure they remain both economical and socially relevant through full, indiscriminate public participation;

- The identification and improvement of appropriate institutional, legal and financial instruments that ensure that water policies and their execution positively contribute to sustainable social progress and economic growth.

Following the above principles as well guidelines from other NGOs and development agencies, the Water Environment Research Foundation (U.S.) proposed a framework for Sustainable Water Resource Management [114]. This framework makes the distinction between “integrated” and “sustainable” water resources management, based on the concept that sustainable use of water resources should be a natural outcome of IWRM as much as it is set as a goal. In lieu of this, they developed the process flow-chart, shown in Figure 2. 1, to guide entities responsible for water resources management and related decisions. The framework consists of parallel proactive- and crisis- components of water resources management, and is adaptable to any water-related management problem. Step 1, the realisation that a water crisis has emerged, is omitted in this representation of the process flow diagram since the steps that need to be taken prior to this, and in response, are of interest. It is important to note that the principles of Steps 2 to 9 of the crisis management process are encapsulated in Steps 10 to 20 of the proactive management process, which highlights the need for strategic planning.

The Sustainable Water Resource Management framework also highlights the need for participation and inclusion in considering the management and allocation of water resources so that water resources management is tailored to local needs. This consultation and inclusivity must be considered at different levels, with consideration of local communities, but within the regional (or national) context and policy perspective [115].

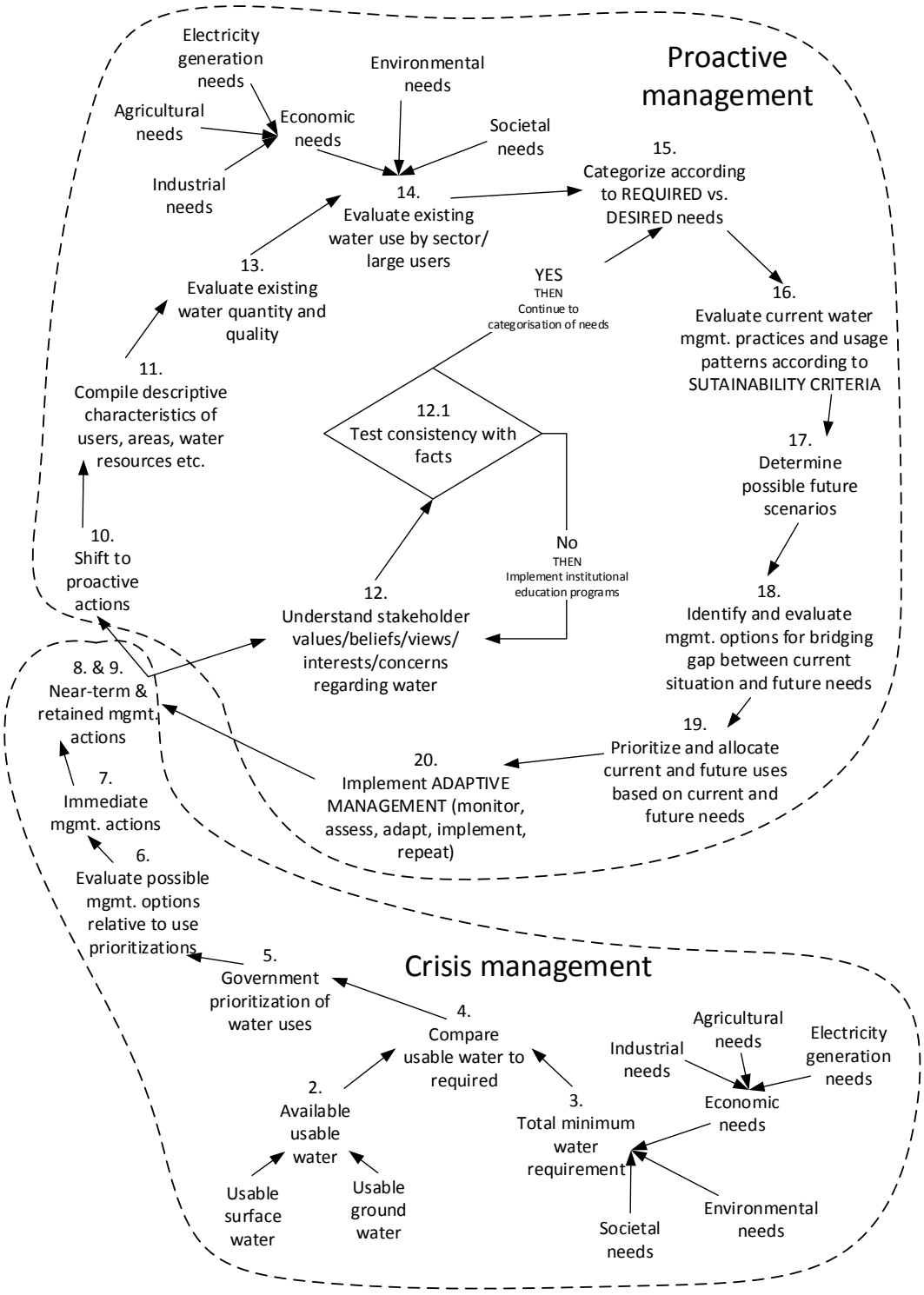

Figure 2. 1: Sustainable Water Resource Management framework process flow-chart. Recreated from [114].

2.4. Water resource constraints to CSP deployment

In order to explore the constraints posed to CSP deployment, the details regarding water consumption at CSP plants and water resource availability in countries of high solar irradiation need to be examined in some detail.

2.4.1. Estimating water available for CSP deployment.

Estimating water availability for industrial water use, particularly for CSP, needs to consider both the water quantity and quality [116]. Both can be modelled according to complex runoff models that attempt to accurately approximate the hydrological cycle from a sub-catchment to a national and in some instance global scale [117]–[119]. These intricate computer models consider a range of input variables on water quantity and quality, and approximate water resource availability using clearly defined parameters for surface water and aquifer balances, an overview of typical inputs and outputs is shown in Table 2. 2 [120]–[122].

Table 2. 2: Overview of runoff water model input variables and outputs.

Model inputs	**Model outputs**
Topography on runoff quantities and directions.	Potential recharge.
The impact of geology on the absorption of water into different ground types and this impact on aquifer recharge rates.	Aquifer recharge.
The quantification of evapotranspiration rates for different plant and crop types.	Surface water baseflow.
The prevalence of crop types in different areas.	Groundwater baseflow.
The withdrawal and consumption rates of various industries and socio-economic activities.	Stream interflow.
Evaporation rates.	Transmission losses.
Rainfall estimates from detailed weather forecasting models.	Groundwater evapotranspiration.
Dam storage capacities and historic levels.	Groundwater outflow and storage.
Silt deposit rates in dams.	Rainfall and runoff.

These models use existing rainfall and hydrological data to model stream flows and storage capacities, and can also carry out scenarios analysis to understand various system interdependencies; such as ground water salinity and the impact of agricultural and mining activities on local water resource quality [123], [124]. These water resource modelling packages typically take the form of system network models [120]. They are comprised of various modules describing the underlying factors that interact with water resources; such as irrigation modules, mining modules, demand nodes and consumption nodes [122]. These modules need to be developed in adequate detail to assess water availability in support of water allocation decisions and formulation of water policy [123]. In South Africa, the recent water resources appraisal used measured stream-flow data to calibrate the WRSM2000 hydrological model; in order to more accurately estimate the mean annual runoff and hence surface water availability and its level of assurance, given the current and future demands [125], [126].

2.4.2. Estimating water requirements for CSP deployment.

In the light of Sustainable Water Resource Management, water requirements take into account social, economic and environmental needs. Minimum water requirements refers to the minimum amount of water required to sustain the most necessary activities under drought conditions; and typically refers to the water required to fulfil basic human-needs and the functioning of critical ecosystems. To estimate the local water availability for CSP deployment, one needs to first ensure available water resources are allocated to the basic human needs reserve and the ecological reserve. Once these needs are met, the water available for CSP deployment can then be considered in the context of various other industrial, domestic and agriculture water demands.

The water withdrawals of CSP plants are similar to that of other thermal power plants, in that the majority of water being used at a plant is for cooling purposes [127], [128]. Water withdrawals refer to the gross amount of water abstracted from a source, and encompass water that is used and lost from the point of abstraction (non-return flows) as well as water that is used and then returned to the point of abstraction (return flows). Consumptive use refers to water that is extracted from a source, and used in a process or incorporated into a product such that it is so altered that it cannot be returned to the source [6]. In the case of CSP, most use is consumptive, with little to no water being returned to the source because it is evaporated to the atmosphere either as part of the cooling process or in evaporation ponds. The water use of a CSP plant consists of: Steam cycle cooling cycle (recirculating wet cooling, air-cooled condenser), mirror cleaning, steam cycle (boiler feedwater closed cycle), auxiliary equipment cooling cycle, firefighting systems, dust suppression, and potable water for operational personnel

Steam cycle cooling

By far, the largest portion of water used at a CSP plant is steam cycle cooling (in the case of wet-cooling). This is the major concern when it comes to water use at any thermal power plant since the condensing and cooling of the steam exiting the low-pressure turbine is critical to plant efficiency and operation [4]. There are two major methods used for cooling at CSP plants: recirculating (evaporative) wet-cooling and dry-cooling[3].

Wet-cooling technology uses water as the cooling fluid, absorbing the latent heat of condensation from the steam exiting the low-pressure turbine. There are two types of wet-cooling technologies: (i) Once-through cooling- water is extracted from a source, used to cool the steam in a condenser and returned to the source to replenish the water abstraction, albeit with water at an elevated temperature [129]. (ii) Recirculating, evaporative cooling- cooling water is circulated between a cooling tower and a condenser; but the warm cooling water is evaporated into the atmosphere. These two wet-cooling technologies are depicted in Figure 2. 2 [130]. Once-through cooling has never been used for CSP because of the lack of adequate water resources in high DNI areas. Recirculating wet-cooling is, however, very prevalent, with almost 80% of all operational plants using this cooling technology[4]. This is due to the lower capital cost of wet-cooling technology and greater efficiency, compared to dry-cooling [4]. Furthermore, compared to recirculating wet-cooling (hereafter referred to as wet-cooling only), the reduced efficiency of dry-cooling results in a larger solar field required to maintain the power output, at higher capital costs [35].

[3] Based on NREL's global projects database available at https://www.nrel.gov/csp/solarpaces/

[4] Calculated from NREL's Concentrating Solar Power Projects database at https://www.nrel.gov/csp/solarpaces/, and excluding unreported cooling technologies.

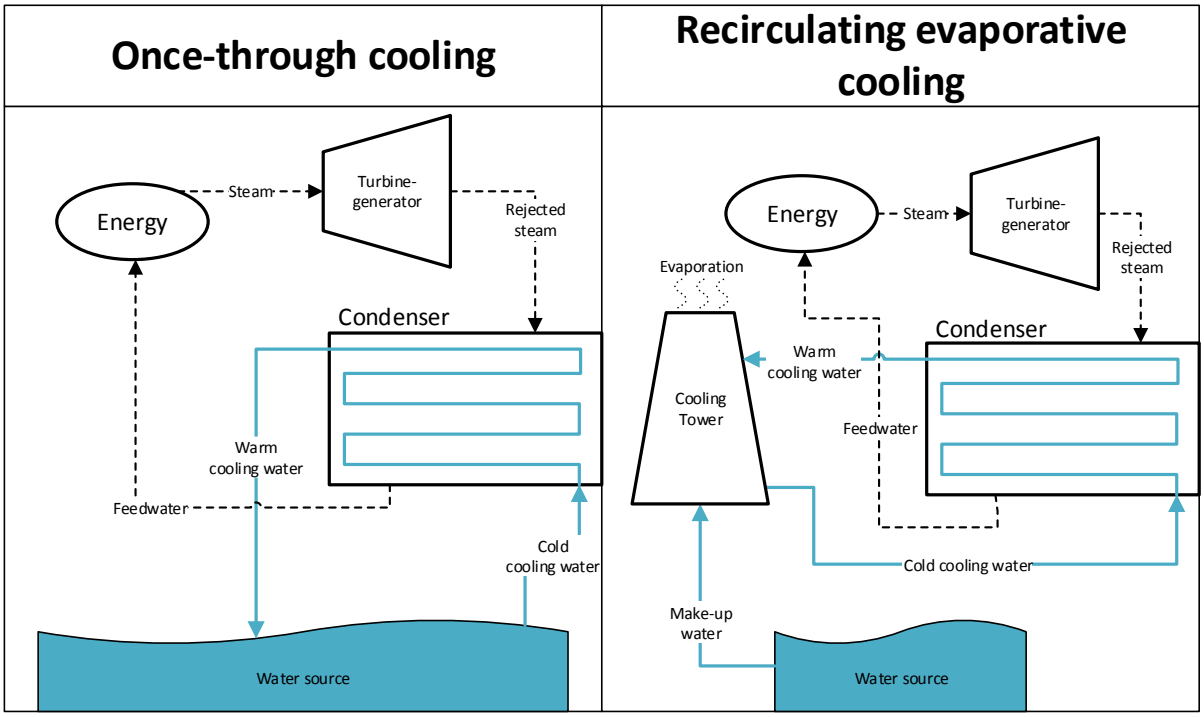

Figure 2. 2: Schematic comparing once-through and recirculating evaporative cooling. Recreated from [131]

Wet-cooling is very effective because the heat from the steam is rejected to the air through the evaporation of the cooling water. Therefore, compared to dry-cooling, the wet-cooling process is less affected by variations in ambient air temperature, since the evaporative cooling is dependent on wet bulb temperature, and as a result of this, wet cooling uses almost 10 times more water than dry-cooling. [35]. There are two major mechanisms of water loss in wet-cooling. Evaporative cooling of the warm water leaving the condenser in the cooling towers, is the primary heat transfer method and water loss mechanism. This results in the concentration of minerals each time water is lost to the atmosphere. Secondly, dilution is required to prevent the cooling water from becoming saturated with minerals; which will result in scale formation and reduced cooling efficiency. Dilution is achieved by adding fresh cooling “makeup water”, and rejecting the higher concentration cooling water, known as “blowdown”, thereby continuously limiting mineral saturation and its consequences[34].

Dry-cooling uses air for cooling instead of water and requires an air-cooled condenser where the steam passes through a bundle of tubes, and ambient air absorbs the heat. This means that the effective cooling that can be achieved is dependent on the dry-bulb temperature of the air; which is always higher than the wet bulb temperature in dry, arid conditions- where CSP is most prevalent. Further, ambient temperatures are highest on days of high solar irradiation, resulting in the highest efficiency losses on days that are supposed to be the most productive [132]. Dry cooling requires minimal water only for cleaning of the condenser tube bundles. This cleaning is carried out at fixed intervals to prevent external fouling on the tubes and ensure efficient operation [133]. As discussed, the main drawback of dry-cooling is the reduced CSP power plant efficiency and higher capital costs, and resulting higher cost of electricity. Studies have found that, depending on the location, dry-cooling can result in increased generation costs of between 5.65% and 7.87% for cool and hot climates, respectively [132].

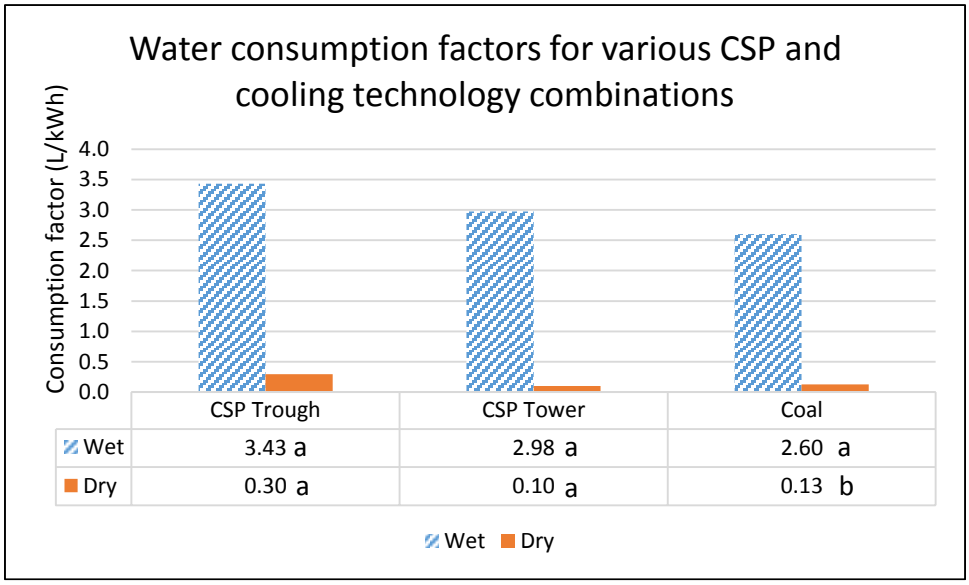

Figure 2. 3: Comparison of water consumption factors for various CSP and cooling technologies, compared to that of Coal.
a – Mean values taken from [134]
b – Mean value calculated from [58]

The overall plant water consumption rates of various power technologies have been compared in other studies [131], [135], [136] and the specific water use for CSP with wet- or dry-cooling were estimated to be in the following ranges (Figure 2. 3). Clearly, dry-cooling uses between 91% and 97% less water than wet-cooling, (trough and central receiver technology, respectively).

Mirror cleaning

Mirror cleaning is the second most significant predictable consumptive use of water at CSP plants. Mirror cleaning is carried out at predetermined intervals using defined amounts of water per square meter of mirrors. Typically, cleaning water is collected, either by the cleaning trucks or the storm water drainage system that conveys possibly contaminated water to the evaporation ponds. Mirror cleaning at trough plants can be between an effective 75-152 L/MWh [137], but typically only accounts for between 1.4% and 2% of total CSP water consumption [4], [138]. In a study to reduce the amount of water required for cleaning, it was found that at SHAMS 1 parabolic trough plant in Abu-Dhabi, cleaning of the 192 loops twice a week, each requiring 1.5m^3 of demineralized water, and has been reported to amount to between 11 and 31 million litres of water per year [134]. There are opportunities to reduce this water use by between 25% and 50%, through the recovery and recycling of water [134], [139].

Steam cycle makeup

Steam cycle makeup water is another consumptive water use at any CSP plant, and is typically between 113-228 L/MWh [137]. This accounts for around 3% of total annual water consumption for wet-cooled plants, and between 44% and 53% for dry cooled plants [35]. Generally, it is assumed that total steam cycle makeup remains almost constant irrespective of the cooling system employed, except for a slight increase for dry-cooled plants at start-up. This is based on the premise that ACCs take longer to achieve full vacuum and reach optimal steam cycle chemistry, resulting in more steam cycle and quench water being consumed in the process [35].

Auxiliary equipment cooling and fire-fighting

Equipment cooling water is circulated between a water-cooling unit (typically a bank of air-cooled condensers) and the components that need to be cooled, such as pump lubrication systems and bearings. Fire-fighting equipment is vital to ensure the safe operation of any CSP plant since receiver temperatures are typically between 290^{O}C and 390 ^{O}C at trough plants and even higher at central receiver plants- in excess of 500 ^{O}C [4], and synthetic oils are often used as the heat transfer fluid, posing a significant fire-risk [140], [141].

2.4.3. Water resources and high solar irradiation areas

Once the available water resources have been estimated, the constraint of water on CSP deployment in areas of high solar irradiation can be assessed. Obviously, areas of high solar irradiation are most suitable for CSP, but are also the most water-scarce, arid regions globally. Figure 2. 4 clearly shows the agreement between high solar irradiation (DNI exceeding 2000 kWh/m^2/year or 6 kWh/m^2/day) and high aridity (chess-board cross-hashing), and that these are areas where most CSP projects are located.

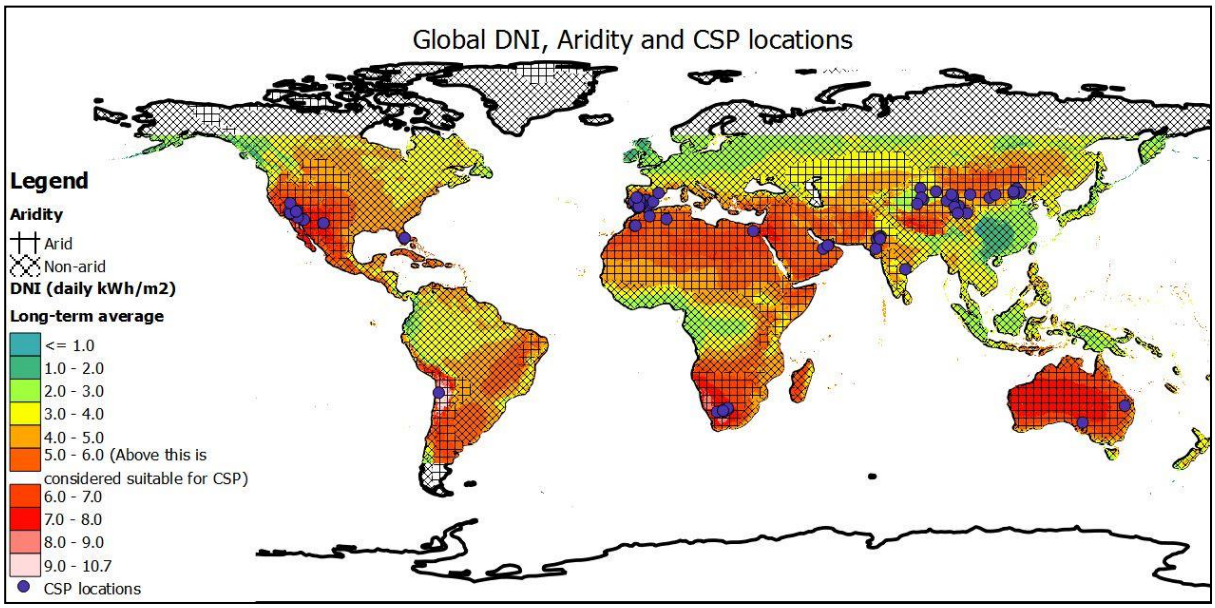

Figure 2. 4: Global DNI, Aridity and CSP locations.

The maps in Figure 2. 5 show the intersection of existing CSP locations with a) arid areas; b) water-stressed areas; c) areas with high seasonal resource variability; and d) areas with high inter-annual resource variability. Map a) clearly shows that CSP plants are mostly located in areas considered semi-arid, arid or hyper-arid, according to the United Nations Environment Programme's (UNEP) aridity index. It is based on the UNEP classification and is a measure of precipitation availability over atmospheric water demand [142]. Map b) shows the intersection between CSP locations and areas with medium to extremely high baseline water stress, showing that CSP-suitable areas already experience lower availability as compared to demands [143]. Map c) and d) shows that these areas are sensitive to variability, both seasonally (monthly) and inter-annually, increasing water-related risks.

Higher temperatures are typically associated with areas of high DNI, and as mentioned before, these warmer atmospheric conditions at CSP plant locations further negatively impact cooling efficiency. Higher atmospheric temperatures are associated with higher cooling-water consumption at wet-cooled plants, and likewise greater efficiency losses in the case at dry-

cooled ones [35]. As a result this, CSP with wet cooling typically uses greater amounts of water when compared to other conventional power generation plants with similar wet cooling technology [135]. This mismatch between optimal CSP locations and impact on cooling efficiency further adds to the disparity between water resource availability and CSP's consumptive demands in these areas and highlights the need to take local conditions into consideration in CSP deployment.

2.4.4. Water-related risks for the power industry

Water constraints are a significant risk for the power industry, as shown by the recent power-plant curtailments in India. CSP operations had to be curtailed at 18 different power plants, because of reduced water availability; with a loss of 14 TWh of power generation in 2016, and curtailment having gradually increased from 6 TWh in 2013 [144]. The Parli Thermal Power Station in Maharashtra, India, had a capacity factor of only 38% due to water availability constraints, and this resulted in a loss of revenue in the order of $1.2 billion in 2016 [144]. The curtailment at the Farakka plant in West Bengal was due to lower than expected rainfall and an inter-boundary water management policy requiring water to be allocated to supply Bangladesh [145]. These incidents highlight the financial risks of poor water resource management in strategic energy infrastructure planning. This risk is even more severe for RETs since their generation relies on the availability of a natural resource (solar irradiation or wind, etc.), and therefore cannot be regained once production has been lost. The above incidents highlights that many developed countries suffer from a lack of integrated water resource management in CSP planning and deployment. In the U.S. between 2000 and 2015, there were 43 separate incidents of power plant curtailment due to water availability and temperature issues [146], [147].Furthermore, the impact of drought conditions on U.S. power plants highlighted that few regulatory bodies have established detailed priority systems for allocating water use to certain water uses during constrained availability [148].

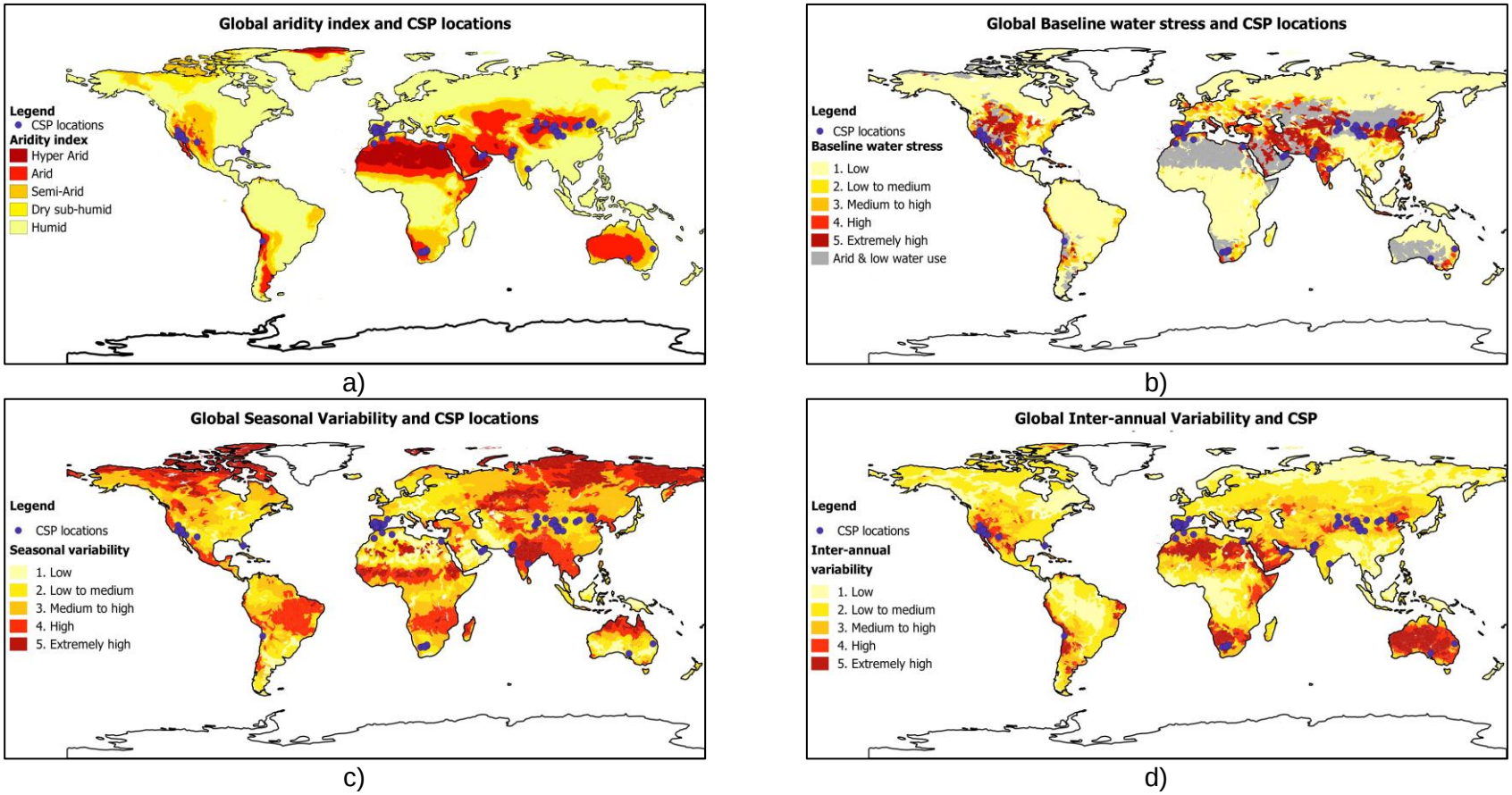

Figure 2. 5: Maps of planned and existing CSP locations and: a) aridity; b) water stress; c) seasonal resource variability; d) inter-annual resource variability.

Maps compiled using aridity data from the UN's Aquastat database (available at http://ref.data.fao.org/map?entryId=221072ae-2090-48a1-be6f-5a88f061431a), water stress data from the World Resources Institute's (WRI) Aqueduct study (available at http://www.wri.org/publication/constructing- decision-relevant-global-water-risk-indicators), Global DNI data from SolrGIS (available at https://solargis.com/maps-and-gis-data/download/world) and NREL's Concentrating Solar Power Projects database (see previous footnotes).

2.5. Discussion: Incorporating water resources management into the strategic planning and deployment of CSP

The suggested approach of this paper is that of combining strategic energy infrastructure planning with integrated water resource management. This integration is essential for the successful deployment of CSP; since the areas of high CSP potential are located in hot and arid areas, where water availability for CSP cooling may be limited and a constraint to CSP reaching its potential for deployment. Strategic planning and policy support is needed to ensure that CSP deployment has minimal impacts on water resources, and that the deployed CSP plants reach their expected performance through the prevention of curtailment due to water availability constraints.

Water is used in different processes within a CSP plant. The water consumption is influenced by the CSP power plant capacity, the cooling technology used, and the solar resource and atmospheric conditions at a particular location. CSP performance at a given locality needs to be modelled in light of seasonal water availability from spatial and temporal variation. The performance of CSP will influence the financial viability or levelised cost of electricity produced. The viability of CSP is also strongly influenced by feed-in tariffs and the market value of dispatachable power. The ability of CSP with storage to produce dispatchable power is an obvious advantage to meet peaking loads, and may receive favourable tariffs to do so. Conversely, the lower night-time tariff may be less favourable due to reduced demand [149]. However, generation during night can reduce CSP water consumption since production during these times will take place under cooler ambient conditions. It is challenging to model CSP deployment potential at a national scale, since various CSP capacities and configurations are possible in each location according to grid expansion requirements, and various possible future feed-in tariff structures. However, the maximum theoretical generation capacity based on the available suitable land and solar resources can be estimated for each quaternary water catchment area and then the water resources availability and assurance of supply in that catchment can be assessed accordingly.

Water resources are spatially and temporally distributed unevenly at a global, continental, regional, national and even sub-catchment level. Drought conditions, defined as periods of restricted water availability due to lower than required rainfall, occur at unpredictable multi-year intervals and result in increased competition for water resources among water users [150]. It is therefore important to be able to evaluate a long period of water resource data in order to see the drought occurrence frequency, as well as establish the baseline water availability in each quaternary catchment to assess potential vulnerability to CSP curtailment and increased water stress.

There are various modelling tools available to increase our understanding of how water resources can limit CSP from reaching higher levels of potential deployment. Aside from engineering modelling of CSP plant design and hydrological modelling of water resources, geographic information systems (GIS) are particularly valuable in planning energy infrastructure and managing water resources, specifically in an integrated manner. GIS is widely used in both water resource planning and infrastructure planning as a means to visually depict specific information such as evaporation rates, flood occurrences, electrical grids, and the energy and water demands. This makes GIS an ideal final tool to represent the results from the modelling and data analysis above, and use these visual representations (maps) to not only inform decisions, but also guide policy developments[151].

Once the water consumption and water resource availability are both represented in accurate models, the CSP potential can be assessed, and appropriate design requirements can be specified for further deployment. For example, in South Africa, the driving regulatory authority

is the Department of Energy, through its Renewable Energy Independent Power Producer Procurement Program (REI4P). This program stipulates various requirements that need to be met by any prospective RET developer, ranging from specifications on the minimum required local content and social and economic development involvement, to minimum plant ramp-up rates and ability to supply electricity when demand is higher. These national policies directly impact RET plant location, design decisions, operating strategies and costs [152].

Water use needs to be regulated and integrated through policy to ensure that water resources are protected, used, developed, conserved, managed and controlled in such a way as to ensure and promote efficient, sustainable and beneficial water use [153], [154]. Coal power plants are highly dependent on water in South Africa, while coal mining also incurs significant impacts to water resources [155]. As a result, guidance notes have been issued to prospective coal independent power producers on water availability for further development in coal-rich areas, recommending various water-use efficiency measures [156]. However, similar recommendations for other RETs such as CSP have not been made. This dependence is also highlighted in the possible impact that loss of water supply from pump stations to these coal power plants could result in loss of generation [157]. Policies can inform and encourage certain power plant configurations to achieve desired water consumption rates and also to promote the use of alternative water sources by power plants [158]–[160]. Coordinated strategic planning between responsible stakeholders can help ensure that targets set out in joint water-energy policies are achieved [161]. Energy infrastructure management and planning will need to integrate water resource availability with the potential for CSP deployment in high solar irradiation areas. In doing so, several questions should guide and frame CSP developments: To what extent is water resource availability and variability a constraint on CSP deployment? Can this constraint be adequately addressed through technology-specific strategic planning? What alternative sources of water are available in areas with inadequate natural water supply? How can policies be used to promote the use of such alternative sources in order to ensure sustainable management of natural fresh water source? What measures need to be put in place to incentivise responsible use and monitoring of water use at CSP plants?

2.6. Conclusions

With the increasing deployment of solar PV and wind in the electricity generation mix, more responsive dispatchable, or peaking generation capacity, is needed to respond to the changes in demand. CSP with storage can overcome the supply intermittency experienced by many RETs. However, the spatial potential of CSP based on the solar resource needs to be tempered by taking into consideration local water availability for CSP power plant cooling. Hydrological models can assess the water availability at various locations, and this can be spatially superimposed with the solar irradiation using geospatial tools to determine areas where biophysical constraints water scarcity hinders CSP reaching its full deployment potential. Integrated water resources management and national policies for sustainable development can be used as a process to explore how local water resources should optimally be used (which takes into account a range of water demands), and therefore enables a more realistic assessment of water availability for CSP deployment. It will be critical to establish a standardised approach to assessing this dualistic managerial problem, and apply it in different countries within the context of national planning. There may also be instances where international water relations need to be considered. Therefore, CSP infrastructure management and planning needs to be integrated with water resources management to allow for contextual differences between different countries, regions, and specific locations. The development of a model-based guiding framework and methodology to achieve this will provide the required insight to tailor policy specifically suited for the country or region in question, which is needed to enable the sustainable development of CSP.

Chapter 3 – Future CSP in South Africa – A review of generation mix models, their assumptions, methods, results and implications

3.1. Introduction

South Africa's energy landscape has undergone turmoil after the 2007/'08 power crisis [162]. This has prompted government to recognize the value of independent power producers (IPPs). Of particular interest, are those using renewable energy technologies (RETs). Global and local climate change targets contributed to the uptake of RETs [163]–[165]. Furthermore, they are becoming cost-competitive with conventional generation options under constrained supply conditions. This is because the can provide much-needed relief within shorter lead-times [101], [166].

Yet, the variability of the renewable energy resources requires more detailed energy planning. Integrated Resource Plans (IRPs), aim to guide government decisions on long-term generation infrastructure expansions. Detailed cost-optimal models, considering various supply options, inform these IRPs [84]. Energy system modelling stems from the need to plan for likely future demand scenarios. The aim is to identify reliable electricity generation options, and achieve a high certainty of supply [90]. South Africa (SA) promulgated its first IRP in 2010. SA released an update in 2013 (not promulgated), and later in 2016 (currently under review) [167], [168]. They form the basis of ministerial determinations. These determinations result in energy procurement programs such as the Renewable Energy Independent Power Producer Procurement Program (REI4P). The REI4P has led to the addition of 6,422 MW installed capacity of renewable electricity generation, of which 3,052 MW is operational [169].

Of this capacity, 3,357 MW and 2,292 MW are onshore wind and PV respectively, with concentrating solar power (CSP) constituting 600 MW thereof [99], [169], [170]. Wind and PV experience great operational variability due to their reliance on natural resources. CSP offers greater stability due to its ability to store thermal energy for dispatchable generation [27]. This gives CSP a competitive advantage over other RETs since it can provide peaking, mid-merit or even baseload generation [171]–[173]. Profitable electricity from CSP requires high direct normal irradiance (DNI) and enough thermal energy storage (TES) for the tariff-structure in place [172][61]. Furthermore, CSP offers opportunities for local and national economic growth. This is through investments, job creation, and the localization of CSP manufacturing sectors [29]. The lower global adoption rates of CSP, and lower allocations in the REI4P, are a result of its higher Levelized Cost OF Electricity (LCOE) [169][12].

The IRPs are the formal reports produced by the SA Department of Energy (DoE). They inform the desired electricity generation mix for future supply expansions [174]. There are, however, other independent studies by research institutions and interested global organizations. These independent studies do not formally contribute to policy-driven decision-making, but provide a benchmark for the IRPs. Furthermore, the results from these studies impact public opinion on generation technologies and influence investments in the electricity sector. Additionally, they often form the basis of assumptions used in further research. In a recent example, a Masters level project used the results of the IRP2013 in its modelling [175]. The IRPs impact investor confidence in SA. Since 2015, CSP bidders were experiencing delays in finalizing agreements with the national utility, Eskom [176], [177]. Additionally, the IRP2016 had no CSP allocations, which lead to an outcry by prospective investors and stakeholders in the media [178]–[187].

In light of this reaction, and subsequent publication of independent studies in response to the IRP2016, a comprehensive review of electricity supply options for South Africa is necessary. Therefore, this paper presents an objective comparison of all such available studies, for South Africa. An analysis of their methodologies, assumptions, and modelling techniques could provide valuable insights for all stakeholders. This paper focuses primarily on CSP because of its capability to provide stable generation. Furthermore, PV and wind are already commercially established, with CSP still in a young, but growing phase. For faster development of the CSP industry, an understanding of which technical, operational and policy factors will influence its future, is necessary.

3.2. Energy System Modelling methods

The modelling packages and approaches used to find the optimal electricity generation mix for a certain country (or area) varies according to method and purpose [90]. Pfenninger et al. discussed the grouping of modelling packages according to the following four paradigms:

1. Energy system optimization models, aiming to determine a variety of possible scenario's based on optimization criteria and goals for all energy sources and demands (scenarios through optimization).
2. Energy system simulation models, aiming to forecast future system developments through simulations, for all energy sources and demands (forecast through simulation).
3. Power systems and electricity market models, aiming to either determine scenarios through optimization or forecasts through simulation, but focused primarily on electricity as a form of energy.
4. Qualitative and mixed-methods scenario's, aiming to produce detailed results (scenario or forecast oriented) for complex energy systems, through a combination of qualitative and quantitative techniques.

These paradigms are not explicit in their boundaries, but are rather fluid in their definitions, approaches, and desired results. Most of the studies reported in this paper focused on finding cost-optimal electricity generation mixes for SA to meet a projected demand (based on separate modelling). Meeting this forecasted demand must take place under certain limitations or constraints; such as meeting future demand at the lowest cost, achieving CO_2 emission reduction targets, and the economies of scale of electricity supply for various generation options. The combinations of these considerations (optimization goals, demands, limitations, and assumptions) constitute "scenarios". These scenarios are then modelled in an appropriate package, and the results are used to understand the implications of the underlying scenario conditions. A simplified representation of the logical process followed to reach final energy mixes in most of the studies is shown in Figure 3. 1 a.

There are many technology-wide energy system modelling packages in use, but the most notable are the PLEXOS and TIMES analysis tools. Industries and research institutions use PLEXOS, and it is the package used by the DoE for the IRPs, and by the National Council for Scientific and Industrial Research (CSIR) for their independent studies and response to the IRP2016. It is a mixed-integer linear programming package with detailed elements for various power plant technologies, the transmission grid and market planning, and with enough detailed input data, is capable of providing analyses at very high resolutions (up to 1- minute detail) [90].

Another widely used package is the TIMES model, developed by the IEA ESTAP[5] consortium of researchers from IEA member countries, and is publicly available, with the aim to present possible future developments of national, regional and global energy systems [90]. TIMES is generally considered to fall in the paradigm of "energy system optimization models", while PLEXOS is considered part of the "power systems and electricity market models" paradigm [90]. Even though these two, among others, might be classified under different paradigms, they can be used in similar ways to determine optimum energy mixes.

The IRPs, the defining regulatory documents used to plan future electricity supply infrastructure builds, uses the outputs of these optimization models to limit the supply capacity of various generation options in a subsequent a competitive bidding process. This relationship between modelling results and its use in national electricity supply planning is shown in Figure 3. 1 b.

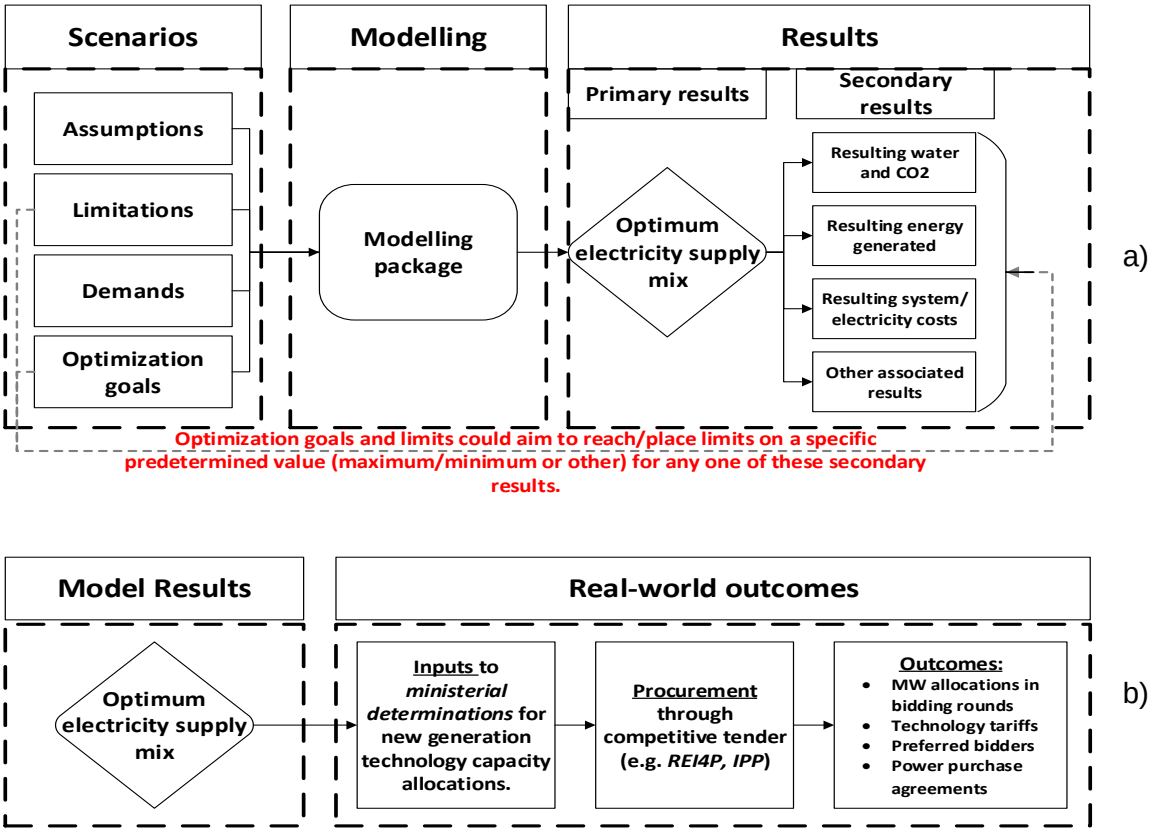

Figure 3. 1 a) The logical process followed to reach optimized energy mixes for various scenario-specific considerations, b) How the results of modelling for the IRP form the basis of informing future developments.

3.3. Approach

Since this study focuses on the amalgamation of information from other studies, it must report coherently on a large number of results, without meaningless repetition. Thus, it aims to review studies that determine various electricity generation mixes for South Africa, and which look in particular detail at RETs options, especially CSP. As discussed, the rationale is that

[5] International Energy Association - Energy Technology Systems Analysis Program

such studies inform industry decisions, public opinions, and assumptions for further studies. This means that studies were considered that might influence these three stakeholder groups.

Many studies like these have appeared in recent years, and limitations need to be placed on which are considered in this paper to ensure relevance; the following four criteria were subsequently used:

1. Published during or after 2010 (one exception has been made).
2. Consideration must be given to RETs and CSP in particular.
3. If a global report is considered, particular detail must be available for South African results.
4. Must be publicly available.

The sources found to adhere to this criteria are summarized in Table 3. 1, and to cover all available energy mix results for South Africa, their databases were searched for possible contributions to this analysis.

Table 3. 1 Sources of potential reports/studies on energy mixes for South Africa.

Resource type	Institution name	Used in analysis
Governmental institutions	South African government gazettes	N
	National Energy Regulator of South Africa (NERSA)	N
	ESKOM	N
	Department of Energy South Africa (DoE)	Y
	The Council for Scientific and Industrial Research (CSIR)	Y
	Department of Science and Technology	N
Global companies and institutions/agencies	International Energy Agency (IEA)	N
	International Renewable Energy Agency (IRENA)	N
	Renewable Energy Policy Network for the 21st Century (REN21)	N
	World Council for Renewable Energy (WCRE)	N
	Solar Energy Industries Association (SEIA)	N
	World Wildlife Fund (WWF)	Y
	Greenpeace	Y
	United Nations Environment Program (UNEP)	N
Research institutions (Academic)	Centre For Renewable and Sustainable Energy Studies (CRSES – Stellenbosch University)	N
	Energy Research Centre (ERC – University of Cape Town UCT)	Y
	Academic publications in general – theses/dissertations and journal papers	N
Research institutions (Industrial)	National Renewable Energy Laboratory (NREL – DoE of the USA)	N
	Plataforma Solar de Almería (PSA - Centre for Energy, Environmental and Technological Research, Spain)	N

The systematic methodology followed to perform the analysis was:

1. Identify appropriate studies according to the four criteria listed above, from the sources listed in Table 3. 1.

2. For each study determine the main objective, modelling approach and package, base scenario, maximum CSP scenario, and minimum CSP scenario.
3. Identify key input parameters, assumptions, limitations, demand profiles, cost profiles/learning curves, forced/relaxed builds, assumed lead times and assumed capacity factors.
4. Find the key results: system costs and/or investment requirements and installed capacities per technology.
5. Enter above information into the database.
6. Analyse trends and correlations according to groupings of CSP development cases.
7. Draw conclusions from above analyses and make informed suggestions.

3.4. Results and discussion

From the various sources of potential studies listed in Table 3. 1, nine studies were found to adhere to the criteria, and are listed in

Table 3. 2. One exception to the criteria was the Greenpeace Energy Revolution report of 2009, since it forms part of a series of two studies, being followed by the Greenpeace Energy Revolution report of 2011.

Table 3. 2 Reports/studies identified which contribute to determining energy mixes for South Africa.

Report/Study Name	Goal of Study	Optimization Parameter
IRP 2010 [84] and 2016 [168]	Determine how long-term electricity demand should be met by new generating capacity, type, timing, and cost, with a balance between affordability, and a government determined policies.	Cost-optimal (with various limits, forced builds, and relaxed options)
IRP 2013 [167]	Determine how long-term electricity demand should be met by new generating capacity, type, timing, and cost, taking changes in technology costs and forecasted demands into account, and providing a flexible approach to determining investment decisions in contrast to the fixed capacity plan of the IRP 2010 and 2016.	Cost-optimal (with various limits, forced builds, and relaxed options)
CSIR response to IRP 2016 [102]	Part of the IRP update process, industry stakeholder-engagement for comments and inputs prior to final IRP. Aimed to find the least cost, unconstrained electricity mix by 2050, in line with the IRP 2016, to reflect the latest industry-aligned costs and changes.	Cost-optimal (with various limits, forced builds, and relaxed options)
Greenpeace 2009 [188] and 2011 [189] Energy [R]evolution	The only exception made on relevancy-criteria since it forms part of a series of documents, with the next published in 2011. Scenarios based on the global energy scenario produced by Greenpeace demonstrating how energy-related global CO_2 emissions can be at halved by 2050.	Unclear; limits on CO_2, possibly optimized or simulated to reach the goal.

Report/Study Name	Goal of Study	Optimization Parameter
WWF - 50% by 2030 (2010) [190]	Compare the implications of a reference scenario (where capacity is allocated according to the 2007 Eskom investment plan) to that of an alternative, where CO_2 emissions are reduced through more RE to the generation mix by 2030, but still meeting demand requirements.	Simulation performed to reach the goal of 50% installed capacity by 2030
WWF – feasibility of the WWF renewable energy vision 2030 (2015) [191]	Test feasibility and merits of targeting 20% annual electricity generation from RETs by 2030 by performing a spatial-temporal analysis on the complete electrical system of South Africa.	Simulation performed to test goal of 20% installed capacity by 2030
UCT, ERC – Towards a new power plan (2015) [192]	Looks at key assumptions in the IRP 2010 and the impact that updating some of these assumptions will have on a new power plan. The new assumptions considered are lower demand, updated investment costs of renewable and nuclear technologies and the availability of natural gas import options.	Cost-optimal (with various limits, forced builds, and relaxed options)
UCT, ERC - Nuclear build plan technical report (2015) [193]	Analyse the SA Government's commitment to 9.6GW of nuclear power against other supply options. A flexible planning approach in the electricity sector is compared to a commitment to the full nuclear fleet for two different demand scenarios.	Cost-optimal (with various limits, forced builds, and relaxed options)

For each study, there are multiple sets of results pertaining to each scenario, for the various technologies considered therein. An example of the IRP 2016 Base Case is shown in Figure 3. 2. An issue with this data was that each study presented it at different time-scales (every year, five years, ten years, etc.) and in different ways; for example, some studies consider the total installed capacity, some only new added capacity, while others used the cumulative added capacity since the start of the modelling period, the representation of choice for this paper, since it could be calculated from the previous two presentation styles. From Figure 3. 2 one can see that factors, such as time-scales, modelling period and the sheer amount of information relating to the energy mixes, namely capacity per technology, complicate the representation of this data for multiple scenarios.

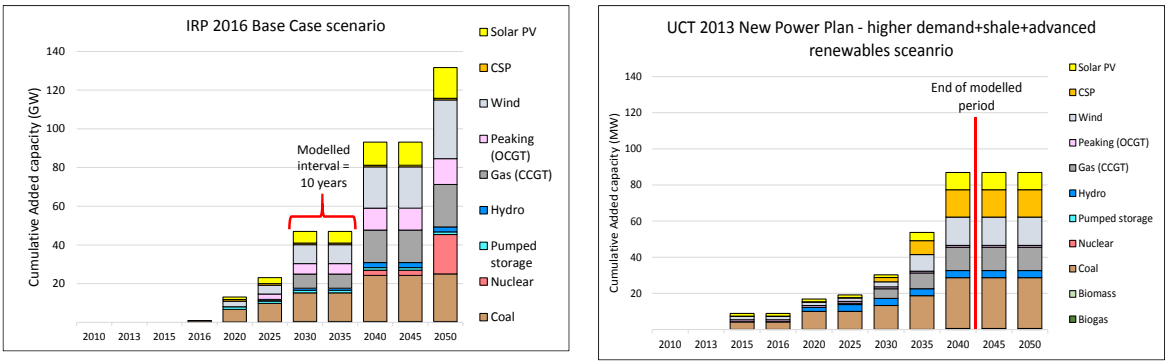

(a) (b)

Figure 3. 2: Cumulative new added capacity for the (a) IRP 2016 and (b) UCT New Power Plan of 2013.

Yet, it is also important to see the capacity allocated to CSP in light of capacities allocated to other technologies to understand how the demand is met by the combination of technologies. For this reason, it was decided to show the CSP build-plan over the entire modelling period, as well as the final total energy mix by the end of the modelling period of each scenario reviewed. Since the aim of this paper is to understand the impact of modelling considerations on the projected development of CSP in South Africa, the scenarios covered in this analysis will be compared to each other on the basis of CSP capacity allocations. Figure 3. 3 (a) shows that there are four distinct groups of CSP development cases stemming from the capacity allocations; high (38.8 GW to 15 GW), moderate (15 GW to 2 GW), low (2 GW to 0.5 GW), and very low (0 GW to 0.5 GW). Figure 3. 3 (b) shows the entire energy mix of each of these scenarios by the end of the modelling period. The full names of each of the scenarios in Figure 3. 3 are given in Table 3. 3 (appended to the end of Section 3.5).

Another key result of these models is the associated total system cost, or calculated average tariff resulting from the energy mix modelled. This information is very relative in nature for each study across the various scenarios aiming to compare relative costs within a study, and not necessarily explicitly predicting the actual future costs. They are also relative across different studies from different countries (currency), different publishing years (inflation), and different input cost data origins (2005 USD for example). This complicates comparing the impact that each energy mix from each scenario has on system costs between different studies.

Therefore, the average cost-results over the modelled period for each scenario in a study are normalized to the lowest average cost over the same modelling period within that study and expressed as a factor greater than the lowest average cost between all the scenarios within a study. This will provide insight into how each scenario compares to the others in the same study, and relatively to those from other studies. It should be noted that a value of one, in Figure 3. 4, refers to the scenario in that study with the lowest system cost, and values greater than one indicates how many times more costly than the least costly energy mix a certain scenario is. This makes the total system costs more comparable between different studies, showing that the higher contribution by CSP does not always result in a higher total system cost.

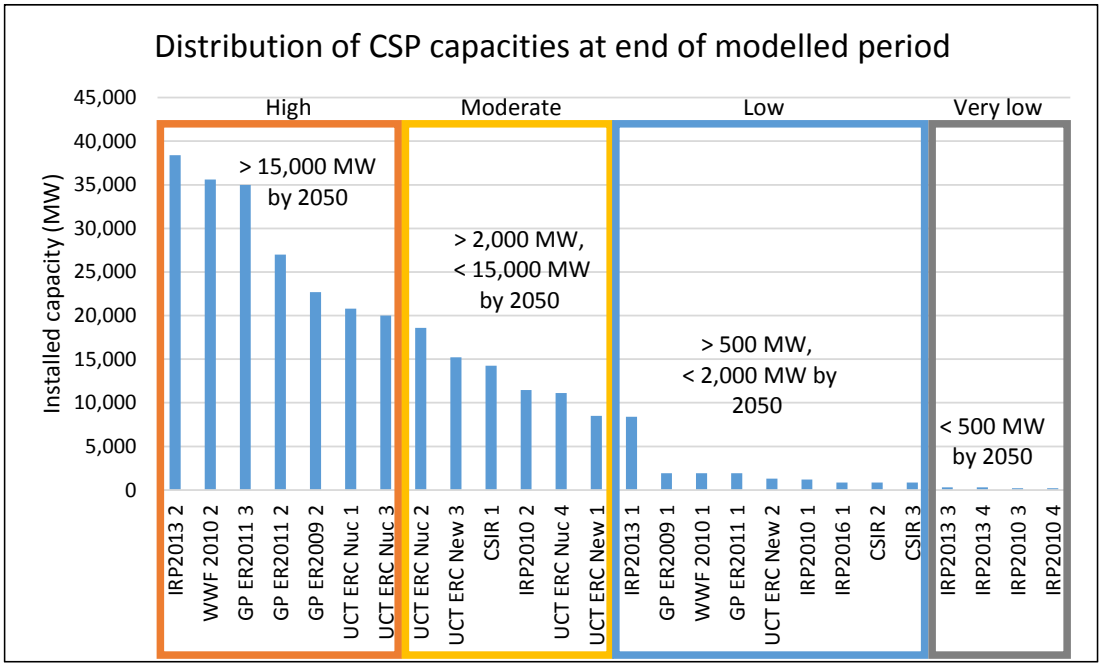

a)

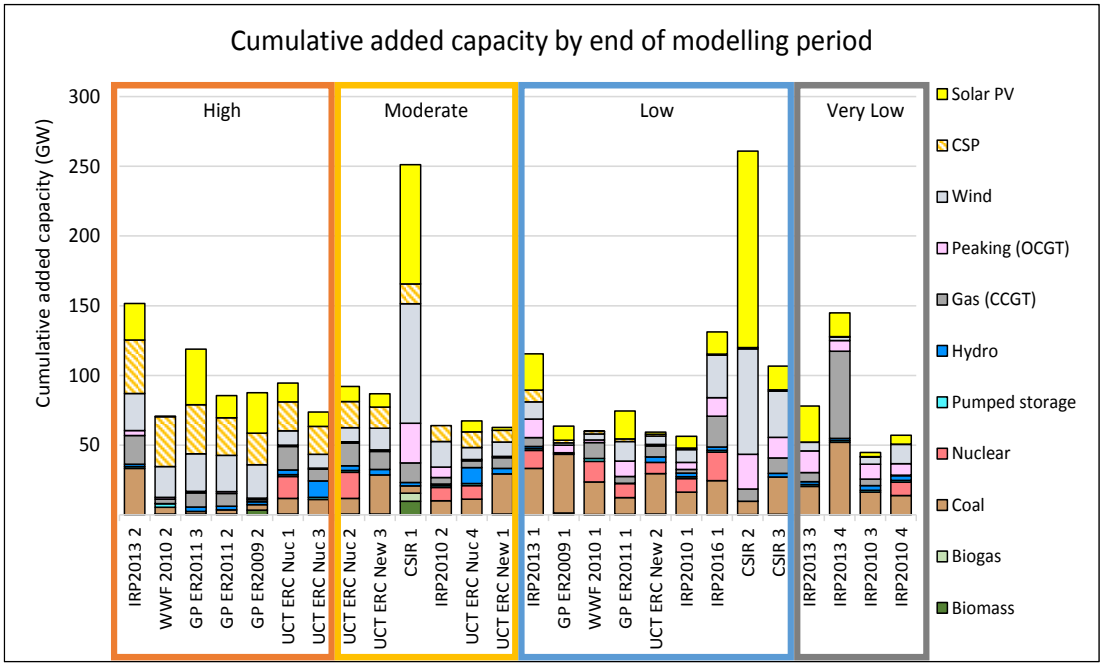

b)

Figure 3. 3: (a) Distribution of capacities allocated to CSP by the end of each scenario's modelling period. (b) Total energy mix by the end of each scenario's modelling period

However, as shown in Figure 3. 4, greater CSP allocations lead to slightly higher system costs when compared to the costs resulting from the other scenarios in the same studies. This is an apparent result of the higher LCOE of CSP, resulting mainly from the current and projected high capital costs. It is furthermore greatly dependent on tariff structures offered by government and bids offered by CSP developers, which are not considered in the modelling. That being said, if the conclusions reached later were systematically implemented, bidding

would be more competitive between CSP developers, and tariffs would be lower, resulting in the desired overall lower system cost-implications by CSP.

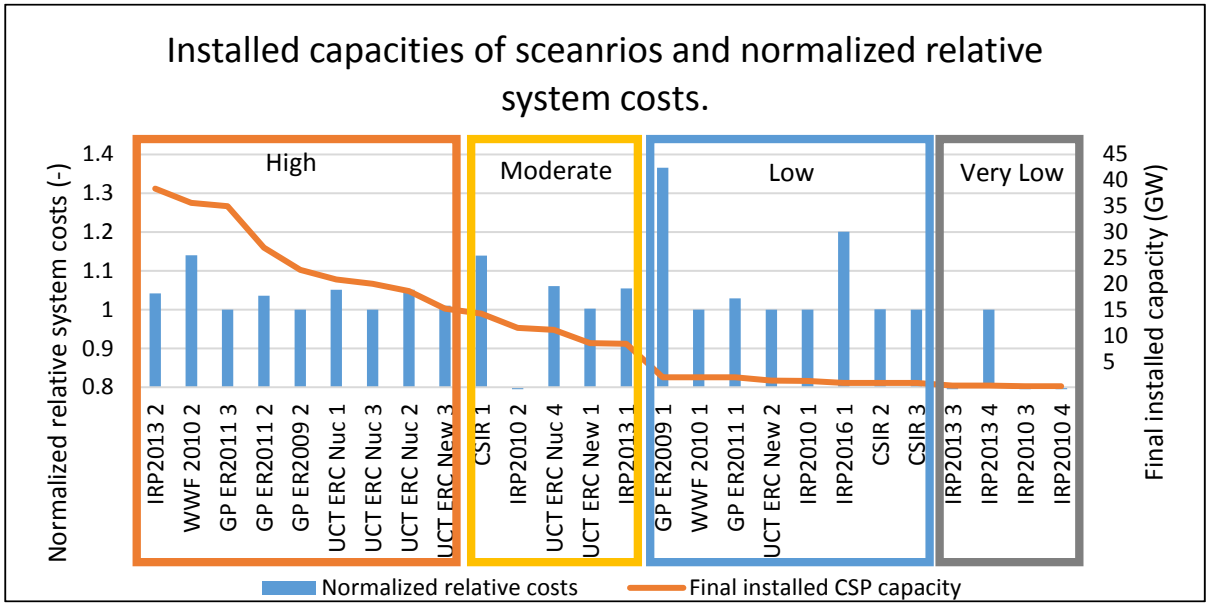

Figure 3. 4: Final installed capacities of each scenario compared to normalized relative system costs.

Greenhouse gas emissions and water consumption are other key considerations for electricity supply planning and modelled energy mixes; to understand the impact of different electricity generation options on natural resources. In all of the studies analysed in this paper, emissions are, however, not used as an optimization parameter, but rather as a limit imposed on the resulting energy mix. For this reason, the presence and magnitude of these limits will be used to analyse impacts on generation technology selections.

The assumptions discussed above can be described as being part of three groups: the attributes of CSP (costs, technical parameters, etc.), the attributes of other electricity generation options (nuclear, coal, PV, etc.), and the attributes of the system itself. When considering the results of these 26 scenarios, their impact on the capacity allocated to CSP cannot be taken in isolation, but need to be addressed as a group. There is very little to no mathematic correlation when, for example, plotting the final CSP capacities against final projected system demand, or any other assumed input parameter. This is because while one assumption in a scenario might be advantageous to CSP (like strict CO_2 limits), another might favour nuclear or PV (lower nuclear costs or lower projected demand growth).

For this reason, the assumptions identified as key driving forces of CSP development/inhibition, are CSP capital costs (relative to alternative generation options; in particular PV and nuclear), CSP learning rates (total reduction over modelling period), demand (final system demand at end of modelling period), meeting greenhouse gas emission reduction targets (final CO_2 emissions goal by end of modelling period) and the inclusion of scenario-specific assumptions of other electricity generation options. For this reason, the parameters used to compare the scenarios' were plotted on radar graphs. Since radar graphs can only compare values of the same scale or order to each other, the values are normalized as far as possible.

The maximum CSP CAPEX refers to the initial overnight capital costs reported in the studies and is compared to the initial CAPEX of PV and nuclear to illustrate the relative cost of CSP

used in the model (higher values indicate that CSP is comparatively more expensive). The cost reduction reported is the total reduction due to learning used in the model, normalized to the average of all the different scenario cost reductions (higher values indicate greater cost reductions). The end-of-period demand is normalized to the minimum demand projected for all the scenarios considered from all studies, thereby giving an idea as to how many times the demand for a certain scenario is greater than the lowest projected demand (higher values indicate greater projected demands). The end-of-period CO_2 emissions limit of each of the scenario are normalized to the average CO_2 emissions limit set for the last year of modelling of all the scenarios considered (higher values indicate more relaxed limits on CO_2).

Figure 3. 5 shows that each of the CSP development cases has different development paths or rates at which CSP is added to the generation fleet. This is partly due to further assumptions, such as decommissioning schedules of existing fleets, carbon emission reduction target years, and projected demand growth rates. Some of the development paths seem to increase too rapidly, but this is due to time-resolution differences between the original report (reporting, for example, every 1 year) and the resolution used for this report (every five years after 2020).

From the High CSP Development Cases, it can be seen that greater technology cost reductions and higher greenhouse gas emission reduction targets to aid in driving the more rapid adoption of CSP into the energy mix. The only exceptions are the three UCT scenarios, which do not report in their published studies that any limits are placed on CO_2 emissions in their models, hence the apparent high levels of CO_2 allowed.

From the Moderate CSP Development Cases, it is clear that the assumption resulting in the slightly lower adoption of CSP is primarily cost-related, with higher CSP/PV and CSP/nuclear costs being used in the models, with generally less strict CO_2 limits placed on emissions. The CSP/PV cost that appears to exceed the maximum bound of the radar graph is that of the CSIR response to the IRP2016, which assumes the highest overnight capital cost for CSP at around 131 R/W, and a much lower PV cost of around 9 R/W. Even though CSP is much more capital intensive in these scenarios, due to the strict CO_2 limits imposed therein, CSP is allocated a large portion of the energy mix.

From the Low CSP Development Cases, it can be seen that the high comparative cost of CSP/nuclear (or lower cost of nuclear compared to CSP) results in CSP being allocated a smaller portion of the generation mix over the modelling period. Here it should also be said that the three cases with the highest final CSP capacities (the two Greenpeace and WWF reference scenarios) appear to not have been optimised as is the case for the IRPs, and CSIR- and UCT studies, since they aim to serve as a projected simulation of the current trends in the electricity generation sector, as brought forward in previous Eskom build plans and the original IRP2010. It is therefore insightful to note that the CO_2 limits have been removed for these scenarios, resulting in lower CSP capacities required, since emissions reductions are not prioritized. It is important to note that the IRP2016 falls in this group, with no CSP learning and very high comparative costs assumed.

In the graphs showing the Very Low CSP Development Cases, the first noticeable characteristic is that there are only four scenarios (out of a total of 26) It is also important to note that maximum end-of-period capacities allocated to CSP have already been surpassed by the current actual installed, and under-construction, CSP projects in South Africa, totalling 500 MW by end-2018. The four of these scenarios form part of the IRP2013 and IRP2010 studies, where very specific conditions are tested, namely a carbon tax instead of CO_2 limits for “IRP 2013 3”, large regional and local gas developments for “IRP 2013 4”, very low economic growth and thus low electricity demand in “IRP 2010 3” and finally high coal and gas costs (with consistently high CSP/PV and CSP/nuclear costs) in the “IRP 2010 4”.

The future electricity demand does not appear to influence the CSP potential installed capacity (Figure 3. 5) as demand is met by the supply mix in all studies and scenarios examined. The opinion of the author is that if the other driving forces were more favourable to CSP (lower CAPEX costs and greater reductions, and stricter CO_2 limitations), irrespective of future demand, CSP would play a greater role in the energy mix. Mention should also be made of the importance of not forcing any annual new-build capacity restrictions on any technology. This was done in all the IRPs, where PV and wind are restricted to 1000 MW/a, and 1600MW/a, respectively. In the initial IRP2010, restrictions were also imposed on CSP, to the order of 500 MW. Since no restrictions are imposed in any of the other studies, they are not used as a basis of comparison.

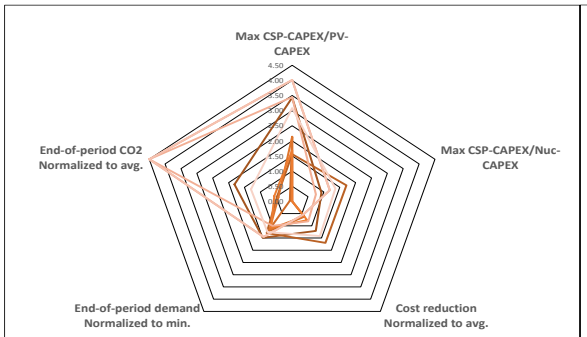

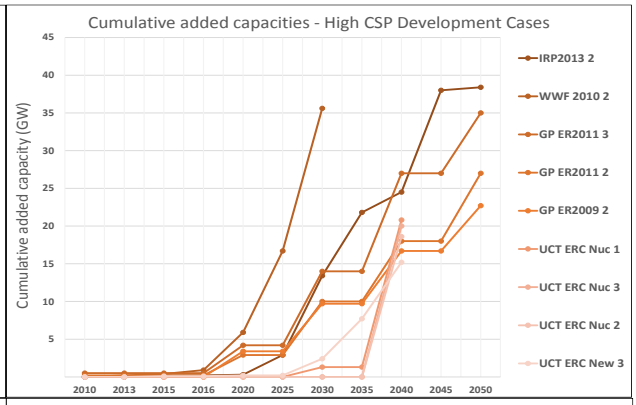

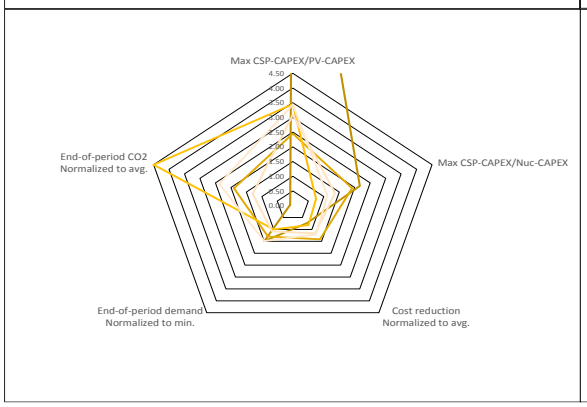

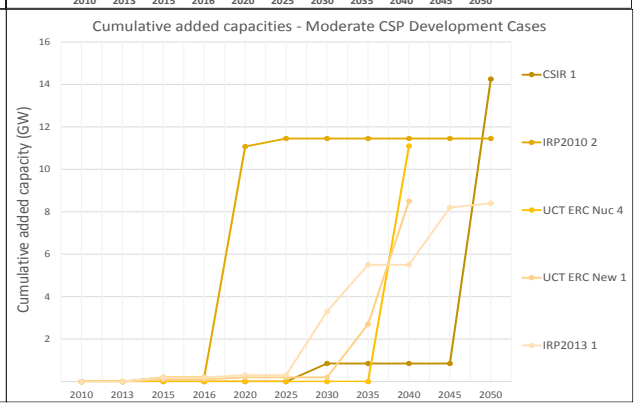

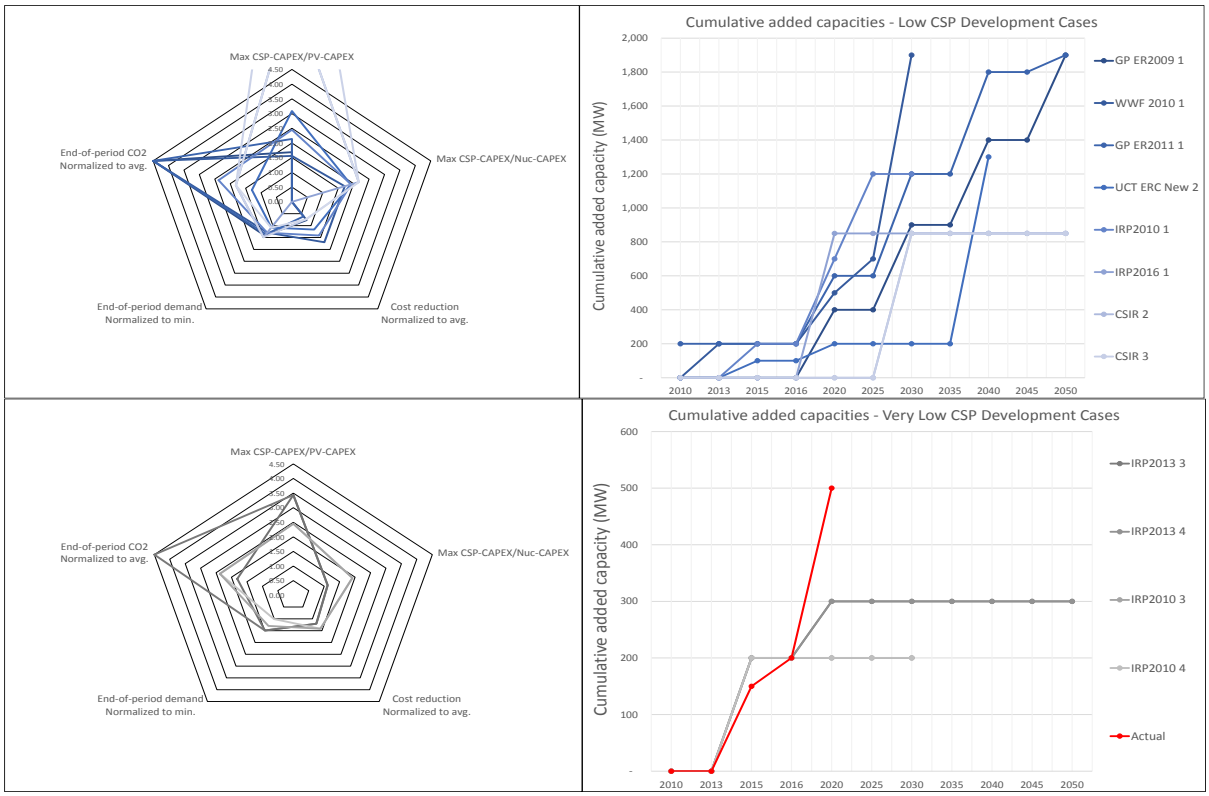

Figure 3. 5: Radar graphs of key drivers and CSP build plans over modelling period for all CSP development cases.

3.5. Conclusions

This work provided an analysis of all of the most relevant energy mix studies for South Africa in light o the Integrated Resource Plans used by the national government to determine which power generation technologies should be included to meet future national electricity demands. Focus was placed on the role that CSP plays in these future energy mixes and which assumptions and model inputs serve as drivers for its inclusion. Furthermore, the results served as an indication of whether the amounts of CSP in the South African power sector are likely to increase, and as such, if there is a valid need to assess the role water resource availability will play in its deployment.

It was found that there are four groups of scenarios for CSP inclusion in the end-of-model period, with certain model inputs and assumptions influencing its inclusion, or prohibiting it. The maximum installed capacities for these four groups were 38,000 MW, 15,000 MW, 2,000 MW and 500 MW. Since there are already 500 MW of installed capacity currently operational in South Africa, it was concluded that the main planning mechanism used for the power sector in South Africa, the IRP, can allow for CSP to grow, depending on:

- The accuracy and relevancy of assumptions relating to techno-economic characteristics of CSP used in the models,
- The way CSP's assumptions compare to other technologies under consideration,

- The climate change goals aimed for in the model, and
- The socio-economic and political agendas that are enforced in the model, outside of the techno-economic merits of each technology.

For energy system modelling, however, it must be emphasized that the models and associated input parameters and assumptions must be as impartial as possible. Modelers need to not only ensure the most realistic technology and demand assumptions are made but also guarantee that least-cost technology selections by the model are the primary driver for selection, preventing modeler bias, and leaving the model and its results "technology-agnostic". This is crucial, since future expansion plans must be based on scientific, objective model results, combined with strategic policy determinations, to ensure new-build options selected do result in the lowest system-costs for the end-consumer.

.

Table 3. 3: Appendix A – Summary of all studies and scenarios assessed

Short name	Study	Scenario name	Brief description
IRP 2013 2	IRP 2013	High Nuclear Cost	Investigated impact of higher nuclear costs on energy mix.
WWF 2010 2	WWF - 50% by 2030 (2010)	Alternative	Investigates the impact of pushing for an energy mix with 50% renewables by 2030.
GP ER 2011 3	Greenpeace Energy Revolution 2011	Advanced Energy Revolution	Aims to reduce carbon emissions to 80% below 1990 levels by 2050.
GP ER 2011 2	Greenpeace Energy Revolution 2011	Energy Revolution	Aims to reduce carbon emissions to 50% below 1990 levels by 2050.
GP ER 2009 2	Greenpeace Energy Revolution 2009	Energy Revolution	Aims to reduce carbon emissions to 54% below 1990 levels by 2050.
UCT ERC Nuc 1	UCT ERC Nuclear build plan technical report	Future 1 - Flexible Build Plan	"Best case for nuclear" conditions; high demand, low nuclear costs and higher RE costs, with a flexible build plan.
UCT ERC Nuc 3	UCT ERC Nuclear build plan technical report	Future 2 - Flexible Build Plan	"Worst case for nuclear" conditions; low demand, high nuclear costs and lower RE costs, with a flexible build plan.
UCT ERC Nuc 2	UCT ERC Nuclear build plan technical report	Future 1 - Committed Build Plan	"Best case for nuclear" conditions; high demand, low nuclear costs and higher RE costs, with a committed nuclear build plan.
UCT ERC New 3	UCT ERC New power plan	High Demand, Shale, and Optimistic RE	Explore impact of higher demand, greater local and regional shale gas developments and aggressive RE learning rates.
CSIR 1	CSIR response to IRP	Decarbonized Scenario	Response to IRP2016, part of public participation process. Aims to reduce CO_2 emissions by 90% by 2050.
IRP 2010 2	IRP 2010	Emissions 3 Scenario	Strict CO_2 emissions limits imposed on electricity sector (220 MT/a from 2020 onwards)
UCT ERC Nuc 4	UCT ERC Nuclear build plan technical report	Future 2 - Committed Build Plan	"Worst case for nuclear" conditions; low demand, high nuclear costs and lower RE costs, with a committed nuclear build plan.

Short name	Study	Scenario name	Brief description
UCT ERC New 1	UCT ERC New power	New Power Plan	Aims to provide a new power plan as an alternative to the IRP 2013, with updated input assumptions.
IRP 2013 1	IRP 2013	Base Case Scenario	Aims to provide a base case scenario with lowest system costs for national planning.
GP ER 2009 1	Greenpeace Energy Revolution 2009	Reference Scenario	Reference scenario for comparing 50% RE against. Based on latest (2007) Eskom builds plans and energy sector conditions.
WWF 2010 1	WWF - 50% by 2030 (2010)	Reference Scenario	Reference scenario for comparing 50% RE against. Based on 2007 Eskom builds plans and energy sector conditions.
GP ER 2011 1	Greenpeace Energy Revolution 2011	Reference Scenario	Reference scenario for comparing 50% RE against. Based on the IRP2010 Policy Adjusted scenario.
UCT ERC New 2	UCT ERC New power	Cheaper Nuclear	Explores the impact of lower nuclear costs on the energy mix.
IRP 2010 1	IRP 2010	Policy Adjusted Scenario	Serves as the basis for current ministerial determinations and national build plans.
IRP 2016 1	IRP 2016	Base Case Scenario	The proposed update to IRP 2010, also to serve as the basis for new ministerial determinations and national build plans.
CSIR 2	CSIR response to IRP	Least cost with expected costs	Response to IRP2016, part of public participation process. Updated cost input parameters for RETs and is cost-optimal.
CSIR 3	CSIR response to IRP	Base Case with low demand	Response to IRP2016, part of public participation process. Same input parameters as IRP2016, with lower demand.
IRP 2013 3	IRP 20133	Carbon Tax Scenario	Investigate the impact of removing CO2 limits and imposing a stricter carbon tax on the electricity sector.
IRP 2013 4	IRP 2013	Big Gas Scenario	Investigate the impact of greater local and regional gas developments on energy mix.
IRP 2010 3	IRP 2010	Low Growth Scenario	Investigates appropriate energy mix associated with lower economic growth.
IRP2010 4	IRP 2010	Peak Oil Scenario	Investigates appropriate energy mix associated higher coal and gas costs.

Chapter 4 – Concentrating Solar Power Potential in South Africa – an Updated GIS Analysis

4.1. Introduction

Global interests in CSP is said to grow with 87% by 2021 [19], with South Africa likely to undergo various possible development scenario', as shown in Section 3. The approach applied in literature for determining potential CSP capacities for a region or country typically follows a generic tiered approach using geographical information systems (GIS). First, certain spatial zones within a region are removed from consideration based on explicit exclusion criteria, while others are regarded as more suitable based on preferred inclusion criteria. Thereafter, considerations are made for distance to and from required supporting infrastructure, such as the electrical transmission network, roads and water sources. Once these limits have been implemented, suitable zones are then identified within the respective region or country.

Second, the CSP potential of these suitable zones are then calculated based on assumptions regarding Land Use Efficiencies (LUE, %) or Power Densities (km^2/GW). Due to the complex nature of multiple criteria being used, these zones can also be ranked based on certain economic, social or technical criteria according to a multi-criteria decision-making method like an analytical hierarchy process. Third, and finally, the potentials for generation are then aggregated and/or ranked according to administrative borders, or some other spatially explicit boundaries of interest. Once this has been done, estimations can be made of the amount of potential energy that can be generated, based on further assumptions regarding plant capacity factor and location-specific conditions. This method is demonstrated graphically in Figure 4. 1.

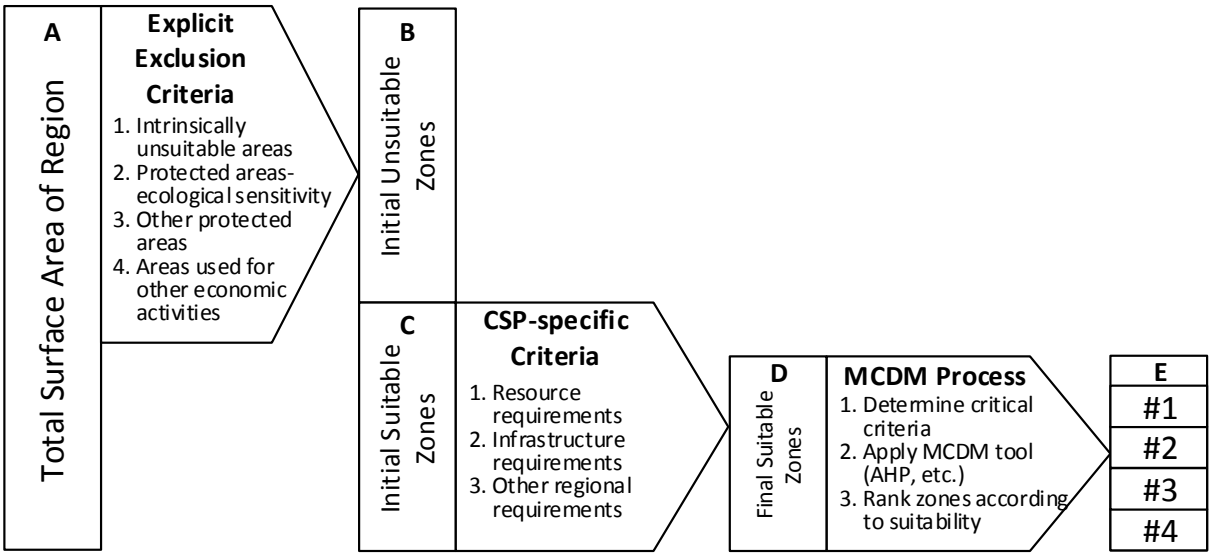

Figure 4. 1: Standard approach for CSP potential studies.

A detailed account of the suitability criteria from various CSP potential studies using the process depicted in Figure 4. 1 is given in Section 5. Apart from CSP with storage, some studies also consider distributed batteries, and their optimal location, based on GIS [194]. The ranking of suitable zones in step E is optional. Typically, after the final suitable zones in Step D, calculations are done to determine the potential CSP capacity associated with those zones. This, of course, requires that certain assumptions are made regarding the CSP technology, the plant configuration and site-specific solar resource (DNI) and meteorological conditions. Finally,

as mentioned before, these capacities, typically in MW installed or total annual MWh, are then aggregated according to user-defined discrete borders, such as administrative boundaries of provinces or districts, economic development areas, or some other definition of interest.

4.2. Suitability criteria and data sources

Before determining whether a certain area is technically suitable for the development of a CSP plant, all explicitly non-suitable areas are to be excluded. These areas generally constitute “no-go” areas for infrastructure development due to intrinsic unsuitability, or because of a conflict of some sort. In the case of SA, these can be grouped into three groups: intrinsic unsuitability, ecological -, and economic conflict.

4.2.1. Exclusion Criteria: Intrinsically unsuitable areas

Since CSP requires large areas of reflective mirror surfaces, typically unsuitable areas include surface water (rivers and dams) and steep slopes. Rivers can be classified based on how their water flows vary seasonally (class) and what order they are within a catchment (1 to 7). The class can be perennial, non-perennial or dry, while the order refers to how many river-branches have joined upstream of a certain river-segment. For example, if Stream A and B converge to form Stream C, but Stream A and B have no converging streams upstream of them, then Stream A, B and C have orders of 1, 1 and 2, respectively. These two classifications are important when deciding which streams can easily be diverted in large, flat catchments, and which cannot. Therefore, streams which adhere to the following classifications have been excluded: Class = Perennial, AND Order >=5. This implies that dry river beds in large flat areas, for example, are considered technically suitable areas, while large perennially flowing rivers with many up-stream converging rivers are not. An arbitrary buffer of 5m was applied to the rivers data file. All dams are excluded, with a 500m buffer around their polygons. The data files for these exclusion criteria are from the Department of Water and Sanitation of SA, and are available online. Figure 4. 2 (a) shows the rivers and dams.

The second most critical technical feasibility criterion for a CSP plant is whether it is physically possible to construct the plant on the ground. The major criterion is slope, or the rate of change in vertical altitude over a certain horizontal distance. This can be expressed in degrees or % change in altitude per horizontal distance. The two existing commercial CSP technologies, Parabolic Troughs (PT) and Central Receivers (CR), are capable of being constructed on surfaces that have a slope of between 1% (0.57^{o}) and 7% (4.00^{o}), relating to a rise of between 1m and 7m over a horizontal distance of 100m [76]. Surfaces with slopes steeper than this range would require intensive civil-works and ground preparation to construct the long rows of mirrors required for PT, or complicate the construction and layout of the thousands of heliostats used to reflect sunlight onto the receiver mounted on a high tower, in the case of CR. The slope used in this study is 3%. A digital elevation model raster file, showing height above sea level, from the South African Environmental Observation Network, was used, with a spatial resolution of 90m x 90m. A slope raster, using the ESRI ArcGIS® Spatial analyst slope toolbox, was generated, shown in Figure 4. 2 (b).

4.2.2. Exclusion Criteria: Unsuitable areas due to ecological conflict

Regarding CSP development, the same basic ecological exclusion criteria apply as to any large infrastructure project. In SA, the following national areas are always considered “no-go” areas: important bird and biodiversity areas, conservation areas, protected areas, and wetlands.

Conservation and protected areas are determined by the national Department of Environmental Affairs under the Protected Areas Act of 2003. These databases contain areas under formal

legislative protection, of which the legal statuses of these areas are audited against official gazettes before inclusion. The inclusion of certain areas into the database is governed by the relevant environmental conventions of the Act and is updated at quarterly intervals. The types of areas considered as conservation or protected include biosphere reserves, botanical gardens, wetlands, forest nature reserves, forest wilderness areas, marine protected areas, mountain catchments, national parks, nature reserves, protected and special nature reserves, and world heritage sites. For wetlands, only those larger than 50ha were excluded, since some dry pans in high DNI areas are classified as wetlands, but are generally smaller and support limited ecologically sensitive biodiversity. Important bird areas (IBA), compiled by Birdlife South Africa, are objectively determined using globally accepted criteria. An IBA is selected based on the presence of the following bird categories: bird species of global or regional conservation concern, assemblages of restricted-range bird species, assemblages of biome-restricted bird species, and concentrations of congregatory bird species [195]. These unsuitable areas are shown in Figure 4. 2 (c).

4.2.3. Exclusion Criteria: Unsuitable areas due to economic conflict

Another basis on which any new large-scale infrastructure development can be excluded from consideration in a particular area is the likely conflict with existing economic activities. In SA, agriculture uses a significant portion of land to support many people's livelihoods and contribute to the economy. In order to determine which areas are not suited to CSP plants because of a conflicting economic activity, the 72-class 2013-2014 South African National Land-Cover Dataset was used, and is a 30x30m raster for the entire SA. This dataset was compiled by Geoterraimage for the Department of Environmental Affairs [196].[6]. Naturally, areas classified as bodies of water were excluded (class 1-2). Indigenous forests were also excluded since special environmental permits are required to clear these for infrastructure developments (4). Cultivated lands with commercial annual rainfed and irrigated crops, commercial permanent crops, and commercial sugarcane crops were excluded due to their high economic value (10,11,13-17,19,20,22,26-31). All forest plantations were excluded (32-34), as well as mine-related bodies of water and buildings (37-39). Finally, all built-up areas were excluded due to conflict with human settlements (42-72). Another type of area excluded from consideration is the area dedicated to the construction and development of the Square Kilometre Array (SKA). This is an international project to build the world's largest radio telescope, with eventually over a million square meters of collecting area (1 km^2). The area within SA which has formally been dedicated to the, is located in the Northern Cape Province, and is shown in Figure 4. 2 (d), along with the other excluded areas from the landcover dataset. This area includes a buffer of 30 km for electrical infrastructure with a rating of greater than 100 kVA, to prevent interference with the sensitive radio telescope equipment [197].

[6] Since the list of excluded classes totals 59, only a brief overview of these shall be given, and readers are invited to review the relevant document, available online, for more detail.

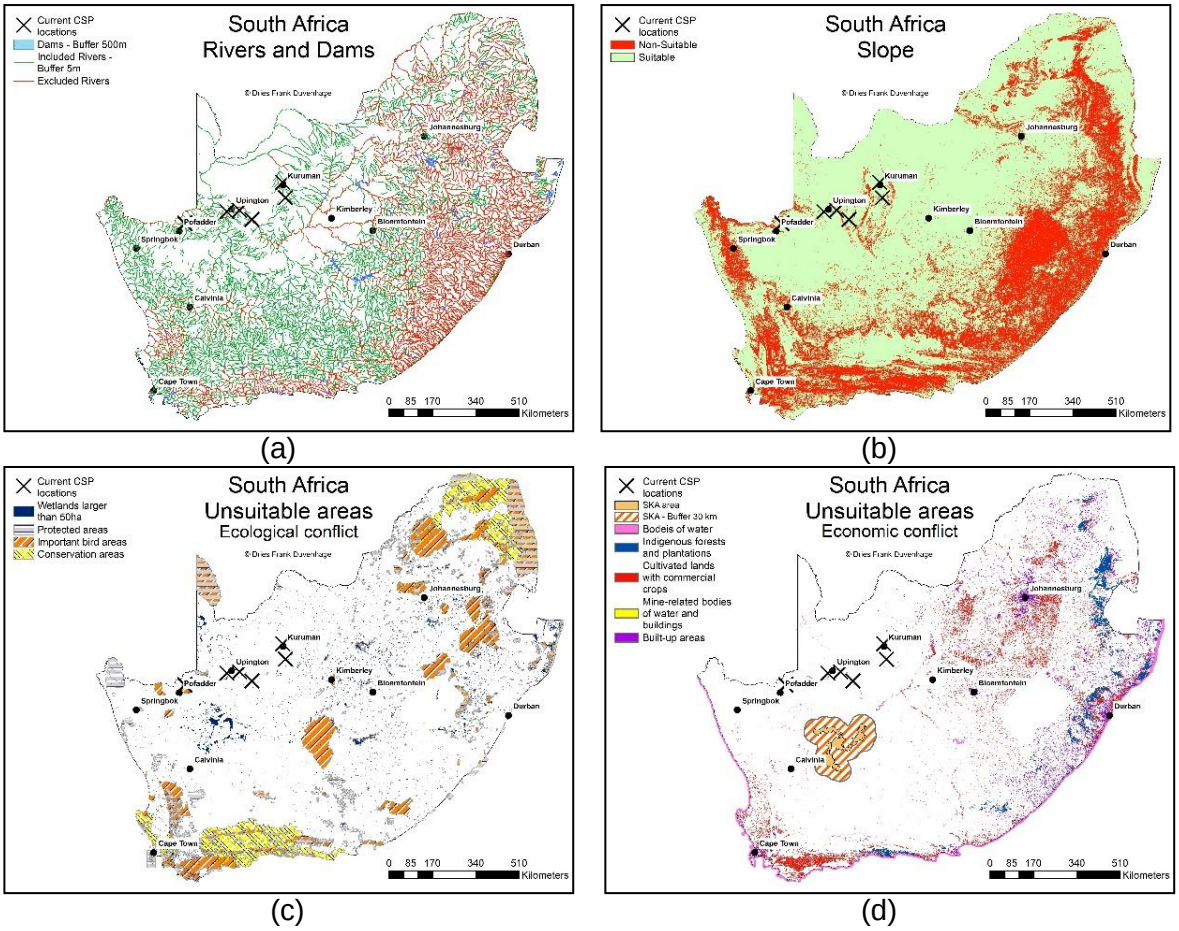

Figure 4. 2: Maps of South Africa showing excluded areas due to A) Rivers and dams, B) Slope, C) Unsuitable areas – Ecological conflict, D) Unsuitable areas – Economic conflict.

4.2.4. CSP-specific Suitability Criteria: DNI

The most critical suitability criteria for the determination of CSP potential is Direct Normal Irradiance (DNI), measured in kWh/m^2 per time period (day, month or year). This is the amount of direct irradiance incident on a surface normal to the direction of the sunrays. The amount of DNI which reaches the earth's surface is influenced by the relative position of the earth to the sun (season and time of day), position on the surface of the earth (elevation, latitude and longitude)and atmospheric conditions (aerosols, dust, water vapor and most importantly clouds) [198], [199]. Since DNI is the primary energy source for a CSP plant, it is the major determining factor of a plant's techno-economic feasibility.

For this reason, the general consensus is that the minimum required DNI is between 1800 and 2000 kWh/m^2/y, with increases in DNI directly related to reductions in cost of generated electricity [200]. The threshold DNI employed in any CSP potential study is relative to the average DNI in the study area. The inclusion of areas with lower DNI, even though it might be equal to or larger than 1800 kWh/m^2/y, will only result in the consideration of areas that are less favourable than others. SA has a minimum, average and maximum DNI of 1290 kWh/m^2/y, 2397 kWh/m^2/y and 3141 kWh/m^2/y, respectively. The annual DNI data source used in this study is from SolarGIS ®, and is a raster file with a spatial resolution of 30 arc-seconds, shown in Figure 4. 3 (a) [201]. Based on the high average DNI of SA, the DNI threshold selected in this study is 2400 kWh/m^2/y.

4.2.5. CSP-specific Suitability Criteria: Distance to required infrastructure

Theoretically, CSP infrastructure only requires suitable land and high DNI to be feasible. However, for this infrastructure to be economically and logistically practical, it must be located near adequate transport, transmission and water-supply infrastructure. In fact, water is the only other natural resource on which CSP depends [3]. The co-location of theoretically suitable areas and man-made infrastructure can be directly due to the development of the CSP infrastructure, or due to independent, existing infrastructure expansion plans. In the case of the former, the costs associated with these infrastructure developments must be added to those of the CSP plant, but not necessarily in the case of the latter.

The same distances to transmission (Tx) infrastructure will be used as in [75], namely less than, or equal to, 20 km. This study did not include consideration for transport infrastructure, since dirt roads are a low-cost option for accessing highly suitable areas. Furthermore, no consideration has been given to proximity to water infrastructure, as was the case in [75], and is not included here; although it is the focus of our current research efforts. This work includes new planned Tx lines in its analysis to explore likely future CSP potential in these areas. The transmission network in SA can be seen in Figure 4. 3 (b), acquired from the national utility, Eskom.

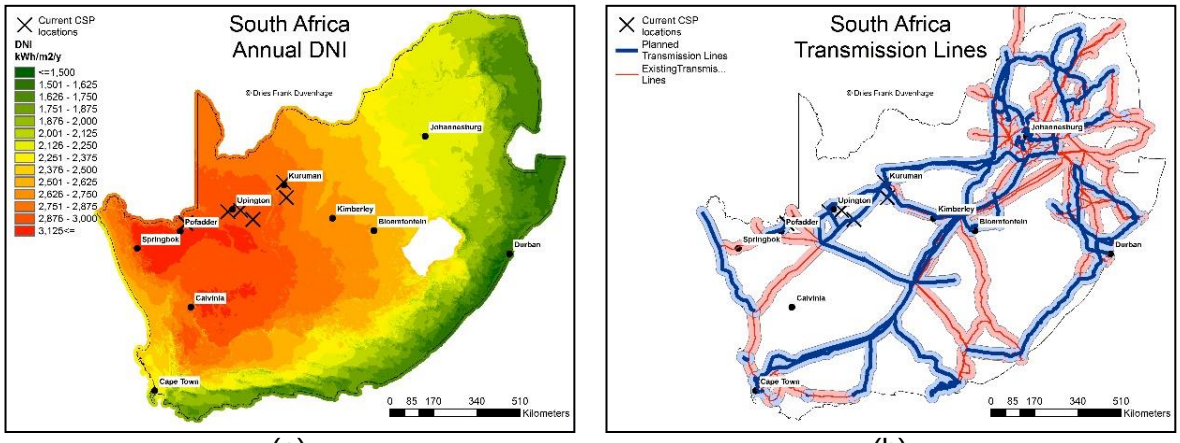

(a) (b)

Figure 4. 3: Maps of South Africa showing CSP-related suitability criteria A) DNI, B) Transmission network.

4.2.6. Suitability conditions at existing CSP plants in SA

In order to align the assumptions used in this work with the actual conditions at existing CSP plants in SA, the available GIS datasets were used to evaluate the locations of these plants. The results are summarized in Table 4. 1 for PT with wet cooling (PTWC) and dry-cooling (PTDC), and CR with wet-cooling (CRWC) and dry-cooling (CRDC).

Table 4. 1: Suitability conditions at existing CSP plants in SA

CSP plant name	CSP + cooling type	Location (decimal degrees)	DNI (kWh/m^2/y)	Slope (%)	km to Exc water body	km to Ecological conflict area*	km to Economic conflict area	km to Tx Line**
Kaxu and Xina	**PTDC**	-28.89, 19.59	2927	1.17	<27	<1 (IBA)	<26	<4(Ex)
Khi Solar One	**CRDC**	-28.54, 28.08	2922	0.58	<11	<12 (wet)	<8	<4(Pl)
Kathu Solar Park	**PTDC**	-27.61, 23.04	2801	0.44	<50	<0.5 (wet)	<7	<9(Ex)
Bokpoort	**PTWC**	-28.78, 21.96	2930	2.44	<2	<5 (wet)	<5	<0.4(Pl)
Illanga	**PTDC**	-28.49, 21.52	2912	2.44	<12	<0.3 (wet)	<11	<31(Pl)
This study	**NA**	NA	>2400	<3.00	5m	NA	NA	<20

* IBA: important bird areas, wet: Wetlands
** Ex: Existing Tx lines, Pl: Planned Tx lines

The DNI in all locations is above 2800 kWh/m^2/y, compared to the generally accepted minimum of 2000 kWh/m^2/y. The slope at these sites varies between 0.4% and 2.5%, hence the use of a maximum acceptable slope of 3% in this study. Generally, the sites are located relatively far from economic exclusion areas. However, they are comparatively close to ecological exclusion zones, due to the emphasis placed on environmental protection and ecotourism by the SA government, and the resulting abundance of such nationally protected areas. It is apparent that the sites are also mostly near to high-voltage Tx lines, and that some of the plants have been built near to those considered “under planning”, indicating that these lines might already have existing by the time the plants were connected to the grid.

4.3. Data processing and potential modelling

4.3.1. GIS data processing

The final aim of this greater project which this work forms part of, is to model monthly CSP operation and water consumption across large geographical areas. To simplify this, SA was divided into a 1x1km grid. Blocks within the grid were then excluded in a systematic manner if they intersected with any of the exclusion criteria. The exclusion reason(s) for a certain block was recorded as attribute data in that block. The result was a grid leaving only suitable blocks, either located near Existing or Planned Tx lines, shown in Figure 4. 4 (a) and (b), respectively. Thereafter, the DNI values intersecting with these suitable areas were stored as attribute data in each block.

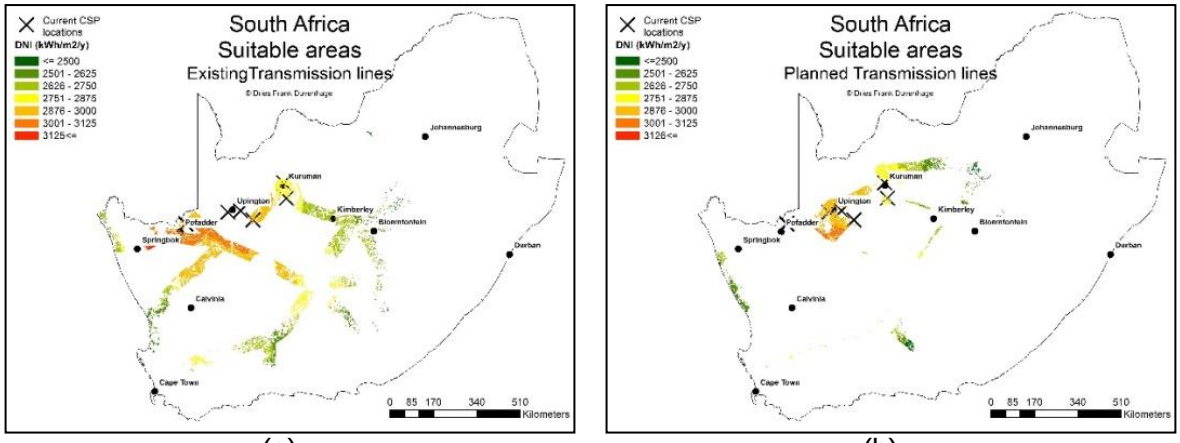

(a) (b)

Figure 4. 4: Maps of South Africa showing suitable areas near A) Existing Tx lines, B) Planned Tx lines.

4.3.2. CSP potential modelling

The potential amount of electrical energy generated from a CSP plant in a specific location depends on the CSP technology configuration in use and the solar resources at that location. The CSP technology configuration used depends greatly on the business model used to generate profit, the tariff structure and various financially driven criteria. However, to determine the theoretical potential at a location, certain high-level assumptions can be made based on the fundamental energy conversions taking place in a CSP plant, and these assumptions can be used to estimate the amount of electricity, in GWh, a CSP plant can generate, based on knowledge of the prospective location's DNI. A common approach is using efficiencies for the energy conversions in a CSP plant. This process was explained in detail, with relevant equations and assumptions, in Section 5 and Section 6. For clarity, the governing equations are given in Equation 4. 1.

Equation 4. 1: Calculation of Annual Net Electricity

$$Q_{ELNET} = LUF \times \eta_{SE} \times DNI \times A \quad \mathrm{Q_{ELNET}} = \mathrm{LUF} \times \eta_{\mathrm{SE}} \times \mathrm{DNI} \times \mathrm{A}$$

Q_{ELNET} represents the net electrical energy (GWh) that is generated, based on the Land Use Factor (LUF) and area (A). LUF refers to the ratio between total footprint and solar field area. The assumptions used in this work, to calculate total annual generation potential, are given in Table 4. 2.The η_{SE} values were determined by modelling the annual operation of a 50 MW PTWC, PTDC, CRWC and CRDC plant, with 9 hrs of storage in the locations of the five existing CSP plants in SA. The annual average η_{SE} was calculated for each configuration and averaged across the five locations, shown in Table 4. 2.

Table 4. 2: Efficiency assumptions used

Parameter description	Symbol	Unit	PTWC	PTDC	CRWC	CRWC
Land Use Factor	LUF	%	28	28	23	23
Solar-to-electric efficiency	η_{SE}	%	14.1	13.7	19.2	18.1

4.4. Results and conclusions

Equation 4. 1 was used to calculate the annual generation potential from the four different CSP and cooling technology configurations for each block in the suitable areas grid. This study calculated the potential for both PT and CR CSP technologies, as well as in combination with wet- or dry-cooling, to reflect the impact that such design decisions will have. In Figure 4. 4, the annual generation potential in GWh is shown for the wet-cooled options for PT and CR, near existing and planned Tx lines, respectively.

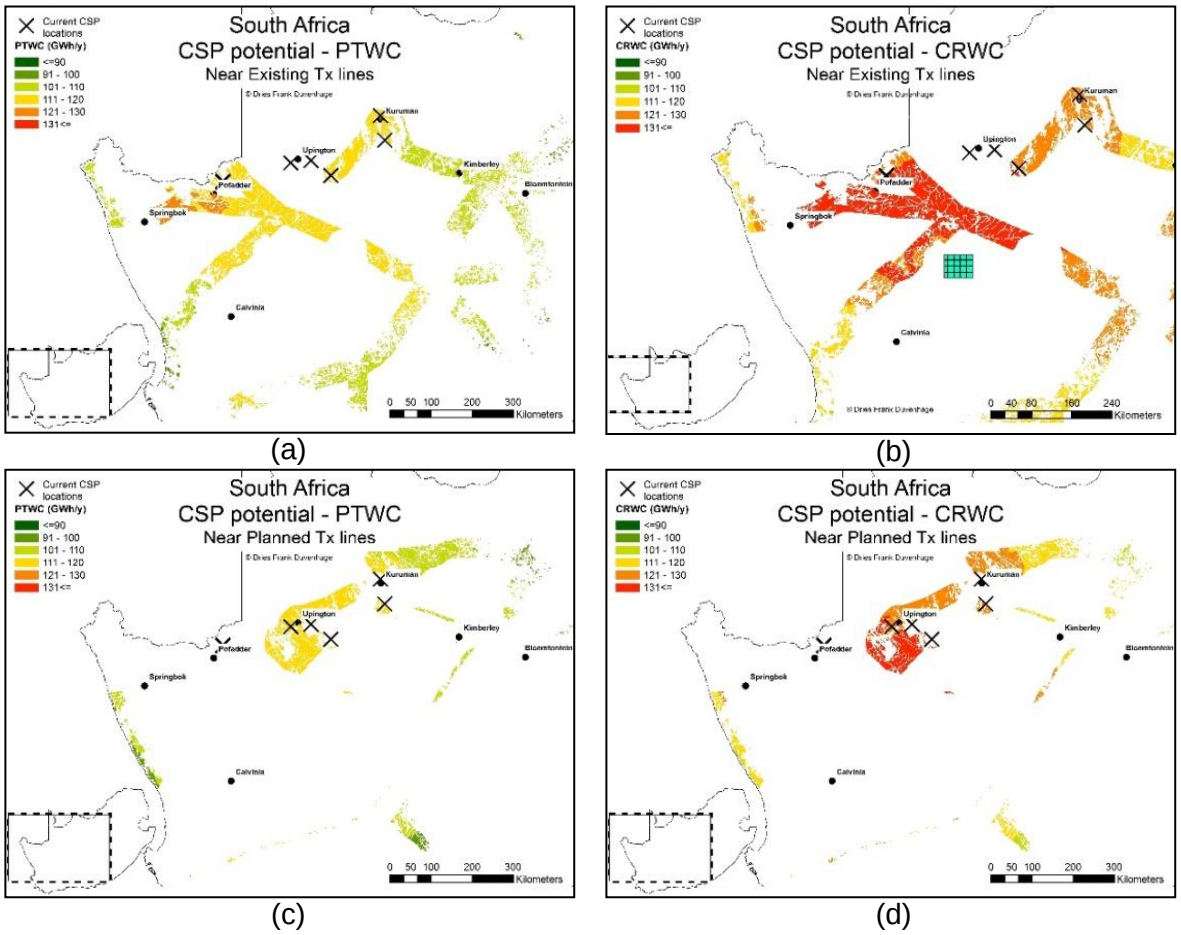

Figure 4. 5: Maps of South Africa showing Annual generation potential from CSP A) PTWC near existing Tx lines, B) CRWC near existing Tx lines, C) PTWC near planned Tx lines, D) CRWC near planned Tx lines.

The higher efficiency of CR plants results in the generally higher annual electricity generation reflected in the colour scale, as shown in Figure 4. 5. The quantitative results are given in

Table 4. 3 shows the theoretical generation potential from CSP, on less than 9% of the total SA surface area, far exceeds the demand for electricity in South Africa. In fact, it would require less than 0.2% of the total SA surface area, or 2% of the identified suitable areas, covered with the least efficient PTDC configuration to generate the annual electricity demand of 231.472 TWh for 2018.This surface area is shown in Figure 4. 5 (b), for a spatial reference. To put this into perspective, the total amount of electricity generated from all RETs in South Africa in 2018 was 10.483 TWh, less than 4.53 % of the 2018 total [202]. The major advantage of CSP, in comparison, is that it is capable of large-scale storage for dispatchable generation. This is a critical benefit over other RETs, since the energy generated (TWh) from CSP can coincide with

when it is needed from the grid, not only with when the resource is available, as is the case for PV and wind. This highlights the priority that countries with high DNI, such as South Africa, could give to CSP in replacing fossil fuels (coal, diesel and natural gas) in the electricity supply mix, and to assist in transitioning to a cleaner energy mix dominated by renewables.

Table 4. 3: Summary of CSP potential results in identified suitable areas

Transmission line	**Area (km²)**	**PTWC (TWh/y)**	**PTDC (GWh/y)**	**CRWC (GWh/y)**	**CRWC (GWh/y)**
Existing	71,457	7,978	7,752	8,924	8,413
Planned	33,252	3,668	3,568	4,102	3,866
Total	104,709	11,646	11,320	13,026	12,279
% SA Total	8.59	5,031	4,890	5,627	5,305

SA area: 1,221,037 km². SA 2018 electricity demand: 231.5 TWh, [203]

This work, therefore, provided an updated appraisal of the theoretical potential for CSP in South Africa, based on best-practice suitability criteria from literature, as well as from existing CSP plants in South Africa. While it was pointed out that the theoretical potential of CSP in South Africa, based solely on the suitability criteria and solar irradiance, far exceeds that of the national annual demand, it must be pointed out that no consideration was given to water resources as a critical suitability limitation. This was intentional since this CSP potential study will serve as the first step to quantifying the limits imposed by water resources on the theoretical potential for CSP. The main goal of this work is to have results for suitable CSP locations at a high spatial resolution in order to assess the potential demand for water from CSP. This is critical in light of the fact that water resources' availability vary spatially, and are impacted at local levels. Therefore, these theoretical locations for CSP will serve as the primary factor for where, and which, resources must be evaluated when considering the limit they might place on CSP generation and deployment potential.

Chapter 5 – Water and CSP – a preliminary methodology for strategic water demand assessment

5.1. Introduction

There have been many studies to determine the amount of potential CSP capacity in a region or country. Understandably, these studies look at the solar resource (DNI) as a primary criterion, accompanied by other land-suitability criteria, summarized in Table 5. 1[7]. From Table 5. 1, it is clear that very little consideration is given to the availability of water for the demands from CSP plants. Certain reports mention the scarcity of water as a potentially limiting factor [137], [204]. However, they then simply proceed to state that dry cooling will address this issue. Although the demands from dry-cooled CSP plants are around 90% less than wet-cooled plants [4], water is still a prerequisite for its successful operation.

It therefore follows that, when determining the CSP potential of any region, not only must the proximity of a potential CSP site to water be considered, but attention must be given to the ability of regional water sources to supply the demand from CSP plants at these sites [3]. Furthermore, when the consumption rate of CSP plants is mentioned in the above studies, crude approximations of different CSP and cooling technology combinations are used. These take the form of over-simplified consumption factors, such as 3.27 m^3/MWh or 3274 L/MWh, mentioned in [75] and [81], respectively. While [75] does briefly mention the need for more detailed consideration of the limits placed by water availability on CSP potential, no study has done this quantitatively.

Hence, this paper aims to present a structured methodological framework, for the case of South Africa. However, it is argued that the framework is reproducible in any region where CSP is considered viable. The framework can then be used to assess potential water demand from CSP and identify constraints placed on potential sites due to water availability.

5.2. Methodology

The approach used to assess spatiotemporally varying water demands from CSP consists of the following fundamental steps:

1. Determine suitable areas for CSP based on solar resource and land suitability criteria.
2. Evaluate monthly generation potential based on CSP technology selection and design, and impact of ambient conditions on cycle efficiency.
3. Evaluate monthly consumption factor for each identified area based on cooling and CSP technology selection and design, and impact of ambient conditions.

Hereafter, CSP fleet deployment scenarios can be evaluated in order to determine the impact of water resource availability on CSP plants, and vice-versa. Such an assessment is part of on-going.

[7] The table in this publication is the exact same table as in Chapter 2 (Table 2.1), since this publication followed the previous one, and based much of the work thereon. It was included in the final paper submitted to SolarPaces 2018 for completeness, but is omitted here to prevent duplication. The references will follow chronologically.

5.3. CSP Area Suitability Assessment

Table 5. 1 provides a detailed list of the various suitability criteria used in previous CSP potential assessments. These criteria are then used to create exclusion and inclusion layers in Geographical Information Systems (GIS). After all the layers have been generated and the required actions have been performed (merging, dissolving, cutting etc. of layers), a final result is produced showing the suitable areas. The particular details of the applied method can be found in Section 4. The results from this detailed, updated CSP capacity analysis of South Africa was used in this paper. It employed the suitability criteria listed in.

Table 5. 1: CSP suitability criteria in this study

Criteria	**Selected value (buffer in km)**	**Information Source**
Minimum DNI	2400 kWh/m^2/y	[201]
Maximum Slope	4 %	[205]
Minimum area	3km^2	NA
Excluded areas (buffer in brackets)		
Formal protected and conservation areas[a]	Yes (0)	[206] EGIS updated
Sensitive bird and biodiversity areas[a]	Yes (0)	[195]
Indigenous forests[b]	Yes (0)	[196]
Wetlands[b]	Yes (0)	[207]
Dams[b]	Yes (0)	[125]
Rivers[b]	Yes (0)	[125]
All Cultivated Lands (Except low-yield and subsistence) [b]	Yes (0)	[196]
All Forest Plantations[b]	Yes (0)	[196]
All built-up areas[b]	Yes (0)	[196]
All Mining activities[b]	Yes (0)	[196]
Square-kilometre array[a]	Yes (37)	[personal communication]

a – Indicated as “Miscellaneous” on map.
b – Indicated as “Landcover” on map.

For the purposes of this study, distance to infrastructure, such as roads and transmission networks, were not considered. The rationale is that since the focus is on water resources and its consumption, the maximum possible ceiling thereof must be evaluated. This requires consideration of all possible suitable land, based on natural resources. A minimum DNI of 2400 kWh/m^2/y, avoiding the unnecessary consideration of lower-yield areas. Further, a detailed list of exclusion criteria was used from various sources, to ensure flat, high-DNI areas that coincide with any inherently unsuitable, or ecologically sensitive areas, were not considered. The resulting suitable areas, based on the criteria and rationale above, are shown in Figure 5. 1. They consist of a grid of 1km x 1km squares that indicate areas that are suitable, and those that are not. Suitable areas have also been graded according to the annual DNI.

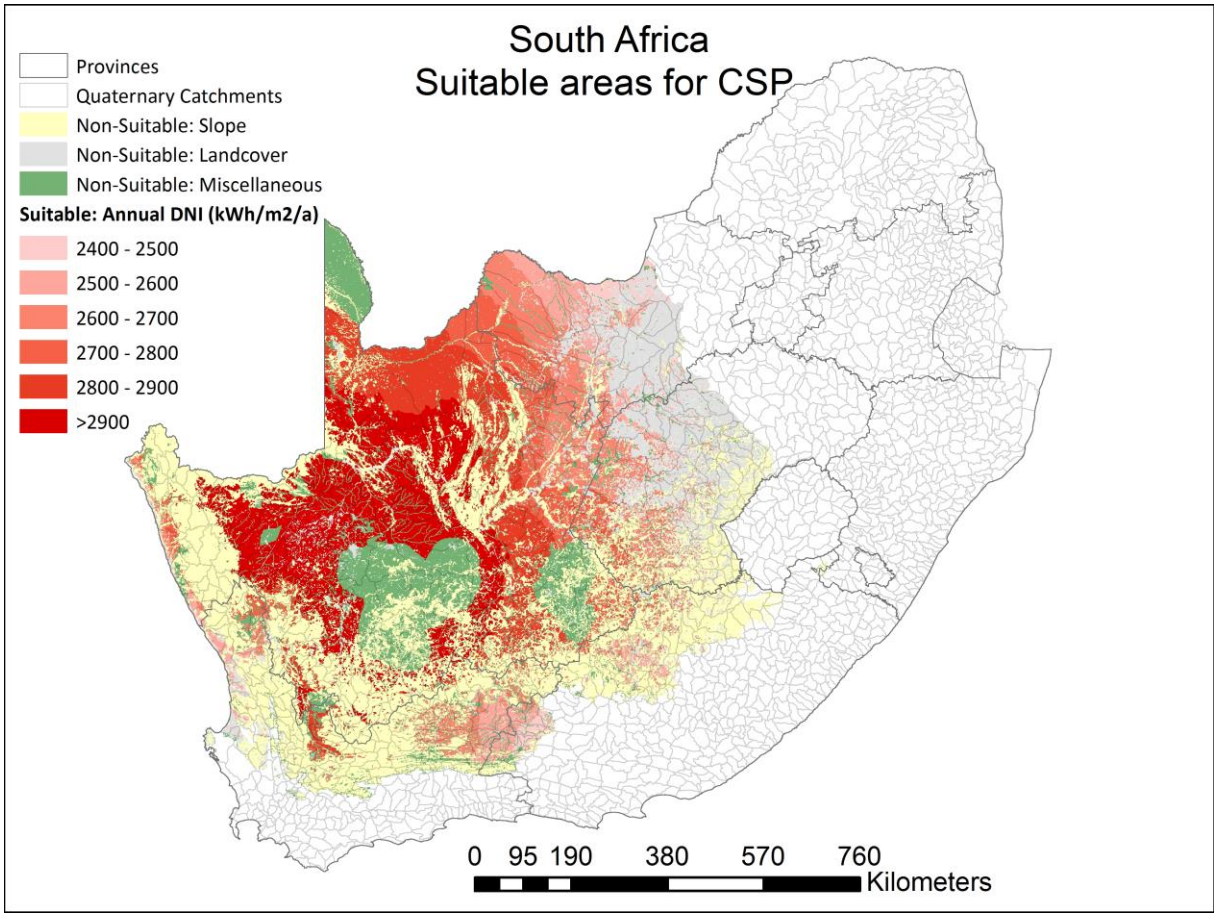

Figure 5. 1: CSP suitable areas

5.4. Monthly Generation Potential

In South Africa, hydrological planning takes place at four levels of detail, based on river basins, from primary to quaternary catchments [208]. These quaternary catchments (QCs) are shown in Figure 5. 1. To evaluate water demand, and ultimately availability too, it therefore makes sense to do so at the same geographical scale at which other hydrological planning is done within a region or country. Accordingly, the total CSP generation potential of the suitable areas identified above, per QC, can be evaluated.

To do so, a similar approach to that of [209] was used. The approach uses the following definitions, in Equation 5. 1 to Equation 5. 3, to calculate potential monthly generation: solar-to-electric efficiency ($\eta_{SE}\eta_{SE}$), annual net power generation (Q_{El})Q_{El}), annual direct irradiance on aperture area (DNI), land use factor (LUF), aperture area of reflectors ($A_{SF}A_{SF}$), total land area required (A_{Tot})A_{Tot}), and land use efficiency (LUE).

Equation 5. 1: Definition of solar-to-electric efficiency

$$\eta_{SE} = \frac{Q_{El}}{DNI}\eta_{SE} = \frac{Q_{El}}{DNI}$$

Equation 5. 2: Definition of Land use factor

$$LUF = \frac{A_{SF}}{A_{Tot}}LUF = \frac{A_{SF}}{A_{Tot}}$$

Equation 5. 3: Definition of Land use efficiency

$$LUE = \eta_{SE} \times LUF \; LUE = \eta_{SE} \times LUF$$

Average land use factors for parabolic troughs (PT) and central receiver (CR) systems were calculated from the NREL database on global CSP projects as 25% and 17%, respectively [210]. The solar-to-electric efficiency is calculated separately for wet-cooled (WC) and dry-cooled (DC) PTs and CRs, based on the simplified method presented in [27], and shown in Equation 5. 4.

Equation 5. 4: Calculation of solar-to-electric efficiency based on composite terms

$$\eta_{SE} = \eta_{optical} \times \eta_{receiver} \times \eta_{power} \eta_{SE} = \eta_{optical} \times \eta_{receiver} \times \eta_{power}$$

Here, $\eta_{optical}$ represents the annual average optical efficiency of the collector area. For PT plants, this value has been shown to be in the order of 59.8%, and for CR plants in the order of 56.3% [211]. The relationship between the energy absorbed by the receiver and that which is transferred as thermal energy to the HTF, is represented by the annual average receiver efficiency, $\eta_{receiver}$. These values are around 85.2% and 83.1% [211], for PT and CR plants, respectively. The power cycle efficiency, η_{power}, is a composite term representing all losses and efficiencies between the absorbed energy in the solar field and the final generation of electricity, in Equation 5. 5.

Equation 5. 5: Calculation of thermal to electric efficiency based on composite terms

$$\eta_{power} = \eta_{PAR} \times \eta_{PIP} \times \eta_{STOR} \times \eta_{AV} \times \eta_{B} \times \eta_{ST} \eta_{power} = \eta_{PAR} \times \eta_{PIP} \times \eta_{STOR} \times \eta_{AV} \times \eta_{B} \times \eta_{ST}$$

In this study, values from various literature sources were used, and are summarized in Table 5. 2. The steam cycle efficiency (η_{ST})η_{ST}) is the component of the power cycle efficiency, which is most dependent on cooling technology and ambient conditions, especially for dry-cooled plants [212]–[215]. In order to reflect this spatially varying dependence in the modelling, the steam cycle efficiency was quantified according to the Chambadal-Novikov cycle efficiency [216], [217]. This method has been shown to be suitable in high-level modelling of CSP operation [26], [218], [219].

Table 5. 2: Annual Average power cycle efficiency composites

CSP+cooling configuration	Efficiency component	Value (%)	Description and rationale	Source
PTWC	Parasitic/auxiliary losses (η_{PAR})	89.0	Efficiency resulting from parasitic losses.	[220]
PTDC	Parasitic/auxiliary losses (η_{PAR})	86.0	Lower efficiency resulting from higher parasitic losses due to fans.	[220]
PTWC/DC	Piping thermal losses (η_{PIP})	96.7	Efficiency resulting from thermal losses from the solar field header and HTF piping.	[221]
PTWC/DC	Storage thermal losses (η_{STOR})	99.6	Efficiency resulting from thermal losses from the thermal storage system.	[221]

CSP+cooling configuration	Efficiency component	Value (%)	Description and rationale	Source
PTWC/DC	Power plant availability (η_{AV})	94.0	Efficiency resulting from forced and scheduled outages and dumping.	[221]
CRWC	Parasitic/auxiliary losses (η_{PAR})	92.2	Efficiency resulting from parasitic losses.	[222]
CRDC	Parasitic/auxiliary losses (η_{PAR})	91.5	Lower efficiency resulting from higher parasitic losses due to fans.	[222]
CRWC/DC	Piping thermal losses(η_{PIP})	99.9	Efficiency resulting from thermal losses from the solar field header and Salt piping.	[221]
CRWC/DC	Storage thermal losses (η_{STOR})	99.5	Efficiency resulting from thermal losses from the thermal storage system.	[221]
CRWC/DC	Power plant availability (η_{AV})	94.0	Efficiency resulting from forced and scheduled outages and dumping.	[221]
PT/CRWC/DC	Boiler losses (η_B)	99.7	Losses in steam generating system	[222]

The Chambadal-Novikov cycle efficiency takes the form of Equation 5. 6, where T_L is determined by the cooling technology in place and ambient conditions. T_H is the temperature of the steam entering the turbine(s) and depends on the load at which the CSP plant is operating and the CSP technology in place. In this study, T_H is defined as 371^{O}C for PT [223] and 540 ^{O}C for CR [222]. T_L is defined as the dry-bulb temperature plus an effective approach of 25^{O}C for dry-cooled plants, and as the wet-bulb temperature plus an effective approach of 10^{O}C for wet-cooled plants [224]. This value is added to ambient temperatures to reflect heat-exchange effectiveness for the different cooling technologies and is dependent on cooling system design as well as ambient conditions. This value should be approximated more closely, but such a detailed approach is beyond the needs of this study. Steam cycle efficiencies calculated in this way are generally 5-8% lower for PT plants and 2-6% lower for CR plants, than reported cycle efficiencies in [222] and [223], and therefore provides a conservative estimation of power generation for CSP plants. Wet-bulb temperatures are calculated based on available dry-bulb temperatures and relative humidity, according to the formula derived in [225].

Equation 5. 6: Calculation of Chambadal-Novikov cycle efficiency

$$\eta_{ST} = 1 - \sqrt{\frac{T_L}{T_H}} \eta_{ST} = 1 - \sqrt{\frac{T_L}{T_H}}$$

The final annual solar-to-electric efficiencies for the four CSP+cooling configurations have the following ranges, depending on ambient conditions: 12.13% to 12.97% for PTWC, 11.36% to 12.53% for PTDC, 15.02% to 15.75% for CRWC and 14.58% to 15.49% for CRDC, respectively. These values correspond well with those in literature [204], [221], [222], [226], [227]. It is, however, known that larger installed net capacities result in higher solar-to-electric efficiencies [220]. Based on the above equations, the final monthly electrical generation potential (Q_{tot})Q_{tot}) for each suitable 1 km x 1 km grid (A_{km2}) A_{km2}) can now be calculated according to Equation 5. 7. Hence, $A_{km2}A_{km2}$ equals 1 square kilometre, or 1,000,000 m^2. The total potential per QC can then be calculated. Long-term monthly DNI values were calculated from satellite derived data between 1983 and 2013, as provided by [228] and validated in [229].

Equation 5. 7: Calculation of total net electricity generation

$$Q_{tot} = LUE \times DNI \times A_{km2} \; Q_{tot} = LUE \times DNI \times A_{km2}$$

5.5. Monthly Consumption Factor

The monthly consumption factor is calculated for each CSP+cooling configuration and each suitable area 1 km x 1 km grid. This value is critical in highlighting the trade-offs between lower consumption factors and higher cycle efficiencies between WC and DC plants [137]. This consumption factor is calculated based on the system-level generic model (S-GEM) of water use in thermoelectric power plants, by [34]. The formula derived for consumption factors (I_{WC}) (i.e. consumption intensities) of wet tower-cooled plants (recirculating wet cooled), is given in Equation 5. 8.

Equation 5. 8: Calculation of water consumption factor

$$I_{WC} = 3600 \frac{(1 - \eta_{TE} - k_{OS})}{\eta_{TE}} \frac{(1 - k_{SENS})}{\rho h_{fg}} \left(1 + \frac{1}{n_{CC} - 1}\right) + I_{PROC}$$

Here, η_{TE} refers to the thermal-to-electric efficiency of the CSP plant, considering heat input at the steam generating system (boiler) and the electrical energy generated. It is calculated as the product of η_{ST} and η_B. The value k_{OS} is heat lost to other sinks, which is particularly applicable to combustion-based thermoelectric power plants, since a large amount of heat is dissipated through the flue stack. For this study, however, k_{OS} is calculated as 1 minus the product of η_{PIP} and η_{STOR}, fromTable 5. 3. In Equation 5. 8, k_{SENS} is the fraction of heat load rejected through sensible heat transfer and depends on the temperature of the incoming air and the design of the cooling tower. It is calculated according to Equation 5. 9, from [34]. coefficient

Equation 5. 9: Calculation of sensible heat transfer coefficient

$$k_{SENS} = -0.000279{T_{DB}}^3 + 0.00109{T_{DB}}^2 - 0.345T_{DB} + 26.7$$

h_{fg} is the latent heat of vaporization of water, assumed constant at 2.45 MJ/kg, and ρ is the density of water, taken as constant at 0.9982 kg/L. n_{CC} refers to the number of cycles of concentration used in the cooling tower, to account for water lost through blow-down, assumed to be 5 for this study. I_{PROC} is the sum of consumption factors allocated to other processes, in this case mirror cleaning, steam cycle blow-down, and air-cooled condenser (ACC) tube-bundle cleaning. For mirror cleaning needs by cleaning trucks, a water usage of 1 L/m^2 and 1.2 L/m^2 was used for CR and PT respectively [230]. Multiplying this value by the LUF and the surface area of each suitable area, as well as the amount of cleans per year (assumed to be once a week, i.e. 52 per year), and dividing by the total annual electrical generation, results in consumption factors around 0.18 m^3/MWh. Values for steam cycle make-up are estimated at 0.24 m^3/MWh [231].

Values for ACC tube-bundle cleaning were estimated at around 0.033 m^3/MWh, based on data from ACC cleaning systems manufacturers [232], [233]. The total amounts for I_{PROC} are around 0.4 m^3/MWh, which compare well with values reported in [231]. Improvements on the quantification of I_{PROC} are required. Furthermore, as stated in [34], k_{SENS} is an empirically derived formula as implemented by [234], and is based on results from the more complicated, but more accurate, Poppe cooling tower model. In light of this, better approximations of k_{SENS} will contribute to the accuracy of water consumption estimations at thermoelectric plants.

The use of k_{SENS} in this methodology provides an acceptably accurate quantification of the change in water consumption with air temperature and relative humidity. This sensitivity of water consumption by WC plants to ambient conditions is clearly demonstrated in [235]. Results for I_{WC}, for the suitable areas identified in South Africa, with varying T_{DB} data from 6°C to 29°C, were calculated. The results for PTWC plants are between 3.29 and 4.15 L/kWh, and between 2.55 and 3.14 L/kWh, for CRWC plants. These values agree well with those reported in [135], such as between 2.74 and 4.20 L/kWh for PTWC, and between 2.84 and 3.45 for CRWC. Other values reported for PTWC, with varying locations and varying thermal storage capacities, are between 3.1 and 4.1 L/kWh, for a cold and a hot site, respectively, both with 6h of TES [35].

5.6. Results

The spectrum of results from this spatio-temporal model of CSP water demand and generation potential are summarised in Table 5. 3. As Table 5. 3 shows, there is a total of 288 different possible results-based maps or graphs that can be generated, when considering each of the six results for the four CSP+cooling configurations are per month. Furthermore, there are a total of 314,931 1km x 1km grid cells (i.e. 314,931 km² of suitable land for CSP), for which calculations had to be done to generate these results. This means that each of the cells must have the input data (dry-bulb temperature, relative humidity and DNI) required for these calculations, as shown in Equation 5. 1 to Equation 5. 9, and therefore a further group of 48 maps/results can be generated to show the monthly variance in these.

Table 5. 3:Possible results combinations from spatio-temporal model

Configu-ration	η_{power} (%)	η_{ST} (%)	η_{SE} (%)	Generation potential (GWh)	Consumption factor (L/kWh)	Total consumption (m^3)
PTWC	Monthly	Monthly	Monthly	Monthly	Monthly	Monthly
PTDC	Monthly	Monthly	Monthly	Monthly	Monthly	Monthly
CRWC	Monthly	Monthly	Monthly	Monthly	Monthly	Monthly
CRDC	Monthly	Monthly	Monthly	Monthly	Monthly	Monthly

Considering this large amount of results, two maps per CSP+cooling configuration are shown. These eight maps show the Summer (January) and Winter (June) generation potentials and consumption factors per configuration. The generation potential (GWh per month) are shown at the 1km x 1km grid level, while the consumption factors are shown as an average within each QC. All the maps have the same scale for generation potential. Each configuration has the same scale for consumption factor between summer and winter, for comparative purposes.

From Figure 5. 2 (a) and (b), and Figure 5. 2 (c) and (d), one can compare both the change in monthly generation potential and average consumption factor between summer and winter, for PTWC and CRWC configurations, respectively. Not only does the generation potential drop dramatically from summer to winter, across all suitable CSP sites, but likewise, the consumption factor drops from an average of 3.89 to 3.42 L/kWh. What also becomes clear is that the consumption factor varies dramatically from site to site. Even though the range in consumption factors for Figure 5. 2 (a) and (b) is only 0.65 L/kWh, this impact translates to a large amount of water over time, when total consumption is considered. For example, a difference in consumption factor of 0.3 L/kWh between two locations with a hypothetically similar monthly generation potential of 7 GWh, translates into a difference in total consumption of around 2.1million m^3 for that month.

The maps in Figure 5. 2 (e) and (f), and Figure 5. 2 (g) and (h), show the seasonal differences for PTDC and CRDC. As one might expect, the dry-cooled configurations have substantially lower consumption factors than for wet cooled ones, ranging between 0.4 and 0.5 L/kWh for both PT and CR technologies. These spatial variances in consumption factor are, however, only due to the statistical calculation of average per QC, and is higher in QC's with more suitable locations than those with fewer. In practice, the consumption factor for all QCs will be the same since in this methodology, there is no spatially-dependent variables forming part of its calculation at this stage. When comparing generation potential, the average for January is lower, at around 7.64 GWh, compare to 8.12 GWh for PTWC, demonstrating the impact of reduced efficiency from DC systems. Furthermore, the change in generation potential between winter and summer is greater for dry-cooled plants than for wet-cooled ones, when comparing Figure 5. 2 (b) and (f), or Figure 5. 2 (d) and (h).

Finally, if Figure 5. 2 (a) and (c) are compared, it is clear that PTWC consumption factors are considerably higher than those for CRWC. This stems from the fact that central receiver systems reach higher temperatures and therefore higher cycle efficiencies, resulting in more efficient use of water in cooling. However, due to the lower LUF of CR systems (17% vs. 25 for PT), there is less generation potential per suitable area than for PT systems.

5.7. Conclusions

This work provided a simple methodology for modelling CSP performance and water consumption both spatial and temporally. The aim was to be able to allow for sensitivities to spatiotemporal changes in meteorological conditions and their impact on generation and water demand, for different CSP+cooling configurations. The assumptions used were highly simplified, and there is a need to refine an validate them based on detailed hourly interval simulations in multiple locations, for the different CSP+cooling configurations. This initial model, however, provides results which are within the ranges found in literature, and can therefore provide insight into the demand for water from CSP in South Africa.

These results can now be incorporated into further studies on water resource availability and variability at QC scales. This can then be used to determine limits placed by water resource availability on CSP capacities in different areas, for different CSP+cooling configurations. Once verified, this methodology can be used to do high-level estimations of generation potential and water demands (and resulting hydrological impact assessments). Furthermore, it can be updated to incorporate improved water use approaches (cleaning strategies and/or technologies, cooling technologies, CSP plant water management strategies, desalination, and alternative sources, for example), and evaluate the likely impact on water resource balances, as well as the impact of variable water supply on plant operations.

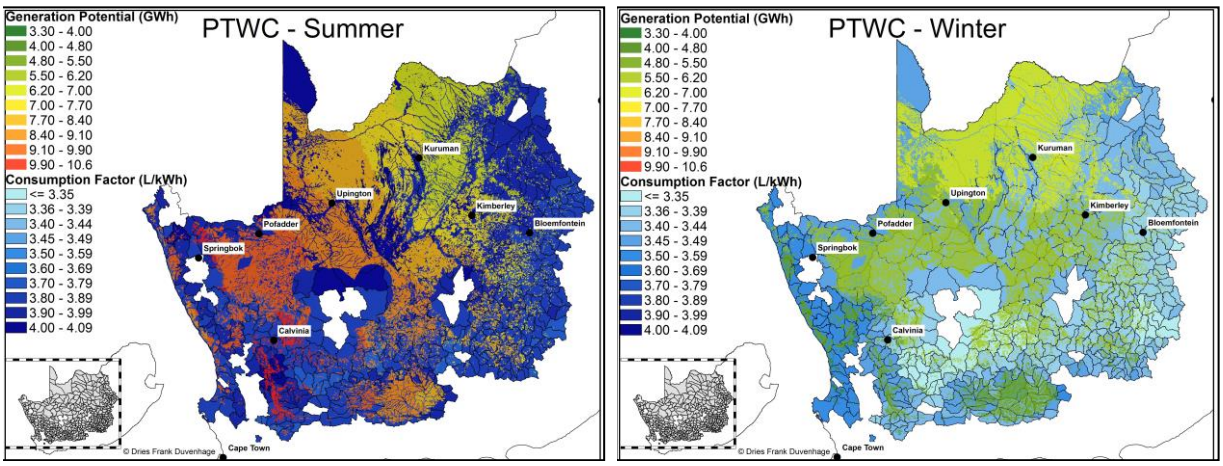

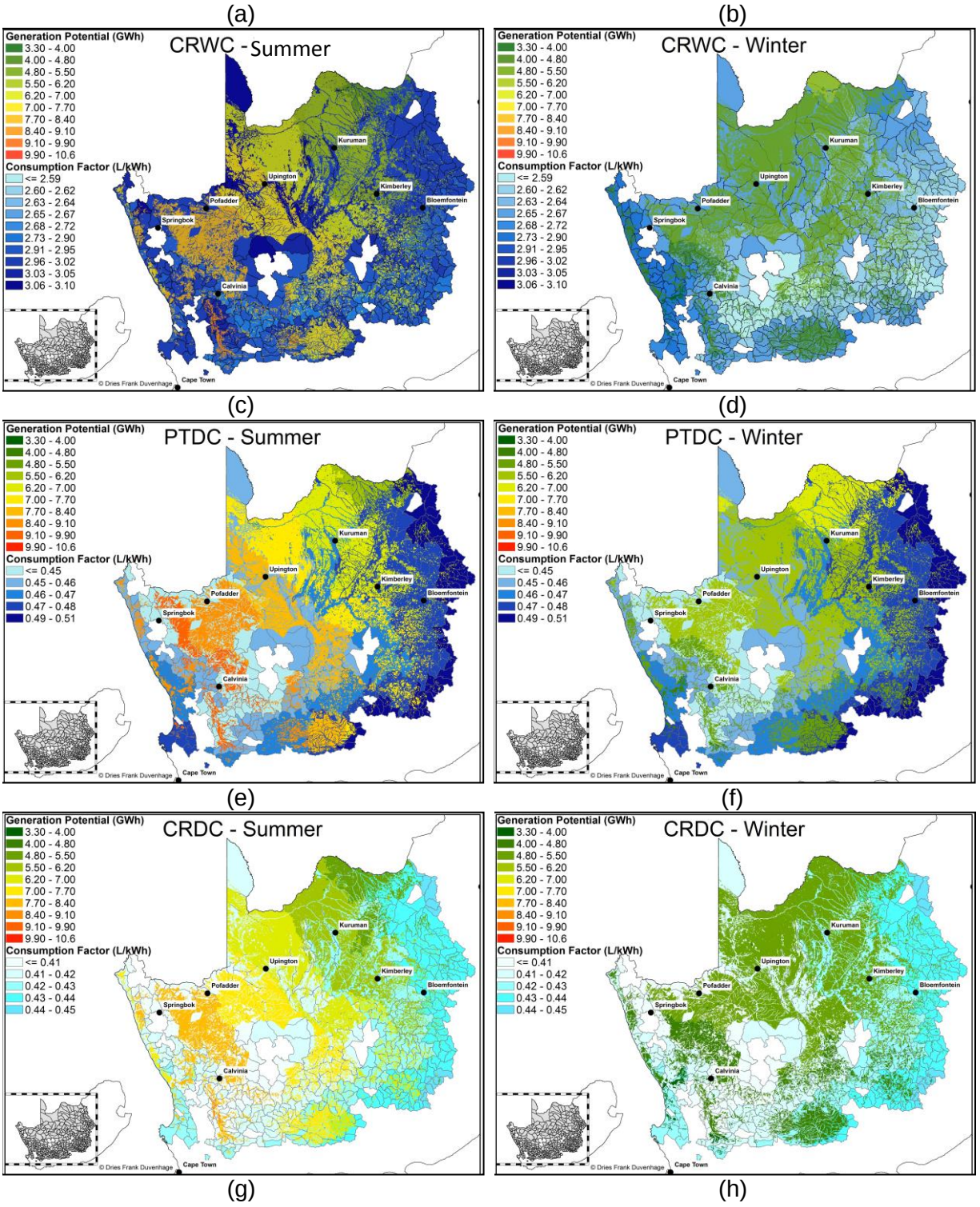

Figure 5. 2: CSP consumption factor and generation potential maps for South Africa

Chapter 6 – Water and CSP – A validated high-level CSP performance and water consumption model based on monthly efficiency calculations

6.1. Introduction – Water Availability and CSP

Concentrating Solar Power (CSP) has shown its ability to address inherent problems experienced with increased uptake of intermittent Renewable Energy Technologies (RETs) [26], [29]. CSP, however, has one particular downfall regarding its sustainability; its current dependence on water [3]. Much work is being done on reducing this dependence; from hybrid cooling systems and solar field cleaning strategies, to improved water management within the plant and cleaning water capturing for treatment and reuse [236]. However, these efforts are generally still in a research and development phase, and current mature CSP technologies remain water intensive. While the main driver of water use is cooling, accounting for more than 90% of total water use in wet cooled plants, dry-cooled plants suffer from higher capital costs and lower plant efficiencies [35], [237]. Considering this, another critical factor is that CSP is most efficient, and therefore profitable, in areas with high Direct Normal Irradiance (DNI). These areas do, however, experience generally drier, more arid conditions.

This coincidence between high DNI and low water availability complicates the sustainable deployment of CSP in these regions. It is therefore necessary for countries where CSP is envisioned as a major part of the energy mix, to strategically manage the deployment of these mature CSP technologies in such a way as to mitigate water-related risks on CSP plant operation, as well as unsustainable water use [3]. This strategic management of CSP deployment and water resources should be informed by detailed technology-based demand modelling, and incorporated into national cross-sectoral, water-energy policies [238]. This work therefore provides a comprehensive approach to the quantification of water demand based on CSP plant performance over large geographical areas, as presented in previous preliminary models for South Africa in Section 5. It builds on this initial high-level quantification through the improvement of CSP plant performance and water consumption estimations based on annual efficiencies, by implementing monthly efficiency factors for a higher temporal resolution. This is deemed necessary since water resource availability varies seasonally, and therefore can potentially impact sub-annual CSP operation.

The paper consists of an Introduction (Section 6.1), a Methodology Overview (Section 6.2), a detailed analysis of each efficiency and assumption required to calculate CSP plant performance based on monthly efficiencies (Section 2.3.1 to Section 2.3.10), a discussion of the error metrics and validation parameters used to compare the final high-level efficiency model (HLEM) results to those from the detailed hourly-interval simulation (DHIS) (Section 6.2.1), a detailed review of the Monthly net generation potential results (Section 6.4.1), the Monthly water consumption factor results and calculation (Section 6.4.2), and the Monthly total water consumption volume (Section 6.4.3). The paper concludes with a discussion of the broader use of the model developed, and the further work required for further refinement (Section 6.5).

6.2. Methodology – Overview

Since the aim of this work is to provide a more accurate, validated high-level modelling approach to estimate CSP plant performance and water consumption based on its location and the month of operation, the use of efficiencies for these calculations was deemed most suitable. This approach, however, is typically only used to roughly estimate the annual operation of a proposed CSP plant based on the design, and its associated efficiencies, and

the location's total annual DNI. These efficiencies, however, are generally static in nature, and cannot reflect any changes due to location- or seasonal dependency. For this reason, an approach was developed to make these efficiency assumptions more sensitive, where applicable, to these dependencies.

The methodology was carried out as follows:

1. Set up a model for an existing CSP plant and validate its results with actual, measured operational data.
2. Design a dry-cooled version of this model capable of handling the same heat load.
3. Scale both these models up to 100 MW.
4. Run annual simulations of this model with hourly meteorological data and one minute simulation time step in multiple locations.
5. Set up a high-level efficiency model (HLEM) as preliminarily described in [239] for each location.
6. Analyse results from detailed hourly-interval simulations (DHIS) for each location and calculate the following monthly efficiencies:
    a. Solar field efficiency (optical and receiver)
    b. Gross to net efficiency (parasitics)
    c. Piping and thermal losses efficiency
    d. Thermal energy storage (TES) losses efficiency
    e. Availability losses efficiency
    f. Boiler and turbine efficiency
7. Compare these to the static efficiencies as reported in Section 5.
8. Adjust these according to monthly variations identified in step 6.
9. Apply adjusted, dynamic efficiencies to the HLEM.
10. Compare results from updated HLEM to those in DHIS.

This approach ensures that the updated, dynamic efficiencies reflect more detailed plant performance variations based on a validated modelling approach and simulation package. The updated HLEM should then be tested for different, independent locations in a similar manner to that used in the above methodology to demonstrate fidelity and applicability of the final model.

6.2.1. Methodology – Detailed Hourly Interval Simulation (DHIS)

The in-house simulation tool of Fraunhofer ISE, *ColSim CSP* [240], was employed for the detailed simulations. Detailed annual simulations with hourly meteorological data were run for 50 MW and 100 MW Parabolic Trough Wet-Cooled (PTWC), Parabolic Trough Dry-Cooled (PTDC), Central Receiver Wet-Cooled (CRWC) and Central Receiver Dry-Cooled (CRWC) plants in 5 different locations. This detailed model was based on plant-specific design data for an operational PTWC plant. After the model was validated against measured operational data, the same plant was modelled in the five locations. The plant was scaled up to a 100 MW installed capacity by proportionately scaling up the solar field size, as well as all other required parameters for the simulation package, *ColSim CSP*[8]. The PTC model of *ColSim CSP* has been validated in a separate study [241]. The detailed water use and treatment models of *ColSim CSP* are presented in [242].The solar field (SF) was not optimised for each location since the annual DNI for each of the locations are similar to each other and initial calculations

[8] A software suite developed by Fraunhofer ISE.

indicated that the optimum SF size would not change drastically between the locations. The meteorological conditions of the selected locations are shown in Table 6. 1. The five locations were selected based on the existing CSP plants in South Africa. Typical meteorological year (TMY) data was obtained from the Meteonorm[9] database through a licensed product.

Table 6. 1: Meteorological conditions at selected locations

Location	DNI (kWh/m²/y)	T_dry_ave (°C)	T_dry_Max (°C)	T_dry_Min (°C)	RH_ave (%)
Bokpoort (*BP*)	2,841	21.13	40.50	-0.55	33.27
Khi Solar One (*KSO*)	2,848	21.34	41.10	-1.15	33.25
Illanga (*ILL*)	2,839	21.34	41.45	-1.25	33.50
Kaxu Solar One (*KaXSO*)[a]	2,958	20.01	39.96	-1.60	36.26
Kathu Solar Park (*KSP*)	2,739	20.45	38.70	-1.75	41.26

a Kaxu Solar One and Xina Solar One are directly adjacent to each other at the same location

The PTWC plant was modelled based on the design of an operational wet-cooled reference plant. The basic design details are given in Table 6. 2. The plant is modelled to operate at full load during day-hours, but not to use TES to compensate for DNI fluctuations, and to operate at full load for as long as the TES can supply during night-hours. The reason for not using TES to compensate for DNI fluctuations, according to operational personnel, is that repeated multiple changes between the TES and the SF for energy to the power block holds adverse maintenance risks for the plant.

Table 6. 2: Reference PTWC design criteria

Parameter Description	Unit	Reference case (50 MW)
Solar collector assembly and receiver	-	Eurotrough and Schott P70 receiver
Number of loops	-	180
Net generator capacity	MW	48
PB gross design efficiency at full	%	38.39
HP turbine Design isentropic efficiency	%	85.50
IP/LP turbine Design isentropic efficiency	%	88.00
Net to gross power ratio	%	89.00
Cycle of Concentration in cooling tower	-	5
Thermal storage capacity	h	9.3
HTF_fluid		Therminol VP1
TES fluid		Hitec Solar Salt

The only change made to the PTDC plant was the cooling technology, which was sized to accommodate the same heat load as that of the PTWC. No optimisation was carried out to increase the performance or reduce the LCOE of the PTDC. Furthermore, no location-specific optimisations were carried out, since this should have little effect on the final application in a HLEM.

[9] https://meteonorm.com/en/

The results from the 50 MW and 100 MW PTWC and PTDC simulations in the five locations produce a total of 20 sets of results, and another 20 sets of results for the 50 MW and 100 MW CRWC and CRDC plants. Due to the large amount of input data associated with these 40 simulations, only the specific data for the reference 50 MW PTWC plant is given in Table 6. 2[10]. The design of the solar fields for the CR plants are discussed separately in Section 6.3.7. From the DHIS results, it was found that not only does the water consumption reduce in winter months (middle months), due to reduced generation from lower DNI, but so does the consumption factor reduce. This is mainly because of the colder conditions under which the plant must operate, resulting in more effective cooling by the wet-cooled tower. Furthermore, it is apparent that the CR plants have a more stable generation profile throughout the year, and higher summer months generation. This is partly due to the lower impact of cosine losses in winter on the mainly north-facing, polar-layout design of the heliostat field, and is discussed in more detail in Section 6.3.7. Across all locations, the 50 MW CRWC plants generate an average of 291.07 GWh per year, while the 50 MW PTWC plants generate only an average of 237.53 GWh per year. This is mainly attributed to the higher thermal efficiency of the CR plants due to their higher operating efficiencies, and is discussed in more detail in Section 6.3.8.

6.3. Methodology – From Annual to Monthly Efficiencies

The classical annual efficiency approach used to estimate annual CSP performance is outlined in Equation 6. 1 to Equation 6. 4. This approach uses the following definitions and nomenclature, as put forward in the SolarPACES Guideline for Bankable STE Yield Assessment [243], to calculate net annual, and later monthly, electricity generation: annual net electricity generation (E_{net}), land use efficiency (LUE), total annual direct normal irradiance per unit area (H_y), total aperture area of all reflectors within a solar field (A_{net}^{SF}), solar-to-electric efficiency ($\bar{\eta}_{net,solar,y}$), land use factor (LUF), and total gross land area required (A_{gross}^{Tot}). These definitions, and their technology- and/or spatiotemporal dependency, will now be discussed in detail.

Equation 6. 1: Classical annual efficiency CSP performance equation

$$E_{net,y} = LUE \times H_y \times A_{net}^{SF}$$

Equation 6. 2: Definition of simplified annual Solar-to-Electric efficiency

$$\bar{\eta}_{net,solar,y} = \frac{E_{net,y}}{H_y}$$

Equation 6. 3: Definition of Land Use Factor

$$LUF = \frac{A_{net}^{SF}}{A_{gross}^{Tot}}$$

Equation 6. 4: Definition of Land Use Efficiency

$$\overline{LUE} = \bar{\eta}_{net,solar,y} \times LUF$$

[10] The corresponding author can be contacted for information on the other CSP configurations simulated for this work.

6.3.1. Land Use Factor (LUF)

In Equation 6. 3, the LUF term is only dependent on the CSP technology in use. This is the ratio between total area used for the CSP plant and the area used by the solar field aperture area to collect and concentrate DNI. It depends greatly on the solar collector assembly used in the construction of the plant, which in turn depends on the decisions of the Engineering Procurement and Construction (EPC) company and owners. A typical LUF can, however, be calculated based on existing operational plants. To do this, some of the most recent projects have been considered, since they are more likely to represent future developments than older projects. Information from project websites, as well as satellite images were used. Table 6. 3 shows these values and their sources, while Figure 6. 1 (a) shows a screenshot of a Parabolic Trough plant, and Figure 6. 1 (b) a Central Receiver plant.

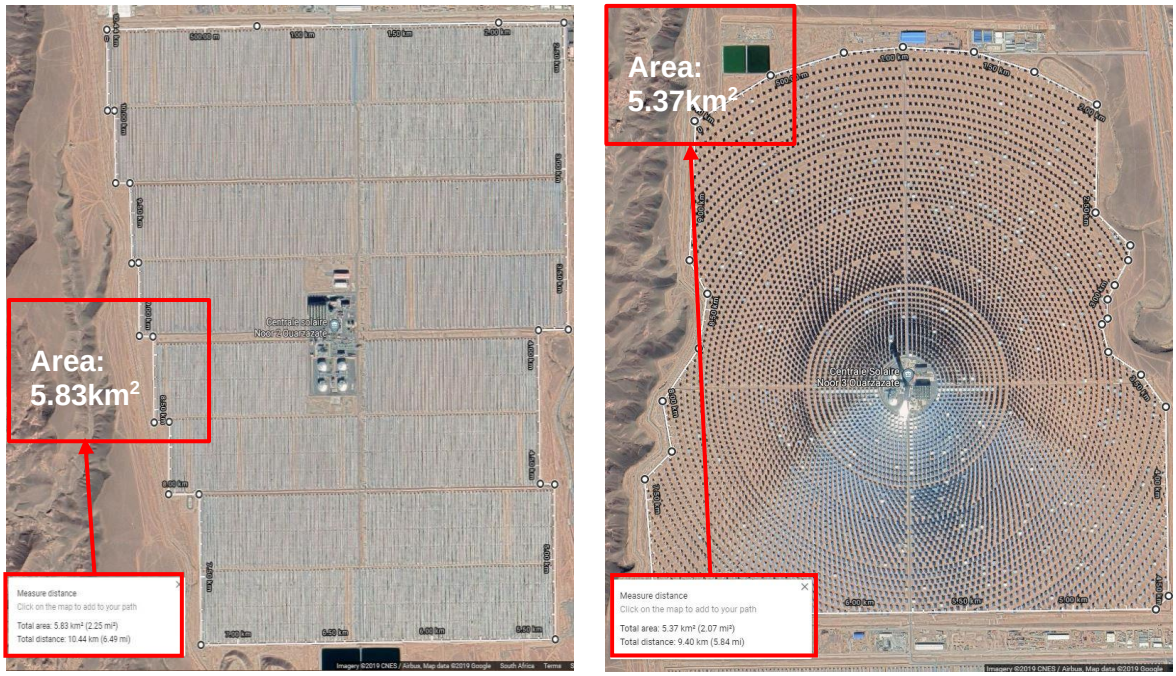

(a) (b)

Figure 6. 1: Screenshot of satellite image for NOOR II (a) and NOOR III (b), Note: the layouts are North-oriented.

Based on the values in Table 6. 3, the average LUF used for Parabolic Trough plants is 28% and for Central Receivers is 23%. This means that if one square kilometre (1 000 000 m^2) is to be modelled for a Parabolic Trough plant, 280 000 m^2 will be occupied by the mirrors, and 230 000m^2 in the case of a Central Receiver plant. This is a seemingly simple parameter, but it is important in high-level models like the one being developed in this work. This is because it serves as the initial, raw energy input from which the net electricity is calculated based on the efficiencies of energy conversions. It should be noted that for CR plants, as installed capacities and solar field sizes increase, the land use factor across the solar field area becomes less consistent as heliostat packing densities vary radially from the base of the tower outward. This is evident from Figure 6. 1 (b), where it is clear that the outer heliostats are less densely packed in order to prevent shading and blocking due to more acute heliostat altitude angles. Because of this variance in reflective surface density across a single solar field at CR plants, compared to a constant reflector density at PT plants, the average LF used for CR plants does not capture the changes in LF with changes in installed capacities. It is, however, deemed adequate for the high-level nature of the intended model for this work, since the

optimization and simulation of solar optics is not part of the scope, nor necessary for the spatiotemporal modelling capabilities of the intended final model.

Table 6. 3: Total area and aperture area values used to calculate LUFs

Plant name	CSP Technology	A_{gross}^{Tot} (km²)	A_{net}^{SF} (km²)	LUF (-)	Source
Bokpoort	PT	2.100	0.588600	28%	[244]
Kaxu Solar One	PT	3.100	0.817500	26%	[245]
Xina Solar One	PT	3.100	0.853306	28%	[245]
Kathu solar park	PT	3.736	1.000000	27%	[246]
Illanga	PT	3.156	0.870000	28%	[246]
NOOR III	CR	5.370	1.321197	25%	[247]
NOOR II	PT	5.830	1.779900	31%	[247]
NOOR I	PT	4.080	1.308000	32%	[247]
Dunhuang 100 MWe	CR	5.860	1.230000	21%	[248]
Atacama 1	CR	7.250	1.484000	20%	[249]

6.3.2. Land Use Efficiency and Solar to Electric efficiency (LUE and $\bar{\eta}_{net,solar}$)

Since LUE is only dependent on the LUF (already discussed) and $\bar{\eta}_{net,solar}$, the latter will be discussed in detail. The $\bar{\eta}_{net,solar}$ refers to how efficiently solar energy is converted into the electrical energy seen by the transmission network which receives it. In its most fundamental form in Equation 6. 2, it is the ratio between the incident DNI, and the net electricity generated. This is, however, an oversimplification if the sensitivity of this ratio to spatiotemporally varying factors must be captured. In order to capture this sensitivity, $\bar{\eta}_{net,solar}$ must be recognised as the composite efficiency, which it ultimately is. This composite equation is shown in Equation 6. 5, and its terms are defined as: η_{SF} refers to the combined optical efficiency of the concentrating mirrors in the solar field and the heat transfer efficiency of the receiver on which the solar flux is concentrated; η_{aux} refers to the loss of efficiency due to auxiliary and parasitic self-consumption, and is typically the ratio between gross and net generated electricity; η_{pipe} and η_{TES} are the efficiency losses due to energy transfer through piping and to and from storage, respectively; F_{avail} is the annual or monthly losses due to limited availability of the plant due to planned and unplanned maintenance and reduced solar field availability from breakages; and finally, η_{gross}^{PB} refers to the combined boiler and steam turbine efficiencies, which take into account the Rankine cycle used in conventional CSP plants.

Equation 6. 5: Detailed Solar-to-Electric efficiency for CSP

$$\bar{\eta}_{net,solar} = \eta_{SF} \times \eta_{aux} \times \eta_{pipe} \times \eta_{TES} \times F_{avail} \times \eta_{gross}^{PB}$$

As described in Section 5, there are various values from literature for each of these efficiencies, which form part of the total energy conversion at a CSP plant. In order to determine the applicability of these literature-based efficiency values, they were compared to the results from the DHIS individually.

6.3.3. Parasitic losses (Net to Gross efficiency, $\bar{\eta}_{aux,m}$)

The parasitic losses of a CSP plant are generally attributed to all the auxiliary electrical loads required to run the plant, which include, among others, HTF pumps, water pumps, the tracking system of the solar field, TES pumps, the heat-tracing system, compressed air system, and so forth [250]. There are many values for this efficiency in the literature for both PT and CR plants [211], [220], [222], [251]. Typically, they range between 88% and 91%, implying a loss of around 10% of the gross generated electricity to auxiliary loads. This value is calculated from the DHIS results according to Equation 6. 6. In the DHIS, the calculation of the total parasitic load is done on a component-by-component basis, depending on the energy and mass balance equations governing the operation of that component and how it depends on the operation of the plant. For each time interval of the model, the parasitic load is calculated and subtracted from the gross electricity generated, in order to arrive at the net electricity generated. Therefore, in order to calculate the total monthly auxiliary efficiency (m) value, the total monthly net electricity is divided by the total monthly gross electricity generated.

Equation 6. 6: Calculation of monthly efficiency due to Parasitic losses

$$\bar{\eta}_{aux,m} = \frac{E_{net,m}}{E_{gross,m}}$$

This was calculated for each month, and is compared to the reference value of 89% for a PTWC plant from literature in Figure 6. 2 [220]. It can be seen that the average of all the monthly averages, for all the locations, is 89%, and there is little change from one month to another. There is a slight increase in general for the winter months for all the locations, in the order of 0.9%. Since this difference is not substantial, a value of 89% is used in the HLEM for PTWC plants. In the case of CRWC plants, in Figure 6. 2 (b), the reference value from literature is 92%, which is 2% greater than the average of all the monthly averages, for all the locations. This may be due to varying assumptions on detailed operation strategies or equipment choices, therefore, the value of 89%, from the DHIS, was used for PT and 90% for the CR plants. There were no substantial differences observed between the DC and WC plants' net to gross ratios, and subsequently these values will be applied to both cooling configurations. It is interesting to note that the CR plants have less variation throughout the year, which is primarily attributed to the fact that the HTF does not need to be circulated through a solar field. As the DNI is lower in winter months, the circulation rate must be lower, to ensure the HTF absorbs enough heat in the SF, resulting in lower pumping losses in PT plants. Since the CR plants do not circulate HTF through long lengths of piping, the auxiliary load is generally lower, and less sensitive to seasonal variations.

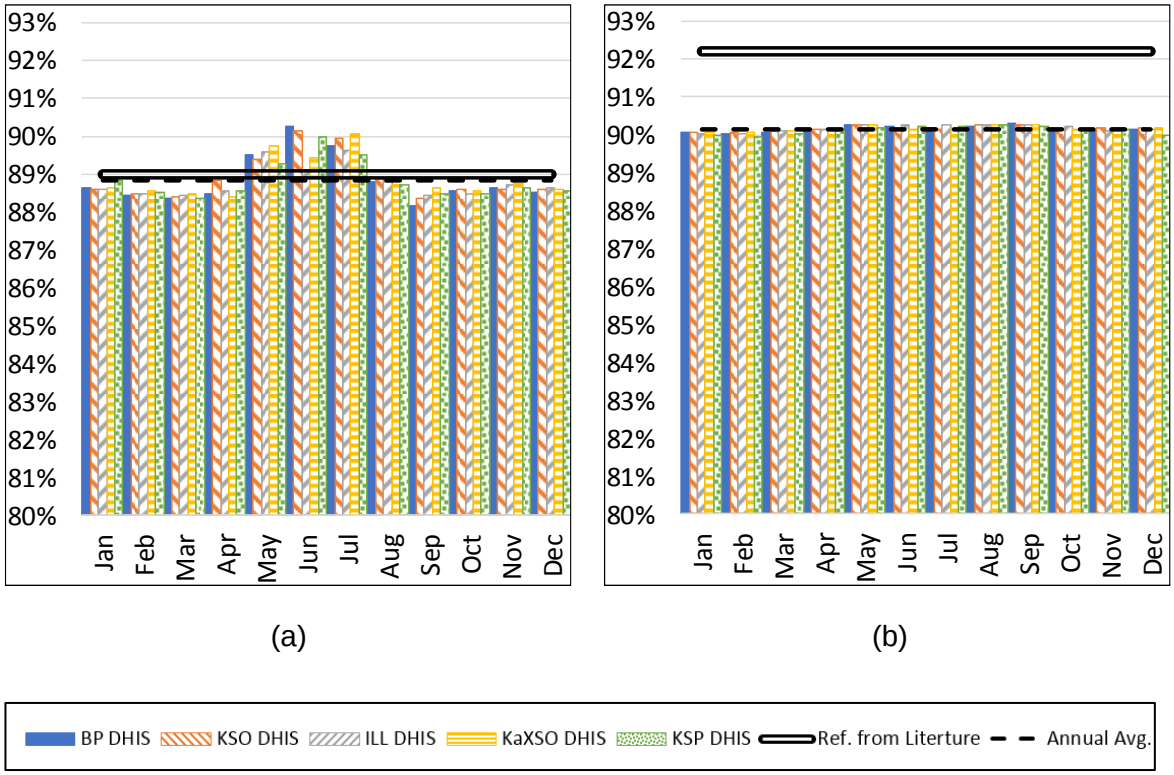

Figure 6. 2: Net to Gross efficiency (Parasitics) – (a) 50 MW PTWC, (b) 50 MW CRWC

6.3.4. Piping losses ($\overline{\eta}_{pipe,m}$)

Piping losses are generally calculated based on heat-loss coefficients for each length of pipe based on the heat transfer properties of the piping and its insulative cladding, as well as the temperatures of the fluid and outside air [252]. In PT plants, most of the heat-loss occurs along the hot HTF headers and piping, which convey the heated HTF, at around ~390^{O}C, from the solar field to the Steam Generating System (Boiler, or SGS) and TES heat exchanger. In CR plants, however, the HTF is solar salt, and operates at higher temperatures of 550^{O}C, but along shorter lengths of piping, only between the receiver, SGS and TES tanks. Losses also occur at valves and joints along the piping. Measures are generally taken to limit this as far as possible using insulation materials and cladding.

From the results of the DHIS, this value is defined as the ratio of total monthly energy absorbed by the HTF in the receiver, to the sum of energy sent to the SGS from the solar field and sent to the TES. Hot HTF from the solar field or central receiver can be sent either to the SGS for power generation only, or to both the SGS for power generation and to the TES heat exchanger for TES charging, simultaneously. The only other destination for energy between the solar field and the power block, is heat loss through the piping. The equation used to calculate the monthly piping loss efficiency is described in Equation 6. 7. $Q_{SF,PB}$ and $Q_{SF,TES}$ refers to the total monthly energy sent from the solar field to the SGS or the TES heat exchanger, respectively, while the $Q_{abs,m}$ is the total monthly energy absorbed by the HTF in the receiver tubes of the solar field or tower.

Equation 6. 7: Calculation of monthly efficiency due to Piping losses

$$\bar{\eta}_{pipe,m} = \frac{Q_{SF,PB,m} + Q_{SF,TES,m}}{Q_{abs,m}}$$

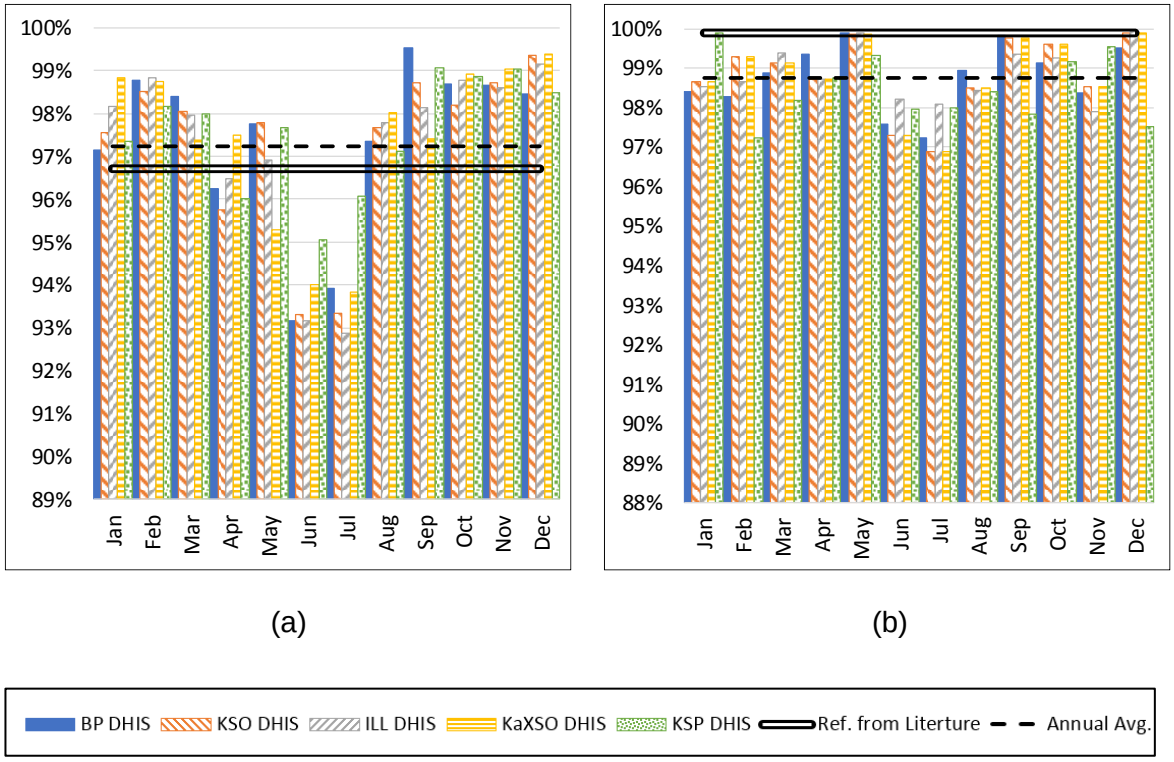

Figure 6. 3: Piping losses efficiency - 50 MW PTWC – (a) 50 MW PTWC, (b) 50 MW CRWC

The reference value from literature for this efficiency for PT plants is 96.7%, and 99.9% for CR plants, and are compared to the results from the DHIS in Figure 6. 3 (a) and (b) [211]. The combined annual average for all the locations for the 50 MW PTWC is 97.3%, and 98.8% for the 50 MW CRWC plants. The reduced efficiency at PT plants between winter and summer months is around 5% due to the colder ambient conditions. Since the monthly variation in this efficiency is not significant, and still above 92% for all locations, the reference values from literature are used in the HLEM. This omission, however, does result in a slight overestimation of final solar-to-electric efficiency in winter months, but in light of the high-level nature of the model, this overestimation is acceptably low.

6.3.5. Storage losses ($\bar{\eta}_{TES,m}$)

Storage losses account for energy lost during discharging of the TES through the TES-HTF heat exchanger. It is typically characterised by a heat loss coefficient and surface area of the storage tank, as well as the temperature of the storage medium inside and the outer ambient temperature [253]. Since the TES is typically discharged at night, this efficiency is only applicable to night-time operation. However, from an annual, or in this case monthly perspective, this efficiency needs to be captured in order to reflect the overall net impact on aggregate performance. These values are calculated from the DHIS results, based on the ratio between energy sent from the TES to the SGS ($Q_{TES,PB}$), and the energy received at the SGS from the TES ($Q_{PB,i}$). It was also calculated based on monthly totals, and this is shown in Equation 6. 8.

Equation 6. 8: Calculation of monthly efficiency due to Storage losses

$$\bar{\eta}_{TES,m} = \frac{Q_{PB,i}}{Q_{TES,PB}}$$

The monthly total storage efficiencies are compared to the reference value for PTWC from literature of 99.6%, in Figure 6. 4 [211]. The combined annual average for all the locations is 99.7%, with little noticeable variation through the year. For this reason, the reference value from literature was used in the HLEM.

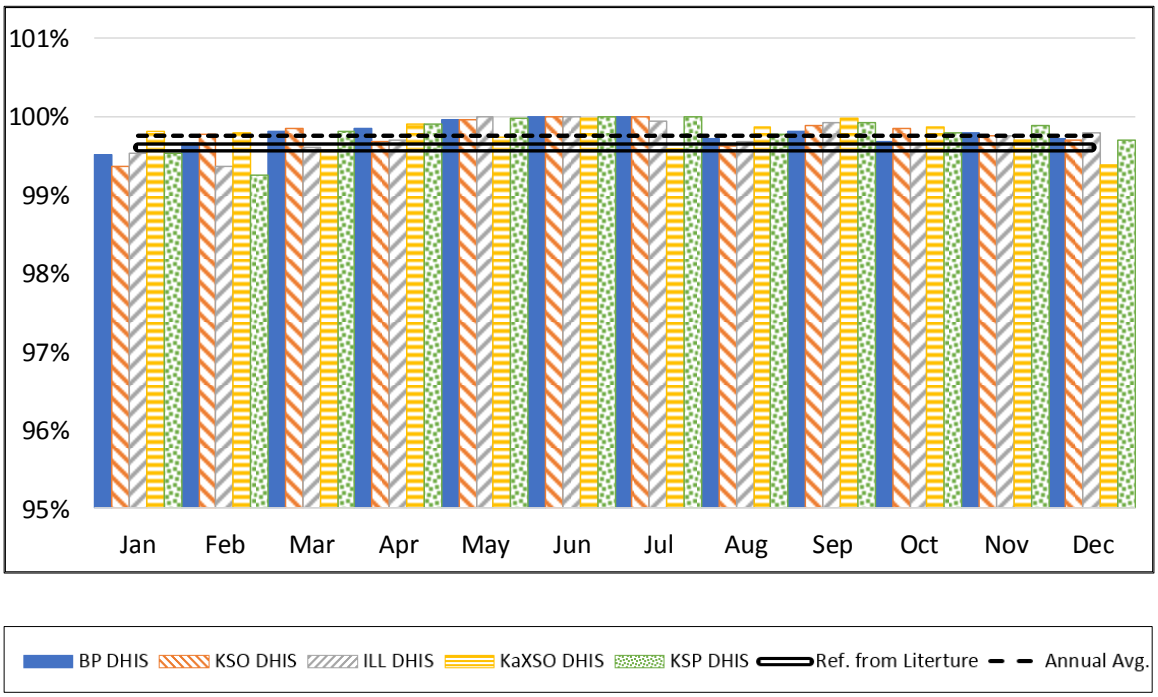

Figure 6. 4: Storage losses efficiency - 50 MW PTWC

In the case of CR plants, there is no heat exchanger between HTF and TES medium as in the case of PT plants using thermal oil as HTF, since solar salt is used for both functions. The solar salt is heated directly in the receiver on top of the tower, and it is then used to generate steam only or to generate steam and charge the TES. Therefore, there is no heat exchanger to measure the energy flow in the CR DHIS, meaning no results for this efficiency can be derived in this case. The reference value from literature is 99.5%, and is used in the final HLEM for CR plants [211].

6.3.6. Availability factor ($F_{avail,m}$)

This efficiency value is typically considered to reflect the impact of planned and unpanned maintenance, as well as losses due to mirror breakages, on the annual operation of a typical CSP plant [211]. However, when conducting a DHIS of a CSP plant, the simulation does not intuitively decide when to keep the plant shut down for maintenance to be performed. Typically, CSP plants conduct this maintenance in the winter months, since the loss in generated energy, and therefore revenue, is inherently lower, due to less daily DNI (lower DNI as well as shorter days). It was observed that applying an annual value of 94% [211] to each of the months will indiscriminately reduce the effective energy generation of each month by 6%, while this will typically only be confined to lower energy yield months. Furthermore, the

implementation of this value on each month resulted in a reduction of around 6% for the total annual energy generation (as would be expected), as well as the same reduction in total annual water consumption relative to the DHIS results. For the purposes of this study, therefore, no availability efficiency was implemented in the final HLEM, effectively resulting in an apparent value of 100%. Although this does not necessarily reflect actual plant performance, the purpose of this study is to validate the results of the updated HLEM with the results of the DHIS, which serves as an industry standard for CSP performance evaluation.

6.3.7. Solar field efficiency (η_{SF})

In this study, the solar field efficiency consists of the optical efficiency of the reflective collectors (parabolic troughs or heliostats), as well as the efficiency of the receiver on which the concentrated solar flux is focussed, meaning that it represent the overall solar-to-thermal efficiency of the plant [27]. This is because the calculation of monthly solar field efficiencies from the results of the DHIS depend on the total monthly incident DNI on the entire solar field aperture area ($Q_{SF,m}$) and the total monthly amount of energy absorbed by the HTF in the receiver ($Q_{abs,m}$), as depicted in Equation 6. 9. Therefore, this calculation inherently includes both the receiver and collector efficiencies, as well as losses due to dumping of excessive incident energy.

Equation 6. 9: Calculation of monthly solar field efficiency from DHIS results

$$\eta_{SF,m} = \frac{Q_{abs,m}}{Q_{SF,m}}$$

The DHIS considers a PT CSP plant based on a very specific design-point, chosen to ensure adequate energy from the SF under the most commonly experienced DNI levels. This inherent overdesign, therefore, means a certain amount of incident DNI will always be dumped. The design point was chosen for a 50 MW PTWC plant in the Bokpoort location. The CR plants' designs, however, were based on a design point selected for each location, based on work the *ColSim CSP* simulation suite, described in Section 6.3.7 *Central Receiver solar field efficiency*.

Typically, the optical efficiency of any CSP system represents the greatest efficiency loss in the system, in the order of between 40% and 60%, depending on the CSP technology in use, as well as the local conditions and time of the year and day [254]. The optical efficiency of solar collectors is the ratio of the reflected (concentrated) solar power absorbed by the absorber under ambient temperature, to the incident solar power on the entire reflector aperture. The denominator of the ratio is the product of the incident DNI and the reflector aperture area. Optical efficiency depends principally on the solar geometry, i.e. the relative angles between the sun and the collector surface. For a detailed explanation of these angles, the reader is invited to refer to Chapter 3 of [255]. Since the physics and functioning of single-axis tracking parabolic troughs are fundamentally different to that of a field of two-axis tracking heliostats and a central receiver, they will be covered separately.

Parabolic trough solar field efficiency

The standard approach to quantify the dynamic impact of solar angles on a PT plant's solar field optical efficiency is to use an Incidence Angle Modifier[11] (IAM), which is defined as the ratio of thermal efficiency at a given incidence angle to the peak efficiency at a normal incident

[11] Sometimes called Incident Angle Modifier or Incidence-angle modifier.

angle [256]. By multiplying the IAM ($K_{PT}(\theta_i)$) with the peak efficiency at a normal incident angle (η_{opt_0}), and accounting for shadowing (η_{shad}) and end-losses (η_{end}), the optical efficiency of a trough, or entire solar field of troughs, can be determined at any incidence angle (θ_i,) as shown in Equation 6. 10 [257].

Equation 6. 10: Calculation of optical efficiency of a trough at incidence angle θ_i

$$\eta_{opt,PT} = \eta_{opt_0} \times \eta_{shad} \times \eta_{end} \times K_{PT}(\theta_i)$$

The IAM is a function of incidence angle. However, this function is different for each parabolic trough design and receiver-tube configuration, and is experimentally determined for each of these different configurations [258], [259]. This level of detail would require the dimensions of the trough and receiver needs, which is excessive and unnecessary for the purposes of the HLEM. Naturally, for detailed thermal designs and economic evaluations, this is important. Therefore, in order to incorporate the monthly variation of optical efficiency due to location and seasonal solar angles, a simplified modifier ($K(\theta_i)$) was used. The alternative is to use a static annual efficiency of 59.8% for PT, and 56.3% for CR plants [211]. The shortfall of this is quite apparent when it is considered that one of the key factors in reduced PT plant performance in winter is the impact of more severe incidence angles on the solar field efficiency.

Two possible approaches would be to account for the solar geometry losses by multiplying a design optical efficiency either with the cosine of an incidence angle for a specific location and date, or with some IAM. In either case, the incidence angle must be calculated based on the hour, date and latitude, from equations brought forward by [255]. Equation 6. 11 to Equation 6. 14 show these equations. The parameters are defines as: δ, the declination angle, based on N, the number of days since January 1st; and α, the altitude angle, based on the declination angle, latitude angle ($\emptyset$) and the hour angle (ω), which depends on the solar time (t_s).

Equation 6. 11: Calculation of declination angle

$$sin(\delta) = 0.39795cos[0.98563(N - 173)]$$

Equation 6. 12: Calculation of altitude angle

$$\alpha = sin^{-1}(sin\delta sin\emptyset + cos\delta cos\omega cos\emptyset)$$

Equation 6. 13: Calculation of hour angle

$$\omega = 15(t_s - 12)$$

Equation 6. 14: Calculation of incidence angle based on α

$$\theta_i = 90 - \alpha$$

From Equation 6. 11 to Equation 6. 14, four variables are required to calculate the incidence angle for any location and any date. The latitude angle is simply the latitude of the location in question in decimal degrees, while the hour angle depends on the solar time at the location. Solar time is also location dependent, specifically longitude, and is different from clock time. For the purposes of this study, the hour angle is taken at solar noon ($t_s = 12$), to reduce the number of calculations required per location, making the hour angle equal to 0. Furthermore, the date selected for approximating the declination angle of each month is selected as the 15th day of each month (1st of each month plus two 7-day weeks). This means that the declination angle is calculated at solar noon for the middle of each month, on the 14th, 45th, 73rd, 104th,

134th, 165th, 195th, 226th, 257th, 287th, 318th and 348th day of the year, since January 1st (N). Previous work suggested using the 16th day of each month, but after comparison, the approach used in this work yielded very similar results [260]. The approximated monthly incidence angle, and monthly incidence angle modifier ($K_{PT}(\theta_i)_m$) can now easily be calculated for any location.

The monthly modifier is a function of the incidence angle, and can be multiplied with a typical PT peak optical efficiency (η_{opt_0}) as well as receiver efficiency (η_{rec}) to calculate the solar field efficiency, as in Equation 6. 15.

Equation 6. 15: Calculation of monthly solar field efficiency based on modifier

$$\eta_{SF,PT,m} = \eta_{opt_0} \times \eta_{rec,PT} \times K_{PT}(\theta_i)_m$$

For comparison, the peak optical efficiency was multiplied with the cosine of the incidence angle, as well as the IAM of the Ultimate Trough, as derived by FLABEG ($K_{PT,FLABEG}(\theta_i)$), shown in Equation 6. 16 [261].

Equation 6. 16: Calculation of IAM

$$K_{PT,FLABEG}(\theta_i) = 1 - 0.008\frac{\theta_i}{cos\theta_i} - 0.117\frac{\theta_i}{cos\theta_i}$$

The values used for η_{opt_0} and $\eta_{rec,PT}$ was 63% [262] and 89.7% [257], respectively. These results are shown in Figure 6. 5. When comparing the IAM- and cosine derived monthly solar field efficiencies, it is apparent that the FLABEG IAM (densely dotted orange bar) resulted in gross overestimations thereof. The cosine-derived solar field efficiencies (solid grey bars) appear to follow those calculated from the DHIS results (according to Equation 6. 9, black line). The final monthly solar-to-electric efficiency profile calculated with this, however, deviated substantially from those calculated from the DHIS results.

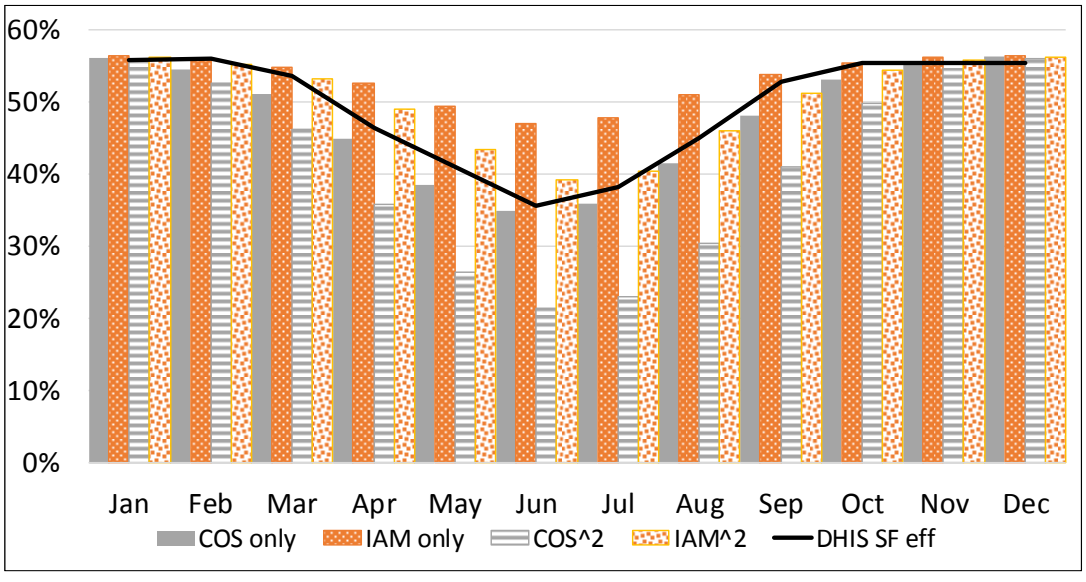

Figure 6. 5:Monthly solar field efficiencies - 50 MW PTWC Bokpoort location

Since it is clear from Figure 6. 5 that the FLABEG IAM modifier does not reflect the reduced efficiencies associated with the winter-months, but did match the summer months very well, it

was decided to take the square of the IAM. This means that the square of the fraction (between 0 and 1) remains close to the original value the greater the value is (closer to 1) but experiences greater reductions at lower values (winter months). The same was done with the cosine-derived η_{SF}, and both are shown in Figure 6. 5. The squared FLABEG IAM η_{SF} (coarsely dotted orange bars) now matches the DHIS η_{SF} very closely, while the square cosine-derived η_{SF} (horizontally striped grey bars) clearly drops too low for all months. The annual average percentage difference and monthly RMSE between the DHIS η_{SF} values, and those derived from the four different modifiers above, for the 50 MW PTWC configuration at all 5 locations, are shown in Table 6. 4. By demonstrating acceptably low annual percentage differences and monthly deviations (RMSE) from the DHIS solar field efficiency values, the squared IAM-derived modifier provides the best approximation for monthly solar field efficiency for PT plants at all the modelled locations.

Table 6. 4: Agreement parameters for solar field efficiencies for all locations - 50 MW PTWC

Modifier approach	Agreement parameter	Bokpoort	Khi Solar One	Illanga	Kaxu/Xina Solar One	Kathu Solar Park
cos	% Annual diff	-3.48%	-3.54%	-3.18%	-3.15%	-3.09%
	% RMSE	3.65%	3.71%	3.38%	3.20%	3.35%
$\cos^2$	% Annual diff	-16.61%	-16.54%	-16.21%	-16.43%	-15.59%
	% RMSE	18.69%	18.59%	18.23%	18.49%	17.45%
IAM	% Annual diff	7.76%	7.59%	7.95%	8.21%	7.57%
	% RMSE	9.34%	9.13%	9.43%	10.03%	8.76%
IAM^2	% Annual diff	1.63%	1.53%	1.90%	1.99%	1.86%
	% RMSE	2.11%	2.01%	2.33%	2.63%	2.17%

Central receiver solar field efficiency

The optical model within the DHIS of *ColSim CSP* is based on a cone optics approach that takes into account cosine/shading/blocking/reflection/atmospheric attenuation/spillage losses [263]. Based on this method, the solar concentration on the receiver surface is assessed for a set of nodes within a sky discretization [264]. The thermal receiver model of the DHIS uses the optical input for transient simulations, where the concentration ratio, CR, for arbitrary sun positions is interpolated with the sky discretization approach and used to calculated absorbed solar radiation as depicted in Equation 6. 17.

Equation 6. 17: Calculation of absorbed heat on Central Receiver absorber within ColSim CSP simulation suite

$$\dot{Q}_{abs} = \alpha_{eff} \cdot G_{b,rec} \cdot A_{rec} \cdot CR$$

In Equation 6. 17, the receiver surface area A_{rec} considers the curvature of the absorber tubes as well as the incident DNI on the absorber tubes, $G_{b,rec}$. Accordingly, an effective solar absorptance, β_{eff}, is derived with the nominal value β and taking into account the micro-cavity effect of the absorber tubes, shown in Equation 6. 18 [265].

Equation 6. 18: Calculation of effective absorptance of Central Receiver absorber within ColSim CSP simulation suite

$$\beta_{eff} = \frac{\beta}{\alpha + (1-\beta) \cdot 2/\pi}$$

Convective losses are calculated with a Nusselt correlation according to [266]. A surface temperature (in Kelvin) of $0.5(T_{in} + T_{out})$ is assumed, which neglects the temperature difference between bulk fluid and tube surface. Thermal radiation losses ($\dot{Q}_{rad}$) are calculated as shown in Equation 6. 19, with Stephan-Boltzmann constant σ, effective surface emittance ϵ_{eff} calculated equivalently to the effective solar absorptance β_{eff} and radiative mean temperature as $T_{rad} = \left(\left(T_{in}^4 + T_{out}^4\right)0.5\right)^{0.25}$.

Equation 6. 19: Calculation of thermal radiation losses of Central Receiver absorber within ColSim CSP simulation suite

$$\dot{Q}_{rad} = \epsilon_{eff} \cdot \sigma \cdot A_{rec}(T_{rad}^4 - T_{amb}^4)$$

While the most conventional solar field layout for PT plants is the North-south orientated, East-west tracking configuration (as shown in Figure 6. 1 (a)), CR plants' heliostat field layouts can be more variable in design. The heliostat field layouts can vary much more drastically based on different design considerations and optimisation criteria. Each heliostat distribution methodology can lead to different seasonal and total annual solar field efficiencies [267]. Furthermore, as in the case of PT plants, the size and shape of the heliostats themselves determine both their individual optical characteristics, as well as the geometrical limitations on field layout [268]. Another key determining aspect of the solar field performance is the position of the entire field in relation to the tower. The two most common layouts in this regard is the surround layout and the polar layout [269], coupled to an external or cavity receiver respectively.

The *ColSim CSP* simulation suite from Fraunhofer ISE, used in the DHIS, includes a heliostat field layout design package which optimizes the Solar Field size and layout based on location and plant design specifications. The pattern-based approach follows the MUEEN principle [270] extended with several compression parameters for enhanced optimization [271]. From an oversized field, the annually best performing heliostats are selected in such a way that the required power at the design point is reached. For heliostat fields in the southern hemisphere, heliostats on the southern side of the tower have on average lower cosine losses than on the northern side [272], [273]. Therefore, surround field designs in South Africa will have a polar tendency towards the south, as depicted in Figure 6. 6 (a) for the Bokpoort location. The receiver characteristics are derived following a design-point approach [274] which aims at reducing optical, thermal and pressure losses, while staying within operational limits.

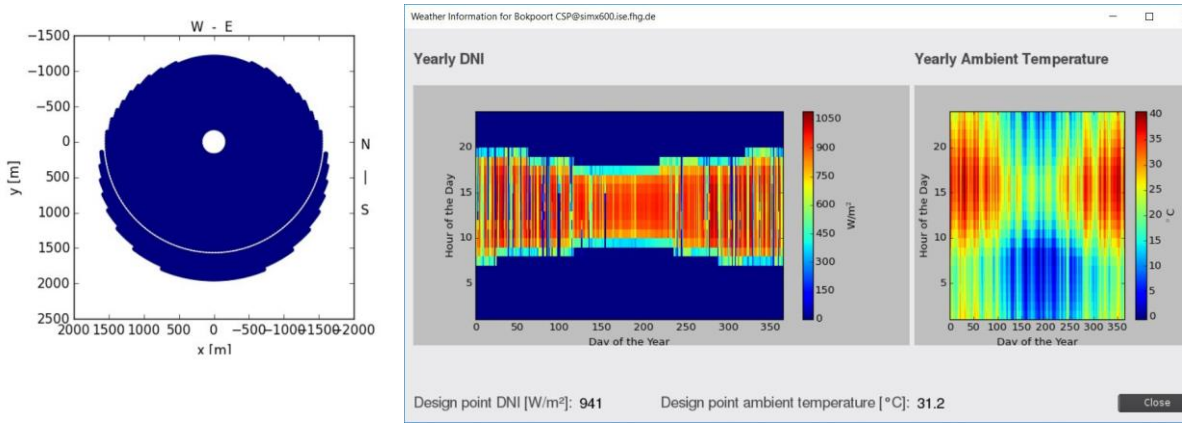

(a) (b)

Figure 6. 6: a) Heliostat field layout and b) design-point conditions used for 100 MW CR plant in Bokpoort location

The overall heliostat field efficiency is typically affected by the reflectivity of the heliostat mirrors (η_{ref}), cosine (η_{cos}), atmospheric attenuation (η_{aa}), interception and spillage (η_{itc}), and shading and blocking (η_{sb}) efficiencies, as shown Equation 6. 20 [56], [275].

Equation 6. 20: Calculation of optical efficiency of a heliostat

$$\eta_{opt,CR} = \eta_{ref} \times \eta_{cos} \times \eta_{sb} \times \eta_{itc} \times \eta_{aa}$$

These efficiencies are all affected by the design of the heliostats themselves, but also by the position of the sun relative to the reflective surface. The cosine efficiency represents the greatest loss in reflectivity, and experiences the greatest variance, from 0% to 90%, depending on the season and time of day [273]. While the solar angles do affect η_{itc} and η_{sb} efficiencies, their seasonal and hourly variance is less extreme and generally less severe. However, η_{cos} experiences the greatest variation with changes in solar angles, but greatly depends on the orientation of the heliostats relative to the tower. Attenuation efficiencies can vary drastically depending on location and atmospheric conditions, as well as the physical size of the heliostat field, with larger fields having more mirrors further away, and therefore experiencing greater attenuation losses (lower η_{aa} values).

For the high-level nature of the HLEM within this study, fixed values for $\eta_{ref}, \eta_{sb}, \eta_{itc}$, and η_{aa} are chosen from literature (84%, 92%, 99% and 95%, respectively) [275], [276]. Here, η_{ref} is slightly lower at 84% because beyond reflectivity (95%), it considers heliostat availability (99%), mirror soiling (95%) and reduced availability due to wind-storage (95%) as well [219]. This gives an estimated overall optical efficiency (not considering solar-geometry losses) of 73%, and is termed the non-geometric optical efficiency ($\eta_{NGO,CR}$).

The approach used to quantify the overall monthly solar field and receiver efficiency from the DHIS results is the same as that used for troughs (Equation 6. 9). The receiver efficiency ($\eta_{rec,CR}$) is a representation of the relationship between the intercepted reflected sunlight on the receiver and the thermal energy absorbed by the HTF. It is affected by ambient conditions such as temperature, as well as incident flux on the receiver surface, however, the seasonal

change is minimum, resulting in the value for $\eta_{rec,CR}$ being constant in the HLEM at 89% [277], [278].

In order to calculate the effect of solar-geometry on optical efficiency, a polynomial equation is used, as derived by [219], and depicted in Equation 6. 21. The advantage of this polynomial is that it captures the impact of the change in incidence angle (θ_i), calculated in Equation 6. 14, on optical efficiency, which is by far the greatest contributor. This polynomial is derived from surround field layouts.

Equation 6. 21: Polynomial for geometric optical efficiency of surround layout heliostat field

$$\eta_{GO,CR} = 0.4254\theta_i^6 - 1.148\theta_i^5 + 0.3507\theta_i^4 + 0.755\theta_i^3 - 0.5918\theta_i^2 + 0.0816\theta_i + 0.832$$

Because of the surround-field layout on which this polynomial is based, it predicts a decrease in Solar Field efficiency in the winter months (June – August for Southern Hemisphere), as shown in Figure 6. 7 (a), with an increase in incidence angle, demonstrated in Figure 6. 7 (b). However, Figure 6. 7 (a) shows that the DHIS results (solid black line with triangle markers) predict an increase in solar-to-thermal efficiency in winter. This is mainly due to two primary factors. First, due to the high DNI conditions in summer, and because of the over-design of the field to accommodate DNI fluctuations yet still maintain the designed plant output, excess thermal load on the receiver must be avoided. This requires that parts of the heliostat field have to be defocused, which causes high dumping losses in summer, as reflected in Figure 6. 7 (a). During the winter months, less DNI fluctuations occur, thereby reducing the dumping due to extreme peaks in DNI. Second, it has been shown that because heliostats track the sun in two axes, the overall effect of cosine losses, the largest contributor to losses in geometric efficiency, is less variable than for PT plants, and in fact results in slightly higher optical efficiencies in the winter months [279], [280]. This can be explained by the fact that the largest part of the field is facing towards the direction of the sun in winter (north-facing polar layout), meaning that cosine losses actually decrease under these conditions. On average, these effects lead to a higher solar-to-thermal efficiency, and therefore solar-to-electric efficiency [281], as will be discussed in Section 6.3.9.

What is immediately apparent from Figure 6. 7 (a) is that the SF efficiency calculated with Equation 6. 21 results in a mirror image of the DHIS results. Because of this observation, the inverse of Equation 6. 21 was calculated around the average line of the calculated Solar Field efficiency values (dashed orange line with square markers). This inverse relationship to incidence angle is shown in Figure 6. 7 (b), and demonstrates the gradual increase in geometric efficiency with increased incidence angle. The inverse equation is shown in Equation 6. 22.

Equation 6. 22: Inverse polynomial for geometric optical efficiency of polar layout heliostat field

$$\eta'_{GO,CR} = -(0.4254\theta_i^6 - 1.148\theta_i^5 + 0.3507\theta_i^4 + 0.755\theta_i^3 - 0.5918\theta_i^2 + 0.0816\theta_i) + 0.7553$$

If Equation 6. 22 is used to calculate the monthly total overall SF efficiency, instead of Equation 6. 21, the profile (solid blue line with circular markers) matches the seasonal variation of the DHIS results much closer, as shown in Figure 6. 7 (a). In this work, Equation 6. 22 will be used throughout to replicate the results from the DHIS in further calculations. The final overall solar field efficiency is calculated according to Equation 6. 23. It is suggested that in-depth ray-tracing simulations are conducted to evaluate the effect of heliostat field layout (polar vs. surround) and the location's latitude and DNI on the seasonal variation of overall SF efficiency in more detail.

Equation 6. 23: Calculation of Central Receiver Solar-to-thermal efficiency

$$\eta_{SF,CR,m} = \eta'_{GO,CR,m} \times \eta_{NGO,CR} \times \eta_{rec,CR}$$

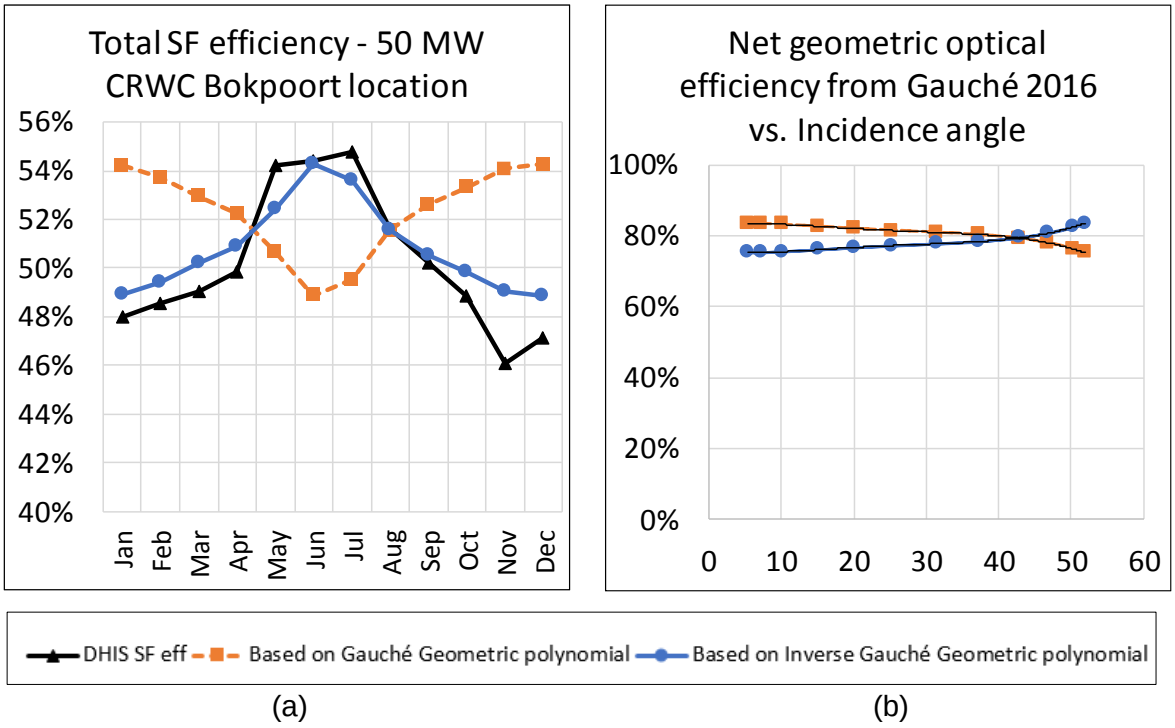

Figure 6. 7: a) Net geometric efficiencies per monthly incidence angle, b) Monthly total Solar field efficiencies

6.3.8. Boiler and steam turbine efficiencies (η_{BST})

The final efficiency required to calculate the monthly solar to electric efficiency of a CSP plant at any location is the combined boiler and steam turbine efficiency (η_{BST}). This efficiency takes into account the efficiency of the thermal processes involved in generating and superheating steam, the expansion of the steam through a turbine-set, and the condensation, or cooling, of the steam in either a wet-cooled condenser (WCC) or air-cooled condenser (ACC), before the steam is returned to the SGS to start the process again. This entire process is known as the Rankine cycle, and is typical in most large-scale thermal power plants. The use of a fixed η_{BST} to estimate annual CSP performance is commonplace, with the only dynamic aspect being to adjust for CSP and cooling technology combinations [282], [283]. However, in order to capture the sensitivity of CSP plants' performance to both cooling technology selection and spatiotemporally varying atmospheric conditions, a more dynamic approximation of η_{BST} is required. One approach that has demonstrated remarkable accuracy is the Chambadal-Novikov cycle efficiency (η_{CH}), shown in Equation 6. 24 [216], [217].

Equation 6. 24: Calculation of the Chambadal-Novikov cycle efficiency

$$\eta_{CH} = 1 - \sqrt{\frac{T_L}{T_H}}$$

The Chambadal-Novikov cycle efficiency relies only on a heat-source (T_H) and -sink (T_L) temperature in Kelvin. As is widely understood in thermal power plants using the Rankine

cycle, the greater the difference between these two temperatures, the greater the amount of work that can be done, and the higher the efficiency. The obvious benefit of WC plants, is that the T_L temperature reaches that of the wet-bulb temperature (T_{WB}) of the atmospheric conditions, which is always lower than that of the dry-bulb temperature (T_{DB}), unless the relative humidity (RH) is 100%, meaning they will be equal. T_{WB} is calculated as shown in Section 5. The T_L value, however, is never exactly equal to the T_{WB} due to thermodynamic limits on the cooling efficiency of the condenser. Generally, the T_L achieved by a WCC is about 10^{O}C warmer than T_{WB}, and this difference is known as the approach (T_{Δ}). It depends on the design of the condenser and cooling towers, and the smaller this value is, the more expensive and larger the cooling tower will be [284]. The results for T_{Δ} from the DHIS are shown in Figure 6. 8, where it can be seen that although there is an apparent increase in T_{Δ}, this is accompanied by a decrease in T_{wb}, in degrees Celsius, resulting in an overall decrease in the cooling tower outlet temperature, thereby improving the cooling tower performance.

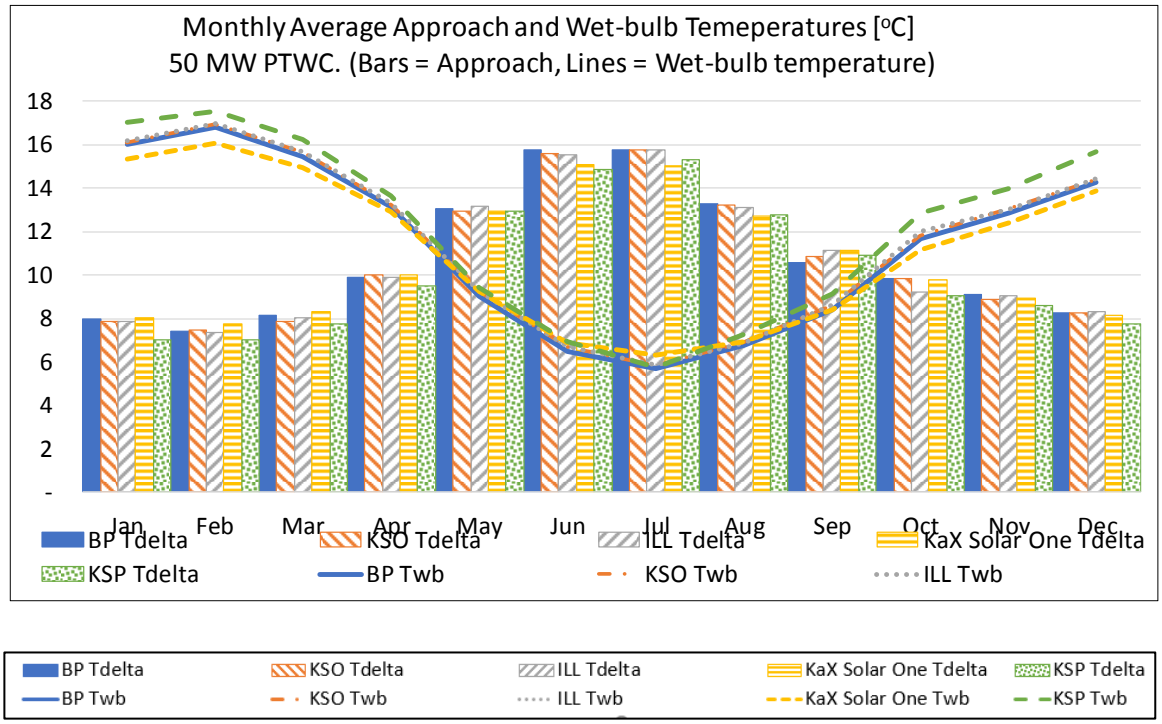

Figure 6. 8: Monthly average approach and wet bulb temperatures for all locations – 50 MW PTWC

It might be argued that this variance in approach needs to be captured in the HLEM. However, it was found that for the PTWC configuration, taking an average T_{Δ} of 10.6^{O}C between all locations' annual averages, the impact on overall solar-to-electric efficiency was minimal. This allows for more simplification of the final HLEM, without compromising extensively on accuracy. Finally, for the T_H value, this is taken as the temperature of the steam reached in the final stages of the SGS, prior to entering the turbine(s), in degrees Celsius [27]. Literature shows that this value is typically around 371^{O}C for PT [223] and 540^{O}C for CR CSP plants [222]. The monthly averages of T_H from the DHIS results are shown in Table 6. 5. Table 6. 5 also shows that the percentage monthly variance from the annual average is acceptably low, allowing for the use of the annual average of T_H between all locations of 375^{O}C for PT plants, and 547^{O}C for CR plants in the HLEM.

Table 6. 5: Annual average T_H values and percentage monthly variance for all locations - 50 MW PTWC

Agreement parameter	Bokpoort	Khi Solar One	Illanga	Kaxu/Xina Solar One	Kathu Solar Park
Annual avg T_H (^{O}C) - PT	375.57	375.38	376.34	377.72	373.63
% Variance from annual avg - PT	1.70%	3.53%	2.50%	2.24%	2.85%
Annual avg T_H (^{O}C) - CR	547.30	547.38	547.35	547.35	546.69
% Variance from annual avg - CR	0.13%	0.13%	0.14%	0.14%	0.77%

This reduces the calculation of $\eta_{gross,m}^{PB}$ to Equation 6. 25 for WC, and Equation 6. 26 for DC, based on the Chambadal-Novikov cycle efficiency and the assumptions discussed above.

Equation 6. 25: Calculation of $\boldsymbol{\eta_{gross,m}^{PB}}$ for WC

$$\eta_{gross,WC,m}^{PB} = 1 - \sqrt{\frac{(\boldsymbol{T_{wb}} + 10.6 + 273.15)}{T_H + 273.15}}$$

Equation 6. 26: Calculation of $\boldsymbol{\eta_{gross,m}^{PB}}$ for DC

$$\eta_{gross,DC,m}^{PB} = 1 - \sqrt{\frac{(\boldsymbol{T_{db}} + 10.6 + 273.15)}{T_H + 273.15}}$$

To compare the results for $\eta_{gross,m}^{PB}$ from this approach to the monthly boiler and steam turbine efficiency results from the DHIS, the calculation in Equation 6. 27 was used. The comparison between the 50 MW PTWC/DC and 50 MW CRWC/DC DHIS $\eta_{gross,m}^{PB}$ and updated Chambadal-Novikov approach are shown in Figure 6. 9 (a) to (d). The black lines indicate the reference values from literature for annual cycle efficiency for PTWC and CRWC plants [223], [285]. It should be noted that the design points for WC and DC plants will differ, depending on the operating conditions achievable by the particular cooling technology under the mean and worst-case atmospheric conditions. The design points, however, were the same for both cooling technologies in the DHIS simulations.

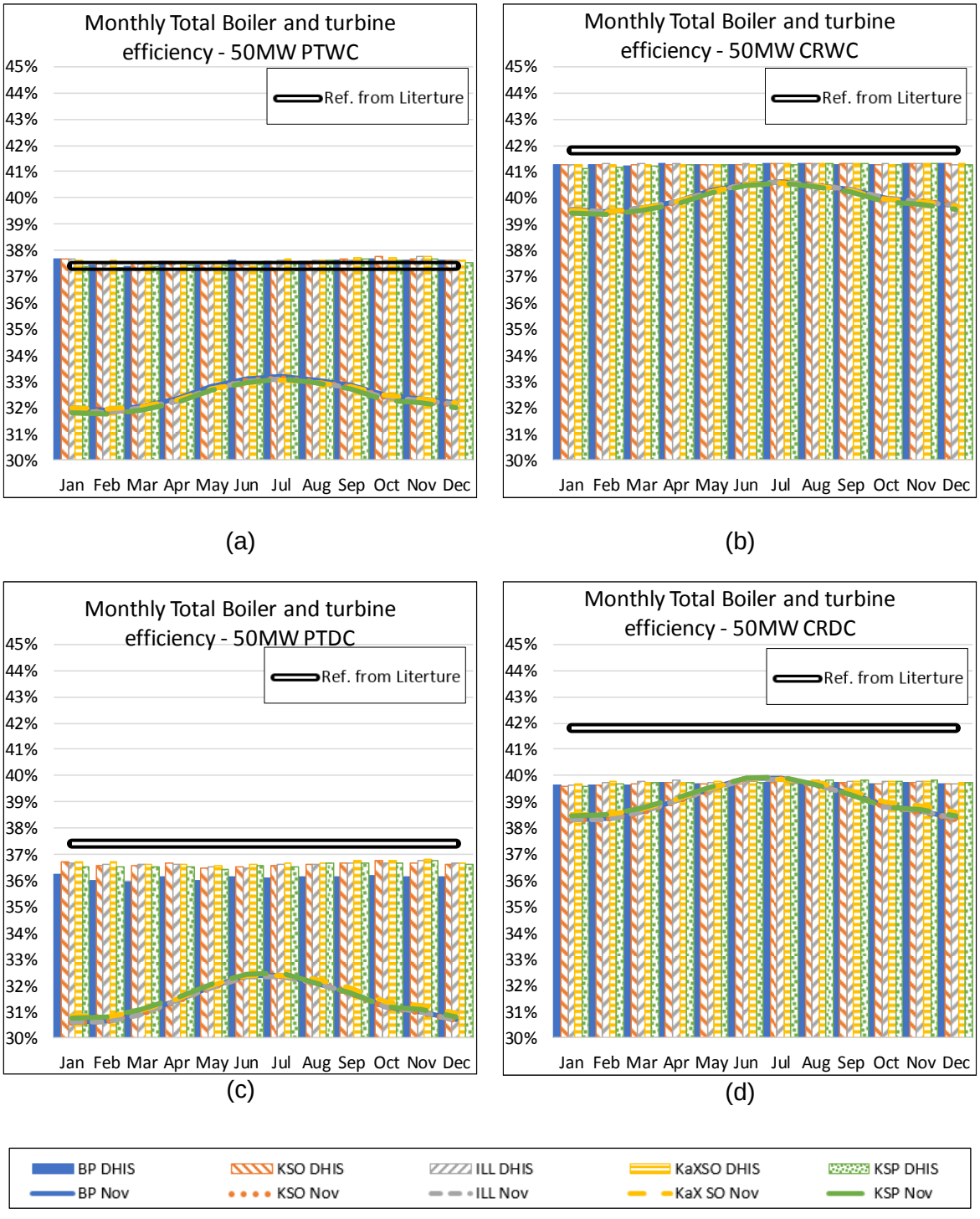

Figure 6. 9: Monthly Total Boiler and turbine efficiency for (a) 50 MW PTWC, (b) 50 MW CRWC, (c) 50 MW PTDC, (d) 50 MW CRDC. NOTE: Nov – Efficiency calculated based on Equation 6. 25 and Equation 6. 26, Values used for Ref. from Literature [223], [285].

Figure 6. 9 shows how the annual mean η_{BST} of the dry-cooled (DC) configurations, calculated from the DHIS results, is 1.06% and 1.55% lower than that of the wet-cooled plants, across all locations, for PT and CR, respectively.

Equation 6. 27: Calculation of monthly $\eta_{gross,m}^{PB}$ from DHIS results

$$\eta_{gross,m}^{PB} = \frac{E_{gross}}{Q_{PB,i}}$$

From Figure 6. 9 it is clear that the $\eta_{gross,m}^{PB}$ calculated according to the updated Chambadal-Novikov approach (lines) are substantially lower than both those calculated from the DHIS results, as well as the reference value from literature for all modelled locations and configurations. However, when this value is incorporated into the final solar-to-electric efficiency from Equation 6. 5, the results compare remarkably well with those calculated from the DHIS results, calculated according to Equation 6. 2. This is shown in Section 6.3.9.

6.3.9. Overall solar-to-electric efficiency (η_{SE})

The overall monthly solar-to-electric efficiency is the final parameter that captures a CSP plant's performance, and how it is impacted by the technology, location, and season. As indicated in Equation 6. 2, the $\bar{\eta}_{net,solar,m}$ is calculated from the DHIS results as the ratio between the monthly total net electricity generated (E_{net}) and the monthly total incident DNI on the solar field ($H_{SF,m}$). The results for the monthly $\bar{\eta}_{net,solar,m}$ values from the HLEM are compared to those calculated from the DHIS for the 50 MW PTWC/DC in Figure 6. 10 (a) and (c), and for the 50 MW CRWC/DC in Figure 6. 10 (b) and (d).

The increases in $\bar{\eta}_{net,solar,m}$ due to increases in $\bar{\eta}_{gross,m}^{PB}$ associated with larger steam turbines (50 MW vs 100 MW) were found to be marginal, as shown in [286]. The relative annual average $\bar{\eta}_{net,solar,m}$ from the DHIS, across all locations for the 100 MW PTWC configurations was 14.44%, compared to 14.06% for the 50 MW PTWC plants. Since the aim of this work is to quantify power generation potential and water consumption over large spatial areas, the slight under-estimation in $\bar{\eta}_{gross,m}^{PB}$, and consequently $\bar{\eta}_{net,solar,m}$, did not result in considerable loss of accuracy, while maintaining calculation ease and robustness.

Table 6. 6 shows how the percentage annual average difference between HLEM and DHIS results for η_{SE} varies between -2.46% and -0.41%, and between -2.16% and 0.05% for PTWC/DC and CRWC/DC, respectively, for all locations.

Table 6. 6: Agreement parameters for solar-to-electric efficiencies for PT and CR configurations for all locations

CSP Configuration	Agreement parameter	Bokpoort	Khi Solar One	Illanga	Kaxu/Xina Solar One	Kathu Solar Park
50 MW PTWC	% Annual diff	-0.89%	-1.40%	-0.71%	-1.32%	-0.41%
	% RMSE	3.37%	3.95%	4.53%	4.80%	3.87%
50 MW CRWC	% Annual diff	-1.49%	-1.56%	-1.20%	-2.16%	-0.39%
	% RMSE	2.58%	2.42%	3.20%	2.82%	2.39%
50 MW PTDC	% Annual diff	-1.36%	-2.46%	-1.88%	-2.07%	-1.36%
	% RMSE	3.84%	4.50%	4.62%	5.04%	4.03%
50 MW CRDC	% Annual diff	-1.89%	-1.96%	-1.88%	-1.61%	0.05%
	% RMSE	2.72%	2.42%	3.19%	2.89%	2.12%

Furthermore, Table 6. 6 shows that the monthly percentage RMSE, an indication of how much each month's $\bar{\eta}_{net,solar,m}$ HLEM results differ from the DHIS results, is only between 3.37%

and 5.04% for PTWC/DC and between 2.12% and 3.20% for CRWC/DC. This shows that the approach used to calculate the HLEM $\bar{\eta}_{net,solar,m}$ is accurately replicating the results from the detailed hourly interval simulations for each both PT and CR configurations[12] and locations.

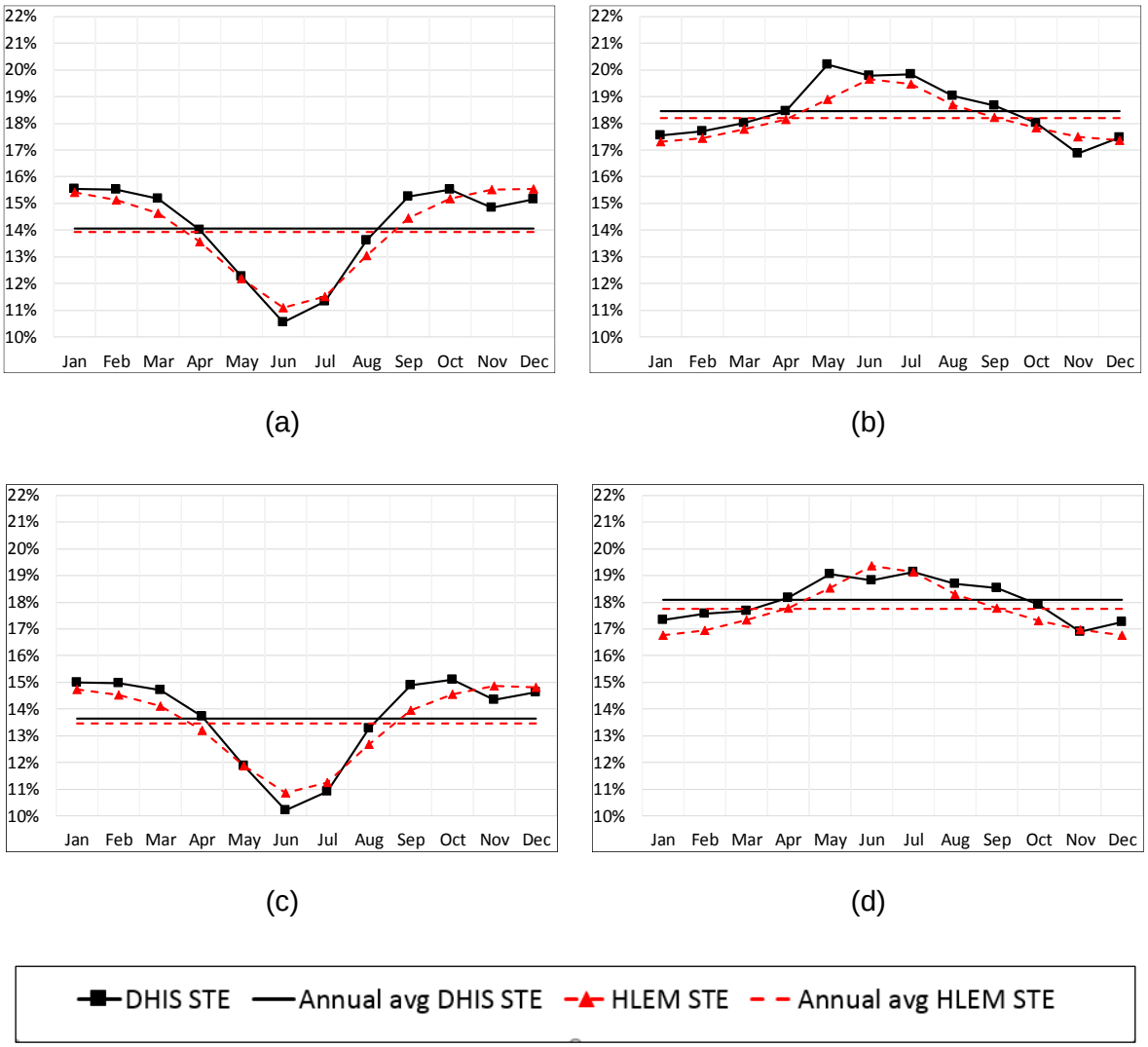

Figure 6. 10: Monthly overall $\bar{\eta}_{net,solar,m}$, results at Bokpoort location for: (a) 50 MW PTWC, (b) 50 MW CRWC, (c) 50 MW PTDC, (d) 50 MW CRDC

Considering the fact that this is a highly simplified approach, capable of estimating CSP plant performance for different CSP technology and cooling technology configurations, and spatiotemporally varying atmospheric and meteorological conditions, this level of accuracy can be considered acceptable. To summarize, Equation 6. 5 was used to calculate these monthly solar-to-electric efficiencies. The adjusted and validated assumptions for each efficiency were discussed in Sections 6.3.1 to 6.3.9.

[12] The configurations considered in this study only, not all possible CSP plant configurations.

6.3.10. Validation parameters

The validation parameters used to test the agreement between the HLEM's results and the reference DHIS results are percentage Annual Average Difference Error (AADE) and percentage Root Mean Square Error (RMSE). The AADE reflects the accuracy of the HLEM's capability to estimate a certain performance parameter based on the percentage difference between the annual total or average of that estimated parameter and the annual total or average of the reference parameter from the DHIS results. It is calculated based on Equation 6. 28, and is illustrated for net electricity for the 50 MW PTWC Bokpoort location in Figure 6. 11 (b). In this example, in Figure 6. 11 (b), A is the sum of the monthly net electricity generation (annual generation) as determined by the reference DHIS, while B is the same parameter, as determined by the HLEM.

Equation 6. 28: Calculation of AADE

$$AADE = \frac{A - B}{A} \ [\%]$$

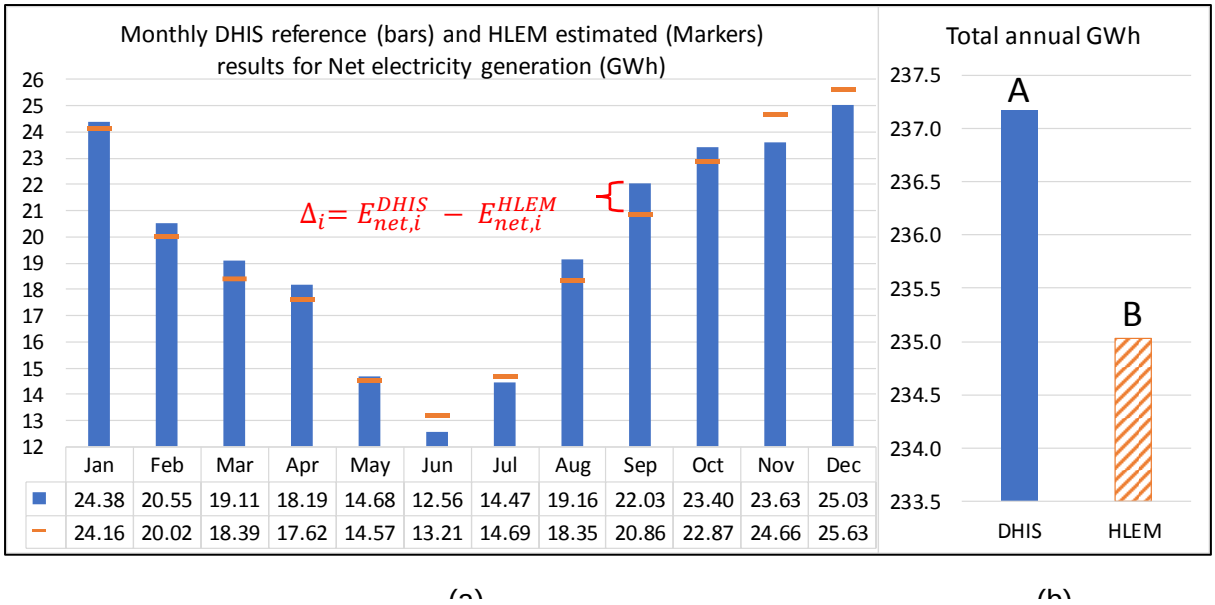

Figure 6. 11: Validation parameters explanation: (a) Monthly Net Electricity, (b) Total annual Net Electricity for 50 MW PTWC Bokpoort location

To calculate the other agreement parameter, RMSE, Equation 6. 29 is used, and illustrated in Figure 6. 11 (a). It is the average of the square root of the squared percentage error for all months. It is an effective indication the percentage error for each month i ($\frac{\Delta_i}{Q_{ELNET\,i}}$) over an entire year, and shows how well the HLEM matches the seasonal changes in performance parameter estimation (in this case, Net electricity generated in GWh). In the data-table below the graph in Figure 6. 11 (a), the values for $E_{net,i}^{DHIS}$ (top row) and $E_{net,i}^{HLEM}$ (bottom row) are given. For example, for the months of January and June, the percentage errors are -0.92% and 5.23%, respectively, between the HLEM and DHIS results. These errors are all squared and then rooted, to remove negative values. The average of all these values are then taken for the number of intervals (n, in this case 12 months), and presented as an agreement parameter showing fit between HLEM and DHIS. In this example, the AADE is -0.90% and the RSME is 3.05%, meaning that the total annual net electricity generation estimation by the HLEM is -0.90% lower than that of the DHIS, and the average monthly percentage error is 3.05%.

Equation 6. 29: Calculation of RMSE

$$RMSE = \frac{\Sigma \sqrt{[\frac{\Delta_i}{E_{net,i}^{DHIS}}]^2}}{n} [\%]$$

6.4. Results – Comparison Between High-level and Detailed Models

6.4.1. Monthly net generation potential (GWh)

The monthly net generation results of the reference DHIS for all five locations, for each configuration of the PT and CR CSP plants, are compared to the results of the HLEM, in Figure 6. 12 (a) to (d). The agreement parameters of this set of results are shown in Table 6. 7. Figure 6. 12 (a) and (c) compare the DHIS and HLEM results for the 50 MW PTWC/DC, respectively, and Figure 6. 12 (b) and (d) show the results for the 50 MW CRWC/DC, respectively.

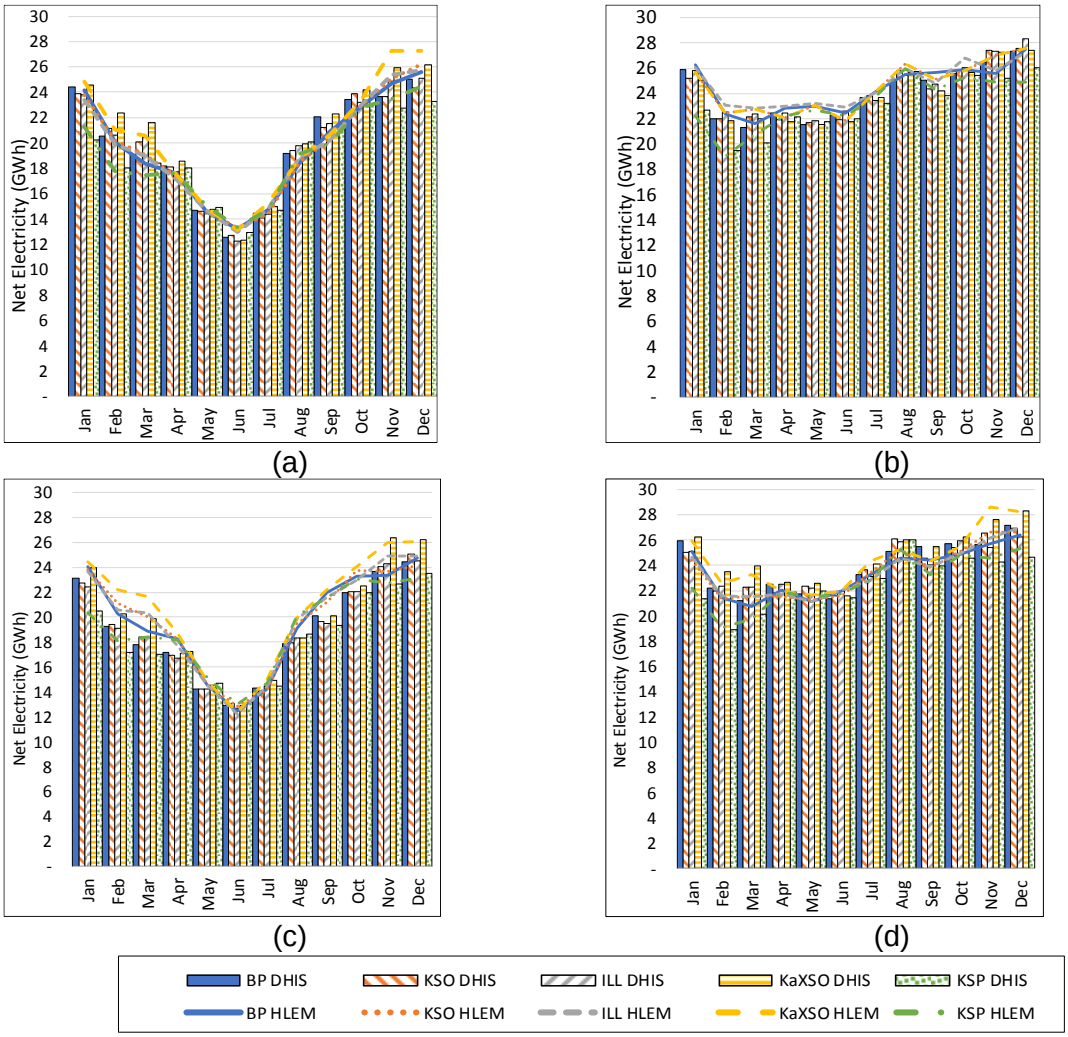

Figure 6. 12: DHIS vs. HLEM results for Monthly Total Net Generation in GWh for: (a) 50 MW PTWC, (b) 50 MW CRWC, (c) 50 MW PTDC, (d) 50 MW CRDC

Table 6. 7 shows that the HLEM results for total annual net electricity differs from the DHIS results by between -4.67% and -0.38% for PT plants, and between -2.05% and 0.11% for CR plants, across all locations and cooling configurations. The observed underestimation of net generation by the HLEM for most plants and locations is attributed to the generally conservative use of assumptions throughout the model.

The RMSE in Table 6. 7, for PT plants, varies between 3.05% and 4.99%, and for CR plants between 2.04% and 3.20%, indicating that the average percentage difference between monthly net generation estimated by the HLEM and the DHIS results is low. This demonstrates a high level of seasonal conformity to the DHIS results. In general, the HLEM results for monthly net generation potential (GWh) is acceptably accurate for all CSP and cooling configurations considered, across all locations, as seen in Figure 6. 12 (a) to (d). This demonstrates the capability of the HLEM to capture impacts on operation from both technology configuration and spatiotemporal changes.

Table 6. 7: Agreement parameters for monthly net generation potential for all CSP configurations and locations

CSP Configuration	Agreement parameter	Bokpoort	Khi Solar One	Illanga	Kaxu/Xina Solar One	Kathu Solar Park
50 MW PTWC	% Annual diff	-0.90%	-1.43%	-0.60%	-1.22%	-0.38%
	% RMSE	3.05%	3.83%	4.36%	4.64%	3.73%
50 MW CRWC	% Annual diff	-1.37%	-1.46%	-0.95%	-2.05%	-0.25%
	% RMSE	2.58%	2.42%	3.20%	2.82%	2.39%
50 MW PTDC	% Annual diff	-3.58%	-4.67%	-3.95%	-4.15%	-3.49%
	% RMSE	4.27%	4.94%	4.98%	4.99%	4.10%
50 MW CRDC	% Annual diff	-1.96%	-1.92%	-1.72%	-1.52%	0.11%
	% RMSE	2.67%	2.38%	3.10%	2.81%	2.04%

6.4.2. Monthly water consumption factor (m³/MWh)

The calculation of monthly water consumption factor for wet-cooled plants, is done as specified in Section 5. For completeness, the equation used to calculate the monthly consumption factor ($I_{WC,m}$, m³/MWh) is given in Equation 6. 31. k_{SENS} refers to the fraction of heat load rejected through sensible heat transfer, meaning that $(1 - k_{SENS})$ represents the fraction rejected by evaporation, and is based on a correlation between it and ambient dry-bulb temperature, as shown in Equation 6. 30, developed by [34]. n_{CC} refers to the cycles of concentration (chosen as 5) and I_{PROC} is the consumption factor allocated to other non-cooling processes. The term $\left(1 - \left(\bar{\eta}_{pipe,m} \times \bar{\eta}_{TES,m}\right)\right)$ refers to the amount of energy lost to other heat-sinks, in this case to piping losses and storage losses, while $(\bar{\eta}_{aux,m} \times \bar{\eta}^{PB}_{gross,m})$ refers to the amount of energy used to generate net electricity output.

Equation 6. 30: Calculation of sensible heat rejection fraction

$$k_{SENS,n} = \left[-0.000279 \times {T_{DB}}^3 + 0.00109 \times {T_{DB}}^2 - 0.345 \times T_{DB} + 26.7\right] \div 100$$

Equation 6. 31: Calculation of consumption factor

$$I_{WC,m} = 3600 \frac{\left(1 - (\bar{\eta}_{aux,m} \times \bar{\eta}^{PB}_{gross,m}) - (1 - (\bar{\eta}_{pipe,m} \times \bar{\eta}_{TES,m})\right)}{(\bar{\eta}_{aux,m} \times \bar{\eta}^{PB}_{gross,m})} \frac{\left(1 - k_{SENS,m}\right)}{\rho h_{fg}} \left(1 + \frac{1}{n_{CC} - 1}\right) + I_{PROC}$$

At dry-cooled plants, $k_{SENS,m}$ is equal to 1, meaning that all heat is rejected through sensible heat exchange with the dry air. Therefore, the parameter I_{PROC} will be the only contribution to consumptive use at any dry-cooled CSP plant, and typically includes the mirror cleaning, boiler blowdown and –tempering, and component cooling make-up. The values used in the DHIS modelling of the dry-cooled plants were found to be too optimistic, resulting in monthly consumption factors of between 0.13 m^3/MWh and 0.19 m^3/MWh, irrespective of installed capacity or location. Data obtained from an operational PTDC plant in South Africa, reflected monthly consumption factors between 0.46 m^3/MWh and 0.78 m^3/MWh, about 274% greater than the results from the DHIS. For this reason, for wet-cooled configurations (both PT and CR), I_{PROC} is selected as 0.3 m^3/MWh, based on extensive modelling by NREL and WorleyParsons on PTWC/DC plants [35].

The consumption data from the operational reference PTDC in South Africa showed no distinct correlation with the month of operation. Furthermore, when it is considered that neither of these consumptive uses depend on thermal processes (cooling), the above observation is not surprising, also alluding to the independence from location-specific conditions. For this reason, the quantification of a consumption factor for dry-cooled plants was based on the annual average of the obtained data, at 0.56 m^3/MWh. When this value, along with the obtained total monthly net generation, is used to calculate the total monthly consumption for the dry-cooled plants in question, the percentage RMSE is 15% and the percentage difference in total annual consumption is 5% greater than the reference PTDC plant amount. For the purposes of the HLEM, this slight over-estimation in total annual consumption is acceptable for dry-cooled plants, since it is still substantially lower than that of wet-cooled plants, yet remains more representative of actual dry-cooled plant data than the results of the DHIS. The validation of the dry-cooled HLEM water consumption results is therefore not relative to the DHIS results, and certainly requires more accurate quantification and detailed investigation to determine actual sensitivity to spatiotemporal conditions.

To calculate the consumption factor from the DHIS results, Equation 6. 32 is used, with V_{tot} representing the total water consumption, and $E_{net,m}$ the net electricity generation for a specific month. V_{tot} is the sum of the makeup water for the cooling tower (losses and blowdown), mirror spray and brush losses, boiler blow-down and -losses as well as miscellaneous losses in the plant (domestic use etc.) for the entire month.

Equation 6. 32: Calculation of monthly consumption factor from DHIS results

$$I_{tot,m} = \frac{V_{tot,m}}{E_{net,m}}$$

The consumption factor used in the HLEM (Equation 6. 31), was calculated for both PT and CR wet-cooled configurations, at each location and every month of the year. The efficiencies used are those discussed in Sections 6.3.1 to 6.3.9. k_{SENS} only depends on the ambient dry-bulb temperature, as presented in Section 5, with the monthly average dry-bulb temperature being derived from the weather files used in the DHIS. It was found that, compared to the DHIS results, Equation 6. 31 underestimates the cooling component of annual mean water consumption factor for PTWC plants on average by -3.08% across all locations. Conversely, it overestimates the cooling component of annual mean water consumption factor for CRWC

plants on average by 3.86% across all locations. This points to the fact that Equation 6. 31 uses the boiler and steam turbine efficiency to determine the amount of heat not converted to electrical energy in the Rankine cycle, and which subsequently needs to be rejected by a cooling process. As shown in Section 6.3.8, the updated Chambadal-Novikov approach in Equation 6. 25 and Equation 6. 26 provide a conservative, low estimation of the boiler and steam turbine efficiency. However, because its accuracy improves at higher heat-source temperatures, as is the case for CR plants, this underestimation becomes less severe than for PT plants. This explains the overestimation in cooling water consumption factor for CR plants, since the efficiency used is higher than for PT plants.

Consequently, if the same I_{PROC} of 0.3 m^3/MWh is used for both PT and CR plants, the results for total water consumption factor can become somewhat distorted. Adding the 0.3 m^3/MWh to the already over-estimated cooling water consumption factor for CR plants results in large annual mean difference errors to the DHIS results, in the order of 11.37% across all locations. However, doing the same for PT plants, results in a much smaller annual mean difference error of 1.02% across all locations. However, if I_{PROC} is taken as 0.09 m^3/MWh for CR plants (the value suggested by the modelling software used), the annual mean difference error is 3.57% across all locations, substantially lower than the 11.37% if 0.3 m^3/MWh is used. It must be considered that the accuracy of the HLEM is being validated against the results of DHIS, based on the modelling software *ColSim CSP*. This software package, in turn, relies on certain assumptions on hourly consumption for the various processes in a CSP plant. Since the aim of this study is to refine a HLEM based on extensive simulations and their DHIS results, assumptions were made in order to most closely reflect the DHIS results, without contradicting literature.

Therefore, for PTWC plants, I_{PROC} is chosen as 0.3 m^3/MWh, and as 0.09 m^3/MWh for CRWC plants [135]. It was decided that this is an acceptable compromise since the final water consumption factor results for both PTWC and CRWC plants is within limits suggested by literature, as depicted in Figure 6. 13 (a) and (b). It shows the total monthly water consumption factor results of the reference DHIS for all five locations, for PTWC and CRWC plants, compared to the results of the HLEM, as well as to values from literature [135]. Figure 6. 13 (a) shows that the HLEM results for total water consumption factor of PTWC plants are closely replicating the values from the DHIS and are also within the range given in literature. Figure 6. 13 (b), however, shows that the HLEM is underestimating total water consumption factor for CRWC plants when the lower I_{PROC} is used, compared to literature, but is slightly overestimating compared to the DHIS results. The selection of I_{PROC} is a simple step, and can therefore be adjusted based on improved input information when the HLEM is finally implemented.

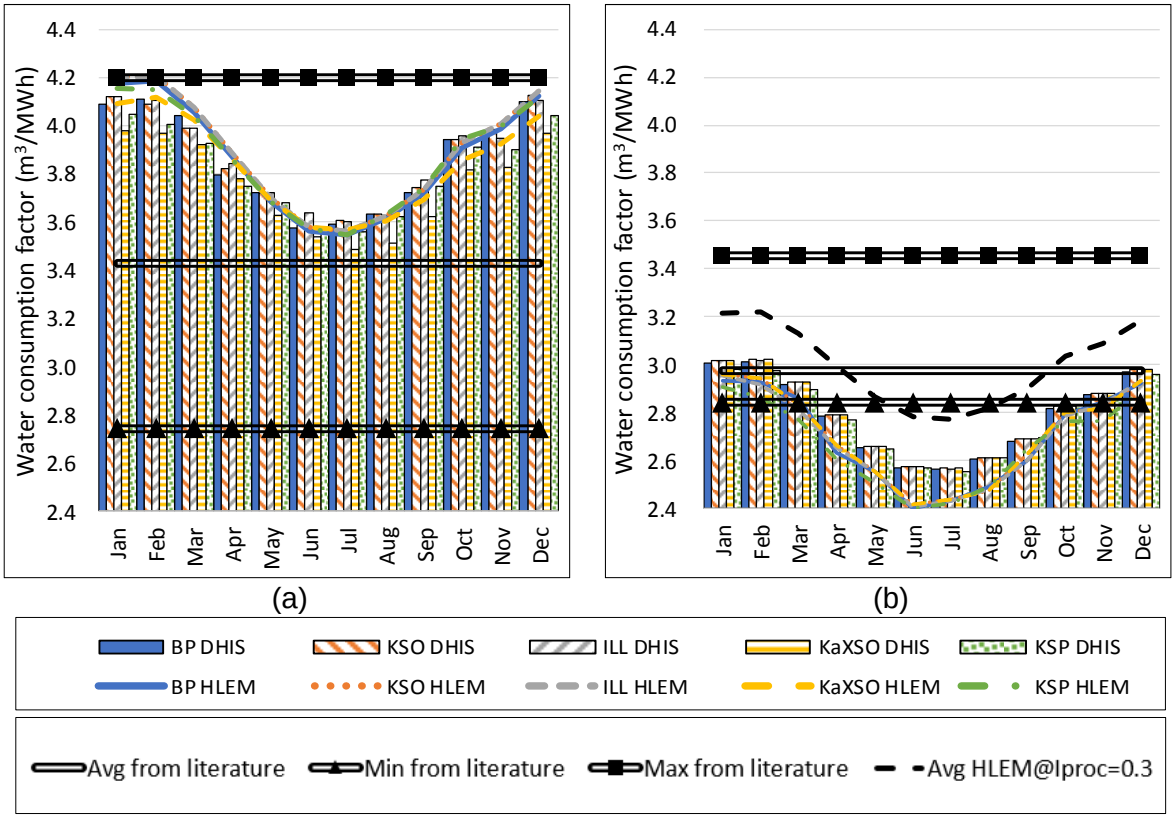

Figure 6. 13: DHIS vs. HLEM results: Monthly consumption factor in m3/MWh for all locations: (a) 50 MW PTWC and (b) 50 MW CRWC

The agreement parameters of this set of results are shown in Table 6. 8.

Table 6. 8: Agreement parameters for consumption factor for all wet-cooled CSP configurations and locations

CSP Configuration	Agreement parameter	Bokpoort	Khi Solar One	Illanga	Kaxu/Xina Solar One	Kathu Solar Park
50 MW PTWC	% Annual diff	0.28%	0.49%	0.60%	2.22%	1.50%
	% RMSE	0.93%	1.27%	1.01%	2.21%	1.55%
50 MW CRWC	% Annual diff	3.35%	3.35%	3.69%	3.35%	4.14%
	% RMSE	3.46%	3.45%	3.79%	3.45%	4.21%

6.4.3. Monthly total water consumption (m^3)

Now that the solar-to-electric efficiency, total monthly net electricity generation, and the total water consumption factor can be calculated, the total monthly consumption can finally be estimated, as shown in Equation 6. 33.

Equation 6. 33: Calculation of total monthly water consumption

$$V_{tot,m} = I_{WC,m} \times E_{net,m}$$

The monthly total water consumption results of the HLEM for all five locations, for each configuration of the Parabolic Trough CSP plants, are compared to the results of the reference DHIS, in Figure 6. 14 (a) and (b). The HLEM results for the two DC configurations are shown in Figure 6. 14 (c) and (d), without comparison to the DHIS results for the reasons discussed in Section 6.2.1.

It might be argued that since the major drivers of consumption at PTDC plants are non-thermal, and generally unrelated to the cooling of the plant, total consumption should not be directly proportional to total generation. However, when it is considered that one of the major contributors to non-cooling water is solar field cleaning, and that the size of the solar field is directly proportional to plant installed capacity, as well as that boiler-related consumption is proportional to generation, this approach is acceptable. Certainly, if plant data were available for PTDC plants of varying installed capacities, these relationships could be more accurately quantified. For the high-level purpose of this work, the use of the constant consumption factor, irrespective of location, season, or plant configuration, will suffice.

Table 6. 9 shows that for the 50 MW PTWC plants the average percentage difference in HLEM results, relative to the DHIS, in total annual water consumption is between -0.82% and 1.25%, and between 1.18% and 3.93% for the 50 MW CRWC plants, across all locations. The RMSE for the PTWC and CRWC plants ranges between 3.32% and 4.75%, and between 2.72% and 4.50%, respectively. This shows that the series of calculations leading up to the total monthly water consumption provides results which show high accuracy as well as corresponding seasonal variation.

As would be expected, the monthly consumption for the 100 MW CSP plants are roughly double that of the 50 MW plants. Furthermore, the total monthly consumption of the PTDC plants are substantially lower, at about only 14% that of the PTWC plants.

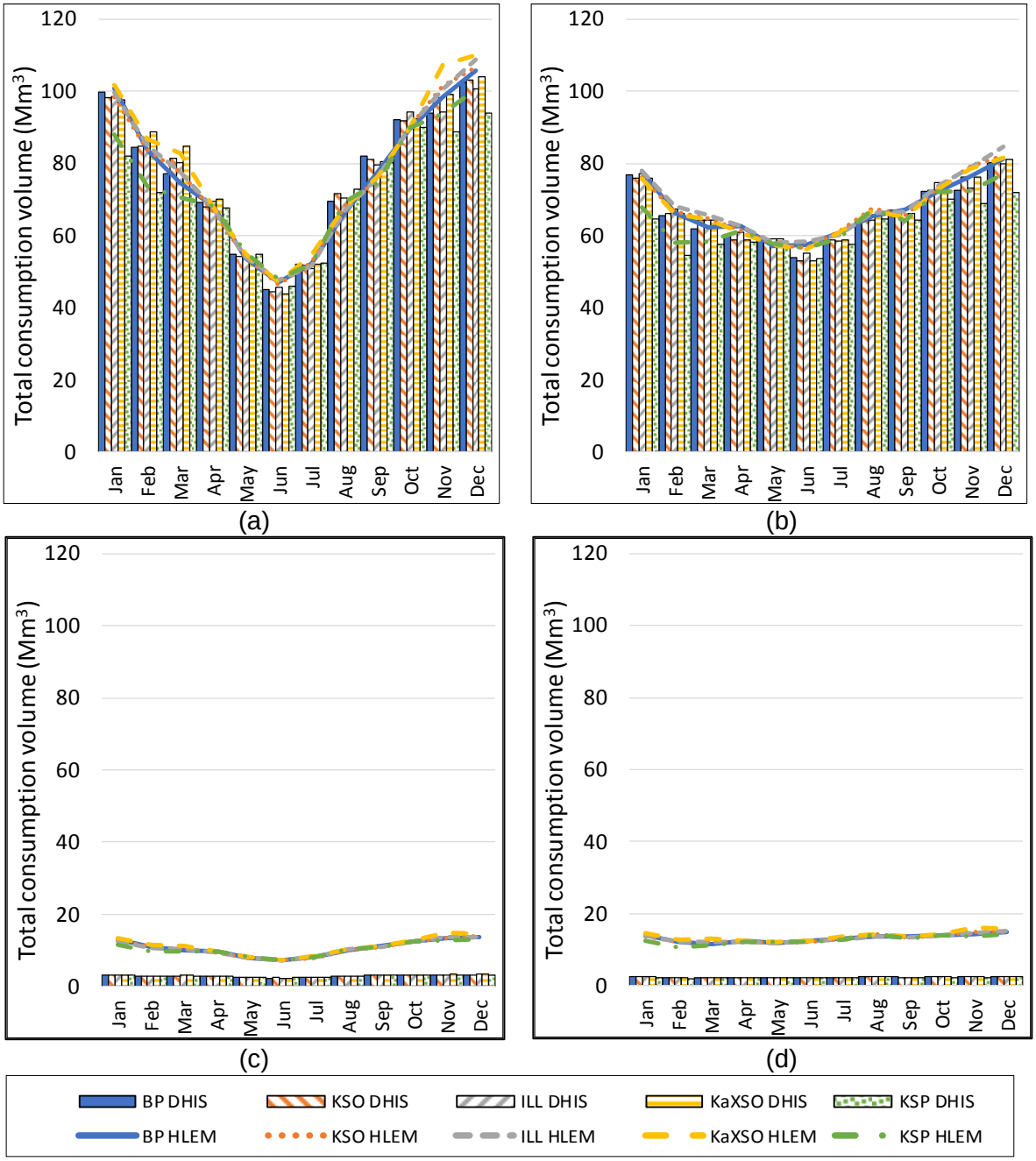

Figure 6. 14: HLEM results for monthly total consumption in Mm3: (a) 50 MW PTWC, (b) 50 MW CRWC, (c) 50 MW PTDC, (d) 50 MW CRDC

It might be argued that since the major drivers of consumption at PTDC plants are non-thermal, and generally unrelated to the cooling of the plant, total consumption should not be directly proportional to total generation. However, when it is considered that one of the major contributors to non-cooling water is solar field cleaning, and that the size of the solar field is directly proportional to plant installed capacity, as well as that boiler-related consumption is proportional to generation, this approach is acceptable. Certainly, if plant data were available for PTDC plants of varying installed capacities, these relationships could be more accurately quantified. For the high-level purpose of this work, the use of the constant consumption factor, irrespective of location, season, or plant configuration, will suffice.

Table 6. 9 shows that for the 50 MW PTWC plants the average percentage difference in HLEM results, relative to the DHIS, in total annual water consumption is between -0.82% and 1.25%, and between 1.18% and 3.93% for the 50 MW CRWC plants, across all locations. The RMSE for the PTWC and CRWC plants ranges between 3.32% and 4.75%, and between 2.72% and 4.50%, respectively. This shows that the series of calculations leading up to the total monthly water consumption provides results which show high accuracy as well as corresponding seasonal variation.

Table 6. 9: Agreement parameters for total monthly consumption – Wet-cooled Parabolic Trough, all locations

CSP Configuration	Agreement parameter	Bokpoort	Khi Solar One	Illanga	Kaxu/Xina Solar One	Kathu Solar Park
50 MW PTWC	% Annual diff	-0.53%	-0.82%	0.12%	1.03%	1.25%
	% RMSE	3.32%	3.53%	4.25%	4.75%	4.45%
50 MW CRWC	% Annual diff	1.91%	1.80%	2.69%	1.18%	3.93%
	% RMSE	3.11%	3.07%	3.81%	2.72%	4.50%

For the PTDC results, since a constant, static consumption factor is used, little can be speculated of the accuracy to the DHIS, since its results were found to be too low compared to operational data for a 100 MW PTDC in South Africa. However, because there is little causal correlation between monthly water consumption factor and season, it is expected that the RMSE will be high, but the total annual percentage difference will be small. Since the scale in difference between the dry-cooled and wet-cooled plants is in the right order of magnitude (around 90% less), the results can be used to compare the variable demands associated with the two cooling technologies.

6.5. Conclusions

This work aimed to provide a validated improved approach to use system efficiencies to estimate CSP plant generation and water consumption. The work is based on the application of the typical annual efficiency approach, with the updated approach being capable of accurately quantifying monthly performance without computationally expensive hourly modelling. The validation process used detailed hourly-interval simulation (DHIS) results for a reference PT CSP plant, and equivalent CR plant, in five different locations, with two different cooling technologies and two different installed capacities. These hourly interval results were used to characterise monthly changes in system efficiencies. These characterisations were then employed in the updated high-level efficiency model (HLEM). The agreement parameter used to measure validity and relative accuracy of the final HLEM was the annual average difference error (AADE) in net generation, total water consumption, and water consumption factor. The agreement parameter used was that of percentage root mean squared error (RSME) between the monthly DHIS results and the HLEM estimations.

The work resulted in a set of simple equations that can be used in the HLEM to quantify the monthly performance (net generation and water consumption) of a CSP plant of a specific technology (Central Receiver or Parabolic Trough) and cooling technology (dry- or wet-cooled) at any location. In order to calculate monthly performance, however, monthly datasets are required for the relevant input parameters, namely monthly total DNI, average dry-bulb temperature, average relative humidity, and location latitude and longitude. Once this input data is available for the location and month of interest, the model can be used to quickly estimate both the total monthly net generation, and the monthly total water consumption. The goal of developing this updated HLEM is to be able to calculate these two performance

indicators for a large geographical area (thousands of locations) for any month of the year, in order to perform spatiotemporal assessments of regional and national CSP plant performance. The specific focus is to assess spatiotemporal changes in water demand from different CSP-cooling configurations and capacities with low computational expense, in order to inform fact-based national policies in CSP infrastructure deployment and water resource management.

The HLEM is not intended to provide bankable yield assessments of CSP plant operations, nor the capability to do any form of operational, scheduling, solar field design, or economic optimization. The HLEM, therefore, makes use of practical, simplified approaches in order to characterise monthly generation potential and water consumption within reasonable accuracy, at the expense of detailed theoretical modelling principles. This enables it to perform these estimations across vast geographic expanses and at sub-annual temporal scales, with reasonably few inputs and calculation steps. The small geographic distribution of sites simulated in the DHIS for South Africa, does pose a potential limit to direct application in other global regions, but this should be tested prior to discounting the current set of equations and assumptions capabilities. The final HLEM, and approach followed, is however easily adaptable to other regions due to the systematic use of localized DHIS simulations and efficiency assumptions from proven, widely used literature-derived values.

Chapter 7 – Water and CSP – Linked CSP water demand models and national hydrology data to manage CSP development and water resource sustainability in arid regions

7.1. Introduction – Water Availability and CSP

The water-energy-food (WEF) nexus is a term used to describe the complex interactions and interdependencies between water as a naturally fluctuating resource, energy as our means to perform work, and food as a source of sustenance. The interactions of these three systems have been well documented since the first international recognition of its importance at the Bonn 2011 Nexus Conference [287]–[289]. Since then, nexus thinking and approaches are becoming more common in creating sustainable development pathways [290], and ensuring resource security of these three systems [291]. However, while using the WEF nexus as the basis for policy planning is crucial for resource security and sustainable development, it can remain stuck as a theoretical ideal only, never finding practical implementation in resource management due to gaps between conceptualisation and application [292]. Beyond gaps in governance and inter-sectoral harmonization in policy planning, the actual quantification of the dynamics between water, energy and food systems remains a challenge, and practical investigations of the spatiotemporal dynamics of variable resource availability and demand are lacking in addressing the WEF nexus [293].

In this work, the focus is placed particularly on the water-energy dynamics of the WEF nexus, with attention to a specific dilemma being faced by Concentrating Solar Power (CSP) developments in arid regions. CSP is a Renewable Energy Technology (RET) uniquely suited to aid the collection of commercial Variable Renewable Energy (VRE) options in addressing global concerns about the impact of a fossil fuel-reliant energy sector on climate change. This is because CSP is ideally positioned with the capacity to incorporate Thermal Energy Storage (TES) to counter problems associated with the unpredictable nature of VREs [26], [29]. However, the dilemma being faced by CSP is that it is highly dependent on solar insolation, in particular Direct Normal Irradiance (DNI), which typically coincides with semi- to hyper-arid regions [3]. This poses a specific instance of the water-energy nexus, where the deployment of a beneficial RET, in the transition away from carbon-intensive energy, needs to be managed strategically to ensure the sustainability of the water resources on which it, and also surrounding communities, economies and ecosystems, rely.

In terms of the water-energy nexus, many studies focus on estimating the water demand from future energy supply pathways within a certain region, based on the water consumption factor of various energy technologies [155], [294]–[296]. This process is considered acceptable considering the vast amount of information (technological, spatial, temporal, political, and so forth) required to synthesize any practical approach to understanding the interaction between energy generation and water resources. However, a critical aspect lacking from most approaches to address the water-energy nexus is that of water availability at different scales – from local, to regional and national, and the intra-annual variability of these resources. This is fundamentally important in developing any practical cross-sectoral policies that aim to manage both the deployment of energy technologies in order to accommodate future energy demand, as well as water resources that must supply water to various sectors and demands. Furthermore, the spatial and temporal variability of these water resources, and the demand for this water, needs to first be understood before model-based policies can be developed and finally implemented [297].

This work represents the culmination of a series of studies aimed at systematically formulating strategic, integrated management policies for CSP deployment and water resources in arid regions to ensure resource sustainability. The study-region of this work is South Africa, the 30th driest country in the world [298], with an increasing amount of installed CSP capacity [202]. First, the fundamental need for the strategic management of CSP plant deployment and water resources was identified and motivated [3]. It was highlighted that the vast majority of global CSP installations are located in semi-arid, arid and hyper-arid regions. Furthermore, not only was the impact of thermal power stations on local and regional water resources identified as a risk, but also the impact of variable resource availability on the operation of thermal power plants, and CSP in particular. It was concluded that due to the need of CSP for high solar irradiance, and the general scarcity of water in these areas, the development of large CSP fleets needs to be undertaken with awareness of the likely constraints placed thereon by limited and variable water resources.

Second, the question of how much CSP is likely to be developed in the region, from a national policy perspective, was addressed in Section 3. The purpose of knowing what the likely amount of CSP deployment in the South African electricity supply market would be, was to provide a foundation on which to base water demand estimations. Although South Africa has an abundance of theoretically suitable land for CSP development (discussed in following sections), the main determining factors are national energy policies, in particular the Renewable Energy Independent Power Producer Procurement Program (REI4P) [149]. This is because South Africa's energy landscape is heavily regulated and based on a single-buyer model, where only the state utility, Eskom, may trade electricity to consumers, meaning that the tariffs at which Eskom buys (or generates) electricity is regulated in order to prevent excessive cost-escalations to the off-takers [299]. A critical part in regulating new power plant construction projects is the Integrated Resource Plan (IRP) [300], which is a strategic report, intended to be regularly updated, and which informs the required installed capacities per power plant technology within a certain planning horizon. The view on the role of CSP in the national energy mix has changed throughout the series of IRPs to date, and will likely change with the release of newer versions. Beyond the IRPs, other studies by governmental and academic institutions, as well as global concerned groups, on energy mix scenarios for South Africa, were included in the study. Various drivers for CSP adoption were identified, and the scenarios of energy mix development were categorised based on the proportion of CSP included in the final year of modelling, and range from in excess of 30 GW to no new installed capacity (0 GW) by the end of their planning horizons (typically 2030).

Thereafter, the question of where (geographically) CSP is likely to be developed was answered in Section 4. The rationale behind addressing this question is that CSP, irrespective of the amounts in which it is adopted, will impact water resources at specific locations, therefore requiring that these locations are identified and considered in the final analysis. These suitable locations were identified based on a Geographic Information Systems (GIS) analysis of a series of inclusion and exclusion criteria from literature, and from actual operational CSP plants' location characteristics. The main determining criterion is Direct Normal Irradiance (DNI), which impacts the plant's generation potential and performance. Because South Africa is endowed with very high annual DNI across the country, a relatively high limit of 2400 kWh/m^2/y was used. Another critical property of the geography is the slope of the land on which CSP can be built, which literature has showed to be between 1% and 7% inclines. Because none of the existing 6 CSP plants in South Africa were built on land with a slope of more than 3%, this was selected as the maximum allowable slope. The study showed that along existing and planned transmission networks, the suitable areas total between 71,457 and 33,252 km^2.

The penultimate question focussed on understanding and quantifying the water consumption patterns at CSP plants in detail. Initially, a preliminary study was conducted using the same GIS approach discussed above for all suitable areas, without regarding the limits imposed by vicinity to transmission infrastructure, as shown in Section 5. It used a high-level efficiency model (HLEM) to quantify the monthly performance of a CSP plant of a certain CSP-cooling technology configuration (Parabolic Trough or Central Receiver with either wet- or dry-cooling) at any location identified in the GIS analysis. This model, however, was based on rough assumptions from literature, resulting in a somewhat inflexible model, incapable of accurately capturing the technology-dependent, sub-annual performance of actual CSP plants. As a result, a validated HLEM was developed, based on eight sets of simulations in five locations in South Africa (two CSP technologies, two cooling technologies, two installed capacities), totalling 40 sets of detailed hourly-interval simulation (DHIS) result, as shown in Section 6. This large group of simulation results was used to validate the use of certain literature-based assumptions of energy conversion efficiencies, and to provide monthly characterizations of particularly the solar-to-thermal conversion efficiency of the solar field, and the thermal-to-electrical conversion efficiency of the Rankine cycle. Furthermore, the DHIS models included an in-depth consideration of water consumption within a CSP plant, enabling the validation of an accurate approach for quantifying the water consumption factor, and finally total monthly water consumption volume for varying CSP-cooling configuration and spatiotemporal conditions. The final HLEM results were found to be within -5% to +1% of the DHIS results for the total annual generation potential, and between -1% to +3% of the DHIS results for the total annual water consumption, with low root mean square error values, indicating a high agreement with monthly DHIS results and seasonal variation.

Finally, before being able to synthesize a set of practical policy guidelines on sustainable management of CSP fleet deployment and water resources, detailed consideration must be given to water availability itself. There are typically three major cost-effective sources for industrial water abstraction: rivers, dams, and ground water. Alternative sources, such as municipal wastewater, industrial waste water, and salt water, can also be considered if sufficient data on their availability and their techno-economic impact can be obtained. In this work, the focus was placed on the former three major sources, since they are both critical to ecosystems and other existing economic activities, as well as subject to natural fluctuation based on climatological impacts on hydrology. Therefore, this paper provides a detailed account of the approach used to quantify water availability, considering the arid regions in which CSP is likely to be developed, and the unbalanced distribution of these resources. Thereafter, the approach used to determine the natural limit imposed by this fluctuating availability on CSP operations and development is discussed. Based on the results from this analysis, guidelines are suggested for how CSP should be developed at a national scale in South Africa.

7.2. Methodology – Reconciling CSP demand with water availability

CSP plants typically require in excess of 3 m^3/MWh when recirculating wet-cooling towers are used [301]. These wet cooled (WC) plants have between 3% and 8% lower levelized cost of electricity (LCOE) than the same CSP technology with dry cooling (DC), depending on site-specific meteorological conditions [35]. These higher generation costs for CSP+DC plants are due to the cooling technology's negative impact on thermal efficiencies, and therefore plant performance in hotter months, the higher cost of the cooling technology itself, and the required over-design of the CSP plant to compensate for lower performance, with increased capital costs of around 10% [302]. This explains the dominance of WC as the cooling technology of choice at existing CSP plants, representing more than 78% of operational and under

construction CSP plants, compared to less than 20% employing DC[13]. With this in mind, Table 7. 1 shows that the top 10 countries in which CSP plants are currently operational, or under construction, and how these same countries are experiencing the highest levels of water stress. They are all ranked in the top 50 water-stressed countries (out of 167), according to The World Resources Institute's water stress index [303]. Water stress is defined as the measure of total annual water withdrawals (municipal, industrial, and agricultural), as a percentage of the total annual available renewable water, with higher values indicating more competition among users [143].

Table 7. 1: Top 10 Countries with the most CSP installed and their water stress ranking

Country	CSP installed capacity (MW)[a]	Percentage of global capacity (%)	Global water stress ranking[b]	Water stress score (-)[c]
Spain	2,702	36.51%	30	3.77
United States	1,881	25.41%	47	3.17
China	871	11.77%	46	3.19
India	504	6.80%	31	3.70
South Africa	500	6.76%	50	2.98
Morocco	488	6.59%	21	4.24
Israel	121	1.63%	8	4.98
Chile	110	1.49%	32	3.69
Saudi Arabia	93	1.26%	7	5.00
Kuwait	50	0.68%	1	5.00

a - See footnote . b * Based on the work by The World Resources Institute, for the Business as Usual Case of 2020 [303].c - [0-1] Low (<10%),[1-2] Low to medium (10-20%), [2-3] Medium to high (20-40%), [3-4] High (40-80%), [4-5] Extremely high (>80%).

In Table 7. 1, it can be seen that South Africa is the least water stressed of the 10 countries, ranked 50th. This might be misleading if it were interpreted as meaning that South Africa is comparatively less stressed than the others. It must be considered that the water stress score represents a percentage of available water being abstracted. This means that a country might have little water in the first place, but is not necessarily abstracting as much of it as other countries, as is the case for South Africa. However, it must be noted that South Africa receives only an average of 400mm rainfall per year, making it the 30th driest country [298]. Beyond this, the rainfall itself is unevenly distributed across the country, as shown in Figure 7. 1 (a) and (b).

As seen in Figure 7. 1 (b), around 60% of the country has an annual rainfall of less than 500 mm [304], while Figure 7. 1 (a) clearly shows that only small clusters of the country receives more than 1,000 mm per year. These high-rainfall areas are mostly near the coastal regions, with the largest of these areas found in the eastern highlands. This results in most of the surface runoff originating from these eastern highlands, flowing either westward to the Atlantic Ocean, or eastward to the Indian Ocean. This uneven distribution highlights the challenges with quantifying water availability across uneven distributions in arid regions.

[13] This is based on the publicly available data at https://solarpaces.nrel.gov/, with the following filters applied: field_status = "Operational" or "Under Construction".

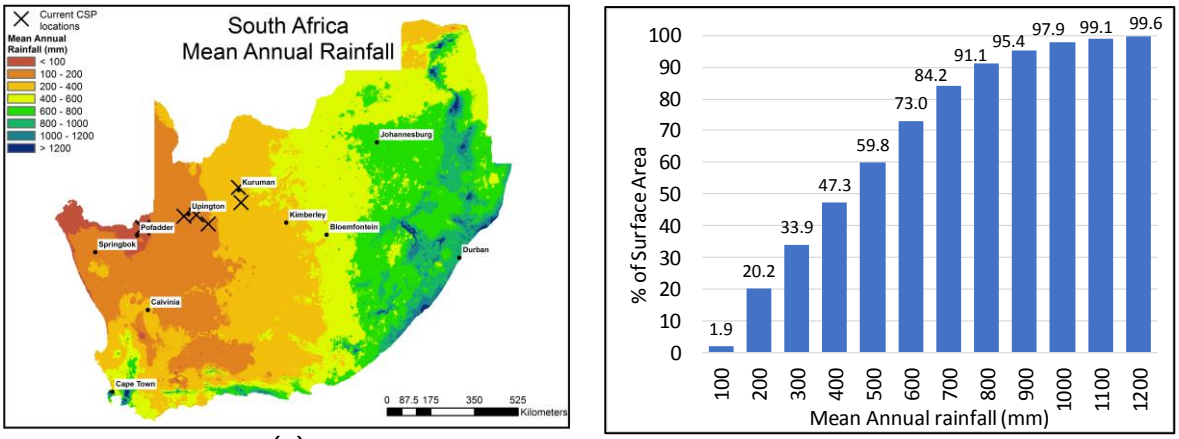

(a) (b)

Figure 7. 1: (a) Map of South Africa - Mean annual Rainfall, (b) Frequency distribution of Mean Annual rainfall across South Africa [305]

7.2.1. Water availability in South Africa.

For the purposes of this work, the concept of water availability needs to reflect what amount of water is readily available for abstraction at the rates required for the operation of a CSP plant at full capacity. This brings up three main principles, which need to be considered: geographic scale, temporal scale, and resource type. With regards to geographic scale, for the purposes of hydrological analyses, the watersheds in South Africa are divided into primary, secondary, tertiary, and quaternary catchments [306]. These 1,946 delineated boundaries represent the most detailed level of operational catchment management and planning by the Department of Water and Sanitation (DWS) in South Africa, and are therefore used as the spatial scale of choice for this work. Secondly, water resources fluctuate seasonally in most regions, following rainfall patterns, and thus the use of annual volumes do not capture the actual minimum available volume available throughout a calendar year. For this reason, monthly available volumes are used to define water availability in this study. Finally, in terms of resource type, only surface water in national dams and perennial rivers, as well as ground water in aquifers, are considered viable sources for CSP in this work.

The seasonal variability of these three types of water resources can typically be determined in two ways: hydrological modelling, such as the Pitman model for South Africa [117], [307], or statistical analysis of historical hydrological records [308]. The use of a detailed hydrological model for the regions where CSP can be developed in South Africa would certainly be a preferred method for long-term planning for the impact of CSP development on the water resources in these regions. However, the development of such a model was outside the scope of this work, which only aims to provide a foundation for the assessment of this potential impact of CSP on water resources in arid regions. As such, the use of long-term hydrological records was chosen. The custodian of hydrological data in South Africa is the DWS, as established in the National Water Act of 1998 [309]. Information logged by DWS is publicly available through hydrological officers who process requests and issue the relevant information.

Another hybrid method for determining water availability is water resource accounting, where the balances of water “stocks” within a defined geographic area or river system, are determine based on an accounting methodology. A detailed methodology is presented in a Water Research Commission (WRC) report, along with a detailed review of water resource data types and availabilities in South Africa [310]. One critical aspect of performing water accounting is the determination of the Resource Base Sheet (RBS), which represents all possible inputs, uses, flows, storages and transfers within a study area to determine the

balance of water resources for a certain period. A schematic representation of the proposed RBS for South Africa is shown in Figure 7. 2. In order to determine the portion of water deemed as “Utilisable Outflow”, which defines the available water for further development [311], all accounting parameters are required for the region in question. Accounting case studies were performed for the Umgeni and Sabie-Sand Catchments in South Africa [310], demonstrating the entire workflow process required to determine the distribution of water uses and finally Utilisable Outflow.

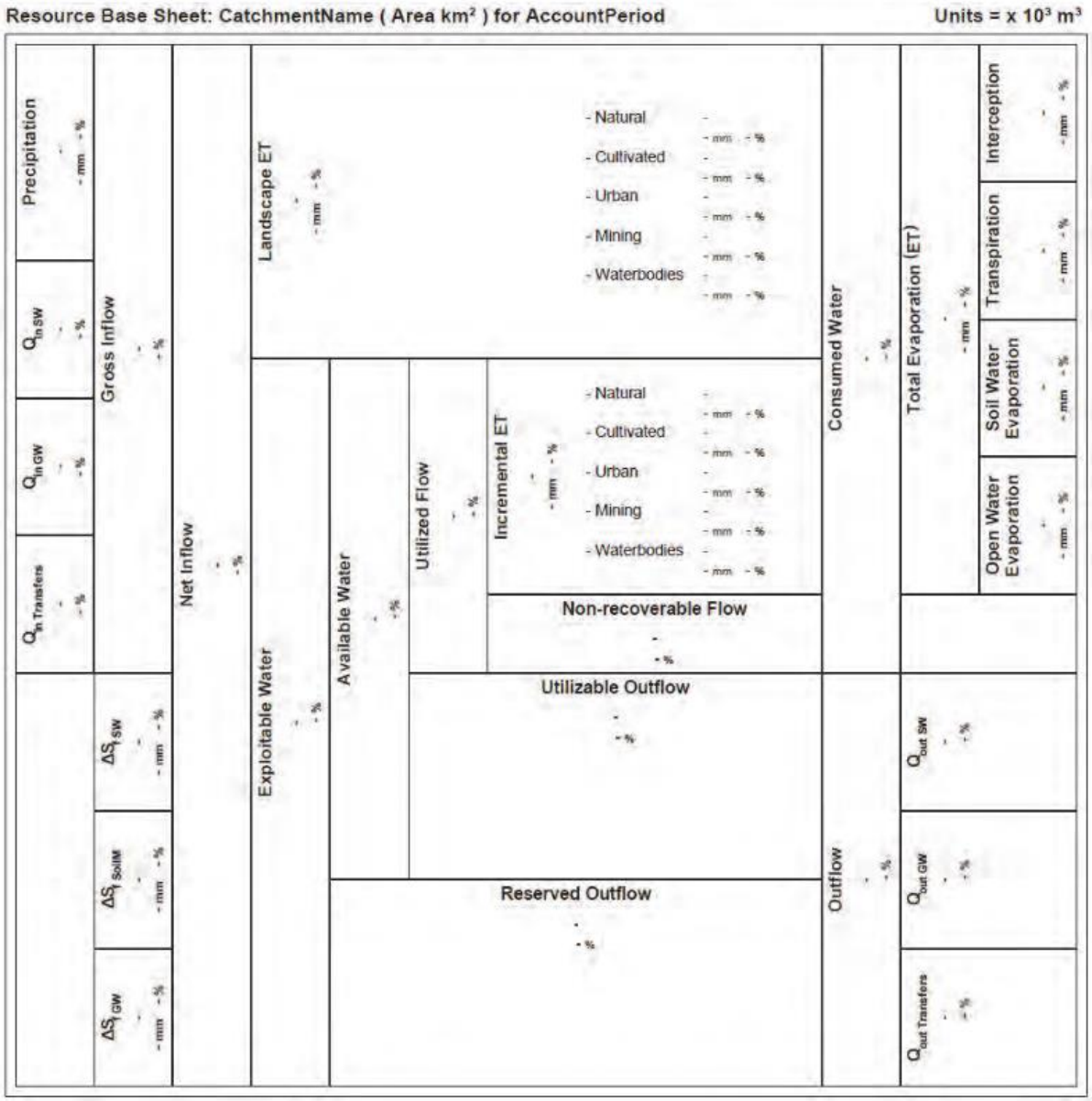

Figure 7. 2: Schematic representation of the modified Resource Base Sheet, from [310]

In order to perform such a water balance across a large spatial area, a large amount of high-quality input data is required, specifically rainfall data. This data serves as the primary input into the hydrological models used in the first step of performing an accounting balance for a region. However, the availability and quality of this data in South Africa has declined over the past years [312]. Beyond data quality and amount, high temporal (daily) and spatial (sub-quaternary catchment) resolutions are required to perform annual simulations of surface runoff and water storage volume as responses to rainfall. This is difficult in regions with sparse

rainfall gauging station distributions, and requires remote sensed data from satellite measurements. To avoid the potentially detrimental impact of the above mentioned data quality and availability issues on performing an initial high-level assessment of the hydrological impact of CSP development in arid regions, an alternative approach was used to quantify water availability at the Quaternary Catchment (QC) level. The Primary (lowest-level detail) and Quaternary (highest-level detail) Catchments are shown in Figure 7. 3, along with the QCs where CSP is likely to be developed, indicating the study region.

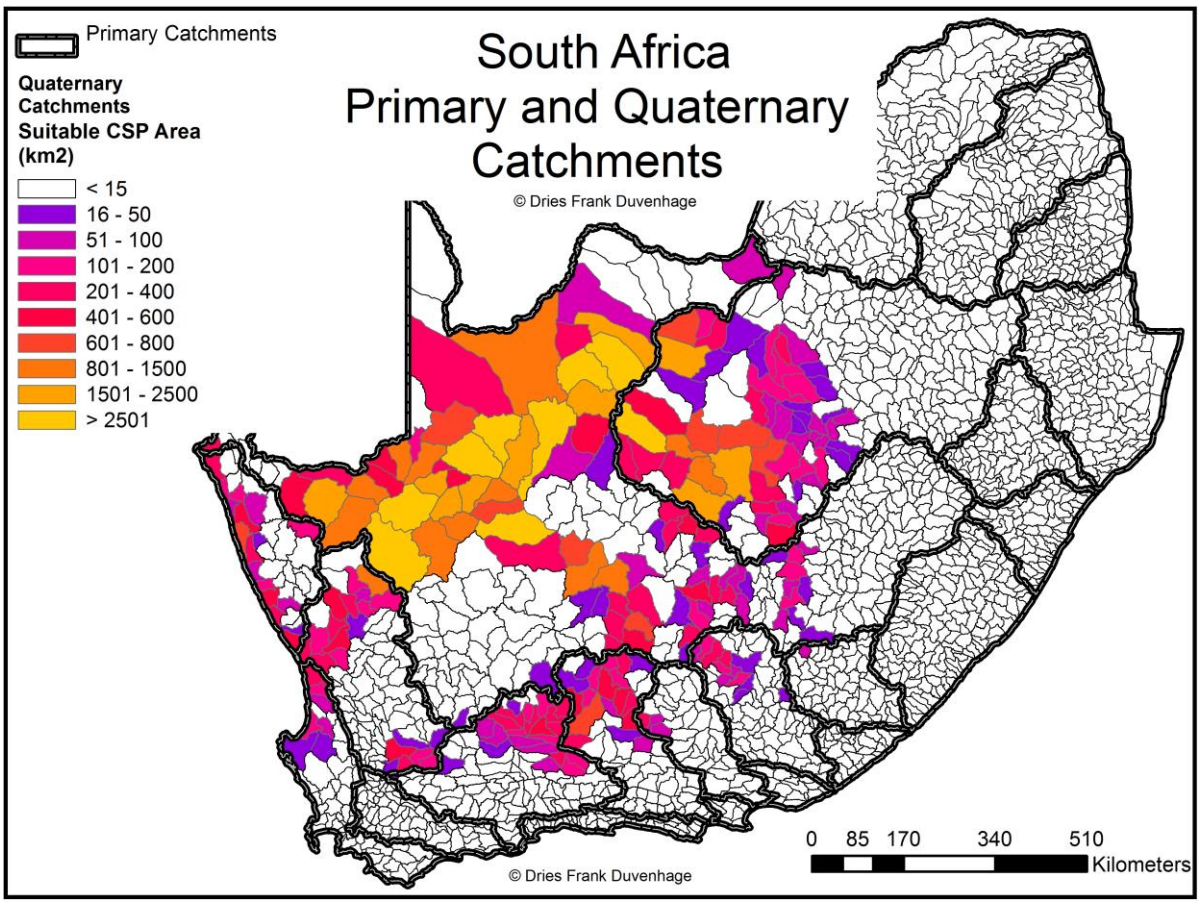

Figure 7. 3: Map of South Africa - Primary and Quaternary Catchments

This approached used large amounts of historical hydrological data kept by the DWS for river flows and dam storage levels in South Africa. It is gathered in near real-time, and stored on the DWS's HYDSTRA database for public access. The advantage is that through using the actual monitored flows and dam storage volumes, the actual responses of the hydrological system to the entire water balance in a certain region are captured. This means that all inputs and abstractions into the water balance are already accounted for when the historical data for a dam or river is analysed. Neither the individual withdrawal rates of upstream processes, nor the rainfall inputs of upstream catchments are required to determine the amount of water readily available for abstraction at a certain location, because their final impact on the system is already reflected.

7.2.1.1 Hydrological data in South Africa

Rivers

Figure 7. 4 shows the river flow lines and flow monitoring points for South Africa in the study region. The river flow lines dataset is publicly available from the DWS website. As can be seen from the River Class symbology used, there are very few perennial rivers in the study region, also reflected by the limited amount of monitoring points along rivers there. In order to determine the quantity of water available for abstraction from a river within a QC boundary, the monthly flow volumes recorded at the monitoring points along that river were analysed. The historical period with available data varied for each monitoring point based on the date they were commissioned by the DWS. The data used represents the total volume of water, which flowed past that monitoring point during the month in question, in million cubic meters (Mm^3). Data periods from available records range between 1 and 108 years, dating as far back as January 1904. The available data for each monitoring point within the primary catchment areas (thick grey boundaries) where CSP development is likely to take place was analysed for each month. A total of 261 monitoring points, representing 111 individual rivers, were analysed.

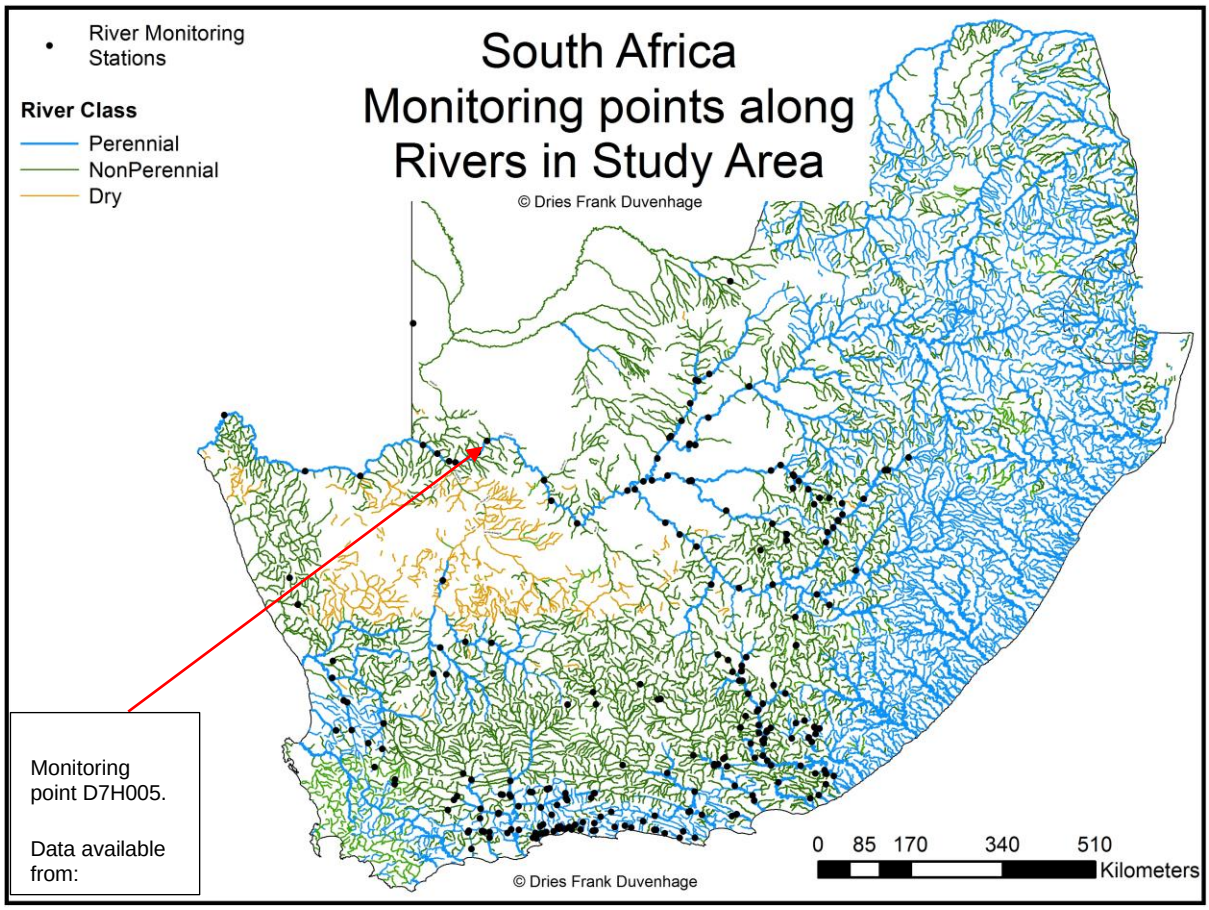

Figure 7. 4: Map of South Africa - Rivers and river data monitoring points within study region

The monthly average, 90th and 10th percentiles were calculated for the period of available data for each monitoring point. The 90th and 10th percentiles represent the total volumes that are exceeded 10% (90th - floods) and 90% (10th - firm yield) of the time, respectively. A sample of this data (black lines) and its calculated average (double blue lines), 90th (red striped) and 10th percentiles (yellow dashed) are shown for monitoring point D7H005 on the Orange River, in

Figure 7. 5, for the period January 2000 to December 2017. A logarithmic scale is used in order to effectively compare the actual monthly volumes to the 90th (low exceedance probability) and 10th (high exceedance probability) percentile values. The 10th percentile was then halved, in line with the approach used in [313], in order to account for the ecological reserve requirements in that river. This value represents a very conservative quantification of water readily available for abstraction from the river section along which that monitoring point is located.

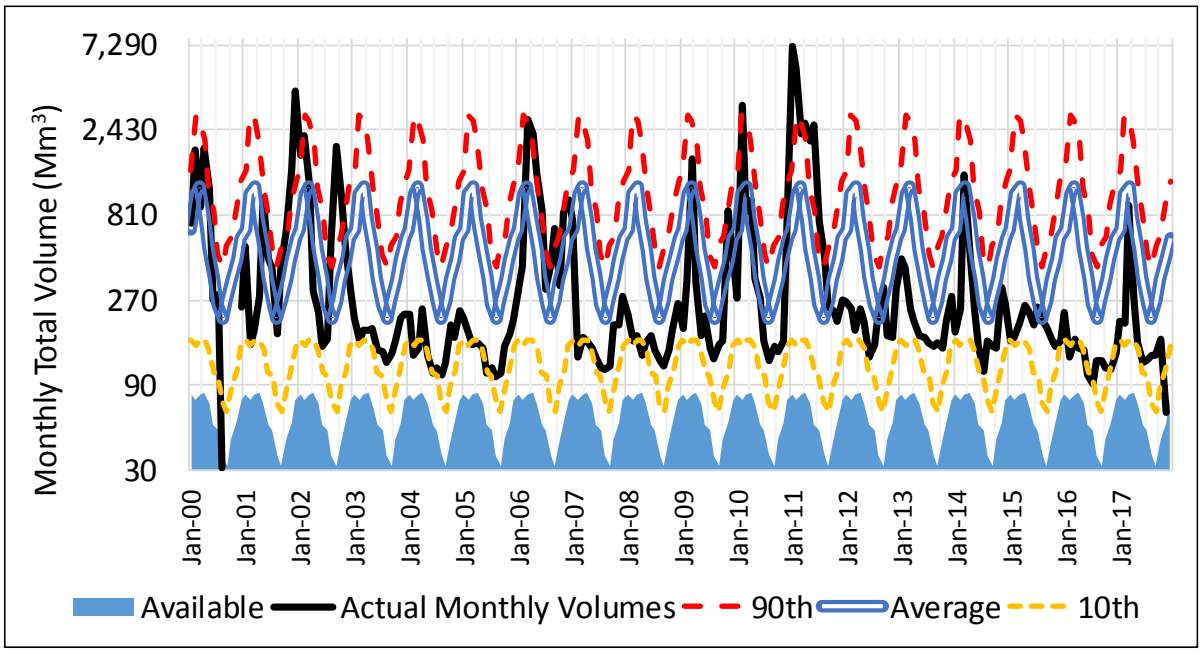

Figure 7. 5: Graph of actual, average, 90th- and 10th percentile monthly river flow volumes for the Orange River at D7H005

After applying the above statistical method to quantify water availability from rivers, an approach was required to aggregate the values from these monitoring points to river sections and ultimately to the QCs in which they are found. There are different cases for monitoring point placement within each QC: there could be multiple monitoring points, one, or none along the same river. Figure 7. 6 shows these cases along the major river in the study region, the Orange River. The QTs have now been coloured graded according to total annual flow volume. For the case of only one monitoring point within a QT, that point was used to calculate the available water from the particular river and QT.

For the case of no monitoring point being located within a QT, data from the next upstream QT along that river with data would be used. No losses are accounted for from one QT to another in this case, since these would have to be based on assumptions with no real-world reference. In the case of D73D and D73C, in Figure 7. 6, there are no monitoring points located in each of them. The next upstream QT with a monitoring point is D73B, with a data record period of 85 years. Therefore, the total annual available water from D73B, of 6,947 Mm^3 was used for D73D and D73C. This method certainly has limitations since it does not account for any abstractions or runoff within D73D and D73C themselves. However, considering that the total annual available water for the next QT with its own monitoring point, D73E, has a total annual available volume of 6,689 Mm^3, which is lower than the upstream volumes, it at least follows the general logic of a mass balance along the river in question.

For the cases of multiple points along the same river within a QT, such as for D73F (D7H004, D7H010, D7H014 and D7H003), the data had to be aggregated in such a way so as to represent available water from the river as accurately as possible, without replacing data from one point with that of another. Furthermore, some of the points would have data for certain periods, while others would not and certain points would have data for longer periods than others. Data were aggregated and combined in these cases according to different criteria based on a hierarchal approach. The criteria used to select data points and their data was data record period length and relative position within the QT, i.e. how far downstream the point is. The rationale is that the most downstream point would be the most representative of how much water is available for abstraction within that particular QT. However, if the data record period of the more downstream is too short, it will not provide an effective indication of long-term available water. If there were gaps in the most downstream dataset, they would be filled with the data of the next upstream point with the longest record period. In this manner, data would be combined to create a congruent, non-conflicting data record for that particular QT.

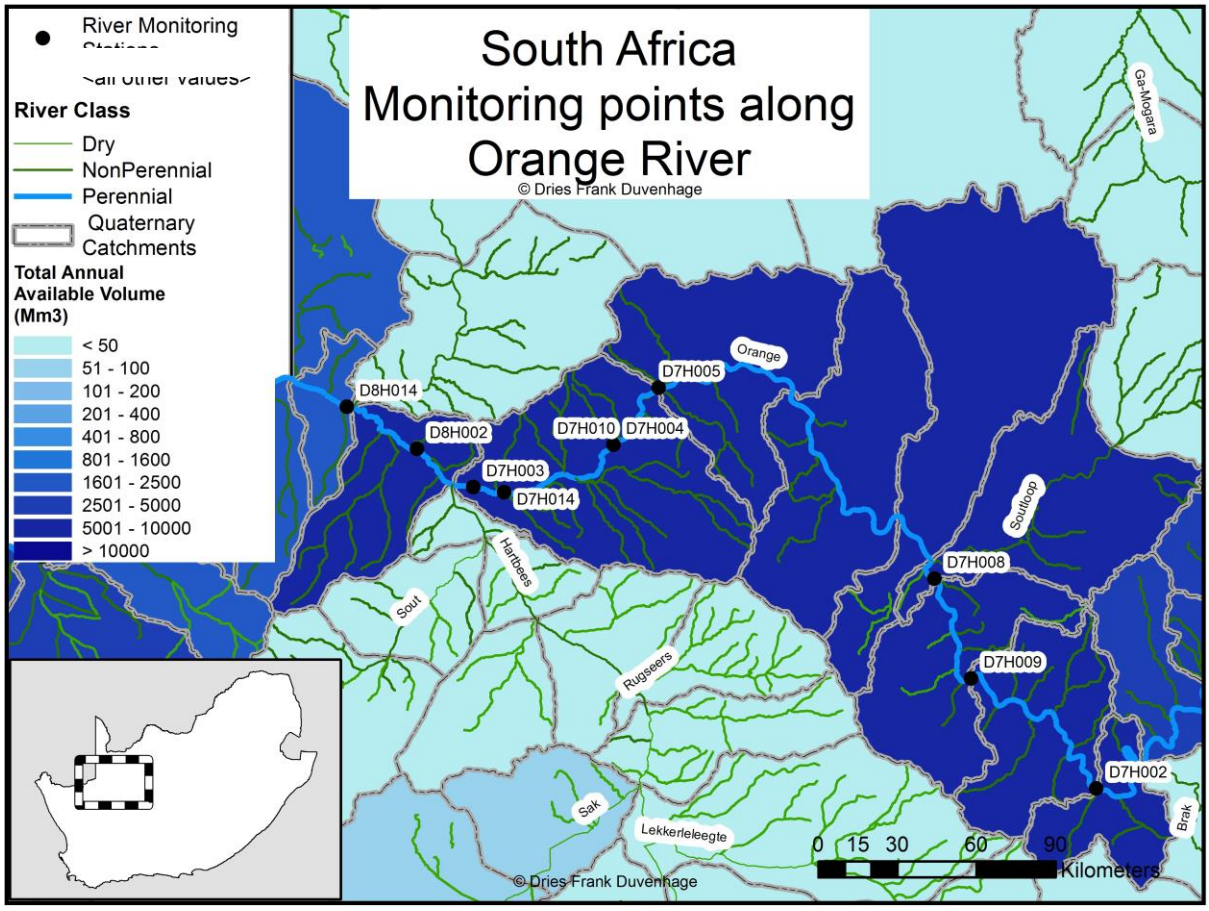

Figure 7. 6: Map of South Africa – Monitoring points along Orange River in study region

Dams

Similarly, the dams across South Africa that are under the administration of the DWS, were considered as potential sources for abstraction. The DWS also keeps data for dams, with records for around 215 dams dating back to February 1900. These records are typically stored as water level readings in meters above sea level (MASL). However, these records alone do not provide a quantifiable indication of what volume of water is stored. Therefore, each dam has a calibrated calculation of the relationship between the MASL readings and volume, and this data can be requested from the DWS's HYDSTRA database. Monthly average volume in

Mm^3 was used, to align with data obtained for total monthly river flow volumes. The dams for which records were obtained are shown in Figure 7. 7.

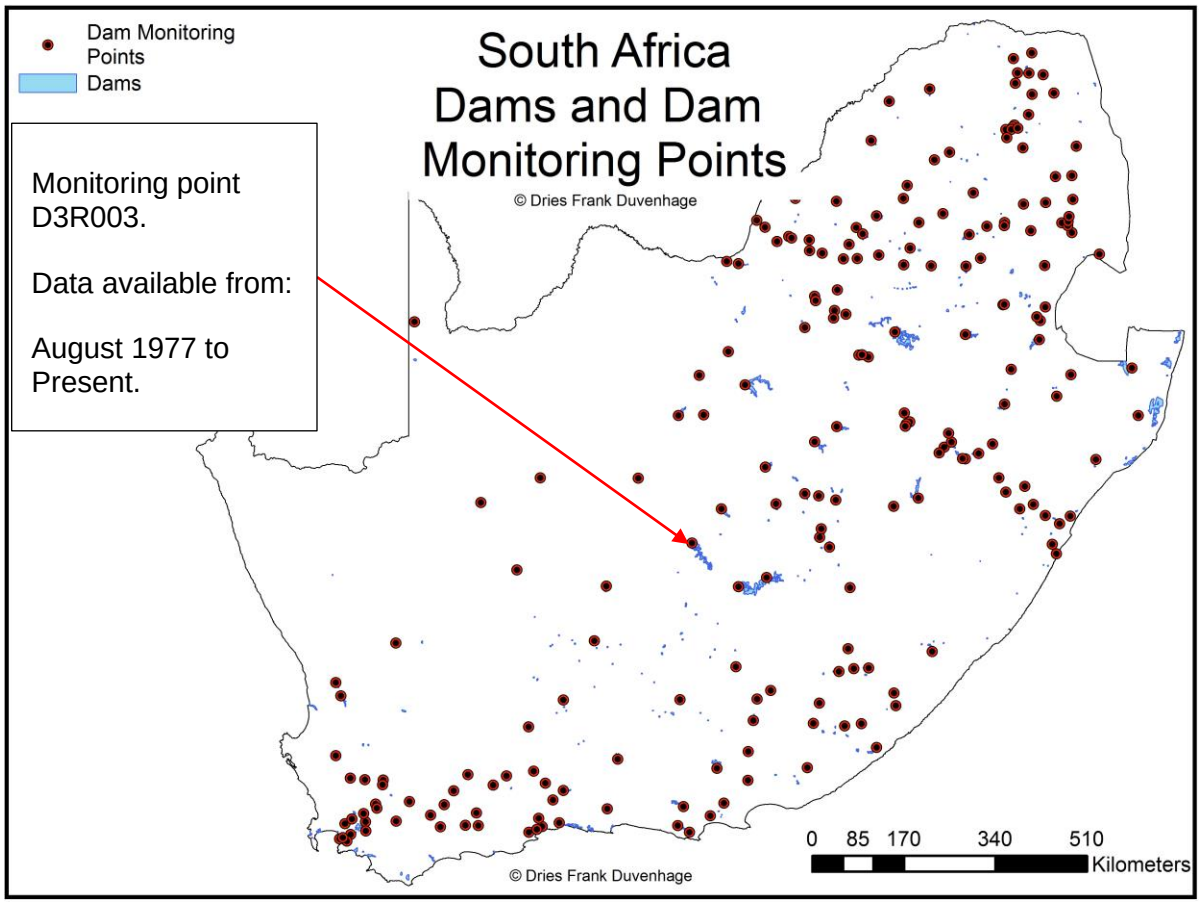

Figure 7. 7: Map of South Africa – Dams and Dam Monitoring points

Since dams do not represent a flow of water, if there are multiple dams in a QC, their combined volume can simply be calculated by adding them to each other for that month. The same statistical approach was used as for rivers, where the acquired records of monthly storage volumes were used to calculate monthly 90th, average and 10th percentile values. A sample of this data is shown for the Vanderkloof Dam, and its monitoring point D3R003 for the period January 2000 to December 2017 in Figure 7. 8.

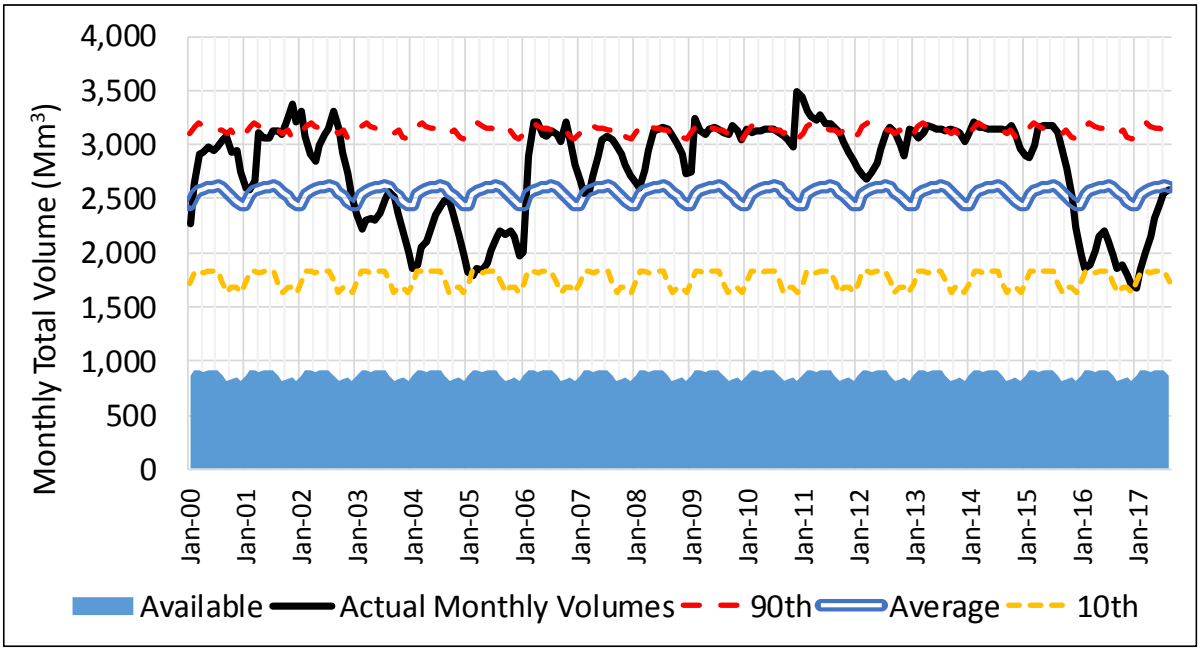

Figure 7. 8: Graph of actual, average, 90th- and 10th percentile monthly dam storage volumes for Vanderkloof Dam at D3R003

The same conservative approach used for rivers was applied to the dams, where half of the monthly 10th percentile values, calculated for the entire record period for each monitoring point, were used to represent available water. This approach makes provision for existing water withdrawals from the dam, as well as the minimum storage required to supply the ecological reserve requirements to downstream rivers.

Ground Water

Ground water refers to water stored beneath the water table of a catchment. These resources have served as affordable, and often high-quality, water sources for development in arid regions, and as a result have become stressed in many regions [314]. The quantification of the usable volume from subterranean aquifers is a difficult task, and typically the safe reliable yield of an aquifer needs to be determined at that specific location based on pump tests [315]. However, detailed studies have been performed to quantify ground water availability at the national level, with a detailed review of the past Groundwater Resource Assessments (GRAs) for South Africa presented in [316]. These GRAs provide estimations of aquifer storage volumes, recharge rates, and yield. These estimations are based on a combination of borehole level measurement records and hydrogeological modelling, and take into account various technical interactions between geology, soil permeability, runoff, withdrawals and the conceptual stratification of aquifers into layers based on the nature of water storage dynamics in them [317]. These estimations are publicly available through the DWS's National Groundwater Archive. In particular, the database of available groundwater, on the DWS's National Integrated Water Information System, was used, which provides groundwater balances in Mm^3/year per QC, as shown in Figure 7. 9.

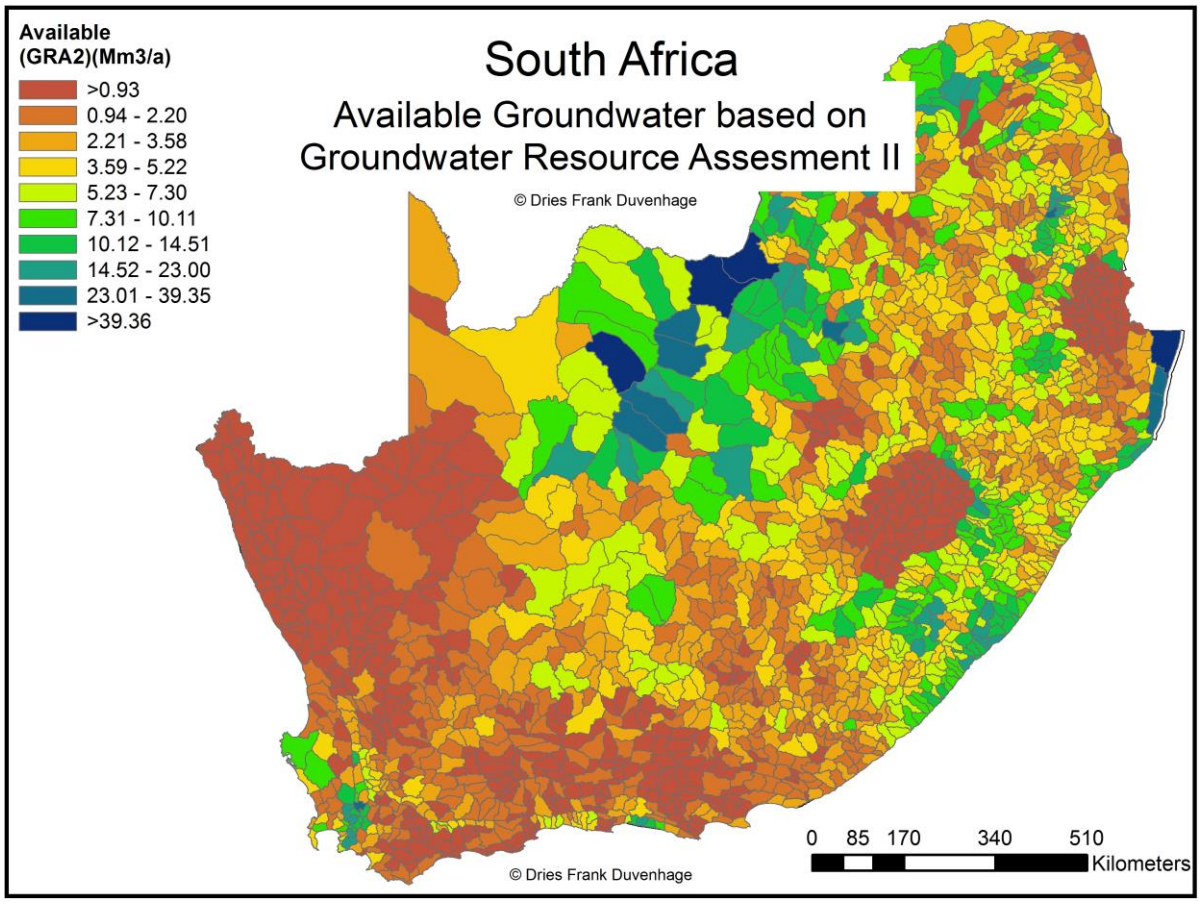

Figure 7. 9: Map of South Africa – Available Groundwater in Mm^3

These annual values for available water from groundwater sources were simply divided by 12 to provide a monthly estimation of availability. Naturally, this approach is limited in its sensitivity to seasonal variations. However, considering the limited availability of up-to-date data on sub-annual groundwater resource balances, this approach at least prevents the exceedance of annual volumes.

7.2.1.2. Aggregated water balance

After identifying, analysing and quantifying the appropriate data for the three water resource types, it was necessary to aggregate them in order to determine a total available water balance. The geographical boundaries of choice are those of the QC, since they serve as the most detailed level at which hydrological planning is undertaken in South Africa. Therefore, they serve as a convenient and appropriate spatial definition for water availability. The final available water from rivers, dams and groundwater are simply summed per QC. The process described in Section 7.2.1.1 for rivers explains what approach was used to prevent double-counting different flow monitoring points along the same river network within a QC. Dams can be summed explicitly. Groundwater is reported for the entire QC, and therefore needs no special spatial considerations. The final aggregate available water balances in Mm^3 (or GL) for the study region within South Africa, for January (summer), April (autumn), July (winter) and October (spring), are shown in Figure 7. 10.

As can be seen when compared to the locations of dams in Figure 7. 7, the QCs with large dams have the most stable monthly water supply throughout the year. Furthermore, the aggregate available water along the Orange River remains the most stable in the arid region

where CSP is likely to be developed. These aggregates were calculated for each month, and based on the demand for water from CSP development in these QCs, the limits imposed by this available water on CSP development can be determined.

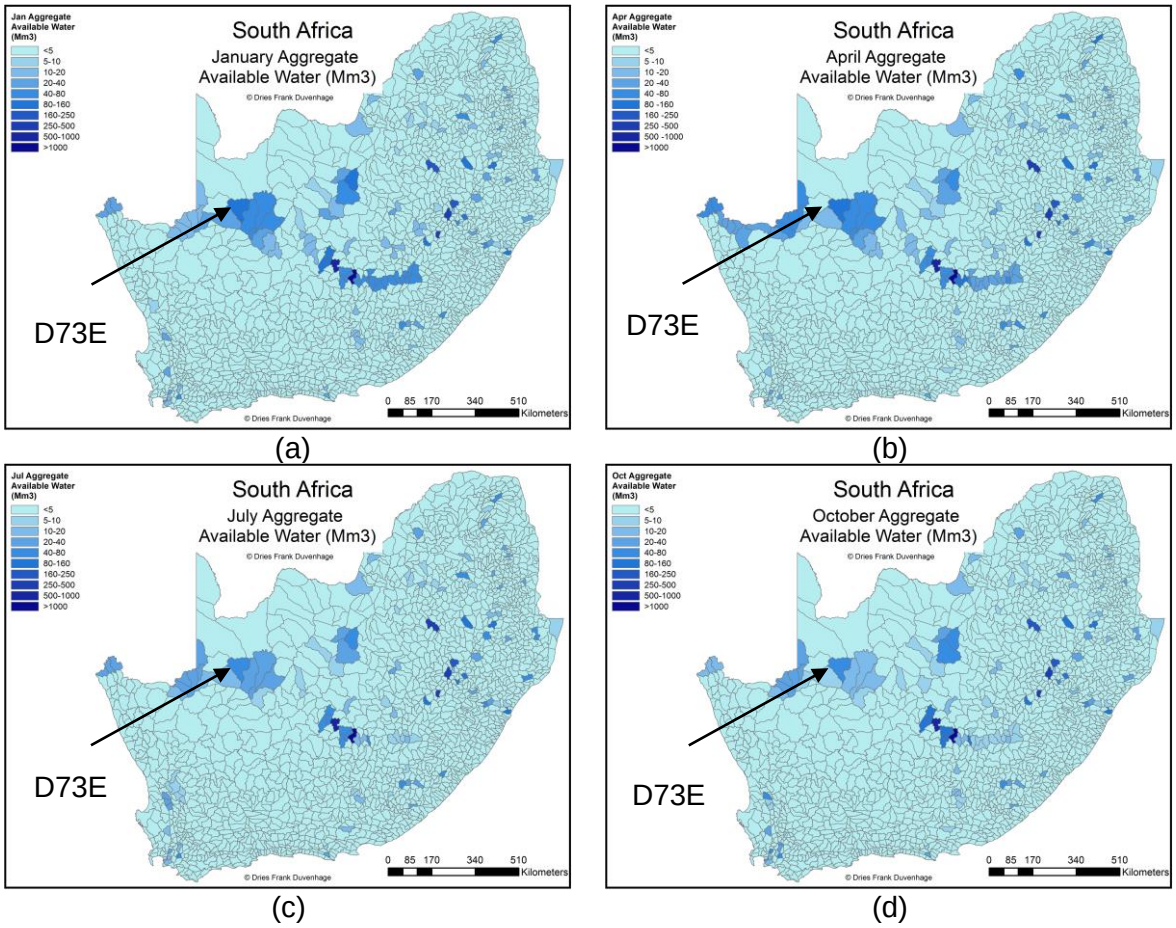

Figure 7. 10: Maps of South Africa: Monthly Aggregate Available Water for (a) January, (b) April, (c) July and (d) October

7.2.2. Water demand from CSP

A high-level efficiency model (HLEM) was developed to calculate water demand from CSP plants based on validated monthly efficiency calculations and assumption, given in Section 6. The model can calculate the monthly performance of Parabolic Trough (PT) and Central Receiver (CR) CSP plants, with either dry- or wet-cooling, at any location. These locations were identified in Section 4, at a scale of 1 x 1 km. The HLEM requires the monthly input data, shown in Table 7. 2. The spatial resolution of the location-linked HLEM model is only limited by the spatial resolution of the input data. However, all input data from Table 7. 2 were resampled to a scale of 1 x 1 km, as shown in Figure 7. 11 for January dry-bulb temperature.

Table 7. 2: Input data required for spatiotemporal HLEM

Input data	Spatial Resolution	Source
Monthly Mean DNI	0.05 x 0.05 deg ~ 5.6 x 6.5 km	(Müller, *et al.*, 2015)
Monthly Mean Dry-bulb Temperature	0.01667 x 0.01667 deg ~ 1.5 x 2.1 km	[318]
Monthly Mean Relative Humidity	0.01667 x 0.01667 deg ~ 1.5 x 2.1 km	[318]

The resampling process involved taking the centroid of each square and applying the input data of the raster grid, which intersects with it. This process was repeated for each month (12) of the three (3) datasets, resulting in the location-linked HLEM model capturing a total of 36 input parameters per square. Each 1 x 1 km square, therefore, represents one cell where a solar field, and likewise the heat input of a CSP-cooling configuration, was modelled.

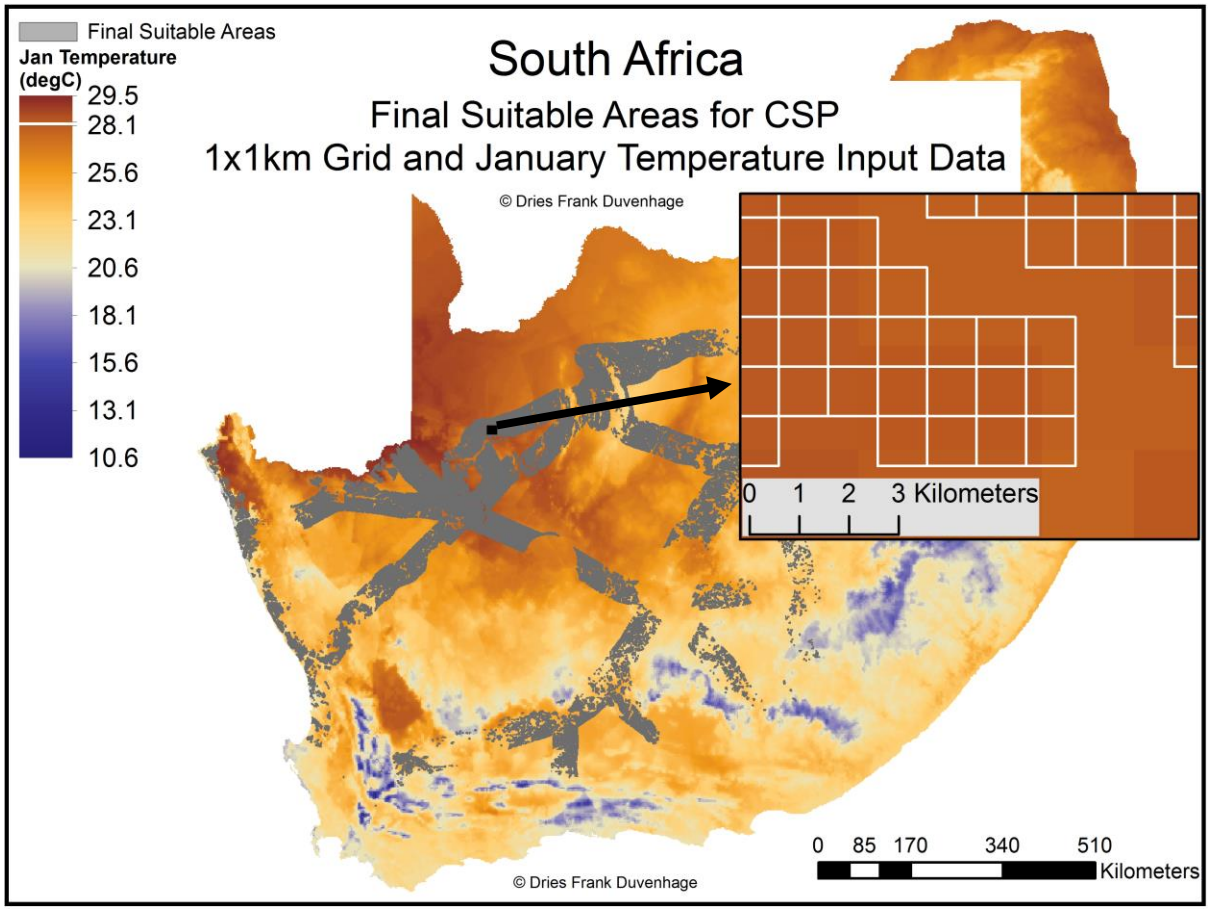

Figure 7. 11: Map of South Africa – Resampling process for input data to the location-linked model grid

The attribute table of this location-linked model and resampled input data was then processed in Microsoft Excel, where the HLEM calculations were used to calculate monthly solar-to-electric efficiencies (%), net generation potential (GWh), water consumption factor (m^3/MWh), and total water consumption volume (m^3), as described in detail in Section 6. The results, calculated at the 1 x 1 km scale, were then aggregated to QC level to determine total potential water withdrawal from the different CSP-cooling configurations inside each QC. This final resampling from 1x1km grid to QC level is shown in Figure 7. 12 (a) and (b). As an illustration,

Figure 7. 12 (a) shows the results for annual net generation potential (GWh) from PTWC at the 1x1km grid level, where the detail insert shows all the suitable areas within QC D73E. Figure 7. 12 (b) shows the aggregated total volume water consumption for January for all QCs, with the detail insert showing how the 1x1km grid is aggregated to QC level for D73E.

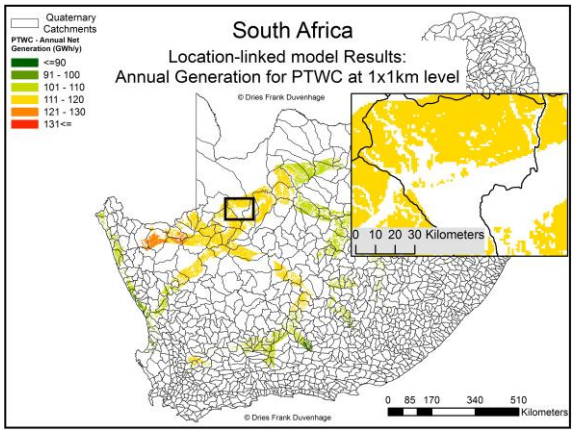

(a) Annual generation potential from PTWC at 1x1km grid level

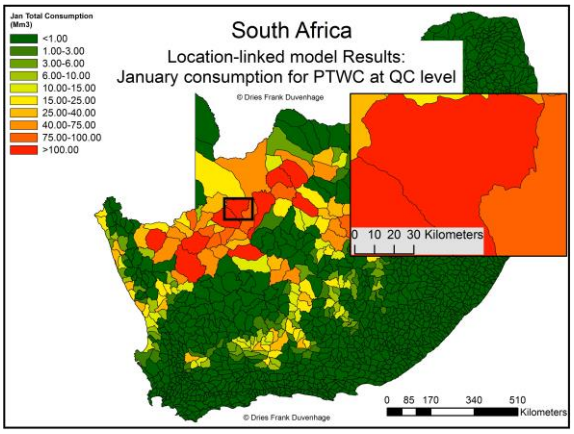

(b) Aggregated January total water consumption from PTWC at QC level

Figure 7. 12: Maps of South Africa – Resampling process for location-linked model results to QC level

While the results shown in Figure 12 (a) and (b) are for specific cases, the model provides monthly (12) results per QC, for four (4) CSP-cooling configurations, totalling 48 sets of results. These results sets are used in further linked calculations to determine what limit the actual volumes of available water in each QC places on the potential for CSP generation.

7.2.3. Linking CSP water demand to water availability

Now that both water availability and water demand from CSP is quantified at the same spatial level of QCs, it is possible to reconcile the two and determine what amount of CSP generation can be supported by the available water resources in each QC. Naturally, because rivers are one of the types of water sources under consideration, the transfer of water between QCs also must be accounted for. A systematic approach was therefore applied, where only the water sources within each QC were first used to determine the amount of CSP that can be supported in each QC individually, without consideration for the downstream impact of this consumption. This was followed by a stream-linked approach, where the impact of this consumption in each QC is considered in downstream QCs along the same river network. This systematic approach allowed for a simple and effective way to estimate the total CSP generation potential that can be supported by the combined water resources, without neglecting the linked nature of QCs through rivers.

7.2.3.1. Isolated approach – Individual catchments

One of the key principles of this work is that the limiting factor on CSP development is not due to annual water availability, but rather sub-annual availability. This is because although a certain total annual volume of water is available in a certain area throughout the course of a year, this total annual volume is unequally distributed throughout the year. Due to this sub-annual distribution, a monthly temporal scale was selected in order to effectively reflect the seasonal changes in availability, without the high computational effort associated with shorter time-periods. As such, the aggregated water balances per QC were analysed per month, as discussed in Section 7.2.1.

To illustrate the process used to quantify the hydrological limit on CSP development, the example of QC D73E from Figure 7. 6 is considered. This QC (D73E) has a relatively stable monthly aggregated available water balance, as highlighted in Figure 7. 10. This monthly aggregate available water balance is shown in detail in Figure 7. 13 as the blue line. The 90th percentiles represent the sum of the monthly 90th percentiles for rivers, dams and groundwater, as discussed in Section 7.2.1.1. The same applies to the monthly averages and 10th percentiles. The allowable maximum monthly abstraction volume for D73E is therefore represented by the Available Balance (blue line), meaning that these volumes may not be exceeded in each of the months.

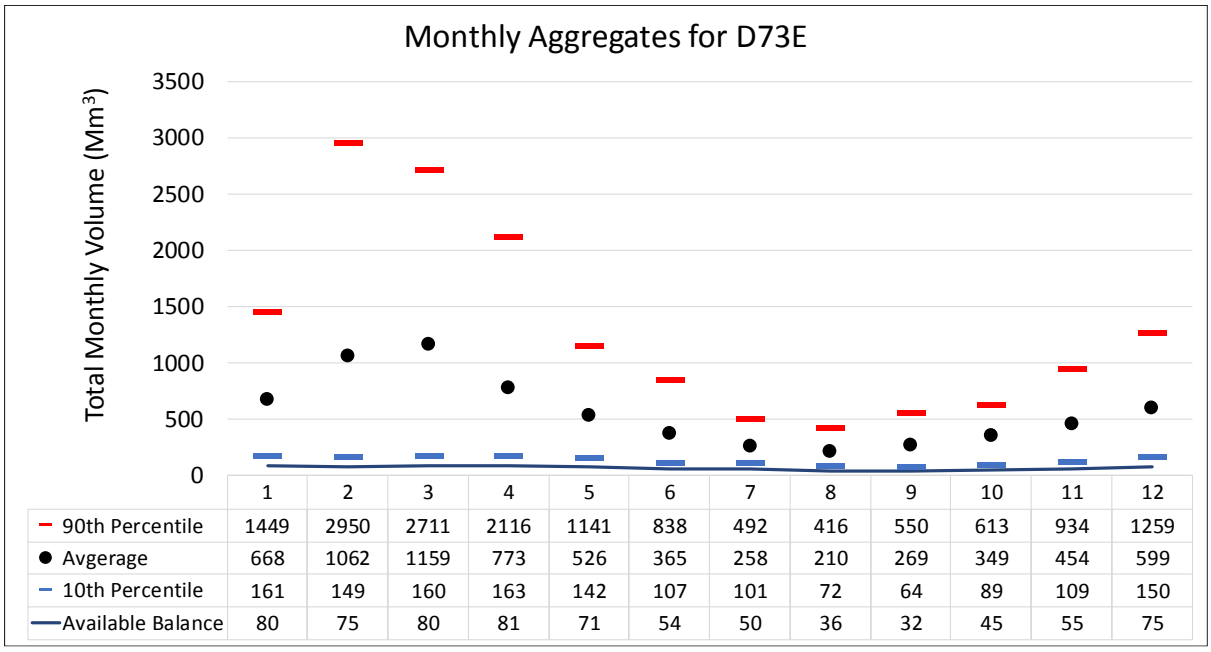

	1	2	3	4	5	6	7	8	9	10	11	12
90th Percentile	1449	2950	2711	2116	1141	838	492	416	550	613	934	1259
Avgerage	668	1062	1159	773	526	365	258	210	269	349	454	599
10th Percentile	161	149	160	163	142	107	101	72	64	89	109	150
Available Balance	80	75	80	81	71	54	50	36	32	45	55	75

Figure 7. 13: Graphs of Monthly Aggregated balances for Quaternary Catchment No. D73E

However, the monthly abstraction volume from CSP would depend primarily on the amount of electricity generated, and therefore the amount of CSP developed in that QC. Therefore, if the amount of CSP developed in that QC was based on the month with the greatest Available Balance (April), the demand for water would always exceed the available volume in every other month. Furthermore, if the amount of CSP developed in that QC was based on the total annual Available Balance (734 Mm^3), then the monthly demand would exceed the Available Balance in some months, and not in others. It therefore follows that the actual limiting factor is the month with the lowest Available Balance, which is September, with 32 Mm^3, in the example of D73E in Figure 7. 13.

In order to determine the amount of generation from a specific CSP-cooling configuration, which can be supported by the water resources in that QC only, a ratio must be determined based on the monthly average consumption factor and monthly theoretical generation potential for that QC. If the monthly Available Balance (Mm^3) is divided by the monthly consumption factor (m^3/MWh) for that QC, the generation potential, which can be supported by that Available Balance, is calculated in TWh. When this value, in turn, is divided by the monthly theoretical generation potential, based on the location-linked HLEM, then the amount of hydrologically limited CSP generation potential is expressed as a fraction thereof. This fraction is calculated for each month, and the month with the lowest fraction is used to calculate the amount of CSP generation potential for a CSP-cooling configuration in that QC. As can be seen in Figure 7. 14, for the case of D73E and the PTWC configuration, the month with the

lowest hydrological limit fraction is September, at 32%. This means that only 32% of each month's unconstrained theoretical generation potential can be supported by the aggregated water resources therein with a 90% assurance level. To illustrate this, the unconstrained theoretical generation potential and hydrologically limited CSP generation potential is shown in Figure 7. 14 on the left axis.

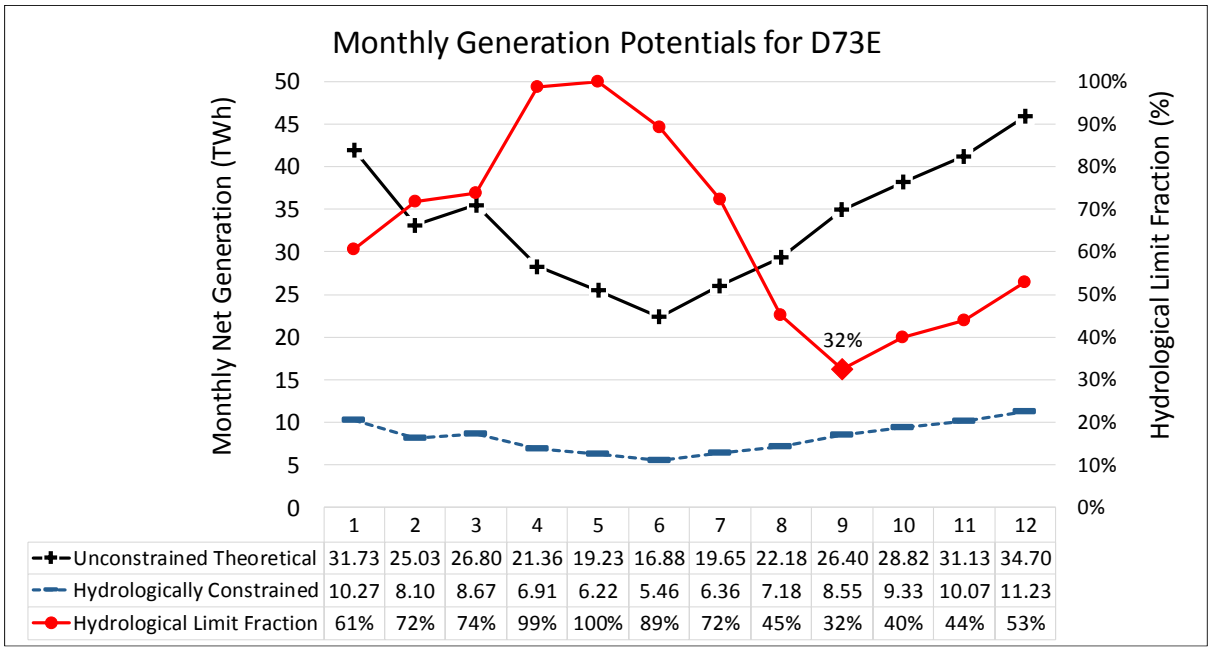

	1	2	3	4	5	6	7	8	9	10	11	12
Unconstrained Theoretical	31.73	25.03	26.80	21.36	19.23	16.88	19.65	22.18	26.40	28.82	31.13	34.70
Hydrologically Constrained	10.27	8.10	8.67	6.91	6.22	5.46	6.36	7.18	8.55	9.33	10.07	11.23
Hydrological Limit Fraction	61%	72%	74%	99%	100%	89%	72%	45%	32%	40%	44%	53%

Figure 7. 14: Graph of Monthly Generation Potentials and Hydrological Limit Fraction for D73E

The monthly total abstraction volumes for the unconstrained, and hydrologically limited cases, can now be calculated by multiplying the monthly generation potentials shown in Figure 7. 14 with the monthly consumption factors. These monthly consumption factors are taken as the average across all the suitable locations' 1x1km squares from the location-linked HLEM model, for a particular QC. The hydrologically constrained abstraction volumes are shown in Figure 7. 15 as the brown, dashed line, relative to the monthly 10th percentile and available balance aggregates for D73E. It shows how the use of the month with the lowest hydrological limit fraction to determine allowed CSP generation potential, prevents the total monthly abstraction volume of this generation potential from exceeding the Available Balance in any month.

Based on this methodology, the hydrological limits placed on CSP generation (and therefore development) by the water resources within a certain QC are calculated, without consideration for downstream impacts. This limit is termed the isolated hydrological limit, since it ignores the relationship between QCs due to abstractions from rivers. This impact, however, cannot be ignored, and a linked catchment approach is required in order to determine the final limit on CSP development for an entire catchment and its resources.

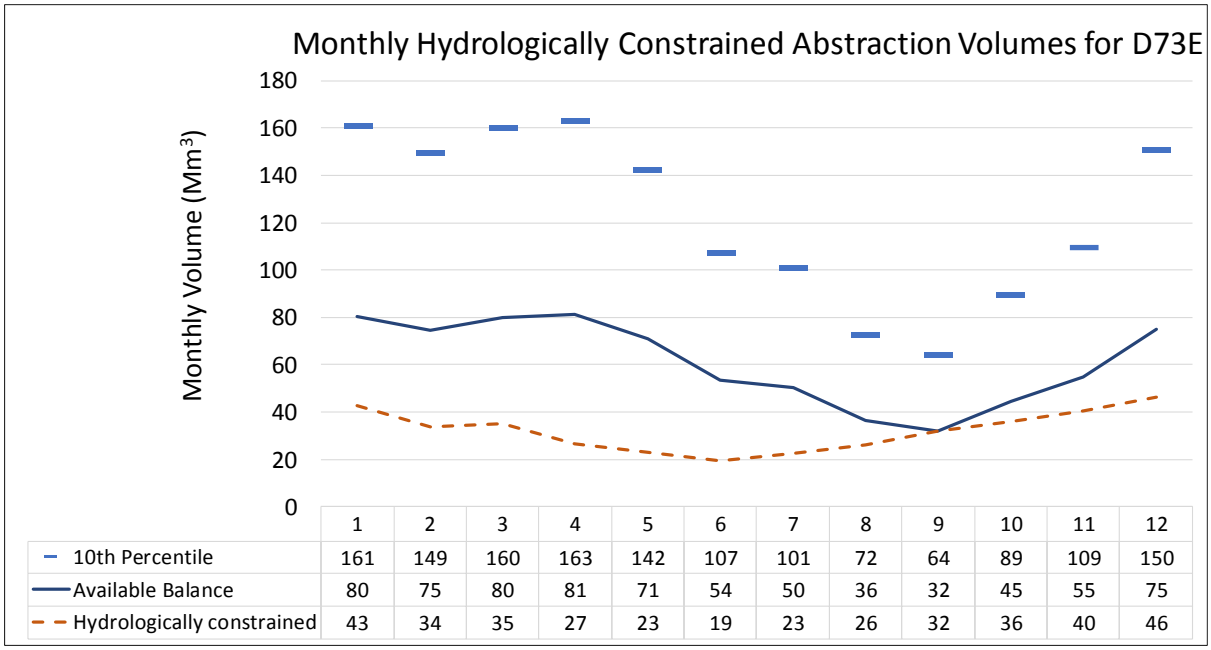

	1	2	3	4	5	6	7	8	9	10	11	12
10th Percentile	161	149	160	163	142	107	101	72	64	89	109	150
Available Balance	80	75	80	81	71	54	50	36	32	45	55	75
Hydrologically constrained	43	34	35	27	23	19	23	26	32	36	40	46

Figure 7. 15:Graph of Monthly Constrained Abstraction volumes relative to 10th Percentile and Available balance for D73E

7.2.3.2. Linked catchment approach – Downstream catchments

The isolated hydrological limit serves as a reference point from which to determine the overall hydrological limit on CSP development. To do this, a mass balance along a primary river must be carried out, with the abstractions due to CSP development in an upstream QC being subtracted from its own water balance, as well as from the downstream QCs's water balances. To perform this mass balance, however, the hydrological data used for each QC along a primary river must be temporally synchronised. If this is not the case, then hydrological data used to quantify the aggregated balance in one QC might be from a drier period, while the data used for another adjacent QC might be from a wetter period.

This is quite common for the data used across the study region, simply because all the river monitoring points weren't built and commissioned at the same time, or certain monitoring points would undergo periods of data loss, while other would still be recording data, or they would stop recording indefinitely. This is illustrated for three monitoring points in Figure 7. 16, with D7H008 being the most upstream, D7H005 in the middle, and D7H004 the most downstream. As can be seen, D7H008 has the longest recording period from October 1932 to present, with a clear data loss from 2008 to 2009. D7H005 has the second longest, from October 1942 to present, and a long period of overlap with D7H008. D7H004 has the shortest recording period, from August 1971 to present. It is noteworthy that the three monitoring points' records roughly follow the same typical response-curves.

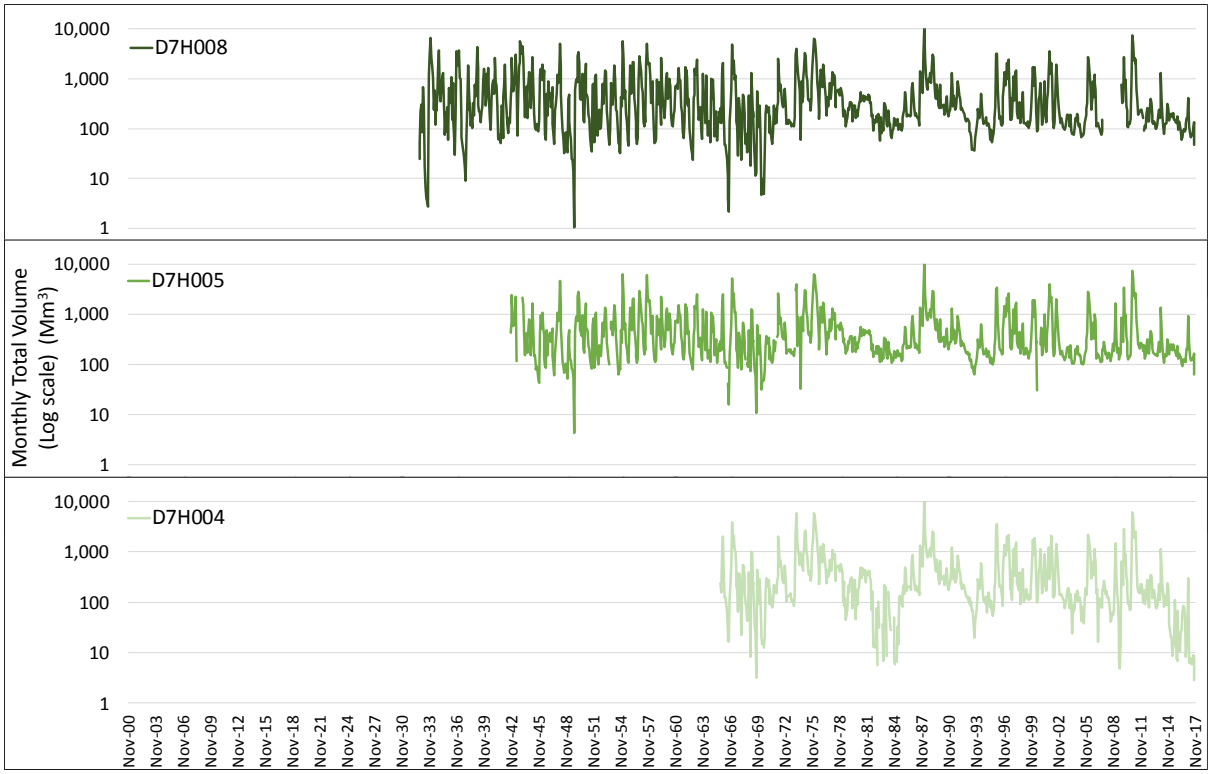

Figure 7. 16: Graphs of monthly total river flow volumes for three adjacent monitoring points along the Orange River

If only the period of overlap is used for the three monitoring points in Figure 7. 16, data fidelity will be lost for points with longer records. As such, the full recording period of each point is used. However, to overcome the lack of temporal synchronisation required for an accurate mass balance, a relative volume reduction ratio is used to represent the links between QCs along the same primary river. This will provide a relatively simple approach to account for the reduction of water availability in downstream QCs because of CSP-related abstractions in an upstream QC. The rationale behind this approach is confirmed by the relative agreement between the three monitoring points' monthly flow volumes in Figure 7. 16.

Therefore, instead of subtracting the consumption of CSP development in one QC from that of downstream QCs' balances, these downstream balances are proportionally reduced based on the abstraction in the upstream QC. For example, if the volume abstracted due to CSP development in the upstream QC represents 15% of that QC's 10th percentile aggregated water balance, then the downstream QCs' aggregated water balance is now only 85% of their 10th percentile volumes prior to CSP development. Naturally, a critical aspect of this approach is which statistical monthly volume (10th, 90th, or average) is used as the denominator in the calculation of the relative reduction in available volume. If the monthly 10th percentile is used, the relative reduction will be larger than if the monthly average is used. The monthly 90th percentile is not considered an effective option since this represents floods, and therefore not typical flow conditions.

To ensure the approach takes into account the most common conditions, and to provide the most conservative relative reduction in available volume, the monthly 10th percentile is used as the denominator in the equation $R_{i,m} = 1 - \frac{V_{CSP,i,m}}{V_{10th,i,m}}$. R represents the percentage volume available after CSP-related abstractions, $V_{CSP,i,m}$ the volume abstracted by CSP developments in QC i only for month m, and $V_{10th,i,m}$ is the original aggregated (river, dam and groundwater)

monthly 10th percentile volume for QC i and month m, as discussed in Section 7.2.1.1. The aggregated balance is used since abstractions from a section of river will ultimately reduce the total volume stored in affected QCs because rivers serve as the main transfer of water between both groundwater and dam storages within the hydrological cycle. The R values of each downstream QC are then multiplied with each other in order to determine the accumulated affect of reduced aggregated water balances along the entire primary river. To calculate the balance in the i^{th} QC along a primary river, the R values of all QCs with stream ranks lower than i (ranked from upstream to downstream, i.e. 1 to i), are multiplied with each other in order to capture the reduced balance in QC i due upstream CSP-related abstractions. The abstractions calculated for QC i are then finally subtracted from the remaining aggregated 10th percentile volumes.

As an example, from Figure 7. 6, the case for D73C, -D, -E and -F is shown in Table 7. 3 for January ($m = 1$). This is for the scenario where all possible CSP developments, based on the isolated hydrological limit for each individual QC, are allowed to abstract water from the aggregated balance for that QC. Naturally, since the 1st QC for this example is ranked 38th, it has 37 other QCs upstream thereof along the primary river (the Orange River). Therefore, its cumulative R value (col. 6) is already low, at 10.93%, meaning because of upstream CSP-related abstractions, only 10.93% of its pre-CSP monthly 10th percentile aggregated balance is available for further abstractions. After the CSP-related abstraction within each QC is subtracted from its the remaining available water due to upstream abstractions, the final linked catchment balance for each QC is calculated (col. 7). The values in column 7 show that if maximum amount of CSP based on the isolated hydrological limits of each QC are fully developed, then, due to reduced transfer between QCs, a hydrological deficit will be reached in downstream QCs.

Table 7. 3: Linked catchment calculated values for QC D73C, D73D, D73E and D73F along the Orange River for PTWC.

1	2	3	4	5	6	7
QC Number (-)	**QC stream rank (-)**	**QC Isolated hyd.[a] limit (Mm^3)**	**Pre- CSP 10th agg.[b] balance (Mm^3)**	**Isolated R value (%)**	**Cumulative R value (%)**	**Final Linked agg.[b] balance (Mm^3)**
D73C	38	16.06	151.52	89.40%	10.93%	0.50
D73D	39	16.50	151.29	89.09%	9.77%	-1.72
D73E	40	42.87	161.80	73.34%	8.70%	-28.88
D73F	41	9.86	78.05	87.36%	6.38%	-4.88

a – hydrological
b - aggregated

Since this 100% development of CSP per QC results in certain QCs experiencing deficits, another approach was needed to prevent this. This presents two questions: which QCs are selected for CSP development, and if they are selected, to what extent? To address this, a sequence of four scenarios were calculated based on the extent to which CSP is developed in each QC.

7.3. Results – Limits imposed by water availability on CSP development

Based on the methodology presented in this paper, a sequence of hydrological constraints on CSP development can be calculated for each hydrological planning area (in this case, QCs). This sequence of hydrological constraints takes the form of four scenarios: no hydrological

constraints (Unconstrained), constraints based on isolated QC balances (Isolated), constraints based on linked catchment balances with an overall relative reduction in CSP capacity from the Isolated QC approach to prevent downstream catchments from being depleted (Downstream), and finally, constraints based on linked catchment balances according on an optimized relative reduction in CSP capacity according to a priority index (Optimized). These four scenarios are carried out at a national scale for the four CSP-cooling technology configurations: Parabolic Trough (PT) with Wet-cooling (PTWC), Central Receiver (CR) with WC (CRWC), PT with Dry-cooling (PTDC) and CRDC.

The rationale behind the four hydrological constraints is to start from a worst-case Unconstrained scenario, where all theoretically suitable CSP development is carried out and the impact thereof on water balances is quantified. This provides a baseline from which to calculate the hydrologically limited CSP development capacities. From this, the Isolated scenario calculates the CSP development capacities based on the isolated impact thereof with each respective QC, with no consideration for downstream impacts of QCs linked by a perennial river. This Isolated constraint is calculated as a percentage of the Unconstrained CSP generation potential, as described in Section 7.2.3, based on the month with the lowest relative water availability for each QC. While this scenario does address the limitations imposed by water resources on CSP development, it does not do so in a way that considers downstream impacts across an entire Primary Catchment. Therefore, a linked catchment scenario is required to determine what percentage CSP development of the Isolated scenario can be supported in each QC while still maintaining a balance in downstream QCs above the reserve margin described in Section 7.2.1. The Downstream scenario does this by reducing all monthly CSP generation potentials from the Isolated scenarios by a flat rate across all QCs. It is done iteratively to ensure the minimum balance in all downstream QCs stays above the environmental reserve (half of the 10^{th} percentile aggregated balance). Finally, the Optimized scenario follows a similar method to the Downstream scenario; however, instead of applying a flat relative reduction to the Isolated constraints across all QCs, the QCs are ranked according to a priority index, and individually optimized along each primary catchment to maintain the ecological reserve in each QC. This optimization allows the QCs with the highest theoretical CSP development potential along a primary river to undergo higher rates of development.

To calculate a priority index, the theoretical annual net generation of each QC (as discussed in Section 7.2.2.), was divided by the total theoretical suitable area for that QC, giving a net generation potential (GWh) per square kilometre. However, in order to capture the rank of that QC along its primary river, this value is multiplied with a primary river area ratio, which is the total theoretical suitable area within each QC, divided by the total theoretically suitable area along its entire primary river.

Table 7. 4 provides the values for these calculation for the same QCs as in Table 7. 3, and seen in Figure 7. 6: Map of South Africa – Monitoring points along Orange River in study region. As seen in column 6, QC D73C has the highest rank because, even though it has the lowest relative net annual generation potential per square kilometre, it has the most theoretical suitable area along the primary river (Orange River), therefore it has the greatest potential for CSP development. These ranking calculations are performed for all QCs, and CSP development can now be prioritised in areas with the highest of these ranks. Since the QCs have now been ranked, the suitable areas within each QC should undergo the same process of prioritization. However, at this stage, an indiscriminately selected percentage is only allocated per QC. What this means is that now the QCs with the highest rank can be allocated the largest development share, relative to the Isolated scenario. For example, for the PTWC CSP-cooling configuration, D73C can be allocated 47%, D73D 11%, D73E 15% and D73F 23% of their respective 100% isolated hydrological limit for CSP development for that CSP-

cooling configuration. These allocations were calculated iteratively, in a similar manner to that of the Downstream scenario. They can be varied depending on what the user wants to optimise for: cost of electricity production – then the suitable areas with highest DNI and which are the nearest to water sources must be given priority; economic development in desired municipal areas – then these can be identified and the QCs within their boundaries can be given priority; minimized flow reduction in low run-off catchments – then the more upstream QCs, with higher self-generated run-off values can receive priority for CSP development, and so on.

Table 7. 4: QC priority calculated values for QC D73C, D73D, D73E and D73F along the Orange River.

1	2	3	4	5	6
QC Number (-)	**QC theo.[a] suit.[b] area (km^2)**	**Ann.[c] theo.[a] generation (GWh)**	**Net ann.[c] generation/km^2 (GWh/km^2/y)**	**Primary river area ratio (-)**	**Development potential rank (-)**
D73C	4,422	477,587	108	0.22	23.33
D73D	1,870	206,167	110	0.09	10.07
D73E	2,755	303,917	110	0.13	14.85
D73F	3,438	385,262	112	0.17	18.82

a – theoretical
b – suitable
c - annual

This prioritization, however, is still somewhat arbitrary, since ultimately, the development of CSP in one location, and therefore one QC, instead of another, depends greatly on the amount and type of government regulation dictating this decision by independent developers. Therefore, the following calculations of linked catchment hydrological limits should serve only as an initial indication of what the hydrologically sustainable development potential for CSP is in each QC. These limits should ultimately be updated as part of an interdepartmental adaptive management strategy for water resources and CSP, between the Department of Energy (DoE) and DWS of South Africa. Part of this strategy should be the addition of new data on hydrological records and proposed CSP plants into the models to ensure the most recent hydrological changes and CSP developments are considered. The results from these hydrological constraint scenarios and CSP-cooling configurations will now be discussed.

7.3.1. Parabolic Trough and Central Receiver with evaporative Wet cooling (PTWC and CRWC)

The 50MW PTWC CSP-cooling configuration, which was modelled in the location-linked HLEM serves as a realistic indication of water consumption at PTWC plants in South Africa. The 100MW configuration was also modelled, with the primary difference in results being a slightly higher turbine efficiency, translating to a higher solar-to-electric (StE) efficiency. While the 100MW configuration does have proportionately lower water consumption rates due to the higher efficiencies, its results were not included in this work since the 50MW case serves as a worst-case point of reference. Despite the marginal improvements in water consumption between the 50MW and 100MW configuration, these improvements are still small in comparison to the relative difference in consumption rates between wet- and dry cooling.

For CR plants, however, the increase in steam turbine efficiency from 50MW to 100MW installed capacities, is countered to a great extent by the reduction in solar field efficiency due to the larger distance from heliostats to the central receiver on the tower. Despite this, the

higher operating temperatures of CR plants with molten salt as the heat transfer fluid (HTF) mean that the steam turbine efficiencies are higher than PT plants, resulting in less heat needing to be rejected through cooling, and more heat being converted to electricity. This results in CRWC plants having much lower consumption factors, and higher StE efficiencies than PTWC plants. Figure 7. 17 shows the average of StEs and consumption factors across all locations modelled within the study region inside South Africa, reflecting the typical operation characteristics of these two configurations.

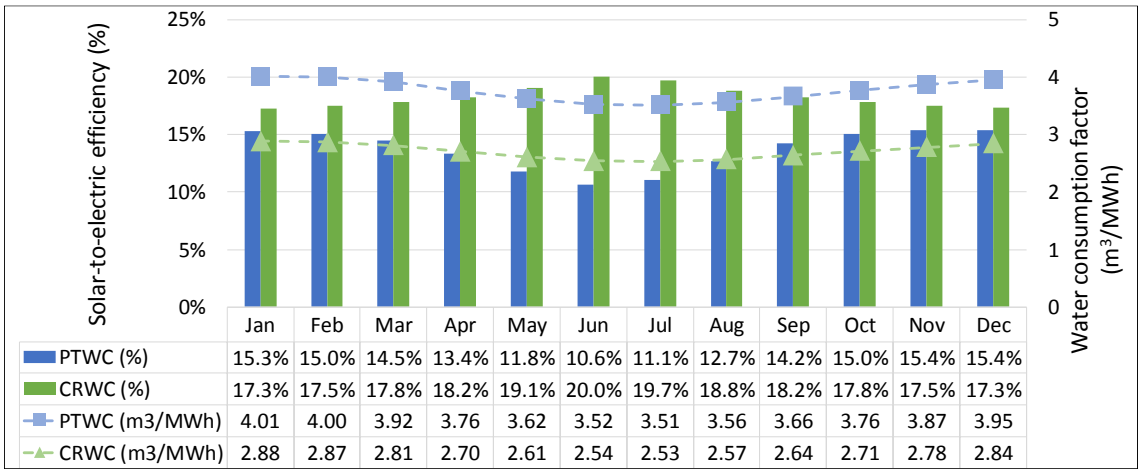

	Jan	Feb	Mar	Apr	May	Jun	Jul	Aug	Sep	Oct	Nov	Dec
PTWC (%)	15.3%	15.0%	14.5%	13.4%	11.8%	10.6%	11.1%	12.7%	14.2%	15.0%	15.4%	15.4%
CRWC (%)	17.3%	17.5%	17.8%	18.2%	19.1%	20.0%	19.7%	18.8%	18.2%	17.8%	17.5%	17.3%
PTWC (m3/MWh)	4.01	4.00	3.92	3.76	3.62	3.52	3.51	3.56	3.66	3.76	3.87	3.95
CRWC (m3/MWh)	2.88	2.87	2.81	2.70	2.61	2.54	2.53	2.57	2.64	2.71	2.78	2.84

Figure 7. 17: National average monthly solar to electric efficiencies and water consumption factors for PTWC and CRWC plants

Figure 7. 18: Total annual abstraction limit and generation limit for South Africa for: (a) PTWC and (b) CRWC (a) and (b) show the national annual abstraction and generation limits for the PTWC and CRWC configurations, respectively, for the four hydrological constraint scenarios. The graphs use logarithmic scales on the y-axes due to the substantial difference in order of magnitude between the four scenarios. The Optimized scenario results in higher abstraction limits reached for both the PTWC and CRWC configurations because of the aim of the optimization approach namely, to maximise the allocation of CSP development to QCs with higher CSP potential, resulting in better use of the available water in those QCs. This increase in both abstraction and generation limit, however, is marginal, at 12% and 15% for PTWC and CRWC, respectively.

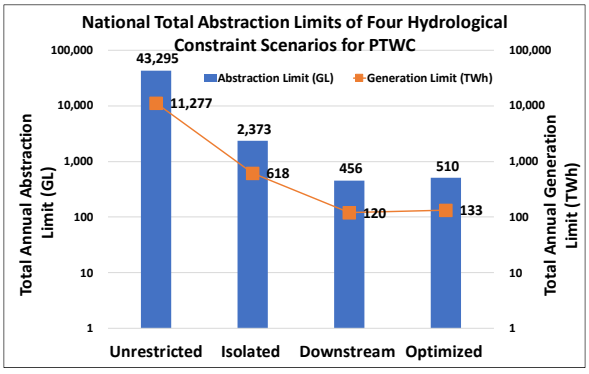

(a)

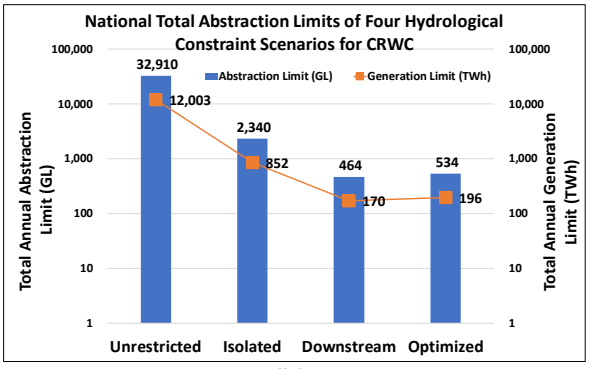

(b)

Figure 7. 18: Total annual abstraction limit and generation limit for South Africa for: (a) PTWC and (b) CRWC

The spatial results for the month of July (winter), from the sequential hydrological constraint scenarios for the PTWC and CRWC configurations, are shown in Figure 7. 21 and Figure 7.

22, respectively. The columns refer to the hydrological constraint scenario, while the rows give different sets of results: abstraction limit in gigalitres (Mm^3) and the generation limits (TWh) associated with these abstraction limits for the CSP-cooling configuration.

Figure 7. 21 and Figure 7. 22 clearly show the decrease in allowable abstraction, and therefore generation potential across the study area in South Africa, from the Unrestricted scenario to the Isolated scenario. Where the Unrestricted scenario shows the theoretical potential for PTWC and CRWC across South Africa per QC, the Isolated scenario takes into consideration the limit imposed by the water resource availability in each QC on this development. The Downstream and Optimized scenarios both show a great reduction in abstraction and generation limits from the Isolated scenarios. This is because the Downstream and Optimized scenarios take into consideration the linked nature of QCs through perennial rivers, where abstractions in one QC are carried over to downstream QCs to reflect the total Primary Catchment impact of CSP related abstractions, and the resulting limit on potential development.

When comparing Figure 7. 18, Figure 7. 21 and Figure 7. 22, the impact of the higher turbine efficiency of CRWC plants, and the resulting reduced consumption factor is clearly seen in the higher generation limits achievable at lower abstraction limits. The decrease in annual national generation potential for South Africa, due to the limits imposed by water availability, is from 11,277 TWh to 120 TWh for PTWC, and from 12,003 TWh to 170 TWh for CRWC. It must be noted that these generation potentials do not consider a specific capacity factor (CF). The assumption is that every unit of solar energy is converted into electrical energy based on a StE from the location-linked HLEM, and therefore serves as the maximum theoretical electricity generation potential. If a desired CF is specified, then the required installed capacity in GW can easily be determined, and with more detailed calculations, the required hours of thermal energy storage can also be established. What is clear, however, is that the hydrological limits placed on CSP development for the wet cooled PT and CR configurations, result in the hydrologically sustainable generation limit being just under 84 (PTWC) and just over 61 (CRWC) times less than the theoretical generation potential.

7.3.1.1. Uncertainty analysis – Climate change and water availability in South Africa and wet-cooled CSP potential

In order to capture the likely impact of climate change on water resource availability in South Africa, the percentage change in streamflow per QC was used. This data is available from the DWS National Integrated Water Information System dashboard, and represents the percentage change in stream flows per QC between the present (1975 – 2006) and projected future (2016 – 2045) [319]. The details of the climate models used are beyond the scope of this work, but are available from the DWS. The percentage changes per QC are shown in Figure 7. 19.

These percentage values were multiplied with the aggregated 10^{th} percentile water balances for each QC. This simple approach was deemed adequate to provide a high-level indication of the likely impact of climate change on total raw water availability across the study area. Naturally, detailed hydrological models would provide a better indication of the complex interactions between changes in precipitation patterns, runoff, ground infiltration, stream flow and dam storage volumes. However, due to the over-all high-level nature of the work done, the simple approach used would serve as an effective and fast estimation of the impact of these climate-related changes on CSP generation potentials. The same process used to determine the initial2 was followed, only substituting the original aggregated balances per QC with those resulting from multiplying the percentage change due to climate change with the original balances.

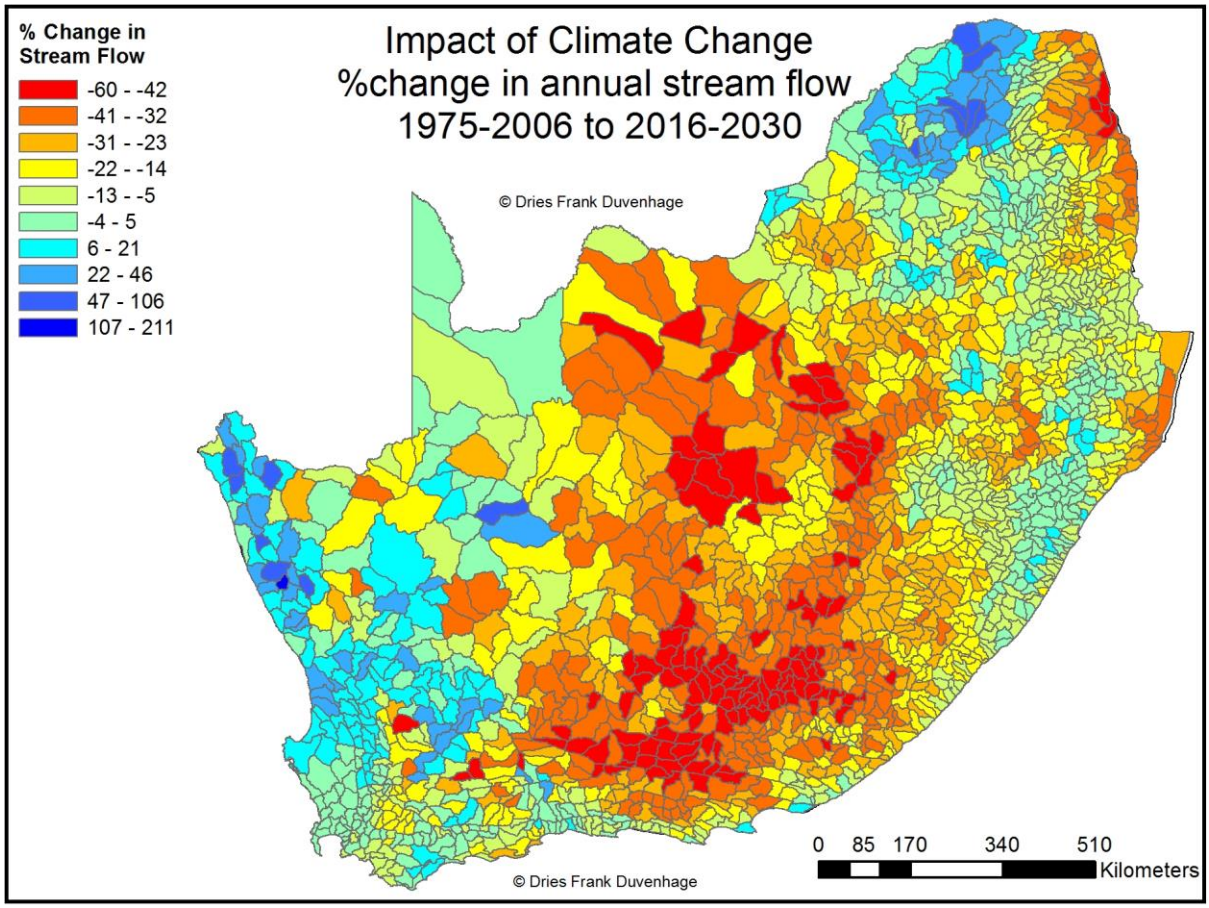

Figure 7. 19: Percentage change in annual stream flow per quaternary catchment due to climate change

The same total national annual generation limits shown in Figure 7. 18 were calculated under the climate change conditions for both PTWC and CRWC, and are shown in Figure 7. 20. When comparing the values in these two figures, it is clear that the implications of climate change are detrimental to the generation potential for wet-cooled CSP plants. The Downstream-linked hydrological national annual generation potential for PTWC is reduced by 15.4% from 120 TWh to 102 TWh. Likewise, for CRWC, it is reduced by 15.2% from 170 TWh to 144 TWh under climate change conditions.

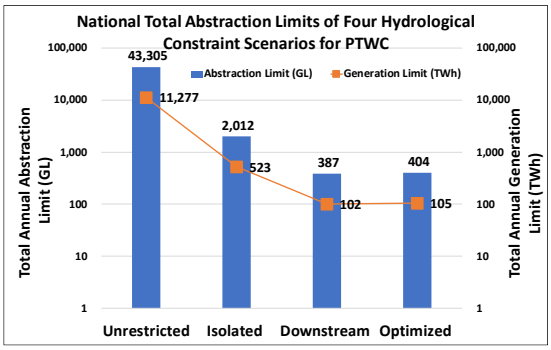

(a)

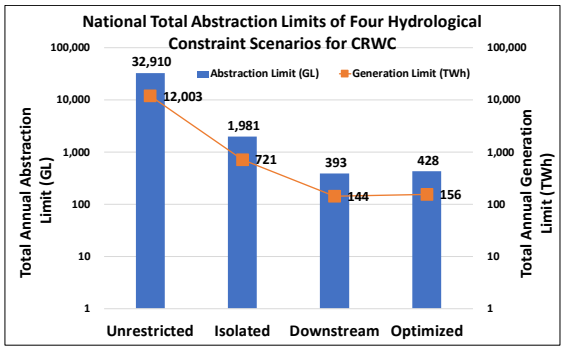

(b)

Figure 7. 20: Total annual abstraction limit and generation limit for South Africa under estimated climate change conditions for: (a) PTWC and (b) CRWC

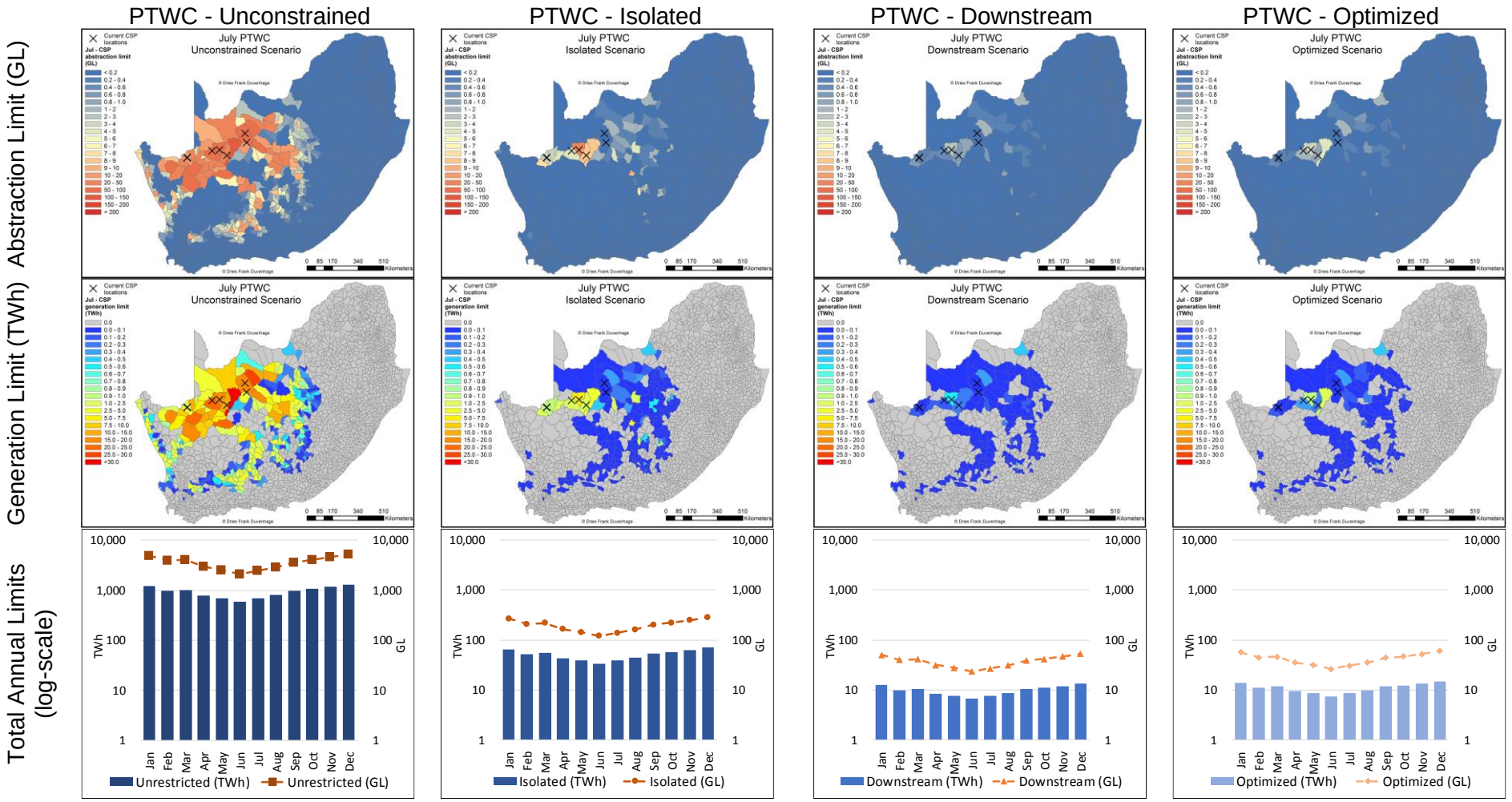

Figure 7. 21: Abstraction and Generation Limit results for Hydrological constraint scenarios for July (winter) for PTWC

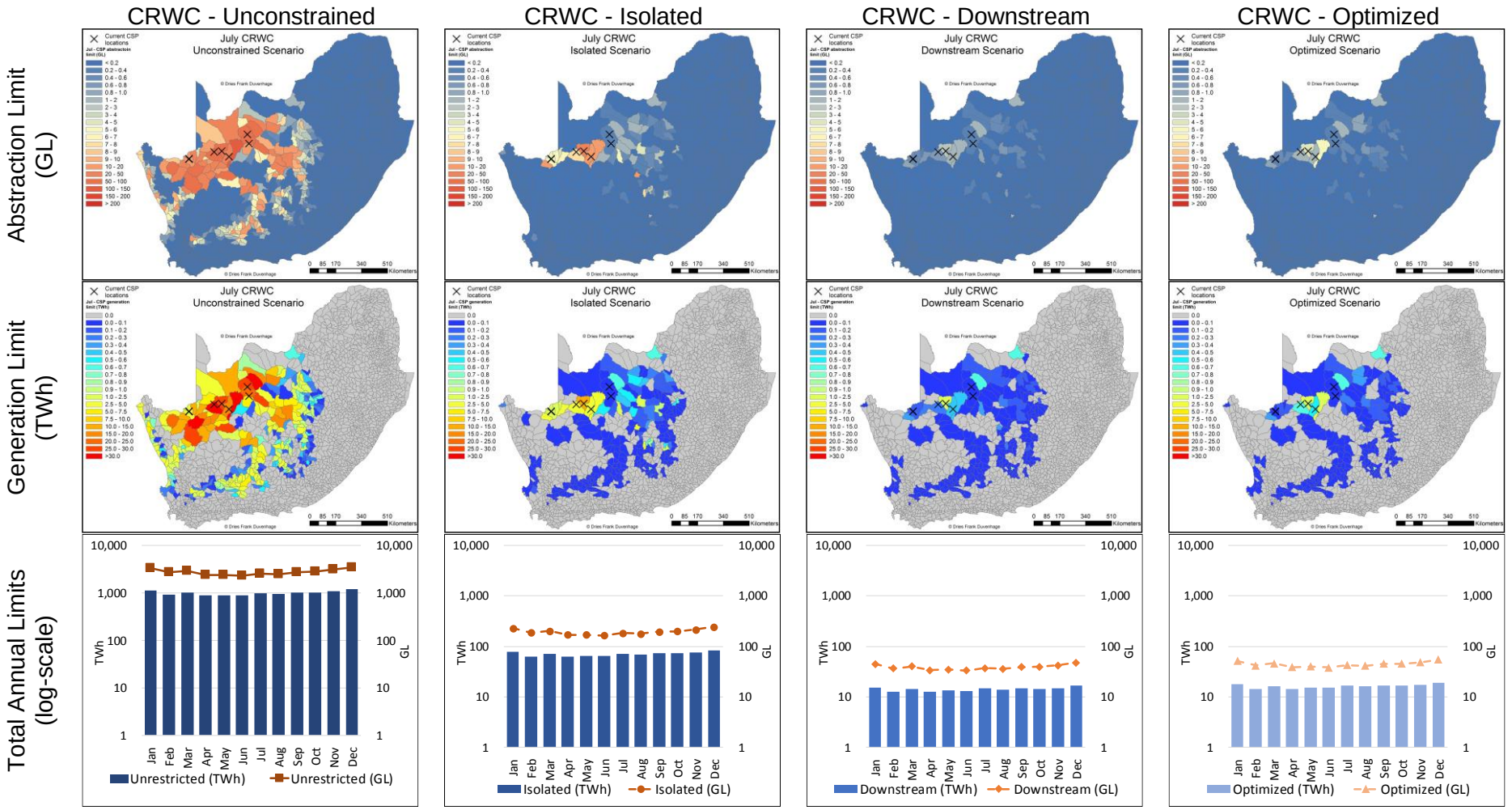

Figure 7. 22: Abstraction and Generation Limit results for Hydrological constraint scenarios for July (winter) for CRWC

7.3.2. Parabolic Trough and Central Receiver with Dry cooling (PTDC and CRDC)

Dry cooling plants in general have lower steam turbine efficiencies due to the reliance on higher ambient dry bulb temperatures for heat rejection. This, in turn, contributes toward an overall decrease in StE at both PT and CR pants compared to wet cooled plants. Dry cooled plants, however, have no water requirements for heat rejection, meaning the consumption patterns are less dependent on seasonal changes in ambient conditions. This ultimately results in the water consumption of dry cooled CSP plants remaining mostly constant throughout the year. A conservative, constant water consumption factor of 0.56m^3/MWh was assumed for all DC plants, based on data obtained from a PTDC plant in South Africa. While this is higher than those (0.1 - to 0.3 m^3/MWh) reported in literature [35], [135], [231], it is still an order of magnitude lower than that of the wet cooling results shown in Figure 7. 17. It is therefore a worst-case estimation of consumption at DC plants in South Africa, yet it maintains the relative improvement in consumption compared to wet cooled plants. The national average monthly StEs and constant consumption factors for PTDC and CRDC plants are shown in Figure 7. 23.

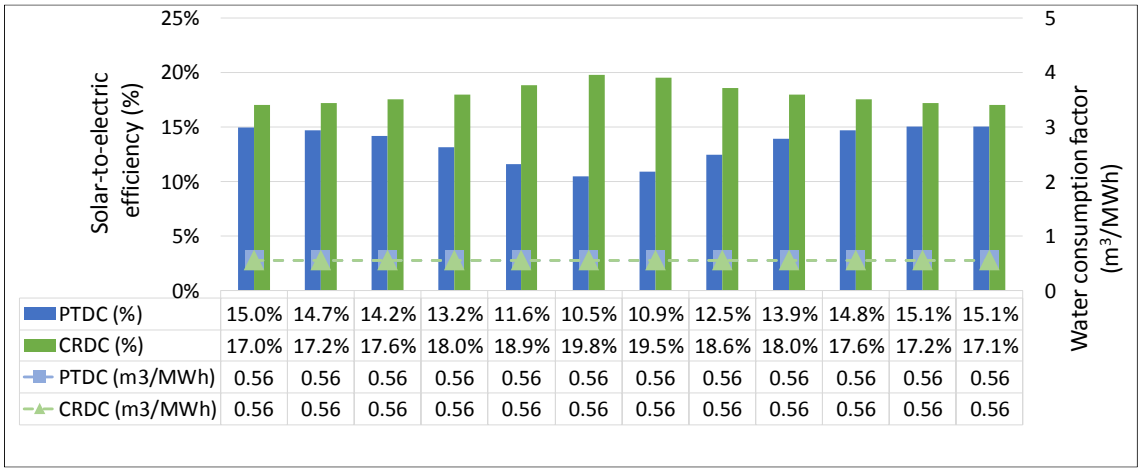

PTDC (%)	15.0%	14.7%	14.2%	13.2%	11.6%	10.5%	10.9%	12.5%	13.9%	14.8%	15.1%	15.1%
CRDC (%)	17.0%	17.2%	17.6%	18.0%	18.9%	19.8%	19.5%	18.6%	18.0%	17.6%	17.2%	17.1%
PTDC (m3/MWh)	0.56	0.56	0.56	0.56	0.56	0.56	0.56	0.56	0.56	0.56	0.56	0.56
CRDC (m3/MWh)	0.56	0.56	0.56	0.56	0.56	0.56	0.56	0.56	0.56	0.56	0.56	0.56

Figure 7. 23: National average monthly solar to electric efficiencies and water consumption factors for PTDC and CRDC plants

Figure 7. 24 (a) and (b) show the national annual abstraction and generation limits for the PTDC and CRDC configurations, respectively, for the four hydrological constraint scenarios. The graphs use the same logarithmic scales on the y-axes as those in Figure 7. 18 for comparative purposes. The Optimized scenario results in higher abstraction limits reached for both the PTDC and CRDC configurations because of the aim of the optimization approach namely, to maximise the allocation of CSP development to QCs with higher CSP potential, resulting in better use of the available water in those QCs. This increase in both abstraction and generation limit is more substantial than for WC plants, at 29% for both PTWC and CRWC, respectively.

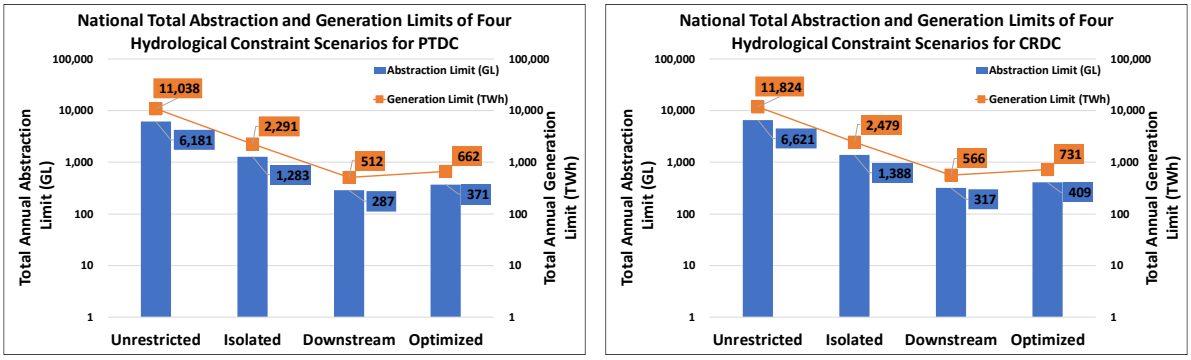

Figure 7. 24: Total annual abstraction and generation limit for South Africa for: (a) PTDC@0.56m^3/MWh and (b) CRDC@0.56m3/MWh

The spatial results for the month of July (winter), from the sequential hydrological constraint scenarios for the PTDC and CRDC configurations, are shown in Figure 7. 27 and Figure 7. 28, respectively.

Figure 7. 24 to Figure 7. 28 clearly show the decrease in allowable abstraction, and therefore generation potential across the study area in South Africa, from the Unrestricted scenario to the Isolated scenario. What is notable, however, compared to the results for the WC plants, is that it is less drastic. Due to the higher efficiencies of WC plants, they have higher national generation potentials under the unconstrained scenarios than DC plants. However, for the Isolated, Downstream and Optimized hydrological constraint scenarios, the limits achievable for DC plants are much higher than those by WC plants. This is not surprising, since WC plants will exhaust water resources much quicker than DC plants and are therefore limited at lower generation limits.

7.3.2.1. Uncertainty analysis – Technological improvements in water use at dry-cooled CSP plants

In order to assess the impact of improved water use, or water use reductions, at CSP plants, more optimistic consumption factors for dry-cooled CSP plants were used in the modelling process discussed in Sections 7.2.2 and 7.2.3. This basically widens the uncertainty range from worst-case water consumption patterns at wet-cooled PT and CR plants to more optimistic, lower water consumption patterns for dry-cooled plants. This approach, therefore provides results which cover the spectrum from optimal water use at advanced dry-cooling plants to standard wet-cooled plants. This therefore accounts for all likely developments that can take place to reduce water use at wet-cooled plants through cooling system hybridisation and better plant-level water management. While these improvements can be quantified and entered into he models used in order to determine their contribution to improving the CSP potential in South Africa, they will fall somewhere within the spectrum of results covered in this work.

Figure 7. 25 shows the results obtained when the same methodology as in Sections 7.2.2 and 7.2.3 is followed, however, with the consumption factor for PTDC set to 0.1262 m^3/MWh and for CRDC to 0.08785 m^3/MWh. These two values represent the most optimistic monthly consumption factors for the two dry-cooled CSP configurations, based on results from detailed hourly-interval simulations of such plants in South Africa. They represent the minimum consumption factors for dry-cooled CSP plants, based on water minimisation strategies employed in the simulation software, ColSimCSP. This highlights the possible range of CSP development potential in South Africa under different hydrological constraint scenarios for

conservative, poor performing PTDC and CRDC plants (Figure 7. 24) and best-of-class future performance of water-efficient PTDC and CRDC plants (Figure 7. 25).

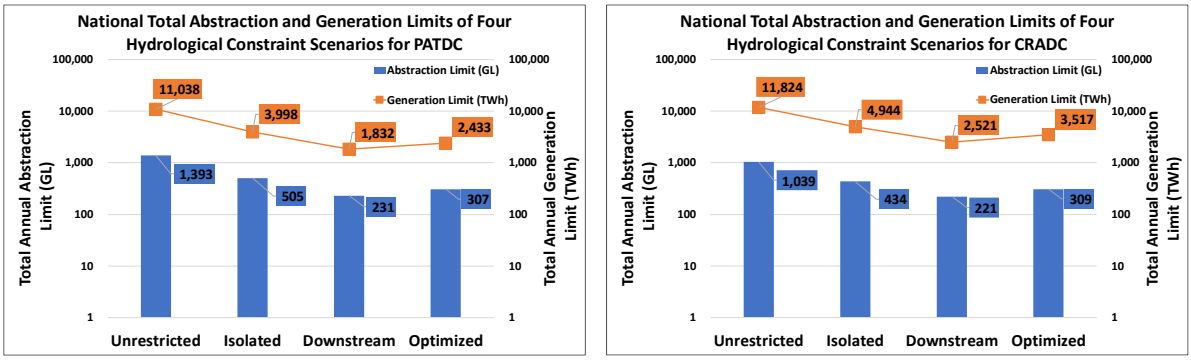

Figure 7. 25: Total annual abstraction and generation limit for South Africa for: (a) PTDC@0.1262m^3/MWh and (b) CRDC@0.08785m^3/MWh

The decrease in annual national generation potential for South Africa, due to the limits imposed by water availability, is from 11,038 TWh to 512 TWh for PTDC@0.56 m^3/MWh and to 1,832 TWh for PTDC@0.1262 m^3/MWh. For CRDC, the reduction from the Unconstrained to the Downstream scenario is from 11,824 TWh to 566 TWh for CRDC@0.56m^3/MWh and to 2,521 TWh for CRDC@0.8785 m^3/MWh. The hydrological limits placed on CSP development for the dry cooled PT and CR configurations, result in the hydrologically sustainable generation limit being just under 30 (PTDC) and 29 (CRDC) times less than the theoretical, unconstrained generation potential. When the optimistic consumption factors are used, however, this reduction is much lower, at just over 6 times for PTDC and 4.7 times for CRDC plants. This translates to the Optimized generation limits for PTDC plants being 2.8 times greater than those for PTWC plants, and those for CRDC plants 2.1 times greater than those for CRWC plants. When comparing Figure 7. 21 and Figure 7. 27, and Figure 7. 22 and Figure 7. 28, it is clear that the generation limits are substantially higher across all QCs for DC than for WC.

7.3.2.2. Uncertainty analysis – Climate change in South Africa and dry-cooled CSP potential

The same approach as discussed in Section 7.3.1 for the impacts of climate change were applied for the advanced dry-cooling cases for Parabolic Troughs (PTADC) and Central Receivers (CRADC). The projected impact of climate change has a larger impact on advanced dry-cooled (ADC) plants in terms of total national annual generation potential than for wet-cooled plants, since the ADC plants can generate more equivalent units of electricity per unit of water. The reduced water availability in catchments where CSP can be developed, results in a reduction of just over 22% for PTADC plants for the optimized scenario (from 2,433 TWh to 1,895 TWh) and a reduction of just over 20% for CRADC (from 3,517 TWh to 2,798 TWh).

However, in spite of the more substantial reduction in generation potential relative to standard water availability conditions, the final generation potential is still substantially higher for ADC plants, at close to 18 times greater than both PTWC and CRWC. This highlights the value of advancements in both technological and plant-level management strategies to reduce water use to further improve the feasibility of large-scale deployment of CSP in arid regions.

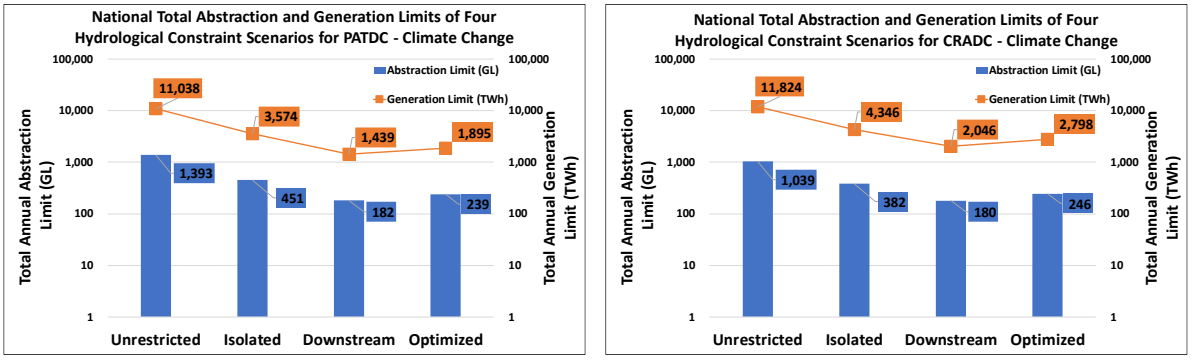

(a) (b)

Figure 7. 26: Total annual abstraction limit and generation limit for South Africa under estimated climate change conditions for: (a) PTADC and (b) CRADC

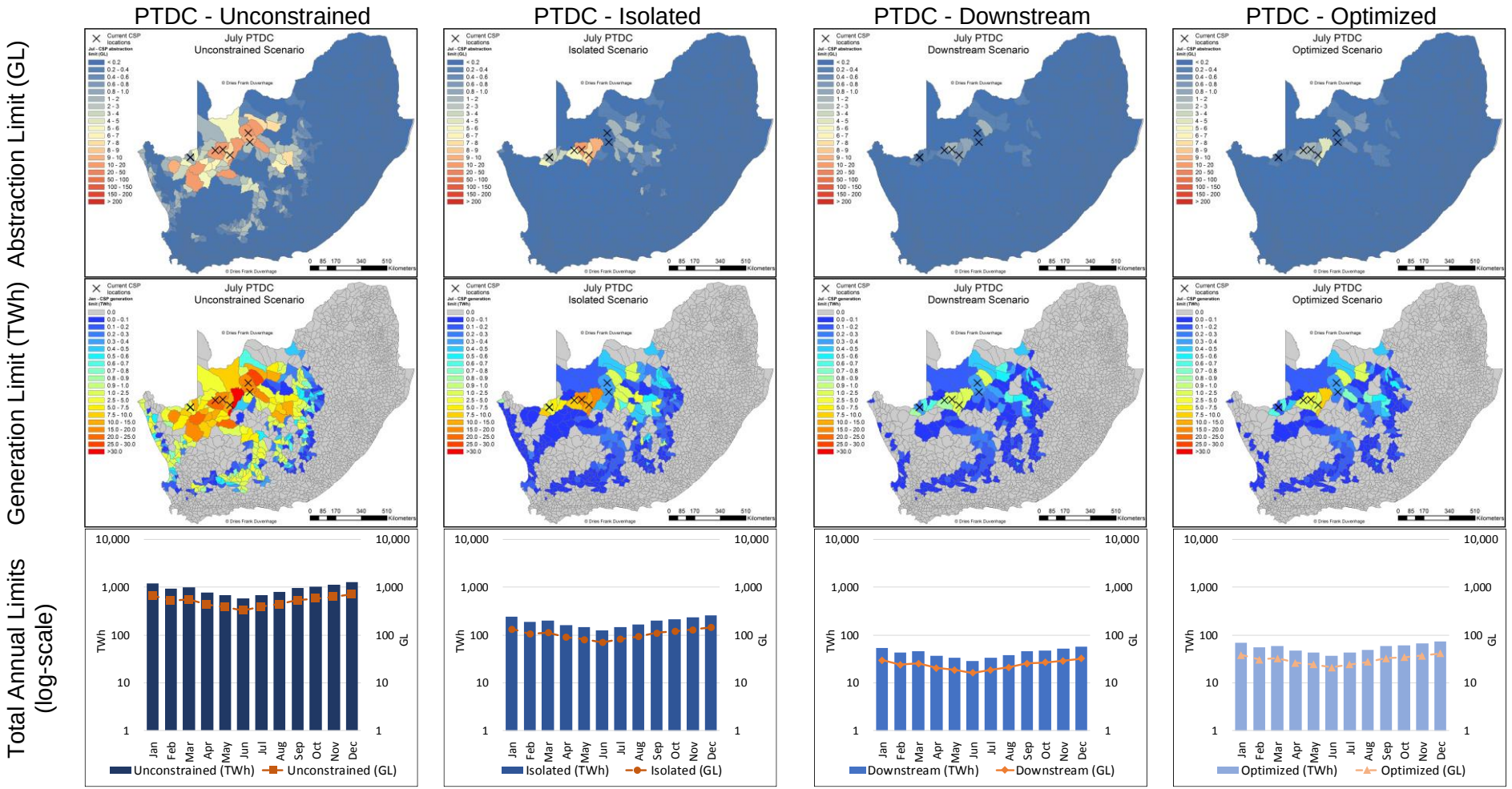

Figure 7. 27: Abstraction and Generation Limit results for Hydrological constraint scenarios for July (winter) for PTDC

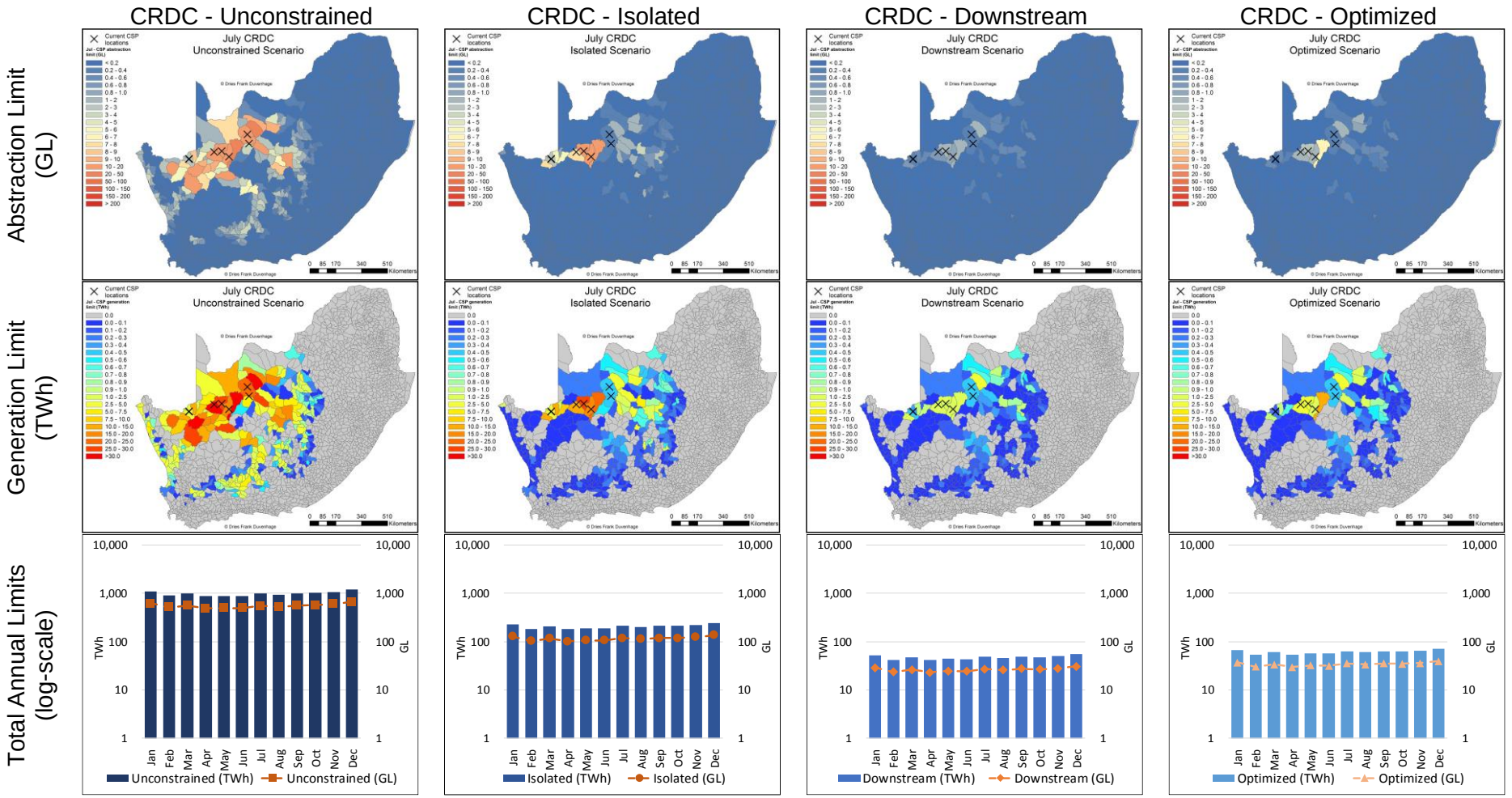

Figure 7. 28: Abstraction and Generation Limit results for Hydrological constraint scenarios for July (winter) for CRWC

7.3.3. CSP and desalination opportunities in South Africa

Of the 104,709 km² of suitable area for CSP in South Africa, is an estimated 6,139 km² within 50 km from the west coast of the country, and are shown in Figure 7. 29. This allows for the possible hybridization of CSP with desalination, in particular Multi-effect distillation (MED) or Multi-stage flash (MSF), which will allow for wet-cooling with ocean water, in combination with the production of potable water. Reverse osmosis is not considered in this brief evaluation since it will require the CSP plant to receive its cooling from wet-cooling, either sourced from the sea, which will be a waste if the water is not used for desalination, or from fresh water sources, which will be counter to locating the CSP plants close to the ocean as a means to prevent the use of fresh water. Alternatively, the cooling can come from dry-cooling, but this would also be counter the idea of locating the plants close to the ocean as a form of fresh-water use prevention. The location of the CSP+dealination plant within a close vicinity to the coast is required in order to prevent pumping and infrastructure costs from escalating beyond techno-economic viability [320]. The limit of 50 km from the coast was arbitrarily selected, based on the fact that shorted distances from the coast would be preferred, but that there are also few other suitable areas further from the coast in the same region, as can be seen in Figure 4. 5.

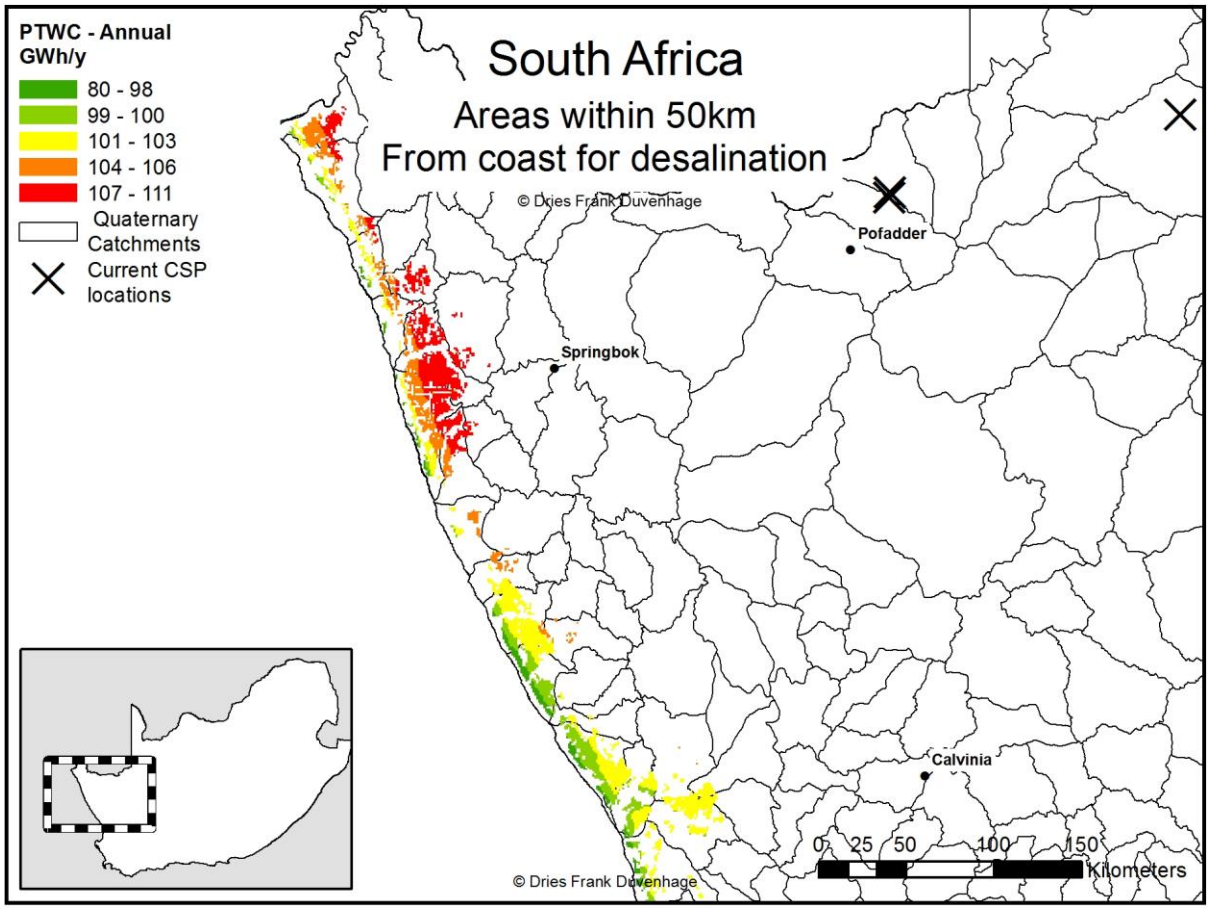

Figure 7. 29: Areas within 50 km of the west coast in South Africa, suitable for CSP and desalination hybridization

It is clear from Figure 7. 29 that the generation potential is higher further away from the coast due to higher DNI values, as there is less attenuation and atmospheric losses due to moisture in the air the further away from the ocean it is. Naturally, the techno-economic feasibility of a

hybrid CSP+desalination plant will depend greatly on the trade-off between higher generation potentials and efficiencies, and pumping distance for sea water. Only MED was considered in order to estimate the amount of desalinated, potable water that can be produced. MED typically has a recovery rate of around 33% of total feedwater, and a specific energy consumption of 1.3kWh/m^3 [321]. With these assumptions, the spatiotemporal HLEM model used in previous sections can be supplemented with simple calculations in order to quantify potable water production. The results for PTWC and CRWC, with MED desalination are presented in Table 7. 5.

Table 7. 5: Monthly results for CSP+desalination (MED) at suitable areas within 50 km of west coast

CSP+ cooling	Unit	Jan	Feb	Mar	Apr	May	Jun	Jul	Aug	Sep	Oct	Nov	Dec	Annual
PTWC	TWh	79	65	66	48	36	29	35	40	50	61	71	81	663
PTWC	GL cons.[a]	319	264	263	184	136	108	128	148	186	234	277	323	2,570
PTWC	GL prod.[b]	105	87	87	61	45	36	42	49	62	77	92	107	848
CRWC	TWh	74	62	67	53	48	46	52	49	53	60	67	75	706
CRWC	GL cons.[a]	213	181	191	149	130	121	136	130	141	164	186	214	1,956
CRWC	GL prod.[b]	70	60	63	49	43	40	45	43	47	54	61	71	645

a – Water demand for cooling
b – Potable water production from MED

What is notable is that the annual generation potential from all suitable areas in this desalination scenario is 663 TWh and 706 TWh for PTWC and CRWC, respectively, both substantially greater than the national annual electricity demand of ~230 TWh. While the water consumption volume is high for both PT and CR plants, since this water is sourced from the ocean, and in actual fact produces fresh water for domestic, agricultural or industrial uses, the net impact on water resources is positive in the Quaternary catchments where these desalination plants are located. In total, PTWC+MED would add a total of 848 million m^3, and CRWC+MED 645 million m^3 to the total water balance for all the Quaternary catchments in question.

7.3.4. Implications in the South African context

Currently, in South Africa, any prospective water user must apply for a water use license (WUL), in accordance with the National Water Act (NWA) of South Africa [309]. The NWA, however, does make special mention of two key strategic use cases: inter-catchment transfers, and power generation. In light of the recognition of power generation as critical to achieving the goal of improved access to electricity, set out in the National Development Plan (NDP), it is important to recognise that the achievement of this goal must not come at the cost of another NDP goal, namely improved access to water [322]. The importance of this trade-off has been recognised by the DWS in a 2015 DWS guidance note on water use by coal independent power producers (IPPs) [323]. This guidance note provides a brief context on water availability across South Africa, and places focus on the areas where coal fields are located, and therefore where coal IPPs are likely to bid to build plants. It emphasizes that water resources in general are stressed, and that bidders who implement water saving technologies and strategies are likely to receive preference during the WUL application process.

As part of the WUL process, such as one undertaken for a CSP plant [324], typically the applicant must perform an integrated assessment of the water availability situation in the QC where it intends to construct the plant. Water availability from the nearby water sources are assessed on an annual basis, and no consideration for the constraint, which the minimum available monthly volume places on generation and associated abstraction, is given. As part of the WUL process, however, the DWS will review the application and supporting documentation, and assess water availability in the area itself, and then approve or decline the WUL.

In South Africa, there are six operational CSP plants, each having already successfully applied for WULs in order for them to be operational. The annual amounts allocated to all commercial, agricultural and industrial water users are publicly available from the Water Authorizations Office (referred to as WARMS) upon request. The water authorizations allocated to the six CSP plants were requested from DWS, and are shown in Table 7. 6 for five of the six, with Kathu Solar Park having to apply for water use authorization from a regional water board, because it abstracts water from a bulk water supply pipeline. These locations are also shown in the maps of Figure 7. 18.

Table 7. 6 also shows the estimated total annual abstraction volumes, based on the locations of these CSP plants, their CSP-cooling configuration, and the results from the location-linked HLEM. It is clear that the values allocated by WARMS to the DC plants are between 56% and 215% higher than the annual abstraction volumes estimated by the HLEM. This suggests that the DC CSP plants in SA have an over-allocation of water, technically allowing them to use much more than the plant should be using. This means that the plant could be wasting water, or using it ineffectively, and the DWS will not raise any alarm because it is still below the registered volumes. The WC CSP plant, however, has a registered volume much closer to the volume estimated by the location-linked HLEM. This suggests that the WC CSP plant might be operating close to its WARMS registered volume, putting it at risk of exceeding its allowance and being subject to penalties.

Table 7. 6: WARMS information for water use authorisations for existing CSP plants in South Africa and HLEM estimated abstraction values

DWS Customer Name[a]	Latitude[a]	Longitude[a]	Registered Volume (m^3) [a]	Quaternary Catchment[a]	CSP-cooling	HLEM annual consumption (m^3)[b]	QC abstraction limit (m^3) [c]
KHI SOLAR ONE RF	-28.536	21.177	300,000	D73F	50MW CRDC	160,000 (4,800 Jun)	8,640,000 (640,000 Jun)
KAROSHOEK SOLAR ONE (RF)	-28.402139	21.497361	300,000	D73E	100MW PTDC	192,000 (3,100 Jun)	15,430,000 (860,000 Jun)
XINA SOLAR ONE RF	-28.62807	19.50579	400,000	D81E	100MW PTDC	190,000 (3,300 Jun)	2,560,000 (130,000 Jun)
KAXU SOLAR ONE RF	-28.628	19.506	600,000	D81E	100MW PTDC	190,000 (3,300 Jun)	2,560,000 (130,000 Jun)
ACWA POWER SOLAFRICA BOKPOORT CSP POWER PLANT	-28.786556	21.881194	875,000	D73D	50MW PTWC	865,000 (42,000 Jun)	13,620,000 (680,000, Jun)

a – The information in these columns is unchanged from the data sent by the WARMS office.
b – Results taken from location-linked HLEM, based on solar field size of existing plants measured on Google Earth®, annual value on top and minimum monthly value on the bottom in brackets.
c – The annual abstraction limit (top value) and minimum monthly abstraction limit (bottom value and month in brackets) based on the Downstream hydrological constraint scenario for the particular CSP-cooling configuration.

These observations demonstrate the need for more informed WUL allocations by the DWS's WARMS office, based on a better knowledge of the typical performance of the various CSP-cooling configurations in a particular location. Beyond an improved approach to quantify suitable allocations for CSP plants, the WUL process also requires a detailed inventory of existing registered users in each QC, accompanied by an inventory of water balances per QC. This will allow the DWS to assess future water use applications, be-it CSP or other water use categories, in greater detail. This will improve the sustainable allocation of water to a specific applicant on grounds of this inventory. This inventory should, however, be updated continuously, as new hydrological data becomes available from the network of monitoring points, and as new applicants are allocated water use rights.

For CSP, as part of future IPP bidding rounds, the methodology presented in this work, with its accompanying models, can be used to guide the development of CSP in certain QCs based on the amount of water already allocated to CSP plants in those QCs. This should also take the form of an inventory of CSP water allocations, and volumes still available for future developments. Like the 2015 Guidance Note for coal IPPs, a guidance note can be generated for CSP in the areas identified in this study where CSP plants are most likely to be developed. The models used in this methodology are adaptable to accommodate the potential impact of water-savings technologies on the four CSP-cooling configurations considered. These impacts can be quantified and incorporated into the models, and the increase in hydrologically sustainable CSP development potential can be determined. Furthermore, once these potential reductions in CSP-related water consumptions are determined and incorporated into the models, the DWS can suggest the use of certain technologies in order to ensure sustainable water use by CSP plants, with cognisance of the potential impact on plant operation.

A set of models is presented to can enable the custodians of water and energy planning in arid regions to better plan for CSP development and ensure hydrological sustainability. It was found that the hydrological limits in South Africa drastically reduce the amount of CSP that can be developed relative to the theoretical, unconstrained potential. This reduction is much greater for water-intensive wet cooled plants, with the Downstream hydrological CSP generation potential being only 1.18% and 1.63% of the theoretical Unconstrained generation potential for PTWC and CRWC, respectively. The much less water-intensive dry cooled CSP plants also experience hydrological limits, albeit much lower than that of wet cooled plants, with the Downstream hydrological constraints being 4.64% and 4.79% of the theoretical Unconstrained generation potential for PTDC and CRDC plants, respectively. These values are shown in Table 7. 7.

Table 7. 7: Total annual generation potential for CSP under theoretically unconstrained and downstream hydrologically constrained scenarios for different CSP+cooling configurations and water availability conditions

CSP-cooling configuration	Water availability conditions	UT [a] (TWh)	DH [b] (TWh)	DH as % of UT
PTWC	**50%**	11,277	74	0.66%
PTWC	**CC**	11,277	105	0.93%
PTWC	**100%**	11,277	133	1.18%
PTWC	**200%**	11,277	252	2.23%
CRWC	**50%**	12,003	108	0.89%
CRWC	**CC**	12,003	144	1.19%
CRWC	**100%**	12,003	196	1.63%
CRWC	**200%**	12,003	376	3.13%
PTDC	**100%**	11,038	512	4.64%
CRDC	**100%**	11,824	566	4.79%
PTADC	**50%**	11,038	1,413	12.8%
PTADC	**CC**	11,038	1,762	15.9%
PTADC	**100%**	11,038	2,433	22.0%
PTADC	**200%**	11,038	3,932	35.6%
CRADC	**50%**	11,824	2,101	17.8%
CRADC	**CC**	11,824	2,798	23.7%
CRADC	**100%**	11,824	3,517	29.7%
CRADC	**200%**	11,824	5,083	42.9%

a – Unconstrained theoretical potential
b – Downstream Optimized hydrological constrained potential

In order to contextualize the limits placed on CSP generation potential in terms of the Integrated Resource Plan (IRP) of South Africa, the four future CSP development cases presented in Section 3 are used as a reference. These four cases indicated that, based on results from various energy mix models performed for South Africa as part of the IRP process, the installed capacities allocated to CSP by 2030 can range between 38 GW and 15.5 GW (High case), between 15 GW and 2 GW (Moderate case), between 2 GW and 0.5 GW (Low case) and less than 0.5 GW (Very low case). There is already 0.5 GW of CSP installed in South Africa, which have reportedly been operating at an average capacity factor (CF) of 45% [325]. To compare these future planned installed capacities to the hydrological limits calculated in Section 7.2.3.1 and Section 7.2.3.2, this capacity factor will be applied to the four future cases for CSP, as presented in Table 7. 8.

Table 7. 8: Comparison of policy mandated future CSP installed capacities to hydrologically constrained CSP generation Potential

Future development case	Maximum Installed GW[a]	CF (%)	Equivalent annual generation (TWh)	As a % of PTWC DH limit[b]	As a % of CRADC DH limit[b]
High Case	38	45%	149.8	113%	4.2%
Moderate	15	45%	59.1	44.4 %	1.7%
Low Case	2	45%	7.8	5.9 %	0.22%
Very Low (Actual)	0.5	45%	1.9	1.4%	0.05%

a – values from Section 3.4.

b – under standard water availability conditions

Table 7. 8 clearly shows that role which CSP can play in the national electricity supply of South Africa is artificially limited by policies which do not reflect resource limits. The IRP is the formal government policy used to dictate how much installed capacity is allocated to various generation technologies to meet the future electricity demand. Naturally, the hydrological limits are not the cornerstone of this process, instead, socio-economic factors such as cost of electricity and economic contribution are. However, these hydrological limits should form part of the IRP process to harmonise inter-departmental planning between the DoE responsible for the IRP and the DWS, responsible for water resource management.

To guide energy policy makers, this work shows that the use of dry cooled plants can allow for higher exploitation of the greater economic benefits associated with CSP above other renewable technologies [326]. Since CSP is comprised of many sub-systems of technologies for which there are mature technical capabilities and skills in South Africa, the use of dry cooled CSP plants will allow for more CSP being hydrologically sustainable, and therefore contribute more to the stimulation of these associated industries. Furthermore, the models and tools presented in this work can be used to assess the hydrological impact of CSP developments in areas of economic interest. This can in turn further motivate the development of CSP in South Africa, without putting water resources under unsustainable stress. The methods used in this work is not exhaustive, and improvements can be made in the spatiotemporal modelling of dry cooled plants in particular, as well as in the hydrological quantification of water availability. The intention of this work, however, is to present an initial high-level strategic assessment of CSP development and water resources in arid regions, and specifically South Africa. It provides a detailed account of the methodology used to determine the first documented investigation of the hydrological limits placed on CSP development.

Chapter 8 – Thesis conclusions

8.1. Thesis Summary

The general aim of this work was to provide a methodological framework which allows for the assessment of national CSP fleet and capacity planning from a hydrological sustainability perspective. This was achieved through the specific goal of determining the hydrological limit placed on CSP development potential per quaternary catchment. A systematic approach was followed to calculate these hydrological limits relative to an unconstrained theoretical limit for each quaternary catchment.

First, the need for the management of CSP fleet deployment and water resources in arid regions was identified based on a narrative literature review in Section 2. Here, the water use at CSP plants was discussed in detail. A global assessment of the locations of CSP plants and water resource characteristics was conducted based on datasets from the World Resources Institute's Aqueduct study and UN's Aquastat study. It was found that existing and planned CSP plants are not only found in the most arid regions, but that these regions' water resources have high seasonal variability. A review of electricity and water infrastructure planning approaches was conducted, and it was found that harmonization between the two are critical to ensure neither power plants, nor water resources, negatively impact each other. This section concludes that CSP poses a particular instance of this water-energy nexus, in that CSP, being thermal, requires water in varying amounts, but that its dependence on solar resources, requires it to be located in arid regions. This necessitates the assessment of the hydrological limits placed on CSP potential in these regions in order to ensure hydrological sustainability.

Once this need was identified in both literature and the cases of existing CSP plants, the potential role that CSP is likely to play in the South African energy supply mix was assessed in Section 3. This was done in light of the national electricity planning that is done in South Africa through the Integrated Resource Plan (IRP). The IRP is based on the results from electricity planning models, and as such, various other institutions have conducted similar studies to test other model inputs and assumptions. These studies' results were evaluated based on the amount of CSP capacity included in the energy mix in the final year of modelling. 10 studies were evaluated, with a final total of 26 different scenarios. From them, a range of possible future CSP development cases were identified, each with their respective drivers for and barriers to CSP. The key take-away was that since there is already 500 MW of CSP installed and operational in South Africa, CSP can account for between 500 MW and 38,000 MW of the installed electricity generation capacity. This, therefore, validates the rationale for this work, since South Africa is the 30th driest country in the world, with these constrained water resources likely to impose considerable limitations on CSP deployment.

Now that the need for strategic management of CSP fleet deployment and water resources for sustainable development, within the South African context has been identified, a systematic methodology was needed to achieve this. The first step was to identify the potential locations where CSP can be developed in South Africa. This was important for three critical reasons:

- CSP performance, and therefore water consumption, depends greatly on the geographic location,

- The water availability varies spatially, and therefore, the impact on water resources is highly localized from the point of consumption and downstream therefrom, and

- A point of reference for the theoretical potential of CSP, based solely on geo-spatial suitability, is required in order to quantify the limits imposed by water resources on this potential.

A standard GIS-study was conducted, using exclusion- and inclusion criteria from literature for South Africa, from publicly available spatial datasets. It was found that there is 104,709 km^2 of theoretically suitable surface area. This area was delineated in the form of explicit 1km x1km squares, enabling the modelling of CSP-performance at a high spatial resolution. Typically, CSP plants are between 2 km^2 and 5 km^2, allowing for sub-plant spatial modelling, and the aggregation of adjacent 1km x1km squares in order to quantify the operation of CSP plants with varying nameplate and TES capacities.

Since the theoretically suitable locations in South Africa have been identified, a robust high-level estimation model (HLEM) is necessary in order to model CSP performance at these 104,709 potential locations. The HLEM must be able to reflect the impact of CSP+cooling configuration, spatially varying meteorological conditions, as well as seasonally changing conditions. Emphasis is placed on seasonal variability of CSP performance in light of the fact that water resources' availability vary seasonally. As an initial attempt in Section 5, an HLEM was developed based on annual efficiency calculations, with simplified additional equations and assumptions used to adapt these calculations to monthly values. This initial HLEM was then further refined through the use of monthly efficiency assumptions from detailed hourly-interval simulations (DHIS) for different CSP+cooling configurations in five representative locations across South Africa in Section 6. This refined HLEM made use of monthly spatial datasets for temperature, relative humidity, and DNI for South Africa to estimate the monthly performance of CSP plants. It was found that this approach provided adequate accuracy to that of the DHIS results in the five locations for the four CSP+cooling configurations considered.

The penultimate step in the methodology was to quantify water availability both spatially and temporally. This was achieved through the use of annual groundwater availability, monthly river flow and dam storage data, collected and maintained by the DWS of South Africa. The monthly water availability per resource was quantified based on statistical analysis of the entire time-series for each data point (dam or river gauging station), which stretched as far back as January 1900 in some cases. The monthly average, 90^{th} and 10^{th} percentile values for each resource was calculated. Half of the 10^{th} percentile value was taken as a conservative indication of the volume of water available at a particular point (along a river or in a dam) for a particular month. The monthly available water (half of the monthly 10^{th} percentile value) for each resource was then aggregated to a total available balance per Quaternary catchment, which served as the most appropriate spatial resolution for water availability studies in South Africa.

These initial available water balances per Quaternary Catchment served as the first step to quantifying the hydrological limitations placed on the theoretical CSP potential calculated based on the suitable areas from Section 4, and the performance model developed in Sections 5 and 6. The first hydrological limit scenario considered was for each Quaternary catchment in isolation. This isolated hydrological limit was calculated as the portion of theoretical CSP potential that can be supported by the minimum monthly aggregated water balance. Since water availability varies throughout the year, the annual amount of available water in a certain location (in this case Quaternary catchment) would not provide a true indication of how much CSP can be supported by the water resources in question, since it would exceed the availability in drier months. As such, the month with the aggregated available water which is the lowest percentage of theoretical CSP water demand serves as the percentage by which the total CSP potential in that Quaternary catchment is

constrained. When this percentage is multiplied with the theoretical unconstrained CSP generation potential for each month, the isolated hydrological limit can be determined for each Quaternary catchment.

Obviously, this isolated hydrological limit does not consider the impact on downstream Quaternary catchments along a perennial river. As a result, a simple approach was needed to link these Quaternary catchments in such a way as to reflect the impact due to abstractions from CSP plants. This was achieved in a step-wise manner by first calculating the percentage remaining aggregated available water for each Quaternary catchment after subtracting the CSP demand. This post-CSP percentage was subsequently multiplied with each Quaternary catchment along the same perennial river before subtracting the CSP water demand for each. This effectively captured the downstream impacts of all CSP related water abstractions along a perennial river, until the aggregated water balance ultimately reduced to 0% of the pre-CSP balance. This, however, would mean that an entire catchment is now completely depleted, a condition that must be avoided since it would represent a man-made drought. As such, the minimum allowed limit would once again be half of the 10th percentile, meaning that this percentile would be assumed to represent pre-CSP aggregated available water for each Quaternary catchment.

Now that the catchments can be linked in a way to reflect the downstream impacts of CSP development, the total catchment hydrological limit due to downstream constraints can be calculated. This was done in an iterative manner for all Quaternary catchments along each perennial river in the study region. The percentage of the isolated hydrological limit was calculated that would prevent the minimum aggregated available water along that river from falling below half of the 10th percentile for that quaternary catchment. This resulted in a dramatically reduced CSP development potential compared to the unconstrained theoretical potential, reflecting the true limit imposed by water resources on CSP in South Africa. However, this downstream hydrological limit percentage was applied indiscriminately across all Quaternary catchments along each perennial river, thus not accounting for the fact that the CSP potential in certain Quaternary catchments could be increased and other decreased in order to exploit the highest possible DNI and efficiencies. As such, a third and final hydrological constraint scenario was considered, where the theoretical potential in Quaternary catchments with the highest average DNI and most suitable area was optimized. This optimized hydrological limit allowed for more CSP generation potential while still preventing downstream Quaternary catchments from falling below the allowed minimum.

These optimized hydrological limits per Quaternary catchment were calculated for six different CSP+cooling configurations, under four different national water availability conditions. The six CSP+cooling configurations considered were PTWC, PTDC, PTADC, CRWC, CRDC and CRADC. The four water availability conditions considered were a standard case, a climate change case, a double standard availability case and half standard availability case. The standard availability case was conservatively chosen as half of the 10th percentile (90% assurance level) monthly aggregated river, dam and ground water volumes for each quaternary catchment. The climate change case was calculated according to the percentage change in streamflow due to climate change, as determined by the DWS per Quaternary catchment. The double standard water availability condition was calculated as 200% of 10th percentile, while the half standard availability case was calculated as 50% thereof.

The total national annual CSP generation potential can be calculated by taking the sum of all the monthly CSP generation potentials for all Quaternary catchments, and serves as an effective measure of the total constraints imposed by water on CSP in South Africa. This allowed for the determination of a range of national annual CSP generation potentials for

both Parabolic Trough and Central Receiver CSP technologies. The range of results vary from low CSP potential, due to water intensive CSP+cooling configurations combined with low water availability, to high CSP potential due to less intensive configurations combined high water availability. Since this range includes the results for 100% wet-cooled and advanced dry-cooled CSP plants, it covers the possible water consumption and performance for all variants of hybrid-cooled CSP plants.

8.2. 8.2 Detail Discussion of Results and Conclusion

To compare the entire spectrum of results for different CSP+cooling configurations and water availability conditions, Figure 8. 1 depicts the total national annual generation potential in TWh on the x-axis, from 0 to 5,500. The top bar-graph shows the spectrum for PT plants and the bottom shows it for CR plants. For both the PT and CR bars, the labels indicate the CSP+cooling configuration and which water availability conditions were considered. These labels, from A to I, and their specific results, are summarised in Table 8. 1.

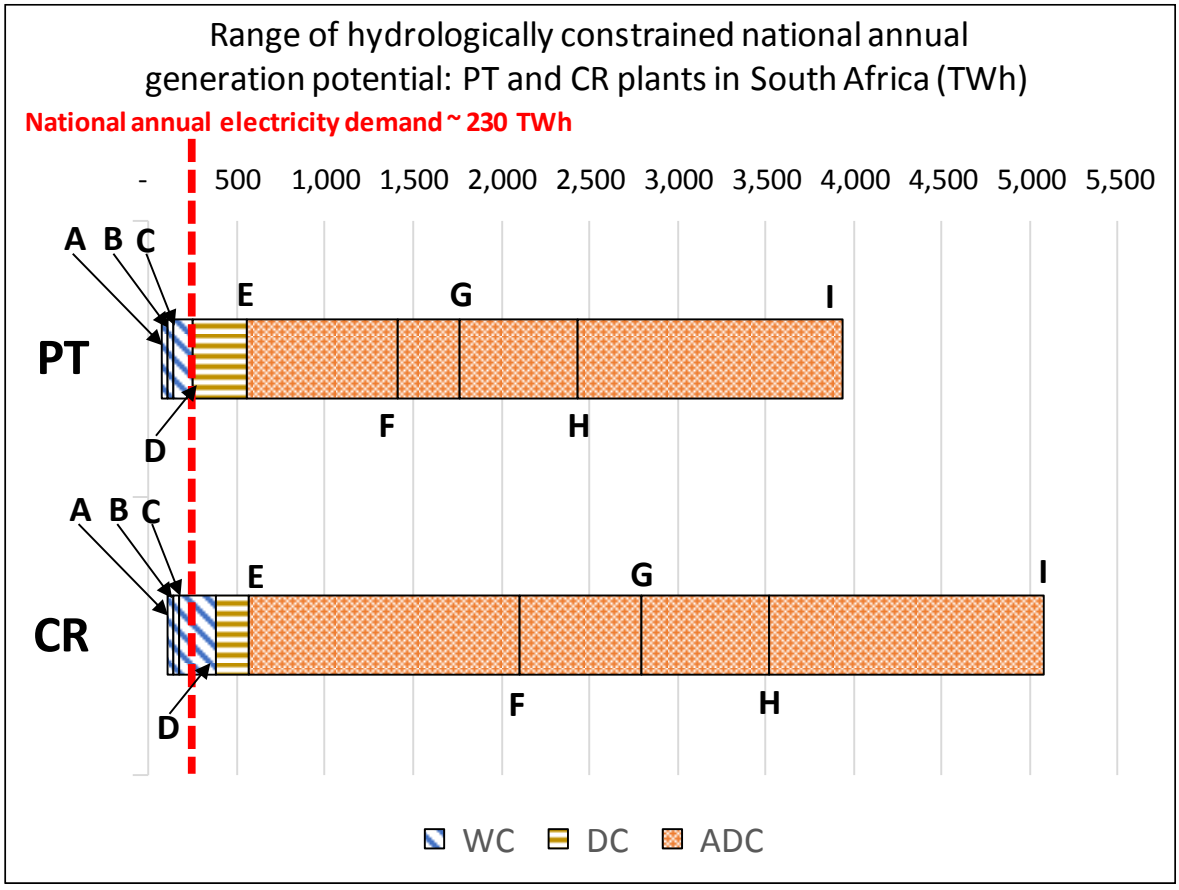

Figure 8. 1: Range of national annual CSP generation potentials for different CSP water use cases and water availability cases. A – WC50%, B – WCCC, C – WC100%, D – WC200%, E – DC100%, F – ADC50%, G – ADCCC, H – ADC100% and I – ADC200%

Figure 8. 1 shows that the worst-case conditions for both PT and CR plants are wet-cooled configurations under half of standard water availability conditions, at 74 TWh and 108 TWh for PTWC – 50% and CRWC – 50% respectively. This is followed by the wet-cooled configurations under climate change water availability conditions, at 105 TWh and 144 TWh for PTWC - CC and CRWC - CC, respectively. Interestingly, even though the conservative

estimation for dry-cooled consumption factors (0.56 m^3/MWh) is substantially lower than the calculated national annual average for wet cooled plants (3.824 and 2.731 m^3/MWh for PTWC and CRWC, respectively), the relative increase is low compared to the relative increase for advanced dry-cooled CSP plants (ADC) with consumption factors of 0.1262 m^3/MWh and 0.08785 m^3/MWh for PTADC and CRADC, respectively. This translates to generation potentials under standard water availability conditions of 662 and 761 TWh for PTDC – 100% and CRDC – 100%, respectively, but increases to 2,433 and 3,517 TWh for the PTADC – 100% and CDADC – 100% configurations, respectively. For comparison, the national annual demand for the entire South Africa is around 230 TWh. This means that mostly the wet-cooled plants are incapable of meeting this demand on their own, unless water availability conditions are double that of the standard, while the dry-cooled plants can meet and exceed this demand several times over due to their more effective use of water, under all water availability conditions. However, at hydrologically constrained total annual generation capacities of 133 TWh and 170 TWh for PTEC and CRWC, respectively, under the standard water availability conditions, wet-cooled plants are still more than capable of meeting the generation capacities put forward in the IRPs discussed in Section 3.

Table 8. 1: Range of results for different sensitivities to water availabilities and water use cases for CSP in South Africa

Label	**A**	**B**	**C**	**D**	**E**	**F**	**G**	**H**	**I**
Water availability conditions[a]	50%	CC[b]	100%	200%	100%	50%	CC	100%	200%
Water use technology	WC	WC	WC	WC	DC	ADC	ADC	ADC	ADC
PT (TWh)	74	105	133	252	557	1,413	1,762	2,433	3,932
CR (TWh)	108	144	170	376	566	2,101	2,798	3,517	5,083
PT (m^3.MWh)	3.824	3.824	3.824	3.824	0.560	0.126	0.126	0.126	0.126
CR (m^3.MWh)	2.731	2.731	2.731	2.731	0.560	0.088	0.088	0.088	0.088

a – as a percentage of Standard Availability conditions discussed in Section 7.2.
b – CC: Climate Change conditions as discussed in Section 7.3.1.

The range for Parabolic Troughs is presented in Figure 8. 2, and for Central Receivers in Figure 8. 3, with a detail frame for the wet-cooled configurations of each. The relative changes in total national annual CSP generation potential for the wet-cooled CSP plants under different water availability conditions are smaller than for the advanced dry-cooled plants. This is because for each unit of water available, the ADC plants can generate much more electricity.

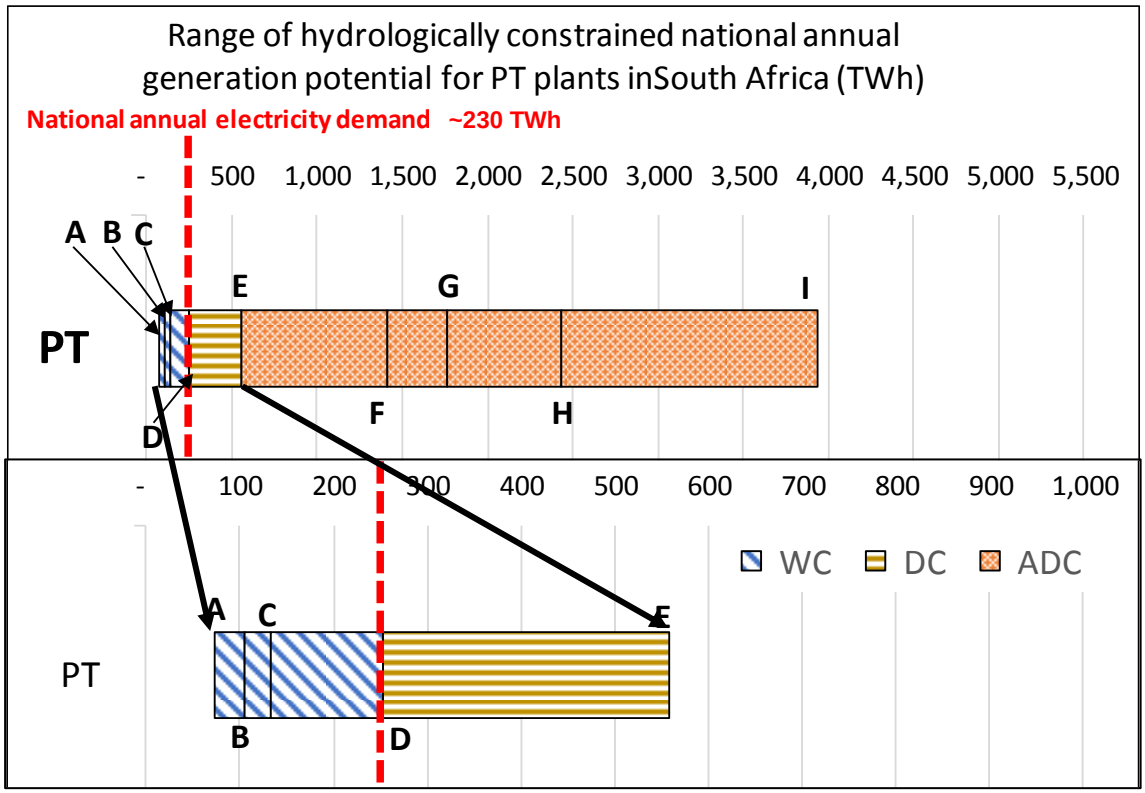

Figure 8. 2: Detail range of total national annual CSP generation potential for Parabolic Troughs: A – WC50%, B – WCCC, C – WC100%, D – WC200%, E – DC100%, F – ADC50%, G – ADCCC, H – ADC100% and I – ADC200%

What these results point out is that the amount by which CSP potential in South Africa is constrained due to water resources depends greatly on the consumption factor of the CSP+cooling configuration. If the consumption factor for dry-cooled plants were to increase, from a conservative 0.56 m^3/MWh, to around 0.1 m^3/MWh for advanced dry-cooling plants, under the same water availability conditions, it would allow for between 430 and 620 times more CSP generation potential (for PT and CR, respectively). This illustrated the importance of placing more focus on CSP plant level water consumption reduction, than necessarily on increasing water availability in areas with high CSP suitability. It also highlights the increased resilience of DC, and ADC plants to changes in water availability, since even under the half of standard water availability conditions, the total national annual generation potential for ADC plants is still more than 19 times greater than that for wet-cooled plants under the same conditions.

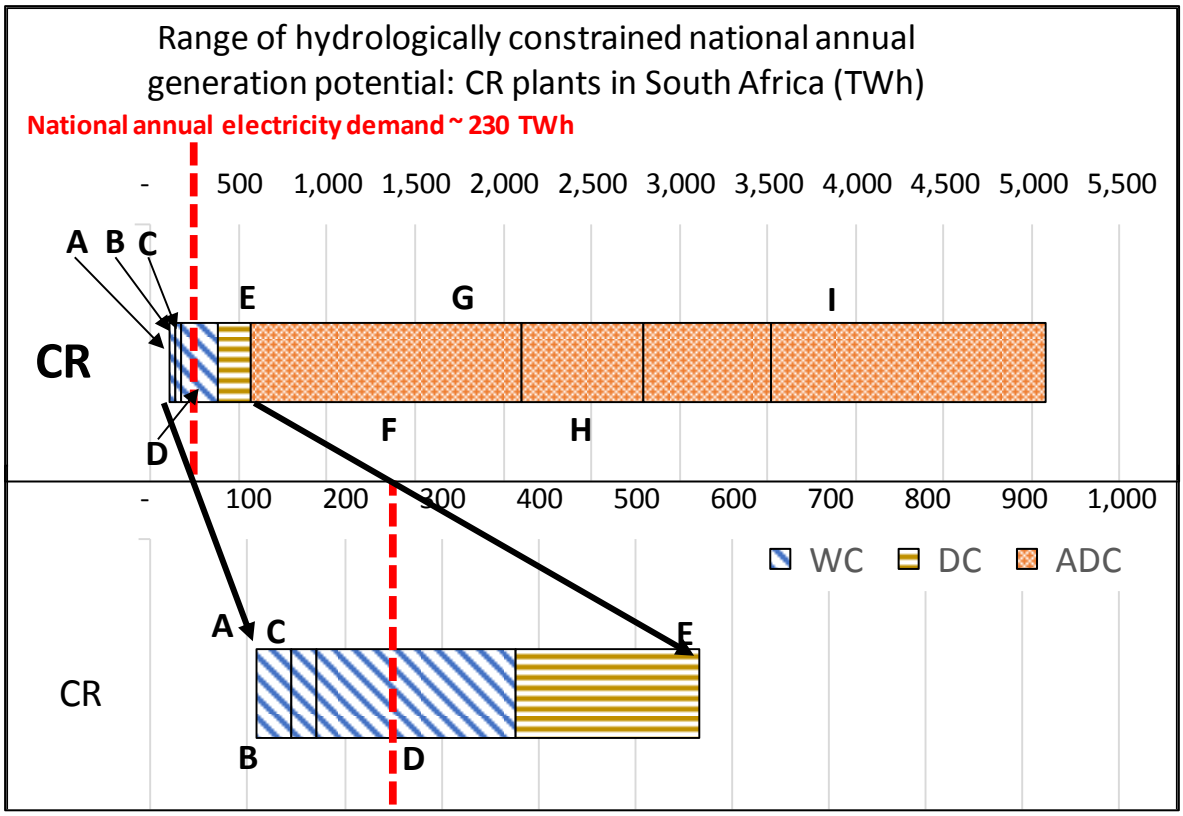

Figure 8. 3: Detail range of total national annual CSP generation potential for Central Receiver: A – WC50%, B – WCCC, C – WC100%, D – WC200%, E – DC100%, F – ADC50%, G – ADCCC, H – ADC100% and I – ADC200%

The value of the maps in Figure 7. 21 and Figure 7. 22 (for wet-cooled CSP+cooling configurations, and Figure 7. 27 and Figure 7. 28 (for dry-cooled CSP+cooling configurations) is that they can be used to evaluate which Quaternary configurations should be prioritized for CSP development above others. This prioritization will therefore stem from the fact that they can support more generation potential due to higher water availability and less water variability. This is important for both policy makers in the water and energy regulatory frameworks, as well as prospective CSP developers. Policy makers can use this information, in conjunction with regular updates to the models used to derive it, as part of their national decision making with regards to water-use license allocations and national electricity supply studies.

A critical aspect for the Department of Energy would be to assess all power technologies included in any future Integrated Resource plans based on their impact on the local water balance of the Quaternary catchment in which they are located. The methodological approach used in this work is specific to CSP but can easily be replicated for other power technologies, and as such can form part of national energy planning studies and subsequent policies.

The department of Water and Sanitation will also be able to incorporate the results and their models into their national hydrology policies, specifically in terms of water use licences. They can keep an inventory of allocations per Quandary catchment in order to keep track of water use per sector and, by updating the water balances with the latest statistical or hydrological model data, ensure that water resources are not over-allocated and ensure sustainability.

Finally, CSP developers can in future competitive renewable energy bid rounds ensure they focus their attention on the Quaternary catchments which are most able to support the CSP-related demand. They can also assess their options based on the high spatial resolution of the models used. Furthermore, they can mitigate the risks associated with curtailment due to water restrictions in dry periods by selecting CSP+cooling configurations that are less susceptible to fluctuations in water resource availability. Curtailments are a far more severe financial risk for CSP developers than the cost of water, and such, avoiding them is a valuable way to ensure CSP plants are operated sustainably.

8.3. Limitations and future work

The scope of this work considered only the most commercially mature CSP and cooling technologies, and therefore, excluded possible new technologies that might be more efficient or less water intensive. This includes efficiency gains in the CSP technology itself, which would reduce water consumption factors in wet-cooled plants, as well as novel cooling technologies such as various forms of hybrid cooling. Furthermore, generation technology combinations, such as solar PV combined with CSP, allowing CSP plants to generate more at night or cooler periods, are also not included in this work, even though this will impact the water demand from the combined generation. In light of this, it is important to note that the range of results from the models considers the most realistic likely improvements in water use efficiency through the inclusion of advanced dry cooled CSP plants. As such, the results include the water-use and power generation efficiencies that covers the widest range of likely scenarios, from severe consumption efficiencies (wet-cooled) to the afore mentioned highly efficient consumption rates (advanced dry cooling). Most other hybridization options will therefore be covered by the range of results.

The spatiotemporal sensitivity of dry cooled CSP plants is not captured due to a lack of industry data available to refine the detailed sub-hourly interval CSP performance models used to characterize monthly CSP performance. As such, a static, constant water consumption factor is used for both Parabolic Trough and Central Receiver dry cooled plants. This should be investigated in greater detail and updated. This limit, however, does not detract from the work's validity since the static consumption factor selected for dry cooled plants still captures the magnitude of order difference between it and that of wet cooling. Furthermore, the monthly CSP performance model used is sensitive enough to spatiotemporally varying metrological conditions to capture the changes in CSP electricity generation, which is typically the greatest driver of water consumption, irrespective of cooling technology.

The approach used can easily be further applied to the sub-quaternary catchment level in order to determine the localised impact on particular water sources. This was forgone in this work in since it would only marginally have contributed to the value of knowing the hydrological limits at Quaternary Catchment level.

The results from the approach used can also easily be applied as another iterative screening criteria in future GIS suitability studies; meaning the hydrological limits can be spatially defined and the areas can be selected with the highest CSP value within these limits. The distance to water resources can also be incorporated to minimize construction costs related to water conveyance infrastructure.

The approach used to quantify water availability can make use of detailed hydrological model results as well as actual monitored data, in a hybrid approach, instead of only relying on monitored data. This can address limitations due to monitoring station data loss and lack of spatial resolution. This will also improve and refine our understanding of downstream

impacts of CSP abstractions, and more fully consider the mass balance between rivers within the same primary catchment.

The groundwater data used was crude in the fact that it was annual yield values based on estimated groundwater resource assessments from 2005. This data should be captured at seasonal or monthly temporal scales, but is outside the scope of this work since it requires a detailed hydrological model considering data from existing boreholes across the country.

References

[1] A. Doyle, “Vast Moroccan solar power plant is hard act for Africa to follow,” *Reuters*, 2016. [Online]. Available: https://www.reuters.com/article/us-climatechange-accord-solar-idUSKBN1300JI.

[2] Gulf News UAE, “Dubai launches world’s largest Concentrated Solar Power project,” 2017. [Online]. Available: https://gulfnews.com/uae/dubai-launches-worlds-largest-concentrated-solar-power-project-1.2091061.

[3] D. F. Duvenhage, A. C. Brent, and W. H. L. Stafford, “The need to strategically manage CSP fleet development and water resources: A structured review and way forward,” *Renew. Energy*, vol. 132, pp. 813–825, 2019.

[4] U.S. DEPARTMENT OF ENERGY, “Concentrating Solar Power Commercial Application Study: Reducing Water Consumption of Concentrating Solar Power Electricity Generation. Report to Congress,” 2009.

[5] U.S. DEPARTMENT OF ENERGY, *Energy Demands on Water Resources Report To Congress on the Interdependency of Energy and Water*. 2006.

[6] M. A. Maupin, J. F. Kenny, S. S. Hutson, J. K. Lovelace, N. L. Barber, and K. S. Linsey, “Estimated Use of Water in the United States in 2010 Circular 1405,” Reston, Virginia, 2010.

[7] International Energy Agency IEA, “Chapter 17: Water for energy. Is energy becoming a thirstier resource. In: World Energy Outlook 2012, Organization for Economic Cooperation & Development (OECD),” International Energy Agency IEA, Paris France, 2012.

[8] World Energy Council, “Water for Energy,” London UK, 2010.

[9] WWAP (United Nations World Water Assessment Programme), “The United Nations World Water Development Report 2015: Water for a Sustainable World,” Paris, 2015.

[10] S. Orr, R. Sánchez-Navarro, G. Schmidt, R. Seiz-Puyuelo, K. Smith, and J. Verberne, “Assessing Water Risk A Practical Approach For Financial Institutions,” WWF Germany, Berlin Germany, 2011.

[11] International Energy Agency, “Renewables 2017 Analysis and Forecasts to 2022,” Paris France, 2017.

[12] IRENA, “The Power To Change: Solar and wind cost reduction potential to 2025,” 2016.

[13] International Energy Agency, “World Energy Outlook 2017: Chapter 1,” 2017.

[14] M. Milligan and B. Parsons, “A comparison and case study of capacity credit algorithms for intermittent generators,” *Proc. 1997 Am. Sol. Energy Soc. Annu. Conf.*, no. March, pp. 329–334, 1997.

[15] U.S. Energy Information Administration, *Electric Power Monthly with Data for October 2015*, no. November 2017. 2015.

[16] R. Piwko and Miller, “Intermittency Analysis Project: Appendix B: Impact of Intermittent Generation on Operation of California Power Grid,” California Energy Commission, PIER Renewable Energy Technologies Program, 2007.

[17] U.S. Department of Energy, “Staff Report to the Secretary on Electricity Markets and Reliability,” no. August, p. 187, 2017.

[18] P. Denholm, K. Clark, and M. O’Connell, *On the Path to SunShot: Emerging Issues and Challenges in Integrating High Levels of Solar into the Electrical Generation and Transmission System*, no. May. Golden, Colorado: National Renewable Energy Laboratory. NREL/TP-6A20-65800, 2016.

[19] International Energy Agency, *World Energy Outlook 2018*. Paris France: International Energy Agency, 2018.

[20] M. Götz *et al.*, “Renewable Power-to-Gas: A technological and economic review,” *Renew. Energy*, vol. 85, pp. 1371–1390, 2016.

[21] J. DiCampli and W. Schulke, “Grid Stability: Gas Turbines for Primary Reserve,” no. 55188. p. V004T09A002, 2013.

[22] EPRI, “Power Generation Technology Data for Integrated Resource Plan of South Africa: Technical Update, August 2015,” EPRI, Palo Alto California, 2015.

[23] R. Sioshansi and P. Denholm, “The Value of Concentrating Solar Power and Thermal Energy Storage,” NREL, Golden, Colorado, 2010.

[24] S. H. Madaeni, R. Sioshansi, and P. Denholm, “Capacity Value of Concentrating Solar Power Plants,” NREL, Golden, Colorado, 2011.

[25] M. Mehos, C. Turchi, J. Jorgenson, P. Denholm, C. Ho, and K. Armijo, “On the Path to SunShot: Advancing Concentrating Solar Power Technology, Performance, and Dispatchability,” National Renewable Energy Laboratory.NREL/TP-5500-65688., Golden, Colorado, 2016.

[26] P. Gauché, S. Pfenninger, A. J. Meyer, T. W. von Backström, and A. C. Brent, “Modeling Dispatchability Potential of CSP in South Africa,” in *Southern African Solar Energy Conference (SASEC)*, 2012, vol. 1, pp. 1–11.

[27] P. Gauché, J. Rudman, M. Mabaso, W. A. Landman, T. W. von Backström, and A. C. Brent, “System value and progress of CSP,” *Sol. Energy*, vol. 152, pp. 106–139, 2017.

[28] T. Telsnig, L. Eltrop, W. Hartmut, and U. Fahl, “Efficiency and costs of different concentrated solar power plant configurations for sites in Gauteng and the Northern Cape, South Africa,” *J. Energy South. Africa*, vol. 24, no. 1, pp. 77–89, 2013.

[29] P. Gauché, T. W. Von Backström, and A. C. Brent, “A concentrating solar power value proposition for South Africa,” *J. Energy South. Africa*, vol. 24, no. 1, pp. 67–76, 2013.

[30] Z. Jokadar and C. Ponte, *Ouarzazate Solar Power Complex , Phase 1 Morocco Specific Environmental and Social Impact Assessment VOLUME 1*, vol. 1, no. December. Rabat, Morocco: Masen, 2013.

[31] Dubai Electricity and Water Authority, “Facts about the solar park,” 2017. [Online]. Available: https://www.dewa.gov.ae/en/customer/innovation/renewable-energy/facts-about-the-solar-park. [Accessed: 14-Feb-2018].

[32] J. K. Musango, B. Amigun, and A. C. Brent, “Sustainable Electricity Generation Technologies in South Africa: Initiatives, Challenges and Policy Implications,” *Energy Environ. Res.*, vol. 1, no. 1, pp. 124–138, 2011.

[33] Department of Energy, “South African Solar Park Indicative Master Plan,” Department of Energy South Africa, 2011.

[34] M. J. Rutberg, “Modeling Water Use at Thermoelectric Power Plants,” Massachusetts Institute of Technology, 2012.

[35] C. Turchi, M. Wagner, and C. Kutscher, “Water Use in Parabolic Trough Power Plants: Summary Results from WorleyParsons’ Analyses,” NREL, Golden, Colorado, 2010.

[36] J. E. Hoffmann and E. P. Dall, “Integrating desalination with concentrating solar thermal power: A Namibian case study,” *Renew. Energy*, vol. 115, pp. 423–432, 2018.

[37] P. Palenzuela, G. Zaragoza, D. C. Alarcón-Padilla, and J. Blanco, “Evaluation of cooling technologies of concentrated solar power plants and their combination with desalination in the Mediterranean area,” *Appl. Therm. Eng.*, vol. 50, no. 2, pp. 1514–1521, 2013.

[38] A. Pugsley, A. Zacharopoulos, J. D. Mondol, and M. Smyth, “Global applicability of solar desalination,” *Renew. Energy*, vol. 88, pp. 200–219, 2016.

[39] J. MacKnick, R. Newmark, and C. Turchi, “Water Consumption Impacts of Renewable Technologies: The Case of CSP,” in *AWRA 2011 SPRING SPECIALTY CONFERENCE*, 2011.

[40] X. D. Wu and G. Q. Chen, “Energy and water nexus in power generation: The surprisingly high amount of industrial water use induced by solar power infrastructure in China,” *Appl. Energy*, vol. 195, pp. 125–136, 2017.

[41] E. A. Byers, J. W. Hall, and J. M. Amezaga, “Electricity generation and cooling water use: UK pathways to 2050,” *Glob. Environ. Chang.*, vol. 25, no. 1, pp. 16–30, 2014.

[42] T. Luo, D. Krishnan, and S. Sen, “WORKING PAPER PARCHED POWER : WATER DEMANDS , RISKS , AND OPPORTUNITIES FOR INDIA ’ S POWER SECTOR,” Washington, DC, 2018.

[43] J. Cullis, N. Walker, F. Ahjum, and D. Rodriguez, “Modelling the Water-Energy Nexus : Should regional variability in water supply impact on decision making for future energy supply options ?,” in *Proc. IAHS, 376*, 2018, pp. 3–8.

[44] B. P. Walsh, S. N. Murray, and D. T. J. O’Sullivan, “The water energy nexus, an ISO50001 water case study and the need for a water value system,” *Water Resour. Ind.*, vol. 10, pp. 15–28, 2015.

[45] G. A. Thopil and A. Pouris, “A 20 year forecast of water usage in electricity generation

for South Africa amidst water scarce conditions," *Renewable and Sustainable Energy Reviews*, vol. 62. Elsevier, pp. 1106–1121, 2016.

[46] P. Kotzé, "Water and energy: How much water will we need to keep the lights on?," *Water Wheel*, vol. 14, no. 3, Pretoria, pp. 22–25, 2015.

[47] M. Govender, S. Leyde, T. Fischer, and M. Weston, "Strategic Assessment and Mapping of Opportunities for Water Desalination and Water- Use Optimisation of Concentrated Solar Power. Report No.2382/1/16.," Water Research Commission, Pretoria, 2016.

[48] D. J. Rodriguez, A. Delgado, P. Delaquil, and A. Sohns, "THIRSTY ENERGY," Washington DC, 78923, 2013.

[49] IRENA, "Renewable Energy in the Water, Energy & Food Nexus," IRENA, 2015.

[50] International Energy Agency, "Water Energy Nexus - World Energy Outlook 2016 Excerpt," IEA, Paris France, 2016.

[51] World Bank Group, *Modeling the Water-Energy Nexus : How Do Water Constraints Affect Energy Planning in South Africa?* Washington DC: World Bank Group, 2017.

[52] US DOE, "The Water-Energy Nexus: Challenges and Opportunities," US DOE, 2014.

[53] M. R. Nogueira Vilanova and J. A. Perrella Balestieri, "Exploring the water-energy nexus in Brazil: The electricity use forwater supply," *Energy*, vol. 85, pp. 415–432, 2015.

[54] K. Hussey and J. Pittock, "The Energy–Water Nexus: Managing the Links between Energy and Water for a Sustainable Future," *Ecol. Soc.*, vol. 17, no. 1, 2012.

[55] G. Simbolotti, "Concentrating solar power Technology Brief E10," IRENA, 2013.

[56] A. Sastry, D. F. Duvenhage, and J. E. Hoffmann, "A Parametric Study of Heliostat Size for Reductions in Levelized Cost of Electricity," in *Southern African Solar Energy Conference 2016*, 2016, pp. 1–8.

[57] G. Cáceres, M. Montané, S. Nasirov, and R. O'Ryan, "Review of Thermal Materials for CSP Plants and LCOE Evaluation for Performance Improvement using Chilean Strategic Minerals: Lithium Salts and Copper Foams," *Sustain.*, vol. 8, no. 2, 2016.

[58] C. Turchi, M. Mehos, C. K. Ho, and G. J. Kolb, "Current and Future Costs for Parabolic Trough and Power Tower Systems in the US Market Preprint," in *SolarPACES 2010*, 2010, no. September, p. 11.

[59] M. Liu *et al.*, "Review on concentrating solar power plants and new developments in high temperature thermal energy storage technologies," *Renew. Sustain. Energy Rev.*, vol. 53, pp. 1411–1432, 2016.

[60] C. Parrado, A. Marzo, E. Fuentealba, and A. G. Fernández, "2050 LCOE improvement using new molten salts for thermal energy storage in CSP plants," *Renew. Sustain. Energy Rev.*, vol. 57, pp. 505–514, 2016.

[61] IRENA, "Renewable Energy Technologies Cost Analysis Series: Concentrating Solar

Power," Abu Dhabi UAE, 2012.

[62] J. Hernandez-Moro and J. M. Martınez-Duart n, "Analytical model for solar PV and CSP electricity costs: Present LCOE values and their future evolution," *Renew. Sustain. Energy Rev.*, vol. 20, pp. 119–132, 2013.

[63] B. N. Green, C. D. Johnson, and A. Adams, "Writing narrative literature reviews for peer-reviewed journals : secrets of the trade," *J. Sport. Chiropr. Rehabil.*, no. 15, pp. 5–19, 2001.

[64] R. A. Day, *How to write and publish a scientific paper. 5th ed*. Phoenix AZ: The Oryx Press, 1998.

[65] J. Baum and P. J. Vlok, "Mapping Primary Constraints In Physical Asset Management Strategy Execution, Using Social Network Analysis," *South African J. Ind. Eng.*, vol. 24, no. 2, pp. 47–58, 2013.

[66] C. Labuschagne and A. C. Brent, "Sustainable project life cycle management: the need to integrate life cycles in the manufacturing sector," *Int. J. Proj. Manag.*, 2004.

[67] H. E. Cardwell, R. A. Cole, L. A. Cartwright, and L. A. Martin, "Integrated Water Resources Management: Definitions and Conceptual Musings," *J. Contemp. Water Res. Educ.*, vol. 135, no. 1, pp. 8–18, 2009.

[68] R. Mahtta, P. K. Joshi, and A. K. Jindal, "Solar power potential mapping in India using remote sensing inputs and environmental parameters," *Renew. Energy*, vol. 71, pp. 255–262, 2014.

[69] J. N. Gathu, P. A. Odera, and E. H. Waithaka, "Determination of Suitable Sites for Establishment of Large-Scale Concentrated Solar Power Plants in Kenya," *Nat. Resour.*, vol. 08, no. 01, pp. 1–23, 2017.

[70] K. Kaygusuz, "Prospect of concentrating solar power in Turkey: The sustainable future," *Renew. Sustain. Energy Rev.*, vol. 15, no. 1, pp. 808–814, 2011.

[71] Y. Le Fol and K. Ndhlukula, "Potential and future of concentrating solar power in Namibia," *J. Energy South. Africa*, vol. 24, no. 1, pp. 90–98, 2013.

[72] K. Ummel, "Concentrating Solar Power in China and India: A Spatial Analysis of Technical Potential and the Cost of Deployment," 219, 2010.

[73] T. V. Ramachandra, R. Jain, and G. Krishnadas, "Hotspots of solar potential in India," *Renew. Sustain. Energy Rev.*, vol. 15, no. 6, pp. 3178–3186, 2011.

[74] A. A. Merrouni, A. B. Mezrhab, and A. Mezrhab, "CSP sites suitability analysis in the eastern region of Morocco," *Energy Procedia*, vol. 49, pp. 2270–2279, 2013.

[75] T. P. Fluri, "The potential of concentrating solar power in South Africa," *Energy Policy*, vol. 37, no. 12, pp. 5075–5080, 2009.

[76] E. W. Ramdé, Y. Azoumah, A. Brew-Hammond, A. Rungundu, and G. Tapsoba, "Site Ranking and Potential Assessment for Concentrating Solar Power in West Africa," *Nat. Resour.*, vol. 04, no. 01, pp. 146–153, 2013.

[77] J. Clifton and B. J. Boruff, “Assessing the potential for concentrated solar power development in rural Australia,” *Energy Policy*, vol. 38, no. 9, pp. 5272–5280, 2010.

[78] J. Dominguez Bravo, X. Garcia Casals, and I. Pinedo Pascua, “GIS approach to the definition of capacity and generation ceilings of renewable energy technologies,” *Energy Policy*, vol. 35, no. 10, pp. 4879–4892, 2007.

[79] L. Dawson and P. Schlyter, “Less is more: Strategic scale site suitability for concentrated solar thermal power in Western Australia,” *Energy Policy*, vol. 47, pp. 91–101, 2012.

[80] D. Dahle *et al.*, “Assessing the Potential for Renewable Energy Development on DOE Legacy Management Lands. DOE/GO-102008-2435,” NREL, Golden, Colorado, 2008.

[81] A. Aly, S. S. Jensen, and A. B. Pedersen, “Solar power potential of Tanzania: Identifying CSP and PV hot spots through a GIS multicriteria decision making analysis,” *Renew. Energy*, vol. 113, pp. 159–175, 2017.

[82] H. Broesamle, H. Mannstein, C. Schillings, and F. Trieb, “Assessment of solar electricity potentials in North Africa based on satellite data and a geographic information system,” *Sol. Energy*, vol. 70, no. 1, pp. 1–12, 2001.

[83] S. Makkonen, “Decision modelling tools for utilities in the dregulated energy market,” Helsinki University of Technology, 2005.

[84] Republic of South Africa Department of Energy, “Integrated Resource Plan For Electricity 2010,” Pretoria, 2010.

[85] Republic of South Africa Department of Energy, “INTEGRATED ENERGY PLAN (IEP),” Pretoria, 2016.

[86] Presidential Infrastructure Coordinating Commission, “A summary of the South African National Infrastructure Plan,” Pretoria, 2012.

[87] Republic of South Africa Department of and Energy, “REVISED STRATEGIC PLAN: 2011/12 - 2015/16,” Pretoria, 2012.

[88] NAMS and IPWEA, *International Infrastructure Management Manual*, 4th ed. Wellington, NZ: New Zealand National Asset Management Steering Group, 2011.

[89] D. F. Duvenhage, O. O. Craig, A. C. Brent, and W. H. L. Stafford, “Future CSP in South Africa – A review of generation mix models, their assumptions, methods, results and implications,” in *AIP Conference Proceedings*, 2018, vol. 2033, no. 1, p. 120002.

[90] S. Pfenninger, A. Hawkes, and J. Keirstead, “Energy systems modeling for twenty-first century energy challenges,” *Renew. Sustain. Energy Rev.*, vol. 33, pp. 74–86, 2014.

[91] NETL, “Estimating Freshwater Needs to Meet Future Thermoelectric Generation Requirements: 2010 Update. DOE/NETL-2011/1523.,” 2011.

[92] D. Yates, J. Meldrum, F. Flores-Lopez, and M. Davis, “Integrated impacts of future

electricity mix scenarios on select southeastern US water resources," *Environ. Res. Lett.*, vol. 8, no. 3, 2013.

[93] J. Macknick, S. Sattler, K. Averyt, S. Clemmer, and J. Rogers, "The water implications of generating electricity: Water use across the United States based on different electricity pathways through 2050," *Environ. Res. Lett.*, vol. 7, no. 4, 2012.

[94] N. Nouri, "Water Withdrawal and Consumption Reduction Analysis for Electrical Energy Generation System," University of Wisconsin-Milwaukee, 2015.

[95] Republic of South Africa Department of and Energy, "FREQUENTLY ASKED QUESTIONS -INTEGRATED ENERGY PLAN (IEP)," Pretoria, 2016.

[96] Republic of South Africa Department of Minerals and Energy, *White Paper on the Energy Policy of the Republic of South Africa*, no. December. Pretoria: Department of Minerals and Energy, 1998.

[97] Republic of South Africa Department of Minerals and Energy, *White Paper on Renewable Energy*, no. November. Pretoria: Department of Minerals and Energy, 2003.

[98] IPP Projects, *The South African Energy Independent Power Producers Procurement Programme (REIPPPP) - Lessons Learned*. Centurion South Africa: IPP Projects, 2016.

[99] A. Eberhard and R. Naude, "The South African Renewable Energy Independent Power Producer Procurement Programme: A review and lessons learned," *J. Energy South. Africa*, vol. 27, no. November 2016, pp. 1–14, 2016.

[100] NERSA, *Monitoring of Renewable Energy Performance of Power PLants*, vol. 2017, no. 10. Pretoria: NERSA, 2017.

[101] D. R. Walwyn and A. C. Brent, "Renewable energy gathers steam in South Africa," *Renew. Sustain. Energy Rev.*, vol. 41, pp. 390–401, 2015.

[102] J. G. Wright, T. Bischof-Niemz, J. Calitz, C. Mushawana, R. van Heerden, and M. Senatla, "Formal comments on the Integrated Resource Plan Update Assumptions, Base Case results and Observations 2016," Council for Scientific and Industrial Research (CSIR), Pretoria, 2017.

[103] C. K. Ho, "Software and Codes for Analysis of Concentrating Solar Power Technologies," *Sandia Natl. Lab. Rep. SAND2008-8053*, no. December, pp. 1–35, 2008.

[104] NREL, *System Advisor Model 2017.9.5 User Manual*. Palo Alto, CA: NREL, 2017.

[105] MinWaterCSP, "CSP plant simulation tool," 2018. [Online]. Available: http://www.minwatercsp.eu/technologies/csp-plant-simulation-tool/. [Accessed: 03-Jun-2017].

[106] C. Wiiwer *et al.*, "ColSim - A NEW SIMULATION ENVIRONMENT FOR COMPLEX SYSTEM ANALYSIS AND CONTROLLERS," in *International IBPSA Conference*, 2001.

[107] “About IWRM,” *Global Water Partnership*, 2012. [Online]. Available: https://www.gwp.org/en/gwp-SAS/ABOUT-GWP-SAS/WHY/About-IWRM/. [Accessed: 22-Jan-2018].

[108] S. Pollard and D. Du Toit, “Integrated water resource management in complex systems : How the catchment management strategies seek to achieve sustainability and equity in water resources in South Africa,” *Water SA*, vol. 34, no. 6, pp. 671–679, 2008.

[109] K. W. Thornton, C. Laurin, J. Shortle, A. Fisher, J. Sobrinho, and M. Stewart, “A Framework And Guidelines For Moving Toward Sustainable Water Resources Management,” in *Proceedings of the water environment federation WEFTEC 2006*, 2006, pp. 2762–2777.

[110] J. Denison and G. Mazibuko, “MSB III Mid-Term Review Implementation of Integrated Water Resource Management in Key Priority Areas,” DWAF, Pretoria, 2010.

[111] F. Zare, S. Elsawah, T. Iwanaga, A. J. Jakeman, and S. A. Pierce, “Integrated water assessment and modelling: A bibliometric analysis of trends in the water resource sector,” *J. Hydrol.*, vol. 552, pp. 765–778, 2017.

[112] United Nations, “Earth Summit‘92. The UN Conference on Environment and Development,” United Nations Division for Sustainable Development, Rio de Janerio, 1992.

[113] H. H. G. Savenije and A. Y. Hoekstra, *WATER RESOURCES MANAGEMENT*, vol. I. UNESCO-EOLSS.

[114] K. W. Thornton *et al.*, *Moving Toward Sustainable Water Resources Management: A Framework and Guidelines for Implementation. Synthesis Report*. Alexandria, VA: Water Environment Research Foundation, 2006.

[115] K. Thornton *et al.*, *Moving Toward Sustainable Water Resources Management: A Framework and Guidelines for Implementation. Technical Report 00-WSM-6b*. Alexandria, VA: Water Environment Research Foundation, 2006.

[116] “Sustainable Water Resources Management Volume 1: Executive Summary,” EPRI and WERF, Palo Alto, CA and Alexandria, VA, 2010.

[117] W. V PITMAN, “A Mathematical Model for Generating Monthly River Flows from Meteorological Data in South Africa. HRU Report No. 2/73.,” Hydrological Research Unit, University of the Witwatersrand, Johannesburg, 1973.

[118] World business council for sustainable development, “Global Water Tool Version 2015 1.3,” no. July. World business council for sustainable development, Geneva, Fr, pp. 1–9, 2015.

[119] N. Hanasaki *et al.*, “An integrated model for the assessment of global water resources – Part 1 : Model description and input meteorological forcing,” *Hydrol. Earth Syst. Sci.*, vol. 12, pp. 1007–1025, 2008.

[120] D. Juizo and R. Liden, “Modeling for transboundary water resources planning and allocation: The case of Southern Africa,” *Hydrol. Earth Syst. Sci.*, vol. 14, no. 11, pp.

2343–2354, 2010.

[121] O. I. Nkwonta, B. Dzwairo, F. A. O. Otieno, and J. A. Adeyemo, “A review on water resources yield model,” *South African J. Chem. Eng.*, vol. 23, no. July 2016, pp. 107–115, 2017.

[122] A. Bailey, “WRSM2000/Pitman Water Resources Simulation Model for Windows: Theory,” HaskoningDHV Ltd, WRC and DWS, Pretoria, 2015.

[123] N. J. Van Wyk, J. A. Van Rooyen, P. G. Van Rooyen, and F. G. B. De Jager, “Proposed Modelling Approach and Procedures for Water Availability Assessment studies.” Miya Luxemburg Holdings S.a.r.l, Ettelbruck Luxembourg, pp. 1–10, 2005.

[124] R. Mckenzie and C. Seago, *Current Analytical Methods and Technical Capacity of the four Orange Basin States*. Pretoria: ORASECOM, 2007.

[125] A. Bailey and W. Pitman, “Water Resources of South Africa 2012 Study (WR2012) Executive Summary,” HaskoningDHV Ltd, WRC and DWS, Pretoria, 2015.

[126] W. V Pitman, J. P. Kakebeeke, and A. K. Bailey, “WRSM/Piman Water Resources Simulation Model: Users Manual,” HaskoningDHV Ltd, WRC and DWS, Pretoria, 2015.

[127] D. Sparks and A. Dane, “Renewable energy choices and their water requirements in South Africa,” vol. 25, no. 4, pp. 80–92, 2014.

[128] H. M. Cekirge and A. Elhassan, “A Comparison of Solar Power Systems (CSP): Solar Tower (ST) Systems versus Parabolic Trough (PT) Systems 2 . Comparison of Solar Tower (ST) and,” *Am. J. Energy Eng.*, vol. 3, no. 3, pp. 29–36, 2015.

[129] M. J. Rutberg, H. J. Herzog, A. F. Ghoniem, and A. Delgado, “A SYSTEM-LEVEL GENERIC MODEL OF WATER USE AT POWER PLANTS AND ITS APPLICATION TO REGIONAL WATER USE ESTIMATION,” in *IMECE2011*, 2011, pp. 1–11.

[130] A. Kohli and K. Frenken, “Cooling water for energy generation and its impact on national-level water statistics,” Rome, Italy, 2011.

[131] V. Fthenakis and H. C. Kim, “Life-cycle uses of water in U.S. electricity generation,” *Renew. Sustain. Energy Rev.*, vol. 14, no. 7, pp. 2039–2048, 2010.

[132] M. J. Wagner and C. F. Kutscher, “Assessing the impact of heat rejection technology on CSP plant revenue,” in *SolarPACES 2010*, 2010, no. October, pp. 1–9.

[133] R. Putman and D. Jaresch, “The Cleaning of Air Cooled Condensers to Improve Performance,” in *International Joint Power Generation Conference*, 2002.

[134] A. Raza, A. R. Higgo, A. Alobaidli, and T. Zhang, “Water recovery in a concentrated solar power plant,” *AIP Conf. Proc.*, vol. 1734, 2016.

[135] J. Macknick, R. Newmark, G. Heath, and K. C. Hallett, “Operational water consumption and withdrawal factors for electricity generating technologies: a review of existing literature,” *Environ. Res. Lett.*, vol. 7, no. 4, 2012.

[136] J. Macknick, J. Meldrum, S. Nettles-Anderson, G. Heath, and A. Miara, “Life cycle

water use for photovoltaic electricity generation: A review and harmonization of literature estimates," *Environ. Res. Lett.*, vol. 8, no. 015031, pp. 1–18, 2013.

[137] N. Bracken, J. Macknick, A. Tovar-hastings, P. Komor, M. Gerritsen, and S. Mehta, *Concentrating Solar Power and Water Issues in the U.S. Southwest*, no. March. Golden, Colorado: Joint Institute for Strategic Energy Analysis, 2015.

[138] G. E. Cohen, D. W. Kearney, and G. J. Kolb, "Final report on the operation and maintenance improvement program for concentrating solar power plants. SAND99-1290.," Sandia National Laboratories, Albuquerque, New Mexico, 1999.

[139] MinWaterCSP, "MinWaterCSP," 2018. [Online]. Available: http://www.minwatercsp.eu/. [Accessed: 06-Aug-2016].

[140] L. Heller, "Literature Review on Heat Transfer Fluids and Thermal Energy Storage Systems in CSP Plants-STERG Report," Stellenbosch, RSA, 2013.

[141] International Association of Engineering Insurers, "IMIA Working Group Paper WG 84 (14) - Solar Thermal Power Plant," Cannes, France, 2014.

[142] N. Middleton, D. S. G. Thomas, and United Nations Environment Programme, *World Atlas of Desertification*. Arnold, 1997.

[143] F. Gassert, M. Landis, M. Luck, P. Reig, and T. Shiao, "Aqueduct Global Maps 2.1: Constructing decision-relevant global water risk indicators," Washington, DC, 2014.

[144] T. Luo, "Droughts and Blackouts: How Water Shortages Cost India Enough Energy to Power Sri Lanka," *WRI*, 2017. [Online]. Available: http://www.wri.org/blog/2017/07/droughts-and-blackouts-how-water-shortages-cost-india-enough-energy-power-sri-lanka. [Accessed: 02-Feb-2018].

[145] D. Das, "NTPC plant shutdown hits power supply in 5 States," 2018. [Online]. Available: http://www.thehindubusinessline.com/companies/ntpc-plant-shutdown-hits-power-supply-in-5-states/article8352253.ece. [Accessed: 02-Mar-2018].

[146] J. McCall, J. Macknick, and D. Hillman, "Water-Related Power Plant Curtailments: An Overview of Incidents and Contributing Factors. NREL/TP-6A20-67084.," NREL, Golden, Colorado, 2016.

[147] M. Van Vliet, J. R. Yearsley, F. Ludwig, S. Vögele, D. Lettenmaier, and P. Kabat, "Vulnerability of US and European electricity supply to climate change," *Nat. Clim. Chang.*, vol. 2, pp. 676–681, 2012.

[148] NETL, "Impact of Drought on U.S. Steam Electric Power Plant Cooling Water Intakes and Related Water Resource Management Issues. DOE/NETL-2009/1364.," National Energy Technology Laboratory, 2009.

[149] C. Silinga, P. Gauché, and W. van Niekerk, "CSP scenarios in South Africa: Benefits of CSP and the lessons learned," in *SolarPACES 2015*, 2015, vol. 070031, pp. 0–8.

[150] N. Shand, "Guidelines for Water Supply Systems Operation and Management Plans During Normal and Drought Conditions (RSA C000/00/2305).," DEPARTMENT OF WATER AFFAIRS AND FORESTRY, Pretoria, 2006.

[151] G. T. Klise, V. C. Tidwell, M. D. Reno, B. D. Moreland, M. Katie, and J. Macknick, “Water Use and Supply Concerns for Utility-Scale Solar Projects in the Southwestern United States. SAND2013-5238.,” Sandia National Laboratories, Albuquerque, New Mexico, 2013.

[152] A. Eberhard and R. Naude, “THE SOUTH AFRICAN RENEWABLE ENERGY IPP PROCUREMENT PROGRAMME Review, Lessons Learned & Proposals to Reduce Transaction Costs,” University of Cape Town Graduate Business School, Cape Town, 2017.

[153] Department of Water Affairs and Forestry, “External Guideline: Generic Water USe Authorisation Application Process,” Department of Water Affairs and Forestry, Pretoria, 2007.

[154] National Water Act, “Department of Water Affairs and Forestry,” no. 36, p. 94, 1998.

[155] A. Pouris and G. A. Thiopil, “Long term forecasts of water usage for electricity generation: South Africa 2030. Report No. 2383/1/14.,” Water Research Commission, Pre, 2015.

[156] South African Department of Water and Sanitation, “Department of Water and Sanitation (DWS) Guidance Note regarding water availability and water use licensing for the Coal Baseload Independent Power Producer (IPP) Procurement Programme,” Pretoria, 2015.

[157] D. F. Duvenhage, M. Kleingeld, and A. J. Schutte, “Integration of DSM interventions into bulk water supply strategies,” in *2016 International Conference on the Industrial and Commercial Use of Energy (ICUE)*, 2016, pp. 2–8.

[158] T. A. DeNooyer, J. M. Peschel, Z. Zhang, and A. S. Stillwell, “Integrating water resources and power generation: The energy-water nexus in Illinois,” *Appl. Energy*, vol. 162, pp. 363–371, 2016.

[159] A. S. Stillwell, “Water Impacts on Thermoelectric Power Generation,” University of Texas at Austin, 2013.

[160] GAO, “Water in the energy sector Reducing freshwater use in hydraulic fracturing and thermoelectric power plant cooling. GAO-15-545,” United States Government Accountability Offi, Washington, DC, 2015.

[161] C. A. Scott and M. J. Pasqualetti, “Energy and Water Resources Scarcity: Critical Infrastructure for Growth and Economic Development in Arizona and Sonora,” *Nat. Resour. J.*, vol. 50, pp. 645–682, 2010.

[162] Financial Mail, “South Africa’s Energy Crisis: Eskom 2008-2005,” 2015. [Online]. Available: http://cdn.bdlive.co.za/ebooks/Eskom and the SA energy crisis.pdf.

[163] United Nations, “United Nations Framework Convention on Climate Change,” 1992.

[164] United Nations, “KYOTO PROTOCOL TO THE UNITED NATIONS FRAMEWORK CONVENTION ON CLIMATE CHANGE,” 1998.

[165] United Nations, “The Paris Protocol – A blueprint for tackling global climate change beyond 2020,” 2015.

[166] Y. Haffejee, “Renewable Energy IPP Program South Africa,” no. January. IRENA, Abu Dhabi, 2013.

[167] Republic of South Africa Department of and Energy, “Integrated Resource Plan for Electricity (IRP update 2013),” 2013.

[168] DoE, “Integrated Resource Plan,” 2016. [Online]. Available: http://www.energy.gov.za/IRP/irp-2016.html. [Accessed: 28-Mar-2017].

[169] Independent Power Producer Office, “Independent Power Producers Procurement Programme (IPPPP) An Overview,” Centurion, 2017.

[170] DoE, “Renewable Energy IPP Procurement Programme (REIPPPP) for South Africa,” 2015.

[171] C. Silinga and P. Gauché, “Scenarios for a South African CSP peaking system in the short term,” *Energy Procedia*, vol. 49, pp. 1543–1552, 2013.

[172] C. Silinga, P. Gauché, J. Rudman, and T. Cebecauer, “The South African REIPPP Two-tier CSP Tariff: Implications for a Proposed Hybrid CSP Peaking System,” *Energy Procedia*, vol. 69, pp. 1431–1440, May 2015.

[173] U. Desideri and P. E. Campana, “Analysis and comparison between a concentrating solar and a photovoltaic power plant,” *Appl. Energy*, vol. 113, pp. 422–433, 2014.

[174] J. Wright, D. T. Bischof-Niemz, J. Calitz, and C. Mushwana, “Least-cost electricity mix for South Africa by 2040,” Cape Town, 2016.

[175] C. Auret, “Scenario modelling for short to long term rollout of concentrating solar power in South Africa,” no. March, 2015.

[176] L. Omarjee, “Eskom postpones IPP signing with Redstone Fin24 Tech,” *Fin24*, 2016. [Online]. Available: http://www.fin24.com/Economy/Eskom/eskom?postpones?ipp?signing?with?redstone?20160728. [Accessed: 10-May-2017].

[177] T. Tsanova, “Eskom again avoids signing PPA for 100 MW CSP park - report,” *Renewables Now*, 2016. [Online]. Available: https://renewablesnow.com/news/eskom-again-avoids-signing-ppa-for-100-mw-csp-park-report-538099/. [Accessed: 10-May-2017].

[178] C. Yelland, “Analysis : The Draft 2016 Integrated Resource Plan – lightweight , superficial and downright dangerous,” *The Daily MAverick*, 2016. [Online]. Available: https://www.dailymaverick.co.za/article/2016?11?30?analysis?the?draft?2016?integrated?resource?plan?lightweight?superficial?and?downright?dangerous/. [Accessed: 13-Mar-2017].

[179] C. Yelland, “Money Talk on Radio 2000 CSIR’s outlook for South Africa’s future electricity mix,” *Moneyweb*, 2016. [Online]. Available: https://www.moneyweb.co.za/news/industry/csir?presents?its?outlook?for?south?africas?future?electricity?mix/. [Accessed: 06-Apr-2017].

[180] P. Ndebele, “Comments for submission to the DOE on the IEP and Draft IRP 2016 Base Case,” 2017.

[181] W. Pierce, T. Bischof-Niemz, M. Mehos, J. Badeda, and P. Gauche, “The Role and Value of CSP in the South African Power System - CONSENSUS STATEMENT,” Pretoria, 2017.

[182] J. Wright and T. Bischof-niemz, “Comments on the Integrated Resource Plan 2016 Draft South African Integrated Resource Plan 2016 public hearing,” 2016.

[183] B. Martin, “South African Renewable Energy Council (SAREC) Response To The Integrated Resource Plan 2016 Update,” 2017.

[184] R. Lilley and C. Yelland, “DoE’s draft IRP 2016 roasted,” *Moneyweb*, 2017. [Online]. Available: https://www.moneyweb.co.za/news/industry/does?draft?irp?2016?roasted/. [Accessed: 10-May-2017].

[185] A. Eberhard, “Structure of the market needs to be revised to ensure least-cost energy,” *Businesslive*, 2017. [Online]. Available: https://www.businesslive.co.za/bd/opinion/2017?05?09?structure?of?the?market?needs?to?be?revised?to?ensure?least?cost?energy. [Accessed: 10-May-2017].

[186] T. Creamer, “As DoE prepares to release IRP, all eyes will be on nuclear,” *Engineering News*, 2017. [Online]. Available: http://www.engineeringnews.co.za/article/as-doe-prepares-to-release-irp-all-eyes-will-be-on-nuclear-2016-11-17/rep_id:4136. [Accessed: 10-May-2017].

[187] S. Njobeni, “Government erred in IRP draft,” *IOL*, 2017. [Online]. Available: http://www.iol.co.za/business?report/energy/government?erred?in?irp?draft?8413556. [Accessed: 10-May-2017].

[188] S. Teske, “energy [r] evolution: A sustainale South Africa energy outlook,” 2009.

[189] S. Teske, “The advanced energy [r] evolution: A sustainale energy outlook for South Africa,” 2011.

[190] M. du Plessis, R. Worthington, S. Fakir, L. Tyrer, and J. Cox, “50% by 2030: Renewable Energy in a Just Transition to Sustainable Electricity Supply,” Rosebank, 2010.

[191] WWF, “Feasibility of the WWF Renewable Energy Vision 2030 – South Africa: A spatial-temporal analysis of the WWF Renewable Energy Vision 2030 – South Africa,” 2015.

[192] ERC, “Towards a new power plan,” no. April, p. 21, 2013.

[193] Energy Research Centre, “South Africa’s proposed nuclear build plan: an analysis of the potential socioeconomic risks. Technical Report,” Cape Town, 2015.

[194] V. Sultana, “Solving electric grid network congestion problem with batteries — An exploratory study using GIS techniques,” *Int. J. Smart Grid Clean Energy*, vol. 7, no. 2, pp. 117–124, 2018.

[195] M. Marnewick, E. Retief, N. Theron, D. Wright, and T. Anderson, “Important Bird and Biodiversity Areas of South Africa,” Johannesburg, 2015.

[196] GEOTERRAIMAGE, “2013 - 2014 South African National Land Land-Cover Dataset.,” 2015.

[197] Government Gazette, *Regulations On The Protection Of The Karoo Central Astronomy Advantage Areas In Terms Of The Astronomy Geographic Advantage Act, 2007*, no. 41321. Republic of South Africa, 2017, pp. 171–226.

[198] M. Sengupta *et al.*, “Best Practices Handbook for the Collection and Use of Solar Resource Data for Solar Energy Applications. NREL/TP-5D00-63112,” Golden, Colorado, 2015.

[199] D. H. W. Li, W. Chen, and S. Li, “Evaluation of the performance of different models for predicting direct normal solar irradiance,” *Int. J. Smart Grid Clean Energy*, vol. 8, no. 2, pp. 231–238, 2019.

[200] AT Kearney and ESTELLA, “Solar Thermal Electricity 2025,” Duesseldorf, Germany, 2010.

[201] SolarGIS, “Solar resource maps of South Africa,” 2018. [Online]. Available: https://solargis.com/maps-and-gis-data/download/south-africa. [Accessed: 22-Mar-2018].

[202] IPP Office, “Independent Power Producers Procurement Programme An Overview December 2018,” Pretoria,RSA, 2018.

[203] Statistics South Africa, “Electricity generated and available for distribution (Preliminary),” Pretoria,RSA, 2019.

[204] U.S Department of Energy, “Solar parabolic trough,” 1997.

[205] South African Environmental Observation Network, “South African Risk and Vulnerability Atlas - Digital Elevation Model.” [Online]. Available: http://media.dirisa.org/inventory/archive/spatial/beeh/raster/s20e0.zip/view. [Accessed: 25-Mar-2018].

[206] P. Bradshaw, “GIS METADATA : DETAILED REPORT. Formal protected areas in South Africa,” Port Elizabeth, RSA, 2010.

[207] J. Nel, “GIS METADATA : DETAILED REPORT. Wetland Freshwater Priority Areas.,” Stellenbosch, RSA, 2011.

[208] Department of Water Affairs and Forestry, “National Water Resource Strategy, First Edition, September 2004,” Pretoria,RSA, 2004.

[209] F. Trieb, “Global potential of concentrating solar power,” *Conf. Proc.*, 2009.

[210] NREL, “Concentrating Solar Power Projects with Operational Plants,” 2018. [Online]. Available: https://www.nrel.gov/csp/solarpaces/projects_by_status.cfm?status=Operational. [Accessed: 31-Jan-2018].

[211] Sargent and Lundy, “Assessment of Parabolic Trough and Power Tower Solar Technology Cost and Performance Forecasts. NREL/SR-550-34440,” Golden, Colorado, 2003.

[212] A. Ramani, B. Paul, and D. Saparia, “Performance Characteristics of an Air-Cooled Condenser Under Ambient Conditions,” *Int. Conf. Curr. Trends Technol.*, pp. 1–6, 2011.

[213] D. V. . B. Manish Baweja, “A Review on Performance Analysis of Air-Cooled Condenser under Various Atmospheric Conditions,” *Int. J. Mod. Eng. Res.*, vol. 3, no. 1, pp. 411–414, 2013.

[214] N. Nirmalakhandan, V. Gadhamshetty, and A. Mummaneni, “Improving Combined Cycle Power Plant Performance,” *6th Int. Conf. Heat Transf. Fluid Mech. Thermodyn.*, no. MN1, pp. 1–6, 2008.

[215] T. Tang, J. Xu, S. Jin, and H. Wei, “Study on Operating Characteristics of Power Plant with Dry and Wet Cooling Systems,” *Energy Power Eng.*, vol. 5, no. July, pp. 651–656, 2013.

[216] I. I. NOVIKOV, “The efficiency of atomic power stations (a review),” *J. Nucl. Energy*, vol. 7, no. 1, pp. 125–128, 1958.

[217] F. L. Curzon and B. Ahlborn, “Efficiency of a Carnot engine at maximum power output,” *Am. J. Phys.*, vol. 43, no. 1, pp. 22–24, 1975.

[218] L. Heller, “Investigation of the Thermal Storage System for a 5 MWel Concentrated Solar Power (CSP) Pilot Plant,” 2012.

[219] P. Gauché, “Spatial-temporal model to evaluate the system potential of concentrating solar power towers in South Africa,” Stellenbosch University, 2016.

[220] L. Qoaider and A. Liqreina, “Optimization of dry cooled parabolic trough (CSP) plants for the desert regions of the Middle East and North Africa (MENA),” *Sol. Energy*, vol. 122, pp. 976–985, 2015.

[221] L. Llc and C. Group, “Assessment of Parabolic Trough and Power Tower Solar Technology Cost and Performance Forecasts,” *Group*, vol. October, no. October, p. 344, 2003.

[222] G. J. Kolb, “An Evaluation of Possible Next-Generation High-Temperature Molten-Salt Power Towers. SAND2011-9320,” Sandia National Laboratories, Albuquerque, New Mexico, 2011.

[223] C. Turchi, “Parabolic Trough Reference Plant for Cost Modeling with the Solar Advisor Model (SAM),” no. July, 2010.

[224] J. E. Hoffmann, “Personal communication via email.” Stellenbosch, RSA, 2018.

[225] R. Stull, “Wet-bulb temperature from relative humidity and air temperature,” *J. Appl. Meteorol. Climatol.*, vol. 50, no. 11, pp. 2267–2269, 2011.

[226] H. Müller-Steinhagen and F. Trieb, “Concentrating solar power A review of the Technology,” *Ingenia*, vol. 1, no. 2, pp. 1–9, 2004.

[227] O. Behar, A. Khellaf, and K. Mohammedi, “A review of studies on central receiver solar thermal power plants,” vol. 23, pp. 12–39, 2013.

[228] R. Müller, Richard; Pfeifroth, Uwe; Träger-Chatterjee, Christine; Cremer, Roswitha; Trentmann, Jörg; Hollmann, “Surface Solar Radiation Data Set - Heliosat (SARAH) - Edition 1.” Satellite Application Facility on Climate Monitoring, https://doi.org/10.5676/EUM_SAF_CM/SARAH/V001, 2015.

[229] A. Riihelä, T. Carlund, J. Trentmann, R. Müller, and A. V. Lindfors, “Validation of CM SAF surface solar radiation datasets over Finland and Sweden,” *Remote Sens.*, vol. 7, no. 6, pp. 6663–6682, 2015.

[230] ECILIMP Termosolar, “ECILIMP termosolar MinwaterCSP conference presentation: PT and HE Cleaning.” Marrakesch, Morocco, 2018.

[231] A. Colmenar-santos, D. Borge-diez, C. P. Molina, and M. Castro-gil, “Water consumption in solar parabolic trough plants : review and analysis of the southern Spain case,” *Renew. Sustain. Energy Rev.*, vol. 34, pp. 565–577, 2014.

[232] F. Noack, “JNW CleaningSolutions presentation to ACC User Group,” no. September. ACC Users Group, Available at: http://acc-usersgroup.org/wp-content/uploads/2015/10/11.F.Noack_.Fin-Cleaning-ACCs.pdf, Gettysburg, USA, 2015.

[233] N. Bester, “Personal Communication via email.” JNW CleaningSolutions SA (Pty) Ltd, Germiston, RSA, 2018.

[234] J. C. Kloppers and D. G. Kröger, “A critical investigation into the heat and mass transfer analysis of counterflow wet-cooling towers,” *Int. J. Heat Mass Transf.*, vol. 48, no. 3–4, pp. 765–777, 2005.

[235] S. Taghian Dehaghani and H. Ahmadikia, “Retrofit of a wet cooling tower in order to reduce water and fan power consumption using a wet/dry approach,” *Appl. Therm. Eng.*, vol. 125, pp. 1002–1014, 2017.

[236] Steinbeis-Europa-Zentrum, “H2020 Project to minimize the water consumption in CSP plants has started,” 2016. [Online]. Available: http://cordis.europa.eu/project/rcn/200380_en.html. [Accessed: 04-Jan-2018].

[237] K. Damerau, K. Williges, A. G. Patt, and P. Gauché, “Costs of reducing water use of concentrating solar power to sustainable levels: Scenarios for North Africa,” *Energy Policy*, vol. 39, no. 7, pp. 4391–4398, 2011.

[238] K. Damerau, A. G. Patt, and O. P. R. van Vliet, “Water saving potentials and possible trade-offs for future food and energy supply,” *Glob. Environ. Chang.*, vol. 39, pp. 15–25, 2016.

[239] D. F. Duvenhage, A. C. Brent, W. H. L. Stafford, and O. O. Craig, “Water And CSP – a Preliminary Methodology for Strategic Water Demand Assessment,” in *SolarPACES 2018 - in review*, 2018.

[240] S. Rohani, “Blog #30 – Simulation software ColSimCSP: a tool to optimise CSP plant operation,” *MinWaterCSP*, 2018. [Online]. Available: https://www.minwatercsp.eu/blog-30-simulation-software-colsimcsp-a-tool-to-optimise-csp-plant-operation/. [Accessed: 16-Mar-2019].

[241] S. Rohani, T. P. Fluri, F. Dinter, and P. Nitz, “Modelling and simulation of parabolic

trough plants based on real operating data," *Sol. Energy*, vol. 158, no. October, pp. 845–860, 2017.

[242] S. Rohani, J. Went, R. Gerards, and T. Fluri, "Poster presentation. Modelling and Simulation of Water Use and Treatment in CSP Plants," in *SolarPACES Conference, 2 – 5 October 2018*, 2018.

[243] T. Hirsch, "SolarPACES Guideline for Bankable STE Yield Assessment," 2017.

[244] NREL, "Concentrating Solar Power Projects - Bokpoort," 2017. [Online]. Available: https://solarpaces.nrel.gov/bokpoort. [Accessed: 04-Jan-2019].

[245] J. Lopez, "CSP Innovations in South Africa – Experience and Lessons Learnt in Khi, Kaxu and Xina Julian Lopez." Abengoa Solar, S.A., Stellenbosch, RSA, 2016.

[246] A. Cuellar, "CSP Market Status. http://sterg.sun.ac.za/wp-content/uploads/2017/03/Mott-Macdonald-STERG-Symposium_2017.pdf." Mott Macdonald, Stellenbosch, RSA, 2017.

[247] MASEN, "Case Study: Masen NOOR Ouarzazate Solar Complex." Moroccan Agency for Solar Energy, 2017.

[248] HelioCSP, "Shouhang Dunhuang 100MW Molten Salt Tower Concentrated Solar Power Project," 2018. [Online]. Available: http://helioscsp.com/shouhang-dunhuang-100mw-molten-salt-tower-concentrated-solar-power-project/. [Accessed: 04-Jan-2019].

[249] NREL, "Concentrating Solar Power Projects - Atacama 1," 2015. [Online]. Available: https://solarpaces.nrel.gov/atacama-1. [Accessed: 04-Jan-2019].

[250] R. J. Ramorakane and F. Dinter, "Evaluation of parasitic consumption for a CSP plant," *AIP Conf. Proc.*, vol. 1734, pp. 1–9, 2016.

[251] H. L. Zhang, J. Baeyens, J. Degrève, and G. Cacères, "Concentrated solar power plants: Review and design methodology," *Renew. Sustain. Energy Rev.*, vol. 22, pp. 466–481, 2013.

[252] B. Kelly and D. Kearney, "Parabolic Trough Solar System Piping Model: Final Report, May 13, 2002 - December 31, 2004," no. July, 2002.

[253] I. Sarbu and C. Sebarchievici, "A comprehensive review of thermal energy storage," *Sustain.*, vol. 10, no. 1, 2018.

[254] N. Kincaid, G. Mungas, N. Kramer, M. Wagner, and G. Zhu, "An optical performance comparison of three concentrating solar power collector designs in linear Fresnel, parabolic trough, and central receiver," *Appl. Energy*, vol. 231, no. September, pp. 1109–1121, 2018.

[255] W. B. Stine and M. Geyer, *Power from the sun*. PowerFromTheSun.net, 2001.

[256] M. Marefati, M. Mehrpooya, and M. B. Shafii, "Optical and thermal analysis of a parabolic trough solar collector for production of thermal energy in different climates in Iran with comparison between the conventional nanofluids," *J. Clean. Prod.*, vol. 175, pp. 294–313, 2018.

[257] I. V. Poole, “Concentrating solar power in South Africa - a comparison between parabolic trough and power tower technologies with molten salt as heat transfer fluid,” Stellenbosch University, 2017.

[258] A. Mokhtaria, M. Yaghoubia, P. Kananb, and A. V. R. Hessamia, “Thermal and optical study of parabolic trough collectors of shiraz solar power plant,” *Int. Conf. Therm. Eng. Amman, Jordan*, 2007.

[259] M. Larcher, M. Rommel, A. Bohren, E. Frank, and S. Minder, “Characterization of a parabolic trough collector for process heat applications,” *Energy Procedia*, vol. 57, pp. 2804–2811, 2014.

[260] S. A. Klein, “REVIEW PAPER CALCULATION OF MONTHLY AVERAGE INSOLATION ON TILTED SURFACES,” *Sol. Energy*, vol. 19, pp. 325–329, 1977.

[261] K. Riffelmann, T. Richert, P. Nava, and A. Schweitzer, “Ultimate Trough® - A significant step towards cost-competitive CSP,” *Energy Procedia*, vol. 49, pp. 1831–1839, 2013.

[262] J. Bonilla, L. J. Yebra, S. Dormido, and E. Zarza, “Parabolic-trough solar thermal power plant simulation scheme, multi-objective genetic algorithm calibration and validation,” *Sol. Energy*, vol. 86, no. 1, pp. 531–540, 2012.

[263] T. M. Chaudhry, “Development of a Program for Fast Design of Solar Tower Power Plants. Masters Thesis,” University of Stuttgart, High Performance Computing Center Stuttgart and Fraunhofer Institute for Solar Energy Systems ISE, 2015.

[264] P. Schöttl, K. Ordóñez Moreno, D. W. van Rooyen, G. Bern, and P. Nitz, “Novel sky discretization method for optical annual assessment of solar tower plants,” *Sol. Energy*, vol. 138, pp. 36–46, 2016.

[265] C.-J. Winter, R. L. Sizmann, and L. L. Vant-Hull, *Solar Power Plants: Fundamentals, Technology, Systems, Economics*. Springer, 1991.

[266] D. L. Siebers and J. S. Kraabel, “Estimating Convective Energy Losses From Solar Central Receivers. SAND 84 - 8717.,” Albuquerque, New Mexico, 1984.

[267] A. Mutuberria, J. Pascual, M. V Guisado, and F. Mallor, “Comparison of heliostat field layout design methodologies and impact on power plant efficiency,” vol. 69, pp. 1360–1370, 2015.

[268] F. J. Collado and J. Guallar, “Campo : Generation of regular heliostat fi elds,” vol. 46, pp. 49–59, 2012.

[269] M. Topel, “Improving Concentrating Solar Power Plant Performance through Steam Turbine Flexibility,” KTH Royal Institute of Technology, 2017.

[270] F. M. F. Siala and M. E. Elayeb, “Mathematical formulation of a graphical method for a no-blocking heliostat field layout,” vol. 23, pp. 77–92, 2001.

[271] E. Leonardi, L. Pisani, I. Les, A. Mutuberria, S. Rohani, and P. Schöttl, “Techno-economic heliostat field optimization : Comparative analysis of different layouts,” vol. 180, no. December 2018, pp. 601–607, 2019.

[272] K. Lovegrove and W. Stein, *Concentrating solar power technology Related: Principles, developments and applications*. 2012.

[273] F. Eddhibi, M. Ben Amara, M. Balghouthi, and A. Guizani, “Design and analysis of a heliostat field layout with reduced shading effect in southern Tunisia,” *Int. J. Hydrogen Energy*, no. 42, p. 28973e28996, 2017.

[274] J. S. M. Jebamalai, “Receiver Design Methodology for Solar Tower Power Plants,” Fraunhofer ISE, KTH Royal Institute of Technology, 2016.

[275] C. J. Noone, M. Torrilhon, and A. Mitsos, “Heliostat field optimization : A new computationally efficient model and biomimetic layout,” *Sol. Energy*, vol. 86, pp. 792–803, 2012.

[276] M. Gadalla and M. Saghafifar, “Thermo-economic and comparative analyses of two recently proposed optimization approaches for circular heliostat fields : Campo radial-staggered and biomimetic spiral,” vol. 136, pp. 197–209, 2016.

[277] C. Xu, Z. Wang, X. Li, and F. Sun, “Energy and exergy analysis of solar power tower plants,” *Appl. Therm. Eng.*, vol. 31, pp. 3904–3913, 2011.

[278] O. A. J. de Meyer, “Optimisation in Plant Operations for a 100 MW Central Receiver CSP Plant with Focus on the Plant Operating Strategies,” Stellenbosch University, 2017.

[279] M. A. Mustafa, S. Abdelhady, and A. A. Elweteedy, “Analytical Study of an Innovated Solar Power Tower (PS10) in Aswan,” vol. 2, no. 6, pp. 273–278, 2012.

[280] F. Rinaldi, M. Binotti, A. Giostri, and G. Manzolini, “Comparison of linear and point focus collectorsin solar power plants,” *Energy Procedia*, vol. 49, pp. 1491–1500, 2013.

[281] G. Franchini, A. Perdichizzi, S. Ravelli, and G. Barigozzi, “A comparative study between parabolic trough and solar tower technologies in Solar Rankine Cycle and Integrated Solar Combined Cycle plants,” *Sol. Energy*, vol. 98, pp. 302–314, 2013.

[282] F. Trieb, C. Schillings, M. O. ’ Sullivan, T. Pregger, and C. Hoyer-Klick, “Global Potential of Concentrating Solar Power,” in *SolarPaces Conference 2009*, 2009, no. September, pp. 1–11.

[283] C. Breyer and G. Knies, “Global Energy Supply Potential of Concentrating Solar Power,” in *SolarPACES 2009*, 2009.

[284] D. R. Baker and H. A. Shryock, “A Comprehensive Approach to the Analysis of Cooling Tower Performance,” *J. Heat Transfer*, vol. 83, no. 3, pp. 339–349, Aug. 1961.

[285] B. Ehrhart and D. Gill, “Evaluation of annual efficiencies of high temperature central receiver concentrated solar power plants with thermal energy storage,” *Energy Procedia*, vol. 49, pp. 752–761, 2014.

[286] A. Poullikkas, C. Rouvas, I. Hadjipaschalis, and G. Kourtis, “Optimum sizing of steam turbines for concentrated solar power plants,” *Int. J. Energy Environ.*, vol. 3, no. 1, pp. 9–18, 2012.

[287] T. R. Albrecht, A. Crootof, and C. A. Scott, “The Water-Energy-Food Nexus: A systematic review of methods for nexus assessment,” *Environ. Res. Lett.*, vol. 13, no. 043002, 2018.

[288] L. Bizikova, D. Roy, D. Swanson, D. H. Venema, and M. McCandless, “The Water–Energy–Food Security Nexus: Towards a practical planning and decision-support framework for landscape investment and risk management,” Winnipeg, Canada, 2013.

[289] A. Endo, I. Tsurita, K. Burnett, and P. M. Orencio, “A review of the current state of research on the water, energy, and food nexus,” *J. Hydrol. Reg. Stud.*, vol. 11, pp. 20–30, 2017.

[290] J. Liu *et al.*, “Nexus approaches to global sustainable development,” *Nat. Sustain.*, no. September, 2018.

[291] G. B. Simpson, G. P. W. Jewitt, and G. B. Simpson, “The Development of the Water-Energy-Food Nexus as a Framework for Achieving Resource Security: A Review,” *Front. Environ. Sci.*, vol. 7, no. February, pp. 1–9, 2019.

[292] N. Weitz, C. Strambo, E. Kemp-benedict, and M. Nilsson, “Closing the governance gaps in the water-energy-food nexus: Insights from integrative governance,” *Glob. Environ. Chang.*, vol. 45, no. July, pp. 165–173, 2017.

[293] D. Mabrey and M. Vittorio, “Moving from theory to practice in the water–energy–food nexus: An evaluation of existing models and frameworks,” *Water-Energy Nexus*, vol. 1, no. 1, pp. 17–25, 2018.

[294] B. Ali, “Forecasting model for water-energy nexus in Alberta , Canada Canadian Association of Petroleum Producers the United States of America,” *Water-Energy Nexus*, vol. 1, no. 2, pp. 104–115, 2018.

[295] L. Liu *et al.*, “Water demands for electricity generation in the U.S.: Modeling different scenarios for the water-energy nexus,” *Technol. Forecast. Soc. Change*, vol. 94, pp. 318–334, 2015.

[296] E. G. R. Davies, P. Kyle, and J. A. Edmonds, “Advances in Water Resources An integrated assessment of global and regional water demands for electricity generation to 2095,” *Adv. Water Resour.*, vol. 52, pp. 296–313, 2013.

[297] Z. Khan, P. Linares, and J. García-gonzález, “Integrating water and energy models for policy driven applications . A review of contemporary work and recommendations for future developments,” *Renew. Sustain. Energy Rev.*, vol. 67, pp. 1123–1138, 2017.

[298] DWS, “Strategic Overview of the Water Sector in South Africa 2015. Department Water and Sanitation, South Africa,” Pretoria, 2015.

[299] B. G. Pollet, I. Staffell, and K.-A. Adamson, “Current energy landscape in the Republic of South Africa,” *Int. J. Hydrogen Energy*, vol. 40, no. 46, pp. 16685–16701, 2015.

[300] ERC, CSIR, and IFPRI, “The developing energy landscape in South Africa: Technical Report. Energy Research Centre, University of Cape Town,” 2017.

[301] J. Macknick, R. Newmark, G. Heath, and K. C. Hallett, “A Review of Operational Water Consumption and Withdrawal Factors for Electricity Generating Technologies A Review of Operational Water Consumption and Withdrawal Factors for Electricity Generating Technologies,” *Natl. Renew. Energy Lab.*, no. March, p. 21, 2011.

[302] A. Madhlopa, S. Keen, D. Sparks, M. Moorlach, and A. Dane, “Renewable energy choices and water requirements in South Africa. Report for the Water Research Commission.,” Cape Town, 2013.

[303] T. Luo, R. Young, and P. Reig., “Aqueduct Projected Water Stress Country Rankings,” *World Resour. Inst.*, no. August, pp. 1–16, 2015.

[304] J. King and H. Pienaar, *Sustainable use of South Africa’s inland waters*. 2011.

[305] R. E. Schulze and S. D. Lynch, “Annual Precipitation. In: Schulze, R.E. (Ed). 2007. South African Atlas of Climatology and Agrohydrology. WRC Report 1489/1/06, Section 6.2,” Pretoria,RSA, 2007.

[306] R. E. Schulze *et al.*, “South African Quaternary Catchments Database. In: Schulze, R.E. (Ed). 2007. South African Atlas of Climatology and Agrohydrology. WRC Report 1489/1/06, Section 2.3.,” Pretoria, RSA, 2007.

[307] D. A. Hughes, “A review of 40 years of hydrological science and practice in Southern Africa using the Pitman rainfall-runoff model,” *J. Hydrol.*, vol. 501, pp. 111–124, 2013.

[308] S. Grimaldi *et al.*, *Statistical Hydrology*, vol. 2, no. December. 2010.

[309] Republic of South Africa, *National Water Act. Act No 36 of 1998*, no. Act No. 36. Cape Town, 1998, p. 94.

[310] D. Clark, “DEVELOPMENT AND ASSESSMENT OF AN INTEGRATED WATER RESOURCES ACCOUNTING METHODOLOGY FOR SOUTH AFRICA. WRC Report No 2205/1/15,” Pretoria, RSA, 2015.

[311] P. Karimi, W. G. M. Bastiaanssen, and D. Molden, “Water Accounting Plus (WA+) – a water accounting procedure for complex river basins based on satellite measurements,” *Hydrol. Earth Syst. Sci.*, no. June 2014, 2013.

[312] W. Pitman, “Overview of water resource assessment in South Africa: Current state and future challenges,” *Water SA*, vol. 37, no. 5, pp. 659–664, 2011.

[313] J. Macknick, S. Cohen, R. Newmark, A. Martinez, P. Sullivan, and V. Tidwell, “Water Constraints in an Electric Sector Capacity Expansion Model,” *Natl. Renew. Energy Lab.*, no. July, 2015.

[314] Y. Zhou, “A critical review of groundwater budget myth, safe yield and sustainability,” *J. Hydrol.*, vol. 370, no. 1–4, pp. 207–213, 2009.

[315] A. Rezaei and Z. Mohammadi, “Annual safe groundwater yield in a semiarid basin using combination of water balance equation and water table fluctuation,” *J. African Earth Sci.*, vol. 134, pp. 241–248, 2017.

[316] K. Witthuser, J. Cobbing, and R. Titus, “Review of GRA1, GRA2 and international assessment methodologies. P RSA 000/00/11609/6.,” Pretoria, RSA, 2009.

[317] A. Woodford, P. Rosewarne, and J. Girman, “HOW MUCH GROUNDWATER DOES SOUTH AFRICA HAVE?”

[318] R. E. Schulze, “Preface and Executive Summary. In: Schulze, R.E. (Ed). 2007. South African Atlas of Climatology and Agrohydrology. WRC Report 1489/1/06.,” Pretoria, RSA, 2007.

[319] G. of R. of S. A. Department of Water and Sanitation, “NATIONAL INTEGRATED WATER INFORMATION SYSTEM,” 2019. [Online]. Available: http://niwis.dws.gov.za/niwis2/ClimateChange. [Accessed: 30-May-2019].

[320] E. P. Dall, “Integrating desalination with concentrating solar power: Large scale cogeneration of water and electricity,” Stellenbosch University, 2017.

[321] M. Govender, S. Leyde, T. Fischer, and M. Weston, *STRATEGIC ASSESSMENT AND MAPPING OF OPPORTUNITIES FOR WATER DESALINATION AND WATER- USE OPTIMISATION OF CONCENTRATED SOLAR POWER*, no. 2382. 2016.

[322] National Planning Commission, “NATIONAL DEVELOPMENT PLAN 2030,” 2011.

[323] Department of Water and Sanitation, “Department of Water and Sanitation (DWS) Guidance Note regarding water availability and water use licensing for the Coal Baseload Independent Power Producer (IPP) Procurement Programme,” Pretoria, RSA, 2015.

[324] C. Grobbelaar, “Integrated water use application: Technical report (for public review) The construction and operation of a 75 MW CSP concentrating thermal power plant on the farm Bokpoort in the !Kheis local municipality, Northern Cape Province,” Johannesburg, RSA, 2010.

[325] IPPPP Office, “Independent Power Producers Procurement Programme (IPPPP) An Overview March 2019,” Centurion,RSA, 2019.

[326] O. Craig, “Concentrating Solar Power (CSP) technology adoption in South Africa,” Stellenbosch University, 2018.